Characterizing the Role of microRNAs in the Modulation of Host Responses to Viral Infection

by

Nadine Ahmed

Thesis submitted to the University of Ottawa
in partial fulfillment of the requirements for the
degree of doctorate in philosophy in Chemistry

Department of Chemistry and Biomolecular Sciences
Faculty of Science
University of Ottawa

Abstract

microRNAs (miRNAs) are a class of noncoding RNAs that regulate gene expression. This class of 18-25 nucleotide-long non-coding RNAs has been found to play critical roles in the modulation of a wide spectrum of cellular processes including immunity, development, and metabolism. They modulate their interactions by binding to the 3' untranslated region of the target messenger RNA to mediate the repression of gene expression. Given their emerging critical roles in the regulation of biological processes, it is not surprising that miRNAs play a significant part in modulating host-virus interactions. Viruses are obligate parasites that hijack the host cellular machinery and processes to promote their life cycle and their propagation. Emerging evidence suggests that miRNAs add an extra regulatory layer to fine-tune viral pathogenesis. This offers novel opportunities not only to delineate the crosstalk between the host and the virus but also allows for the development of novel therapeutics and the identification of novel potential biomarkers of viral infection. Herein, we examine the roles of various miRNAs in the modulation of host-virus interactions. In this thesis, we identify a polycistronic miRNA cluster (miR-183, miR-96, and miR-182) to possess antiviral properties against RNA viruses by augmenting innate immune responses to viral infection. We as well identify miR-383 to possess novel antiviral potential against Dengue virus (DENV), through its targeting of PLA2G4A, a pro-viral host factor essential for the production of infectious particles. Finally, we examine miR-185's role in the modulation of SARS-CoV-2 infection where we show that miR-185's regulation of fatty acid and cholesterol metabolism suppresses the virus's entry and propagation in lung and liver cells. Collectively, the findings in this thesis demonstrate the critical role that miRNAs play in the modulation of host-virus interaction through modifying the host's cellular environment essential for the regulation of viral pathogenesis.

Acknowledgments

I would like to thank my supervisor, Dr. John Pezacki, for his continuous support and mentorship throughout my graduate studies. His support and guidance have been invaluable to my research and have made me the scientist I am today.

I would like to extend my gratitude to former Pezacki Lab members including Dr. Ragunath Singaravelu, Dr. Dave Prescott, Dr. Dennis Özcelik and Dr. Miroslava Strmiskova. Thank you for your help throughout the years and your assistance whenever I had questions in the lab.

I would like to thank my colleagues and friends, Roxana Filip, Rhea Alonzi, Dr. Genevieve Desrochers, Mariam Serhan, Tyler Shaw, Didier Bilodeau, and Dr. Shadi Masoud whom I met in the lab and developed long-lasting friendships with.

I would like to thank my sister, Noreen Ahmed, who shared this journey with me through its ups and downs. Your support makes me a better person.

Finally, I would like to thank my parents for always believing in my abilities and for always providing support whenever I needed it.

Table of Contents

List of Figures

List of Tables

List of Abbreviations

25-HC	25-hydroxycholesterol
27-HC	27-hydroxycholesterol
3'UTR	3’ untranslated region
ABC	ATP binding cassette
ABPP	activity-based protein profiling
ACC1 or ACACA	acetyl-coenzyme A carboxylase 1
ACE2	angiotensin-converting enzyme 2
AGO	Argonaute
ALRs	AIM2-like receptors
AMPK	AMP-activated protein kinase
AP-1	activator protein-1
CARDs	caspase activation and recruitment domains
cGAS	Cyclic GMP-AMP Synthase
CLRs	C-type lectin receptors
CYP7A1	Cholesterol 7α-hydroxylase
DAMPs	damage-associated molecules patterns
DBR1	debranching enzyme 1
DENV	Dengue Virus
DENV-2	DENV serotype 2 strain
DGCR8	DiGeorge critical region 8
DHODH	Dihydroorotate dehydrogenase
ds	double-stranded
ENCODE	Encyclopedia of DNA Elements project
FASN	fatty acid synthase
FOXO1	Forkhead box protein O1
G3P	glycerol-3-phosphate
HBV	Hepatitis B virus
HCoV-229E	coronavirus 229E
HCV	Hepatitis C virus
HDL	high-density lipoprotein
HHV-6	human herpesvirus 6
HIV	human immunodeficiency virus
HMGCR	3-hydroxy-3-methyl-glutaryl-coenzyme A reductase
HMGCR	HMG-CoA reductase
HSV	Herpes simplex virus
IFN	interferons
IFNAR	The interferon-α/β receptor

IKKs	I Kappa B kinases
INSIG1	Insulin-induced gene 1 protein
IRFs	Interferon regulatory factor
ISGs	interferon-stimulated genes
ISRE	IFN-stimulated regulatory elements
JAK	Janus kinase
LDL	low-density lipoprotein
LGP2	laboratory of genetics and physiology 2
LSS	Lanosterol synthase
LXR	liver X receptor
MAPK	mitogen-activated protein kinase
MAVS	mitochondrial associated antiviral signalling
MDA5	melanoma differentiation-associated protein 5
MERS-CoV	Middle East respiratory syndrome coronavirus
MHV	mouse hepatitis virus
miR-183	microRNA-183
miR-185	microRNA-185
miR-383	microRNA-383
miRNAs	microRNAs
MVK	mevalonate kinase
MyD88	Myeloid differentiating factor 88
ncRNAs	non-coding RNA molecules
NF-κB	nuclear factor κB
NK cells	Natural killer cells
NLRs	Nod-like receptors
NR0B2	Nuclear Receptor Subfamily 0 Group B Member 2
NS3	non-structural protein 3
NS4B	non-structural 4B
NS5A	Non-structural protein 5A
OAS	2′-5′-oligoadenylate synthetase
PAMPs	pathogen-associated molecular patterns
pDC	plasmacytoid dendritic cells
piRNA	small interfering RNA
PKR	dsRNA-activated protein kinase R
PPP2CA	Protein Phosphatase 2 Catalytic Subunit Alpha
Pre-miRNA	precursor miRNA
Pri-miRNA	primary miRNA transcript
PRR	pattern recognition receptors
RABV	rabies virus
RC	replication complexes
RIG-I	retinoic acid inducible gene – I

RISC	RNA-induced silencing complex
RLRs	RIG-I-like receptors
RO	replication organelles
rRNAs	ribosomal RNAs
SACRB1	HDL-scavenger receptor B type 1
SARS-CoV-2	Severe Acute Respiratory Syndrome Coronavirus 2
SCAP	(SREBP) cleavage-activating protein
SCD1	Stearoyl-CoA desaturase-1
siglec	sialic acid-binding Ig-like lectin
siRNA	small interfering RNA
SMART	small molecule–mediated annotation of miRNA targets
snoRNA	small nucleolar RNA
snRNA	small nuclear ribonucleic acid
SQLE	squalene epoxidase
SREBF1	Sterol Regulatory Element Binding Transcription Factor 1
SREBF2	Sterol Regulatory Element Binding Transcription Factor 2
SREBP-1c	sterol regulatory element-binding protein 1c
SREBPs	sterol regulatory element-binding proteins
SRING	stimulator of interferon genes
ss	single-stranded
STAT	signal transducer and activator of transcription
TBK1	TANK binding kinase 1
TIR	Toll/interleukin1 receptor (IL1R) homology domain
TLR	Toll-like receptors
TRAF	tumor necrosis factor receptor-associated factors
tRF	tRNA-derived fragments
TRIF	TIR-domain-containing adapter-inducing interferon-β
TRIM27	E3 ubiquitin ligase tripartite motif-containing protein 27
tRNAs	transfer RNAs
TYK2	tyrosine kinase 2
vmiRNAs	virally encoded miRNA
VOC	variants of concern
VSV	Vesicular Stomatitis Virus
WNV	West Nile virus
XPO5	exportin 5
ZIKV	Zika Virus

Chapter 1

Introduction

1.1 Preface

This chapter serves as background and introduction for the topics covered in the following chapters (Chapters 2-5). This thesis explores the role of microRNAs (miRNAs) in modulating host-virus interactions with a focus on miRNAs which we have identified to regulate the innate immune response to RNA virus infection, and immunometabolic responses to dengue virus and severe acute respiratory syndrome coronavirus 2 infections. Portions of this chapter, specifically sections 1.4.1 and 1.4.3, were previously published and adapted from (N. Ahmed, N. Ahmed, R. Filip, and J. P. Pezacki "Nuclear Hormone Receptors and Host-Virus Interactions") with permission from the publisher under license number 5386540630700.

Host-virus interactions are one of the main areas of research and focus of the Pezacki lab. This thesis aims to identify miRNAs with novel roles in the regulation of host-virus interactions and delineate the mechanism of action of these miRNAs in modulating viral pathogenesis.

1.2 Non-coding RNAs and the non-coding transcriptome

Recent advancement in RNA biology and research has led to the discovery of non-coding RNA molecules (ncRNAs), which represent the majority of the transcribable genome[1]. ncRNAs are categorized into two distinct criteria based on the length and size of the RNA species. RNAs shorter than 200 nucleotides are referred to as snRNA or short non-coding RNAs while molecules longer than 200 nucleotides are referred to as lncRNA or long-non-coding RNAs[2]. snRNAs include functional non-coding RNAs such as ribosomal RNAs (rRNAs) and transfer RNAs (tRNAs) as well as other regulatory RNAs which includes mammalian RNA species such as microRNA (miRNA), small interfering RNA (siRNA), piwi-interacting RNA (piRNA), small nucleolar RNA (snoRNA), tRNA-derived fragments (tRF), small nuclear ribonucleic acid (snRNA)[2].

Given the abundant nature of these non-coding species of RNAs, it has been widely believed that these genetic species are "junk" components of the transcribable genome. It wasn't until more recently, with results highlighted from large-scale projects which aim to annotate and functionally characterize genes such as the Encyclopedia of DNA Elements project (ENCODE), that the role of the non-coding transcriptome was reconsidered[3]. The over-representation of these species has allowed researchers to further their knowledge and understanding of the regulatory roles these species play in modulating cellular processes and biological functions. Rapid advancement in high through-put next-generation sequencing technologies aided in simultaneous expansion in the development of databases (Such as miRbase[4] and lncRNAdb[5]), which aims to identify and annotate various species of ncRNAs[6]. Not surprisingly, the quantity, abundance, and complexity of the non-coding transcriptome increase with the complexity of the organism, suggesting the crucial regulatory potential of these species[7]. Recently, ncRNAs implication in various biological

processes has been well demonstrated with distinct roles in transcriptional regulation, mRNA cleavage, translational modulation, and epigenetic modification[8,9]. Recent advances in ncRNA research firmly point toward the involvement of miRNAs in the modulation of human pathological diseases and processes[10–13]. This thesis will focus on the role of miRNAs in the modulation of biological processes which ultimately impact host-virus interactions. Rapid advancement in miRNA research has provided a plethora of tools to identify and annotate the roles of miRNAs in healthy and diseased cellular states[13].

1.2.1 microRNAs

MicroRNAs (miRNAs) are small non-coding RNAs, ranging in size from 18-25 nucleotides in length, which post-transcriptionally regulate gene expression by base pairing with the 3'untranslated regions of mRNA[14]. Through this interaction, which is predominantly mediated by 5' end of the miRNA, they induce translational repression and promote RNA degradation. One single miRNA can have multiple binding sites in the 3' untranslated region (3'UTR) of a target mRNA and one single mRNA can be targeted by many unique miRNAs. This allows the miRNAs to regulate multiple components of cellular pathways and regulatory networks, which accumulate to exert a larger effect on physiology and immunity[15]. Generally, miRNAs form a complex network where each miRNA regulate multiple mRNAs and each mRNA is regulated by multiple miRNAs, this results in the complexity of the regulatory layer added by the activity of miRNAs over the complex cellular pathway and signal transduction pathways like those involved in immunity and cellular differentiation and cancer development [15]. Because miRNAs have evolved to be endogenous signaling molecules that regulate gene expression and can target multiple components within the same pathway or even multiple related pathways, they may result in a more pronounced phenotypic effect[16]. In addition, they fine-tune endogenous gene expression by

regulating feed-forward and negative-feedback loop mechanisms, where the mRNA and the miRNA are being modulated, and that allows for endogenous regulation of protein expression levels[16].

1.2.2 Canonical miRNA Biogenesis

miRNAs are generally intergenic where they are encoded independently of protein-coding genes with independent distinct promotors or within introns of protein-coding genes[17]. However, some miRNAs are identified to reside within exons and protein-coding regions of the host's genome[18]. Transcription of miRNAs into distinct polycistronic genomic clusters has been as well identified, where similar seed regions of the miRNAs within the same cluster can be detected[17]. There are two biogenesis pathways for miRNA production, the canonical and non-canonical pathways: the canonical pathway being the dominant biogenesis pathway.

The canonical pathway starts with the transcription of the primary miRNA transcript (Pri-miRNA) which occurs in the nucleus via the action of RNA polymerase II/III. Following transcription, the Pri-miRNA is processed to produce the precursor miRNA (Pre-miRNA) by the action of the microprocessor complex consisting of two endocytic enzymes: RNase III enzyme Drosha and DiGeorge critical region 8 (DGCR8) [19]. Following the action of both enzymes and the processing of the pri-miRNA into pre-miRNA, the shuttling of the pre-miRNA from the nucleus into the cytoplasm takes place via the action of exportin 5 (XPO5)/RanGTP complex where it subsequently gets process by Dicer to generate the miRNA duplex[19,20]. The duplex results in the production of two forms of the miRNA with a nomenclature dependent on the directionality of the miRNA strand. Two forms are produced in this case, with a strand generated from the 5'end of the pre-miRNA, while another stand generated from the 3'end of the pre-miRNA. The mature miRNA containing the miRNA is then loaded on Argonaute (AGO), which together represents the RNA-

induced silencing complex (RISC). Favorable loading of a specific strand depends on various factors such as cell type, stability, and proportion/abundance of one strand relative to the other[21]. The strand which remains incorporated in the RISC complex represents the active strand, while the other strand is referred to as the passenger stand or miR* and would get degraded[22].

The miRNA loaded on the RISC complex mediates the suppression of protein synthesis through various several mechanisms which directly alter the stability of the target mRNA[23,24]. The RISC complex harboring the miRNA mediates mRNA targeting trough base-pairing complementarity, the mRNA target site is usually located in the 3'untranslated region of the target mRNA and it binds to the complementary miRNA seed sequence site which is located in 2-8 nucleotide 5' seed region in the miRNA[25,26]. This binding event results in gene silencing via a combination of translational repression and mRNA degradation. Through this regulatory mechanism, miRNAs are expected to modulate several transcripts which results in pronounced cellular effects[27]. It is essential to note, that although the canonical base-pairing between the miRNA seed site and the 3'UTR of the target mRNA is the predominant interaction driving the biological function of the miRNA, non-conventional interactions were as well observed[28,29]. For example, it has been found that interactions can occur at 3' compensatory sites with significant pairing to the 3'region of the miRNA. This usually compensates for a bulge in the seed region of the miRNA resulting from a mismatch or a G-U wobble in the seed site[28,29]. Although these interactions are present, they contribute less to the biologically relevant outcomes of miRNA:mRNA interaction in comparison to the canonical interactions described above[30]. Figure1.1 summarizes the canonical miRNA biogenesis pathway.

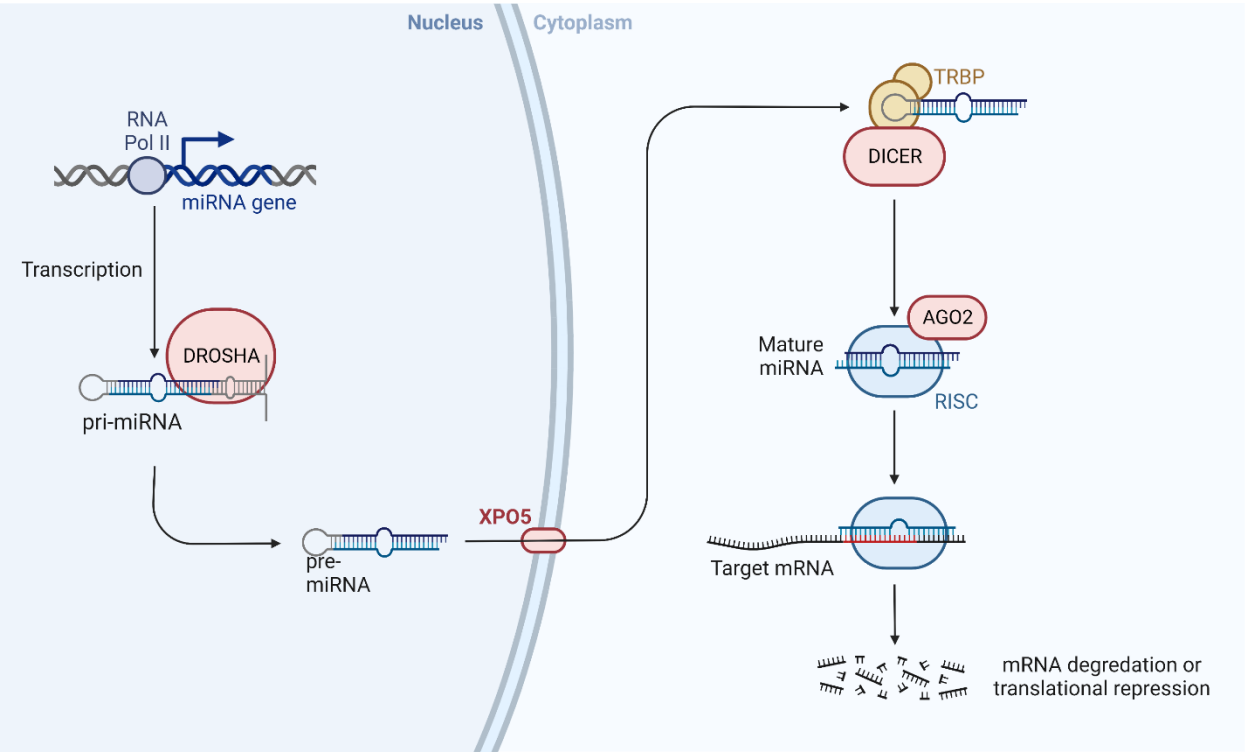

Figure 1.1 The miRNA biogenesis pathway. miRNA biogenesis initiates in the nucleus where the miRNA is first transcribed into pri-miRNA transcript that is further processed by Drosha to produce the pre-miRNA. The pre-miRNA is then translocated to the nucleus by XPO5 where it is initially cleaved by Dicer and its dsRNA-binding protein partner, transactivation response RNA-binding protein (TRBP), into a miRNA-miRNA* duplex. The duplex is then loaded onto RNA-induced silencing complex (RISC) to target the mRNA of interest. Binding of the seed site of the miRNA to complementary sequences in the 3' untranslated region (UTR) of target mRNA results in the repression of gene expression due to mRNA degradation or translational repression. This figure is adapted from "miRNA in Cancer", by BioRender.com (2022). Retrieved from https://app.biorender.com/biorender-templates

1.2.3 Non-canonical miRNA Biogenesis pathways

In addition to the above-described canonical miRNA biogenesis pathway, there are newly described alternative pathways. These pathways are generally categorized as either Drosha/DGCR8-independent or Dicer-independent[31]. An example of the Drosha/DGCR8-independent mechanism is the transcription of mirtrons, which are non-canonical pri-miRNAs encoded within an intron of coding genes[32]. These miRNA species are initially processed in a manner that is similar to introns which results in the formation of species similar to canonical pri-miRNAs, however, with shorter hairpin stem-loops in comparison to the pri-miRNA produced through the canonical pathway[33]. Due to their distinct structural differences, pri-miRNA cannot be processed by DROSHA/ DiGeorge critical region 8 and will get processed by another enzyme; debranching enzyme 1 (DBR1)[34]. Following processing, similar to the canonical pathway, the produced pre-miRNA would be exported by Exportin 5 (XPO5)-Ran-GTP Complex to the cytoplasm cleaved by DICER. Alternatively, there is a Dicer-independent method for the biogenesis of miRNA. Interestingly, pre-miR-451 appears to be the only known miRNAs to be processed in this manner, since the structure of the stem-loop is too short to be processed and cleaved by Dicer and thus requires the catalytic activity of AGO2 for the maturation and processing[35]. Although these non-canonical pathways are present in some cells and required for the biogenesis of some miRNAs, they contribute less to the functional pool of miRNAs in comparison to the canonical miRNA biogenesis pathway.

1.2.4 Prediction and identification of miRNA targets

With the discovery of miRNAs, an increase in the number of tools to identify their targets has been developed. It has since been evident that miRNAs are significantly involved in a variety of processes, and they are found to be crucial regulators of pathways and mechanisms involved in proliferation, differentiation, and host-pathogen interactions[36–40]. Thus, identification and validation of miRNA:mRNA target interactions is essential for uncovering the role that miRNAs play in a given biological process and may aid in uncovering miRNA regulatory networks governing biological processes. Bioinformatic tools for the identification of miRNA targets share similar features. These predictions depend on seed match, free energy which measures the stability and the likelihood of interaction to occur across a biological system and species, and finally site accessibility[41]. Some commonly used prediction software include but are not limited to TargetScan[27,42],miRanda [43], and miRanda-mirSVR[44].

Although these tools are powerful in predicting miRNA targets, they have limitations since they primarily rely on seed-site complementarity for target prediction. This may disregard seed-site accessibility and structural stability[45]. In addition to this, there has been evidence of the functionality of non-canonical and non-conserved sites in the 3'UTR, which may be overlooked by these target prediction tools[46]. Nevertheless, these tools remain instrumental in identifying targets of miRNAs and remain primary tools in miRNA and miRNA-related research since the in-depth understanding of the structural elements of miRNAs has enhanced the predictive power of the miRNA target prediction algorithms. In addition to computational tools, microarray and transcriptomics analysis have been widely utilized to identify miRNA targets. Transcriptomics analysis of cellular gene expression profiles is usually performed following miRNA mimics and inhibitors to either enhance or suppress miRNA function in target cells[47]. These loss-of-function

and gain-of-function approaches offer significant advantages since they allow for not only the identification of potential direct targets of a specific miRNA but also could reveal indirect targets and consequences of miRNA-mediated regulation of gene expression.

1.2.5 microRNAs and host-virus interactions

miRNAs have been implicated in a range of endogenous processes ranging from differentiation, pathological processes, cancer, immunity, and response to viral infections[36–40]. Viruses are obligate parasites that hijack cellular machinery to aid in their propagation and production of viral progeny. Infection of host cells by viruses results in a profound dysregulation of the cellular miRNA profiles. These changes in miRNA profiles could either be beneficial or detrimental to the viral lifecycle, where viruses could either exploit cellular miRNAs to their advantage or cellular miRNA could have antiviral roles or functions by enhancing host antiviral mechanisms. Recent evidence suggests the implication of miRNA in the interplay between the host and viruses, adding a regulatory layer to the intricate cross-talk between both the host and the virus to modulate pathogenesis, antiviral and pro-viral responses[48].

Hepatitis C virus (HCV) represents one prominent example of how viruses can exploit cellular miRNAs to their advantage[49]. HCV is an enveloped RNA virus that belongs to the flavivirus family. HCV infection results in chronic hepatitis in up to 80% of infected individuals leading to chronic liver diseases such as liver steatosis, cirrhosis, and HCV-mediated hepatocellular carcinoma (HCC) [50, 51]. HCV was shown to exploit the function of a host-miRNA, miR-122, which regulates cholesterol biosynthesis, a pathway exploited by HCV to enhance its replication and propagation[52]. Additionally, miR-122 facilitates the replication of HCV by targeting and binding to the viral 5′ non-coding region[38]. MiR-122 is being investigated in a clinical setting as a potential therapeutic target for HCV infection. Miravirsen and RG-101 are clinically developed anti-

miR122 oligonucleotides which have been found, to significantly decrease HCV RNA levels in chronic HCV patients. These clinical trials highlight the relevance of targeting miRNA-mediated virus-host interactions as a potential therapeutic antiviral strategy[53,54]. Other types of interactions between miRNAs and targets have been observed during infections. Some of these examples include interactions between host miRNAs and host target mRNA to either enhance or suppress viral pathogenesis, cellular miRNA targeting viral transcripts for enhancement or suppression of viral life cycle, or virally encoded miRNAs acting on the suppression of host targets to enhance pathogenesis. For example, Li *et al*. profiled dysregulated host miRNAs during HCV infection and identified miR-25, miR-130a/b, and let-7a to be downregulated in levels by infection in cultured cells and human liver tissues[55]. They show that these miRNAs have antiviral capabilities and they are targeted by the virus to enhance replication in the infected host[55]. Additionally, a phenotypic miRNA mimics based-screen performed by Smith and colleagues aided in the identification of miRNAs with anti-flavivirus potential[56]. They identified miR-34, miR-15, and miR-517 to have antiviral activities against Dengue Virus (DENV), West Nile virus (WNV), and Zika Virus (ZIKV)[56]. Moreover, the role of miRNAs in the modulation of Herpesvirus infection is extensively studied, with multiple examples showing the involvement of host miRNAs and virally-encoded miRNA (vmiRNAs) in modulating viral pathogenesis[57]. For example, Herpes simplex virus (HSV), which includes HSV-1 and HSV-2, was shown to encode 27 and 24 functional miRNAs, respectively[58,59]. These encoded miRNAs are found to regulate viral and host gene expression. Overall, evidence has supported the involvement of miRNA in the modulation of host-virus interaction with roles in regulating endogenous pathways that act to combat viral infections (Such as innate immune antiviral pathways[40,60,61]) and metabolic pathways hijacked by some viruses to enhance their replication and pathogenesis[62–66].

1.3 Innate immune response and host-virus interactions

The innate immune response is the first line of defense against invading pathogens, including viruses, parasites, and bacteria[67]. The non-specific nature of the innate immune response is tightly regulated by a set of positive and negative regulators, which enable the host to combat pathogenic microorganisms without over-activation which may result in host cellular damage[68]. The innate immune response is a fast response that is readily activated in the presence of a pathogen[67]. This response will allow for the activation of downstream adaptive immune responses. This defense mechanism represents a rapid response and protection against invading pathogens which include single-stranded (ss) and double-stranded (ds) DNA and RNA viruses, intracellular bacteria, and parasites. These responses are dependent on tightly regulated signal transduction to ensure mounting robust and effective immune response as well as proper resolution of the immune response following pathogen clearance and are mediated by a variety of transcription factors that are instrumental for eliciting proper immune responses [69,70].

The innate immune response is initially triggered by the recognition of pathogen-associated molecular patterns (PAMPs) by pattern recognition receptors (PRR) which can be either expressed on the surface of host and immune cells or endosomal membranes (Such as toll-like receptors (TLR)) or can be detected in the cytosol by cytosolic receptors such as retinoic acid-inducible gene – I (RIG-I) which detects PAMPs in a TLR-independent manner[71,72]. This eventually leads to the activation of a signaling cascade which ultimately results in the synthesis and secretion of interferons (IFN) such as IFN-α and IFN-β, which exhibit antiviral, antiproliferative, and immunomodulatory functions[70,73]. These cytokines are crucial and central to the protective antiviral response in the invaded hosts.

1.3.1 Interferons: modulators of the antiviral response

Type I, II, and III IFNs represent major classes of antiviral cytokines produced as a response to viral infection and they belong to class II family of cytokines[74]. They are integral to eliciting and mounting a potent antiviral immune response against invading viruses[74]. There are 21 different types of human IFNs, with 16 subtypes belonging to type I IFNs and including IFNαs, IFNβ, IFNϵ, IFNκ, and IFNω[74]. Type I IFNs are the most well-defined, with IFNα and IFNβ being predominantly and readily expressed as an innate immune response to viral infection[74].The signal transduction of type I IFNs depends on the binding to the interferon-α/β heterodimeric receptor complex (IFNAR), which is composed of IFNAR1 & IFNAR2[74]. Conversely, Type II consists of IFNγ which acts on a broad spectrum of cell types but is predominantly expressed and produced by specialized immune cells such as T-lymphocytes, B-lymphocytes, macrophages, and Natural killer cells (NK cells)[75]. Unlike, IFNα and IFNβ, IFNγ plays a crucial role in the adaptive immune system, such as modulating and regulating the differentiation and activation of T- and B-lymphocytes, as well as in linking the innate and adaptive immune responses. Type II IFN signaling is initiated by binding of IFN-γ type II IFN receptor complex consisting of IFN-γR1 and IFN-γR2[76]. Interestingly, deficiency of IFNγ response is associated with higher susceptibility to mycobacteria and salmonella infection relative viral infection, however, evidence has emerged suggesting the requirement of IFNγ-modulated responses against some viruses such as mouse hepatitis virus (MHV)[77,78]

A newer antiviral class of IFN was discovered and referred to as type III IFN consisting of IFNλ1, IFNλ2, IFNλ3, and IFNλ4[74,79,80]. These cytokines are similar to the type I IFN family of cytokines but have relatively limited activity and their expression is restricted to epithelial cells and epithelial barriers which include the gastrointestinal, respiratory, and reproductive tracts [80–82]. The signal

transduction of Type III IFN is dependent on the binding to a receptor complex consisting of the IFN-λ-specific IL-28Ra chain and IL-10R2 chain, which includes IL-10 and other members of the IL-10 super-family[80]. All three types of IFN are produced in response to infection following the recognition of PAMPs by PRRs, this initiates a signaling cascade which ultimately results in the production of these antiviral cytokines through the activation of The Janus kinase (JAK)-signal transducer and activator of transcription (STAT) pathway[81].

IFNα and IFNβ are the most well-defined and broadly expressed Type I IFNs. They can establish antiviral states in infected and neighboring uninfected cells in order to restrict various stages of viral lifecycles[83]. Type I IFNs exert a broad range of antiviral activities, which include the induction of dsRNA-activated protein kinase R (PKR) which acts to inhibit the cellular translational machinery, and induction of molecules with the capacity to degrade foreign RNA such as 2′-5′-oligoadenylate synthetase (OAS)/RNAseL[84]. Given this, recombinant IFNs have been extensively utilized and approved for the treatment of various viral infections such as the treatment of HCV and Hepatitis B virus (HBV)[85,86]. Additionally, IFNs were found to be potently effective against other RNA viruses such as Severe acute respiratory syndrome coronavirus 2 (SARS-CoV-2) in clinical and laboratory settings[87,88]. Type I IFN was as well found to be essential to control WNV infection, since mice with defective Type I IFN response were shown to be unable to subvert viral replication and WNV infection[89].

1.3.2 IFN production and signaling

As previously discussed, triggering of the IFN production pathway is dependent on the recognition of PAMPs or self-derived molecules associated with cellular damage referred to as damage-associated molecules patterns (DAMPs) by PRRs[90]. Mammals have evolved to have several classes and types of PRR which includes Toll-like receptors (TLRs), RIG-I-like receptors (RLRs),

Nod-like receptors (NLRs), AIM2-like receptors (ALRs), C-type lectin receptors (CLRs), and intracellular DNA sensors such as Cyclic GMP-AMP Synthase (cGAS)[71,91,92]. TLRs are the most diverse class containing 10 homologs (TLR1-10) in humans. These receptors are predominantly expressed on the cell surface or on the surface of intracellular compartments such as the endosome, lysosome, and ER. Cell surface TLRs include TLR1, TLR2, TLR4, TLR5, TLR6, and TLR10 and they primarily recognize microbial and bacterial membrane components such as lipids, lipoproteins, and proteins, whereas intracellular TLRs are localized in the endosome and include TLR3, TLR7, TLR8, TLR9, TLR11, TLR12, and TLR13 and recognize nucleic acid components of microbes[93,94]. TLRs generally recruit adaptor proteins following PAMP or DAMP binding to initiate the activation of the signaling cascade via Toll/interleukin1 receptor (IL1R) homology domain (TIR). Myeloid differentiating factor 88 (MyD88) and TIR-domain-containing adapter-inducing interferon-β (TRIF) are TIR domain-containing adapter proteins that result in the initiation of signalizing transduction cascade through the activation and recruitment of a cytosolic protein kinase complex involving I Kappa B kinases (IKKs) and TANK binding kinase 1 (TBK1). These interactions ultimately result in the activation and phosphorylation of nuclear factor κB (NF-κB), Interferon regulatory factor (IRFs), or mitogen-activated protein kinase (MAP) kinases to regulate the expression of cytokines, chemokines, and type I IFNs[95–98]. Among TLRs, TLR3 specifically binds to double-stranded RNA and recruits TRIF to activate the tumor necrosis factor receptor-associated factors (TRAF) and IKK-ε, which in turn activates the latent transcription factors IRF-3, IRF-7, and NF-κB[70,73,99]. **Figure 1.2** summarizes the various types of TLRs and their ligands and the downstream signal transduction consequences

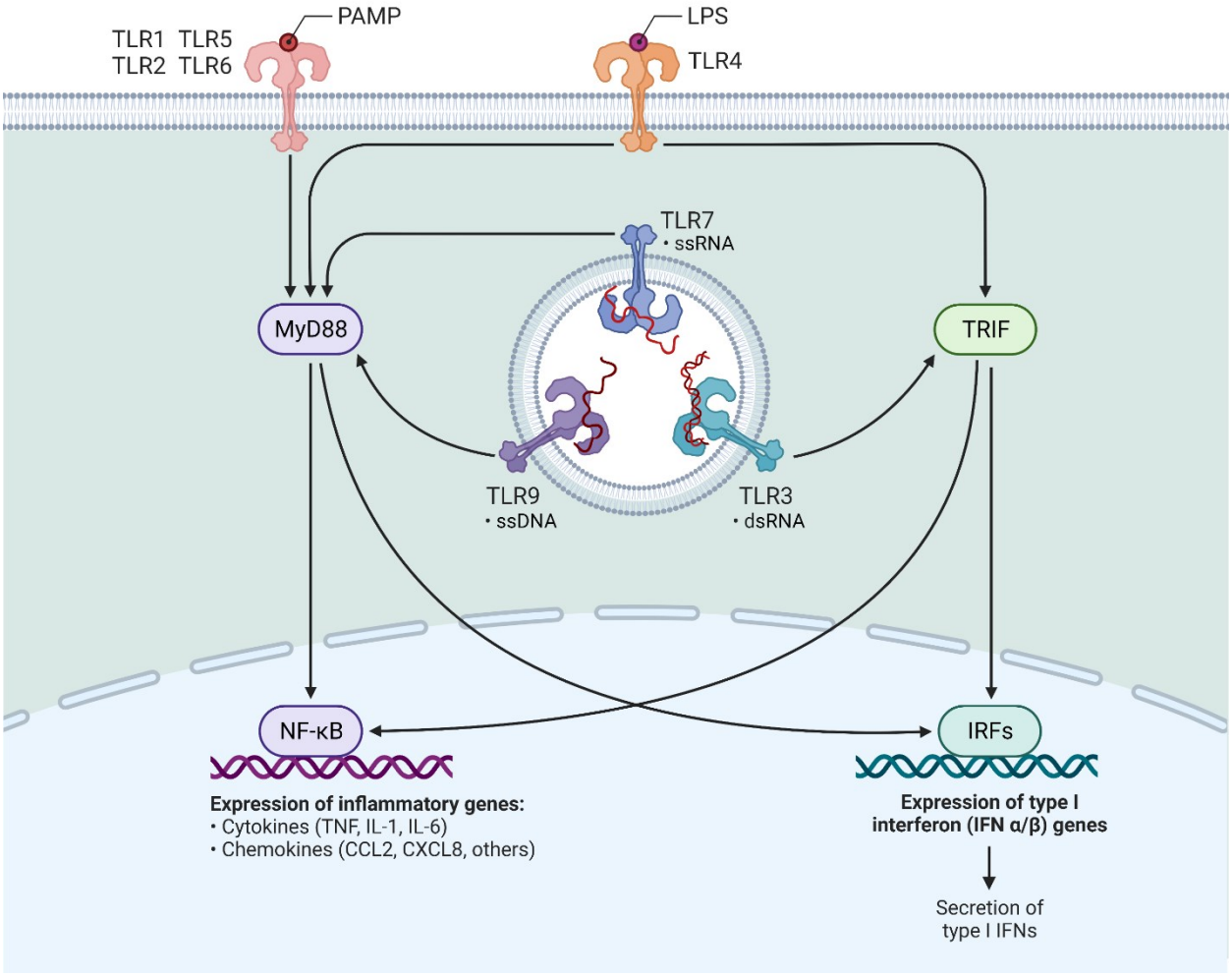

Figure 1.2 Toll-like receptors and their ligands. TLRs act as PRR which recognizes pathogen associated molecular patterns (PAMPs) to elicit a downstream innate response to the invading pathogen. There are several TLRs which recognizes different PAMPS. TRIF is recruited to TLR3 and TLR4 and promotes an alternative pathway that leads to the activation of IRFs and NF-κB for induction of type I IFN and inflammatory cytokine genes. MyD88 is recruited to TLR1,2,4,5,6,7,8 to activate IRF3 and NF-κB for induction of type I IFN and inflammatory cytokine genes. This figure is adapted from "TLR signaling pathway", by BioRender.com (2022). Retrieved from https://app.biorender.com/biorender-templates.

As previously mentioned, in addition to recognition of viral PAMPS by TLRs , they can be recognized by other cytosolic sensors such as RLRs which include RIG-I, melanoma differentiation-associated protein 5 (MDA5) and laboratory of genetics and physiology 2 (LGP2) which localized in the cytosol recognizes cytosolic viral RNA[100].These cytosolic receptors are characterized by the presence of a helicase domain, DExD/H box-containing RNA helicase, and a carboxyl-terminal domain, which are essential for the detection of viral RNAs[101]. Additionally, RIG-I and MDA-5 contain tandem caspase activation and recruitment domains (CARDs) which modulate the downstream interactions with the CARD domain of the mitochondrial-associated antiviral signaling molecule (MAVS), which triggers the activation and recruitment of cytosolic protein kinase complex involving I Kappa B kinases (IKKs) and TANK binding kinase 1 (TBK1) to induce the phosphorylation of downstream transcription factors such as IRF3, IRF7, and NF-κB, which modulates the transcription of type I and III interferons[99,102](Figure 1.3). The functional role of RIG-I in modulating antiviral innate immune responses was first discovered in RNAi loss-of-function studies which validated its importance in the detection of viral double-stranded RNA to initiate the antiviral innate immune responses[71,103]. Currently, the importance of cytosolic sensors in initiating the innate immune response is widely understood with several studies validating their importance in inducing the production of IFNs against various viruses[104–106]. Type I IFN production and signaling model following RNA virus infection consists of a 2-step positive feedback loop process that is modulated by the activity of IRF-3 and IRF-7. The detection of viral RNA by either TLRs or RLR triggers the phosphorylation, dimerization, and localization of IRF-3 or IRF-7 to induce the production, and secretion of type I IFNs from infected cells, which includes IFNαs, IFNβ[70,99].

Activation of IRFs is dependent on the phosphorylation of several possible sites located in the c-terminal signal response domain. For IRF3 possible phosphorylation site is serine 386, while for IRF7 the sites are serine 477 and 479[99,107–110]. Following phosphorylation, IRF3 and IRF7 either homodimerize or heterodimerize and translocate to the nuclease with other transcription factors such as NF-κB or activator protein-1 (AP-1) where they bind to the IFNβ promoter to induce the transcription of Type-I IFNs[108,111]. IRF3 expression is abundant in all cell types, but IRF7 appears to be more restricted to cells, monocytes, and plasmacytoid dendritic cells (pDC)s[112]. Viruses have evolved to antagonize IRF3 phosphorylation to inhibit innate immune responses, for example, Dengue virus restricts antiviral innate immune responses by blocking TBK-1 and IRF3 phosphorylation and thereby IRF3-dependent antiviral responses[113]. Additionally, it has been shown that SARS-CoV-2 acts to inhibit Type I interferon production by deactivating IRF3[114]. Thus, inactivation of IRF3-mediated antiviral gene activation appears to be an innate immunity evasion strategy employed by a range of viruses to allow for viral life cycle progression. Figure 1.3 summarizes and gives an example of how viral-derived nucleic acids can activate the production of interferons in host cells.

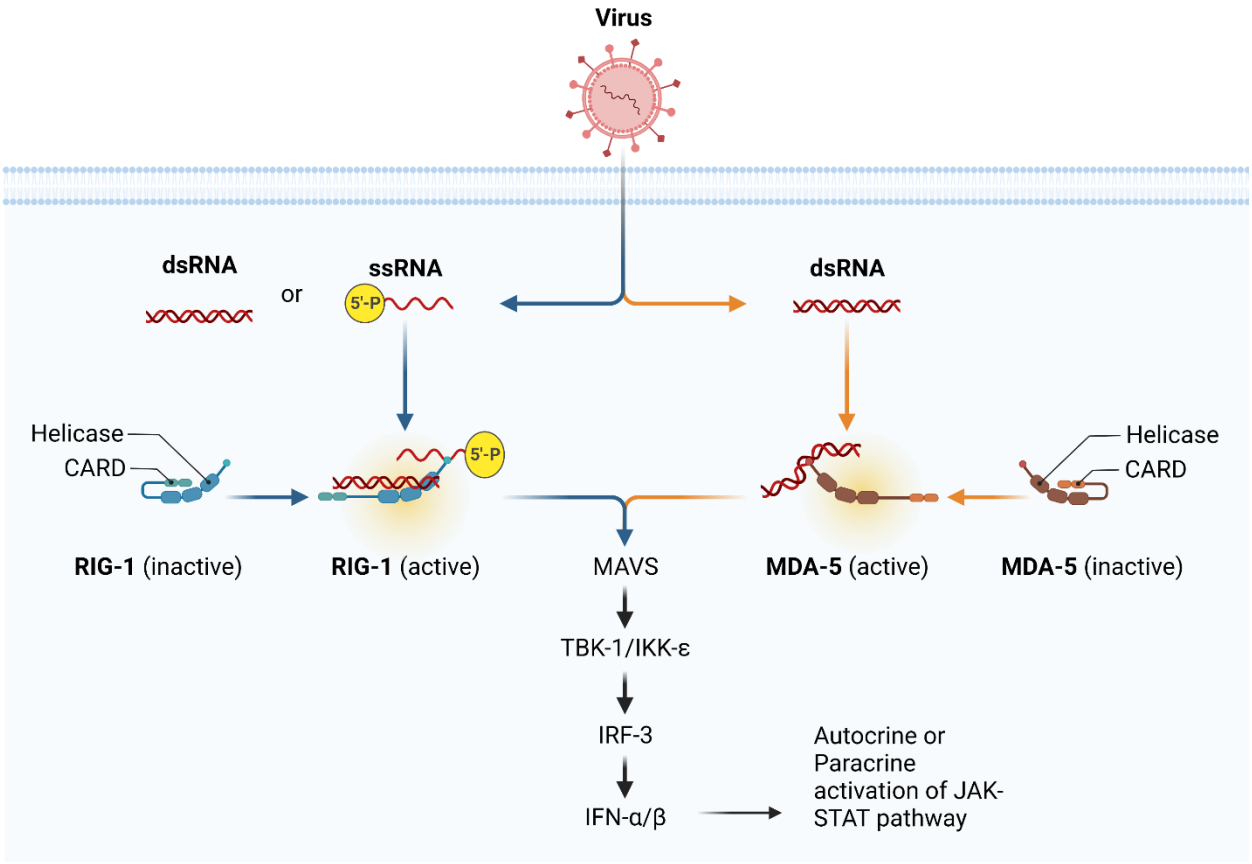

Figure 1.3 IFNα/β synthesis and production. When a virus infects a cell, virus-associated molecular patterns such as viral nucleic acids can be recognized by cytoplasmic sensors such as RIG-I or MDA5. This association leads to the activations of a downstream signaling cascade which ultimately results in the activation of IRF3 and its translocation to the nucleus where it activates the transcription of IFNs which act in a paracrine or an autocrine fashion to activate the JAK-STAT pathway. Figure generated using Biorender. The figure is adapted from "RIG-I and MDA-5 Detects Cytosolic Viral RNAs", by BioRender.com (2022). Retrieved from https://app.biorender.com/biorender-templates.

1.3.3 JAK-STAT signaling and interferon-stimulated gene production

Following stimulation, Type I and II IFN molecules are released and act, in a paracrine or autocrine manner, on the activation of receptor-associated protein tyrosine kinases Janus kinase 1 (JAK1) and tyrosine kinase 2 (TYK2) which ultimately leads to autophosphorylation and activation of downstream STAT1 and STAT 2 molecules (Figure 1.4). Phosphorylated STAT1 and STAT2 complex with interferon regulatory factor 9 (IRF9) and translocate into the nucleus to induce the transcriptional activation and production of interferon-stimulated genes (ISGs) at IFN-stimulated regulatory elements (ISRE)[115]. In addition, phosphorylated STAT1 homodimers are usually activated as a response to IFN γ and induce transcription from IFN γ activation sequence (GAS)[116]. STAT1 activation is dependent on the phosphorylation of two sites, Tyrosine 701 (Y701) and Serine 727 (S727). However, it has been evident that Y701 site full transcriptional activity and biological function[117]. The activation of the JAK-STAT signaling pathway in response to Type I and type III binding results in the production of a wide range of ISGs which ultimately acts at various levels of the viral life cycle to inhibit replication and pathogenesis. Given this, several viruses have evolved to antagonize the phosphorylation and activation of STAT1 to disrupt innate antiviral mechanisms. For example, Adenoviruses have developed mechanisms to inhibit STAT1 activity and ISG production by sequestering phosphorylated STAT1 at replication centers and inhibiting nuclear translocation of activated STAT1 molecules[118]. Moreover, HCV Non-structural protein 5A (NS5A) protein was found to disrupt and antagonize the phosphorylation of STAT1 to reduce ISG production and downstream antiviral responses[119]. Overall, it is evident that STAT1 is a key factor in priming and enhancing antiviral response and is considered a key element of the innate antiviral immune response.

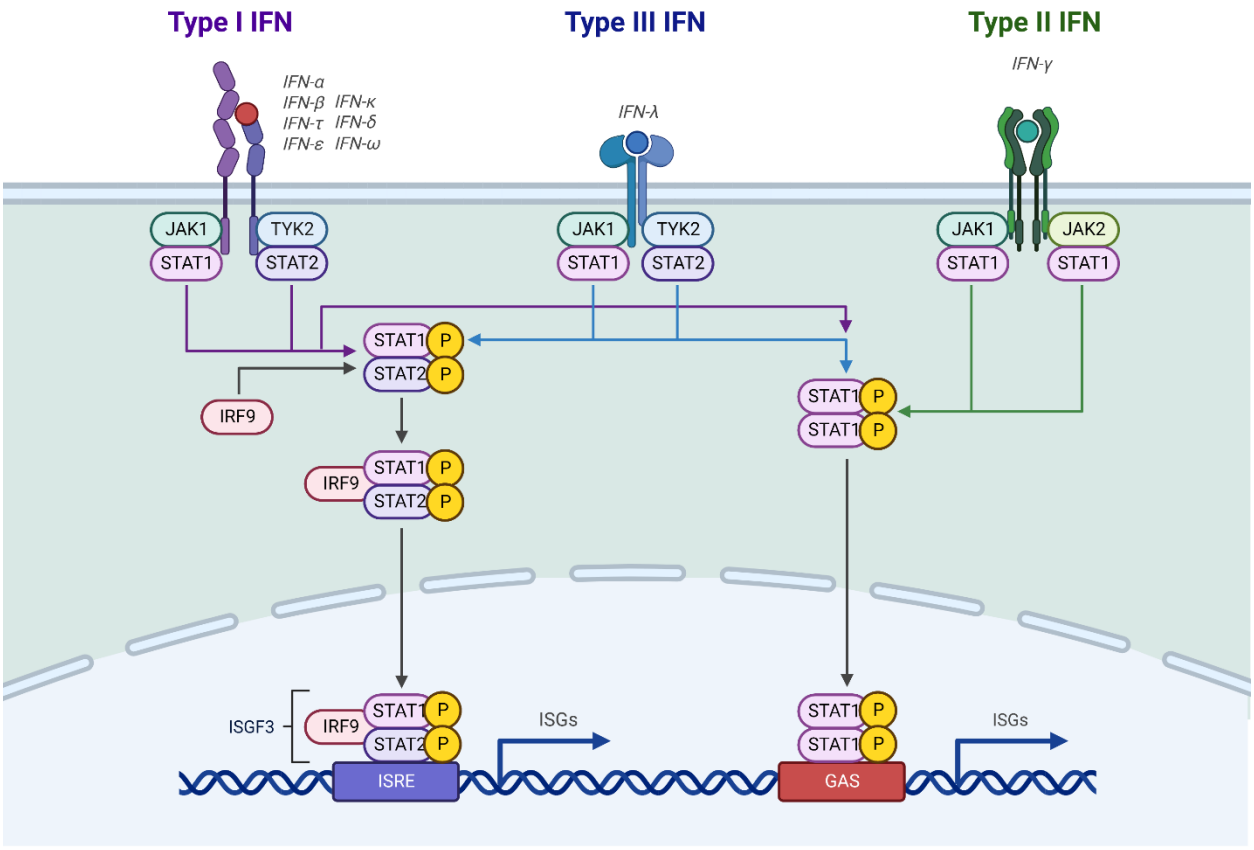

Figure 1.4 JAK-STAT signaling. Activation of the JAK-STAT signaling pathway is initiated by the binding of interferon in an autocrine or paracrine manner to the activate the production of interferon stimulated genes. Binding of interferons to their cognate cell-surface receptor and activating associated Janus kinase 1 (JAK1) and tyrosine kinase 2 (TYK2). JAK1/TYK2 phosphorylates the cytoplasmic domain of the IFN receptor, which serves as a recruitment site for signal transducers and activators of transcription (STATs). STAT1 heterodimerizes with STAT2 in association with IRF9 and bind ISRE to activate ISG production. Conversely, STAT1 homodimerizes, translocate to the nucleus and bind GAS to activate ISG production. The figure is adapted from "Interferon Pathway", by BioRender.com (2022). Retrieved from https://app.biorender.com/biorender-templates

1.3.4 miRNAs and the modulation of antiviral innate immune responses

miRNAs add an additional regulatory layer to the modulation of mammalian pathways which includes pathways involved in the innate immune responses to infection. miRNA profiles were found to be dysregulated in response to various infections, suggesting a regulatory importance of these molecules. Hence, there are several examples of miRNAs that are involved in the regulation of innate and adaptive immune responses. For example, miR-146a was found to be dysregulated in expression in Epstein–Barr Virus positive lymphoma cell line and was shown to dysregulate the production of IFN and ISGs by targeting STAT1 and IRF5 transcripts[120]. miR-27a enhance Type I IFN antiviral response by targeting negative regulator of type I IFN production, sialic acid-binding Ig-like lectin (Siglec)1, and E3 ubiquitin ligase tripartite motif-containing protein 27 (TRIM27). Thus, it has been revealed that miR-27a possesses antiviral capabilities by enhancing Type I IFN production by targeting negative regulators of that response[121,122]. miR-155 is another regulator of the IFN response. It has been shown that miR-155 enhances Type I IFN signaling by targeting the suppressor of cytokine signaling I to enhance antiviral response against viral infection[123]. Interestingly, it has been as well found that miR-155 transcriptionally activated upon RNA virus infection as a host mechanism to inhibit viral replication[123]. Overall, these studies demonstrate an emerging crucial role of miRNAs in the regulation of IFN and innate immune responses to viral infection either directly or indirectly through the manipulation of negative regulators. In Chapter 2, we identify a polycistronic miRNA cluster with novel roles in regulating the innate immune response to viral infection through targeting negative regulators of IRF3 and STAT1 phosphorylation and activation[60].

1.4 Cellular metabolism and viral infection

1.4.1 Host-virus interactions and dependence on lipid metabolism

Viruses are obligate parasites that heavily depend on the host's cellular machinery for the propagation and production of viral progeny. They lack the molecular machinery required for the replication and spread of their viral genetic material. Viruses have evolved to dysregulate the host's metabolic processes and signaling pathways to favor the efficient progression of the viral life cycle[124–127]. Viruses have been shown to redirect the cellular energy towards the production and assembly of progeny virions, thus hijacking the translational and metabolic machinery of the host. This digression in the equilibrium results in the dysregulation of the homeostatic balance in cellular signaling pathways that maintain a stable cellular microenvironment. In addition, the viruses induce the remodeling of the host structural architecture to promote the replication and the multiplication of the viral progeny[128]. For example, *Flaviviridae* family is found to greatly remodel the host's cytoplasm to promote the replication of the viral RNA. Precisely, the virus associates with endoplasmic reticulum-derived membranes and alters the cellular lipid composition to promote the formation of virus-induced cellular enclosures called replication organelles (RO) to facilitate its genomic replication[129]. These remodeling events and alterations in signal transduction pathways are tightly regulated by the action of receptors and transcription factors that control cellular and physiological function at the molecular level to fine-tune and shift the equilibrium towards a more favorable state for the virus. Additionally, viruses alter the metabolic profiles of host cells. Recent evidence suggests that genetically or pharmaceutically modulating modes of the metabolic landscape may regulate host-virus interactions. Several metabolic transcription factors were found to be dysregulated during RNA viral infection and regulating the abundance or activity of these factors in the host cell may be beneficial or detrimental for the virus.

Several studies have demonstrated the importance of various host lipid species in regulating different stages of viral life cycles from attachment to entry, replication, assembly, and release[130,131]. Several omics-based studies have demonstrated that viruses induce large-scale alterations in host cellular metabolism[132,133]. Moreover, it is increasingly becoming obvious that lipid signaling and synthesis pathways in host cells can be remodeled by viral proteins. For example, Nasheri *et al.* found that HCV NS4B was found to induce the expression of fatty acid synthase (FASN) and results in the enhancement of fatty acid pools in the infected cells[134]. Interestingly, however, NS4B does not directly inhibit FASN mRNA or protein expression and abundance. Instead, NS4B activates the sterol regulatory element-binding protein (SREBP-1c), a major transcription factor for FASN expression[135]. In addition to viral protein remodeling specific host pathways, viruses may induce the rearrangement of host membrane structures to support their replication. For example, (+)-strand RNA viruses such as HCV and Dengue virus (DENV), induce the formation of endoplasmic reticulum-derived membranous webs as well as multi-membrane vesicles consisting of various lipid species, namely cholesterol and sphingolipids[131,136–139]. These complexes are referred to as replication complexes (RC) and it is a mechanism of immune evasion which allows the viruses to replication without detection by the innate immune sensors[129]. FASN-derived fatty acids are generally recruited to these specialized structures during HCV infection[134]. Additionally, the DENV NS3 protein sequesters the FASN to the RC, and viral infection increases the cholesterol uptake and cholesterol synthesis[140–142]. In fact, the implication of cholesterol in the modulation of viral entry and replication has been well demonstrated in various viral models. For example, the infectivity of influenza virus and human herpesvirus 6 (HHV-6) is affected by the depletion of cholesterol from their envelopes[143,144]. Furthermore, it has been clear that various other viruses depend on cholesterol for entry such as human immunodeficiency virus (HIV), HSV,

and HCV[145,146]. More recently, cholesterol was deemed essential for the entry of severe acute respiratory syndrome coronavirus 2 (SARS-CoV-2) for entry into host cells[147], with evidence demonstrating that cholesterol depletion from host-cells results in a decrease in infectivity[148]. Although cholesterol in some viruses appears to be essential for promoting infection, there are some cases where cholesterol enrichment results in inhibition of infectivity[149]. This is the case for Rabies virus (RABV), where cholesterol depletion resulted in enhanced infectivity.

Given the importance of cholesterol in modulating various stages of the life cycles of many viruses, it is not surprising that cholesterol metabolism represents a key target when it comes to studying host-virus interactions. Viruses appear to modulate cholesterol and lipid homeostasis through the modulation of sterol regulatory element-binding proteins (SREBPs) and liver X receptor (LXR)-modulated signaling. Regulating the activity or abundance of proteins involved in these pathways may have a significant impact on the life cycles of viruses with demonstrated dependence on the host's lipid metabolism and related pathways. In fact, the impact of genetically or pharmacologically dysregulating lipid biosynthetic pathways has been found to attenuate or augment viral infection[62,126,132,150].

1.4.2 SREBPs and host-virus interplay

SREBPs are lipogenic transcription factors that modulate the expression of genes involved in lipid and cholesterol synthesis, metabolism, and uptake[151–153]. Sterol Regulatory Element Binding Transcription Factor 1-2 (SREBF1) and (SREBF2) encode three major transcription factors: SREBP1c, SREBP1a, and SREBP2. These three proteins are considered master regulators of cholesterol and lipid metabolism with SREBP-1a and SREBP-1c primarily regulating fatty acid metabolism and that SREBP-2 being the regulator of cholesterol metabolism[154,155]. Specifically, SREBP1a activates global lipid synthesis in propagating and rapidly growing cells, whereas

SREBP1c has a role in the regulation of fatty acids and triglycerides in lipogenic organs such as the liver[156]. Conversely, SREBP2 regulates sterol synthesis[157]. The activation of SREBPs is regulated by a processing event modulated by (SREBP) cleavage-activating protein (SACP), which forms a heterodimeric complex with SREBPs in the ER[153]. A decrease in sterol levels triggers the translocation of the SREBP-SCAP complex from the ER to the Golgi where it gets proteolytically activated to a functionally active transcription factor that regulates the transcription of lipogenic genes[158]. It has become clear that SREBPs become less stable in SCAP-deficient cells, where a significant decline in the levels of SREBP-target genes can be observed[159]. Additionally, it has been shown that SREBPs enhance their transcription through a cholesterol-dependent feed-forward mechanism[160]. In addition to regulation by SCAP, a simultaneous regulation by ER-retention membrane proteins can be observed. Insulin-induced gene 1 protein (INSIG1) and INSIG2 negatively regulates the translocation and activation of SREBP-SCAP complex by interacting with SCAP and retaining the complex in the ER in cholesterol-rich conditions[161]. SREBPs drive the expression of various metabolic genes essential for cholesterol biosynthesis and uptake. Some of these genes include 3-hydroxy-3-methyl-glutaryl-coenzyme A reductase (HMGCR) which is an enzyme essential for catalyzing the rate-limiting step of cholesterol biosynthesis[162] and low-density lipoprotein (LDL) receptor which is essential for binding cholesterol-rich lipoprotein particles mediating cholesterol uptake[152].

SREBP-regulated signaling and gene transcription is implicated in various viral infections. Enhancement of cholesterol biosynthesis through the dysregulation of this pathway has been evident during HCMV, HBV, and HCV infections; these viruses were demonstrated to enhance fatty acid and cholesterol biosynthesis by promoting the proteolytic cleavage event to increase the production of functionally active SREBPs[163–165]. Studies suggest a correlation between flavivirus

infection and an increase in cellular cholesterol levels. Specifically, it was shown that during DENV and WNV infection there is an enhancement in LDL cholesterol uptake and cholesterol biosynthesis[141,166]. More recently, it has been demonstrated that DENV hijacks the proteolytic activation of SREBPs[167]. In this specific study, it has been shown that inhibition of the proteolytic function that directs the maturation of SREBPs during DENV infection using site-directed inhibitor PF-429242, resulted in a dose-dependent decrease in DENV infection which can ultimately be reversed using the supplementation of cells with oleic acid to induce lipid droplet biogenesis[167]. Interestingly, a recent study highlighted the interplay between the SREBP pathway and host interferon pathway during flavivirus infection. Specifically, SCAP was shown to antagonize the ubiquitination of DENV non-structural protein 3 (NS3), which results in the inhibition cleavage of host antiviral protein stimulator of interferon genes (STING) by the DENV NS2B-NS3 serine-protease heterocomplex[168]. Overall, the above studies point toward a positive correlation between flavivirus infection and metabolic pathways regulated by SREBPs function.

Additionally, several studies have confirmed the importance of SREBP pathway activation during HCV infection. For example, it has been demonstrated that HCV enhances a lipid-rich microenvironment essential for HCV replication by altering the expression levels of SREBP1c and its targets; acetyl-coenzyme A carboxylase 1 (ACC1) and FASN[169]. HCV has as well been found to induce SREBP activation through oxidative stress-associated pathways. Specifically, NS5A was shown to modulate this response by inhibiting the phosphorylation of AMP-activated protein kinase (AMPK), a major mediator of lipid metabolism and oxidative stress, triggering the accumulation of hepatic LD in a mouse model[169]. Moreover, a study by Park and colleagues demonstrated the interplay between HCV and SREBP-modulated signaling by specifically examining the effects of HCV non-structural protein expression on the pathway[135]. This study

highlighted the positive regulatory effects of HCV non-structural 4B (NS4B) protein on the transcriptional levels of SREBPs and their target proteins[135]. The above studies strongly suggest that HCV may hijack components of lipid metabolism to enhance HCV-associated pathogenesis.

More recently the interplay between SREBP-modulated signaling and coronaviruses has become more evident. A recent study suggests the SREBP proteolytic processes and SREBP-regulated lipid biosynthesis are essential for Middle East respiratory syndrome coronavirus (MERS-CoV) viral protein palmitoylation and double-membrane vesicles formation and virus replication, suggesting that SREBP represents a potent antiviral target[170]. SARS-CoV-2 exocytosis and release were found to be dependent on the biosynthesis of cholesterol mediated by SREBP-2 [171,172]. Some evidence suggests that cholesterol depletion from target cells suppresses viral infection, suggesting that SREBP-2 could act as a therapeutic target when it comes to SARS-CoV-2 infection[171]. Overall, these examples point toward the implication of SREBP-modulated signaling in regulating the life cycles of various viruses. This suggests that targeting lipid and cholesterol biosynthesis may inhibit or dysregulate different stages of viral life cycles.

1.4.3 LXR, cholesterol homeostasis and host-virus interactions

LXRs are nuclear hormone receptors that act as “sterol sensors" and they respond to the physiological concentrations of sterols in the cells[173]. Their roles in the modulation of host-pathogen interactions have been proven integral for both the host and invading pathogens[174]**.** Historically, these receptors were identified as orphan receptors with unclear classification. Later, these receptors were classified as nuclear receptors that respond to cholesterol metabolites, oxysterols[175]. Some of the natural ligands for LXRs include derivatives of oxysterols such as 25-hydroxycholesterol (25-HC), 27-hydroxycholesterol (27-HC), 22(R)-hydroxycholesterol, 24(S),

25-epoxycholesterol [24(S),25-EC], and 5α,6α-epoxycholesterol [5,6-EC] [175–177]. LXRα (NR1H3) and LRXβ (NR1H2) are two distinct genes that encode two isoforms of the LXR nuclear receptors [175]. While LRXβ is ubiquitously expressed, LXRα expression is restricted to metabolic tissues including liver, kidney, adipose tissue, and macrophages[178].

Cholesterol regulation has been found to play an instrumental role in modulating the life cycles of various viruses, especially viruses that require enrichment of the lipid and cholesterol microenvironment for their propagation[179–183]. LXRs play an opposing role to SREBPs. Their primary function is to sense oxysterols in the environment and respond by increasing the expression of various genes that regulates cholesterol transport/efflux and the conversion of cholesterol to bile acid and promote intestinal cholesterol absorption [184]. Some of the genes regulated by LXRs encode phospholipid transport proteins, apolipoproteins and ATP binding cassette (ABC) transporters, ABCG5 and ABCG8[185] as well as Cholesterol 7α-hydroxylase (CYP7A1), one of the first identified targets of LXRs and an enzyme known to be involved in catalyzing the rate-limiting step of the bile acid biosynthesis pathway[186].

LXRs are as well involved in the regulation of triglyceride and fatty acid synthesis. These functions are mediated through LXR-controlled genes such as fatty acid synthase (FASN), ACC, and Stearoyl-CoA desaturase-1 (SCD1) [187–190]. The utilization of LXR agonists has been shown to enhance high-density lipoprotein (HDL)-mediated tissue cholesterol efflux, thus resulting in free-circulating HDL molecules[191]. Moreover, enhanced incorporation of fatty acids into phospholipids and triglycerides is observed in LXR knockout C57BL/6 mice[192]. Thus, given LXR's role in regulating fatty acid, triglyceride, and cholesterol biosynthesis pathways, it is not surprising that it

has been identified as an attractive therapeutic target for various metabolic diseases, such as liver steatosis, and cardiovascular diseases such as atherosclerosis[193,194].

As previously mentioned, for some viruses such as viruses in the *Flaviviridae* family, fatty acid and cholesterol biosynthetic pathways have been proven vital for viral propagation and dissemination. These processes are generally hijacked by the viruses to facilitate viral replication and the production of viral progeny. Given that LXR nuclear receptors are one of the major regulators of such processes, it is not surprising that they play instrumental roles in modulating host-virus interactions. Recently, there is an increasing interest in the development of drugs and small molecules that regulate the activity of LXRs to suppress the life cycle of viruses that depend on fatty acid and cholesterol metabolic processes and thus creating an LXR-dependent intrinsic antiviral state.

Over the past years, the role of LXR in regulating the viral life cycle during infection has become more apparent. In recent studies, LXR has been reported to control HCV infection and particularly the entry of the virus through modulation of the levels of LDL receptor (LDLR)[182,195]. In particular, idol, an LXR inducible E3 ubiquitin ligase has been found to post-transcriptionally regulate the expression levels of LDLR through the promotion of the ubiquitination of its cytoplasmic domain [195]. Zeng *et al*. have demonstrated a decrease in the levels of infection of HCV JFH-1 strain in HCV-susceptible Huh7.5.1 hepatoma cell line with the overexpression of LXR-inducible protein, idol [182]. They were also able to demonstrate the inhibitory effects of LXR synthetic ligands (T0-901317 or GW3965) on HCV entry and intracellular levels. Conversely, Nakajima *et al.* have highlighted the inhibitory effects that a fungus-derived antagonist of LXRs, neoechinulin B (NeoB), exhibits on the HCV life cycle. In particular, the group demonstrated that the treatment of

HCV-permissive cells with the compound results in the inhibition of the formation of specialized HCV replication sites and membrane compartments essential for the viral replication cycle[183]. The formation of these sites is controlled by mechanisms modulated through LXR-mediated transcription[183]. Overall, this work opened potential avenues to explore the impediment of the HCV life cycle through LXR-dependent mechanisms. A more recent study by Singaravelu *et al.* highlighted the role of 25-hydroxycholesterol, an LXRα activating endogenous oxysterol, in inducing the transcription of miRNAs that display potent antiviral activity against HCV infection in Huh7.5 hepatoma cell line[62,180]. In this study, the group identified, through employing a small molecule–mediated annotation of miRNA targets (SMART) screen, 25-HC- induced miR-185 and miR-130b which displayed antiviral activity against HCV[62]. Overall, these studies highlight the role of LXR-mediated transcription and cholesterol depletion in modulating viral pathogenesis and hepatic metabolism during infection.

In addition to the well-documented connection between HCV and LXR signaling, there has been evidence of the effects of cholesterol depletion on other viruses including HIV. Sterols and oxysterols have been shown to play crucial roles in the HIV life cycle and infectivity[196]. Specifically, HIV-1 requires cholesterol for the assembly and budding of the virions from its target cells[196–198]. HIV-1 budding occurs at cholesterol-enriched "lipids rafts", and consequently, it has been shown that there is a higher ratio of cholesterol to phospholipids within the viral envelope[199]. It has been reported that cholesterol depletion markedly reduces HIV-1 particle production and release and decreases infectivity of the produced virions. Due to these connections, it is evident that the LXR-regulated and sterol-modulated signaling can play crucial roles in the modulation of viral progression and production[200,201]. Both the cholesterol-related and trans-repression activities of LXR contribute to the reported suppression of HIV-1 progression and infectivity. Depletion of

cholesterol from lipid rafts leads to a decrease in infectivity and virus production[196,198]. Overall, the above studies highlight the intricate interplay between lipid-associated pathways and viruses, suggesting broad and high degree of dependence on metabolic processes and pathways to regulate their infectious cycles. Given this, metabolic pathways can act as promising targets when it comes to antiviral therapeutics and strategies.

1.4.4 miRNAs and the modulation of metabolic pathways

The interplay between miRNAs and host metabolic processes has been well demonstrated with observed implications in lipid metabolism and antiviral responses. Several miRNAs have been identified to be important regulators of lipid metabolism, this includes miR-122, miR-29, and miR-33[202]. For example, the miR-33 family of miRNAs ae encoded within the introns of the genes encoding SREBP1a, SREBP1c, and SREBP2. Interestingly, the relevance of miR-33 in sterol metabolism was initially identified in mouse hepatocytes and macrophages, showing that miR-33 regulates the expression of ABCA1 and ABCG1 resulting in a consequential decrease in plasma HDL-C levels[202]. miR-29 and miR-33 were as well shown to target the initial steps of the SREBP signaling pathway by negatively regulating the expression of SCAP and SREBP1c, consequently resulting in the downregulation of fatty acid and LD biogenesis[203,204]. Following the discovery of miR-33, several other miRNAs were identified to have roles in cholesterol metabolism and homeostasis with implications in atherosclerosis and cardiovascular disease. Some of these miRNAs include miR-144, miR-148a, and miR-128[205–207]. Interestingly, some of these miRNAs with roles in metabolism are found to modulate viral infections in different models. For example, miR-148a was shown to suppress MAPK signaling which ultimately resulted in the antagonization of HCV infection and hepatocellular carcinoma development[208]. miR-33 as well was shown to promote RNA viral infection through the impairment of RIG-I and MAVS-dependent signaling[209].

Several other metabolic miRNAs were recently identified to play roles in modulating HCV infection through the regulation of the SREBP pathway. For example, exosome-associated miR-24 and miR-223 were found to enhance SREBP processing and cholesterol efflux. These miRNAs were found to be highly expressed in HCV-sustained virologic responders as compared to non-responders[210]. Regulation of lipid metabolism by miRNAs may have a significant intercellular impact. Therefore, miRNAs represent a fine-tuning mechanism of lipid metabolism with great potential for therapeutic antiviral manipulation.

1.5 Rationale and Objective

miRNAs, as previously discussed, are significantly involved in the modulation of various cellular processes and have recently been shown to be involved significantly in the regulation of host-pathogen interaction[36–40]. This is achieved by either directly interacting with the pathogen's genome or indirectly interacting with the host's mRNAs implicated in viral pathogenesis. As discussed above, miRNAs have been shown to extensively modulate innate immune responses to either enhance or suppress antiviral responses. Additionally, evidence has emerged to support the role of miRNAs in the modulation of the lipid microenvironment to regulate viral life cycles[62]. This suggests that miRNAs add a critical regulatory layer that acts to fine-tune molecular and cellular responses to viral infection. For example, miRNAs may target host genes to suppress viral-induced cellular rearrangements that are potentially beneficial to the viral life cycle[62,211,212]. Conversely, viruses may induce the expression of host miRNAs that target antiviral genes and thus enhancing viral-immune evasion and viral accumulation[213]. Thus, miRNAs are considered a determinant of pathogenesis in which they can reprogram the host cellular profiles to regulate viral pathogenesis positively or negatively.

In the presented work, chapters (2-4), we identify miRNAs with novel functional roles in the regulation of RNA viral infections. **In chapter 2**, we identify a highly conserved miRNA cluster, the miR-183 cluster, with antiviral roles specifically against RNA viruses. We demonstrated that this cluster mediates its antiviral potential by enhancing innate antiviral immune responses to suppress viral propagation and infectivity. **In chapter 3**, we identify a miRNA with antiviral properties against DENV and a novel functional role in hepatic lipid metabolism. Finally, **in chapter 4**, we identify immunometabolic miRNA (miR-185), to possess novel antiviral roles against SARS-CoV2 and its variants of concern through the modulation of the cellular lipid microenvironment to suppress entry and infectivity. Overall, the work presented in this thesis highlights miRNAs' potential as therapeutic tools for the manipulation of viral pathogenesis and infection, as well as their role in the identification of targetable host factors or pathways of pro-viral potential.

1.6 References

1. Palazzo, A. F. & Lee, E. S. Non-coding RNA: What is functional and what is junk? *Front. Genet.* **5**, 1–11 (2015).
2. Romano, G., Veneziano, D., Acunzo, M. & Croce, C. M. Small non-coding RNA and cancer. *Carcinogenesis* **38**, 485–491 (2017).
3. Dunham, I. *et al.* An integrated encyclopedia of DNA elements in the human genome. *Nature* **489**, 57–74 (2012).
4. Griffiths-Jones, S., Grocock, R. J., van Dongen, S., Bateman, A. & Enright, A. J. miRBase: microRNA sequences, targets and gene nomenclature. *Nucleic Acids Res.* **34**, 140–144 (2006).
5. Amaral, P. P., Clark, M. B., Gascoigne, D. K., Dinger, M. E. & Mattick, J. S. LncRNAdb: A reference database for long noncoding RNAs. *Nucleic Acids Res.* **39**, 146–151 (2011).
6. Mutz, K. O., Heilkenbrinker, A., Lönne, M., Walter, J. G. & Stahl, F. Transcriptome analysis using next-generation sequencing. *Curr. Opin. Biotechnol.* **24**, 22–30 (2013).
7. Mattick, J. S. Non-coding RNAs: The architects of eukaryotic complexity. *EMBO Rep.* **2**, 986–991 (2001).
8. Matera, A. G., Terns, R. M. & Terns, M. P. Non-coding RNAs: Lessons from the small nuclear and small nucleolar RNAs. *Nat. Rev. Mol. Cell Biol.* **8**, 209–220 (2007).
9. Stefani, G. & Slack, F. J. Small non-coding RNAs in animal development. *Nat. Rev. Mol. Cell Biol.* **9**, 219–230 (2008).
10. Esteller, M. Non-coding RNAs in human disease. *Nat. Rev. Genet.* **12**, 861–874 (2011).
11. Sajjad, N. *et al.* Functional Roles of Non-coding RNAs in the Interaction Between Host and Influenza A Virus. *Front. Microbiol.* **12**, (2021).
12. Mohanty, S. & Chaudhry, R. Emerging role of anaerobes in health and disease. *Indian J. Med. Microbiol.* **39**, 402–403 (2021).
13. Tribolet, L. *et al.* MicroRNA Biomarkers for Infectious Diseases: From Basic Research to Biosensing. *Front. Microbiol.* **11**, 1–15 (2020).
14. O'Brien, J., Hayder, H., Zayed, Y. & Peng, C. Overview of microRNA biogenesis, mechanisms of actions, and circulation. *Front. Endocrinol. (Lausanne).* **9**, 1–12 (2018).
15. Hashimoto, Y., Akiyama, Y. & Yuasa, Y. Multiple-to-Multiple Relationships between MicroRNAs and Target Genes in Gastric Cancer. *PLoS One* **8**, (2013).
16. Ebert, M. S. & Sharp, P. A. Roles for MicroRNAs in conferring robustness to biological processes. *Cell* **149**, 515–524 (2012).
17. Tanzer, A. & Stadler, P. F. Molecular evolution of a microRNA cluster. *J. Mol. Biol.* **339**, 327–335 (2004).
18. De Rie, D. *et al.* An integrated expression atlas of miRNAs and their promoters in human and mouse. *Nat. Biotechnol.* **35**, 872–878 (2017).
19. Denli, A. M., Tops, B. B. J., Plasterk, R. H. A., Ketting, R. F. & Hannon, G. J. Processing of primary microRNAs by the Microprocessor complex. *Nature* **432**, 231–235 (2004).
20. Zhang, H., Kolb, F. A., Jaskiewicz, L., Westhof, E. & Filipowicz, W. Single processing center models for human Dicer and bacterial RNase III. *Cell* **118**, 57–68 (2004).

21. Müller, M., Fazi, F. & Ciaudo, C. Argonaute Proteins: From Structure to Function in Development and Pathological Cell Fate Determination. *Front. Cell Dev. Biol.* **7**, 1–10 (2020).

22. Meijer, H. A., Smith, E. M. & Bushell, M. Regulation of miRNA strand selection: Follow the leader? *Biochem. Soc. Trans.* **42**, 1135–1140 (2014).

23. Guo, H., Ingolia, N. T., Weissman, J. S. & Bartel, D. P. Mammalian microRNAs predominantly act to decrease target mRNA levels. *Nature* **466**, 835–840 (2010).

24. Filipowicz, W., Bhattacharyya, S. N. & Sonenberg, N. Mechanisms of post-transcriptional regulation by microRNAs: Are the answers in sight? *Nat. Rev. Genet.* **9**, 102–114 (2008).

25. Xu, W., Lucas, A. S., Wang, Z. & Liu, Y. Identifying microRNA targets in different gene regions. *BMC Bioinformatics* **15**, 6–8 (2014).

26. Ellwanger, D. C., Büttner, F. A., Mewes, H. W. & Stümpflen, V. The sufficient minimal set of miRNA seed types. *Bioinformatics* **27**, 1346–1350 (2011).

27. Agarwal, V., Bell, G. W., Nam, J. W. & Bartel, D. P. Predicting effective microRNA target sites in mammalian mRNAs. *Elife* **4**, 1–38 (2015).

28. Lee, D. & Shin, C. MicroRNA-target interactions: New insights from genome-wide approaches. *Ann. N. Y. Acad. Sci.* **1271**, 118–128 (2012).

29. Chi, S. W., Hannon, G. J. & Darnell, R. B. An alternative mode of microRNA target recognition. *Nat. Struct. Mol. Biol.* **19**, 321–327 (2012).

30. Agarwal, V., Bell, G. W., Nam, J.-W. & Bartel, D. P. Predicting effective microRNA target sites in mammalian mRNAs. *Elife* **4**, 1–38 (2015).

31. Felekkis, K., Touvana, E., Stefanou, C. & Deltas, C. MicroRNAs: A newly described class of encoded molecules that play a role in health and disease. *Hippokratia* **14**, 236–240 (2010).

32. Berezikov, E., Chung, W. J., Willis, J., Cuppen, E. & Lai, E. C. Mammalian Mirtron Genes. *Mol. Cell* **28**, 328–336 (2007).

33. Westholm, J. O. & Lai, E. C. Mirtrons: MicroRNA biogenesis via splicing. *Biochimie* **93**, 1897–1904 (2011).

34. Ruby, J. G., Jan, C. H. & Bartel, D. P. Intronic microRNA precursors that bypass Drosha processing. *Nature* **448**, 83–86 (2007).

35. Cifuentes, D. *et al.* A novel miRNA processing pathway independent of dicer requires argonaute2 catalytic activity. *Science* . **328**, 1694–1698 (2010).

36. Esau, C. *et al.* miR-122 regulation of lipid metabolism revealed by in vivo antisense targeting. *Cell Metab.* **3**, 87–98 (2006).

37. Hsu, S. hao & Ghoshal, K. MicroRNAs in Liver Health and Disease. *Curr. Pathobiol. Rep.* **1**, 53–62 (2013).

38. Jopling, C. L., Yi, M., Lancaster, A. M., Lemon, S. M. & Sarnow, P. Modulation of hepatitis C virus RNA abundance by a liver-specific MicroRNA. *Science* **1**, 1577–1581 (2005).

39. de Melo Maia, B. *et al.* Design of a miRNA sponge for the miR-17 miRNA family as a therapeutic strategy against vulvar carcinoma. *Mol. Cell. Probes* **29**, 420–426 (2015).

40. O'Connell, R. M., Taganov, K. D., Boldin, M. P., Cheng, G. & Baltimore, D. MicroRNA-155 is induced during the macrophage inflammatory response. *Proc. Natl. Acad. Sci. U. S. A.* **104**, 1604–1609 (2007).

41. Peterson, S. M. *et al.* Common features of microRNA target prediction tools. *Front. Genet.* **5**, 1–10 (2014).

42. Lewis, B. P., Burge, C. B. & Bartel, D. P. Conserved seed pairing, often flanked by adenosines, indicates that thousands of human genes are microRNA targets. *Cell* **120**, 15–20 (2005).

43. John, B. *et al.* Human microRNA targets. *PLoS Biol.* **2**, (2004).

44. Betel, D., Koppal, A., Agius, P., Sander, C. & Leslie, C. Comprehensive modeling of microRNA targets predicts functional non-conserved and non-canonical sites. *Genome Biol.* **11**, R90 (2010).

45. Szostak, E. & Gebauer, F. Translational control by 3'-UTR-binding proteins. *Brief. Funct. Genomics* **12**, 58–65 (2013).

46. Farh, K. K. H. *et al.* Biochemistry: The widespread impact of mammalian microRNAs on mRNA repression and evolution. *Science* **310**, 1817–1821 (2005).

47. Krützfeldt, J. *et al.* Silencing of microRNAs in vivo with 'antagomirs'. *Nature* **438**, 685–689 (2005).

48. Bernier, A. & Sagan, S. M. The diverse roles of microRNAs at the host–virus interface. *Viruses* **10**, 1–26 (2018).

49. Lanford, R. E. *et al.* Therapeutic silencing of microRNA-122 in primates with chronic hepatitis C virus infection. *Science* **327**, 198–201 (2010).

50. Bartenschlager, R., Penin, F., Lohmann, V. & André, P. Assembly of infectious hepatitis C virus particles. *Trends Microbiol.* **19**, 95–103 (2011).

51. Jones, D. M. & McLauchlan, J. Hepatitis C virus: Assembly and release of virus particles. *J. Biol. Chem.* **285**, 22733–22739 (2010).

52. Randall, G. *et al.* Cellular cofactors affecting hepatitis C virus infection and replication. *Proc. Natl. Acad. Sci. U. S. A.* **104**, 12884–12889 (2007).

53. Van Der Ree, M. H. *et al.* Miravirsen dosing in chronic hepatitis C patients results in decreased microRNA-122 levels without affecting other microRNAs in plasma. *Aliment. Pharmacol. Ther.* **43**, 102–113 (2016).

54. van der Ree, M. H. *et al.* Safety, tolerability, and antiviral effect of RG-101 in patients with chronic hepatitis C: a phase 1B, double-blind, randomised controlled trial. *Lancet* **389**, 709–717 (2017).

55. Li, Q. *et al.* Cellular microRNA networks regulate host dependency of hepatitis C virus infection. *Nat. Commun.* **8**, (2017).

56. Smith, J. L., Jeng, S., McWeeney, S. K. & Hirsch, A. J. A MicroRNA Screen Identifies the Wnt Signaling Pathway as a Regulator of the Interferon Response during Flavivirus Infection. *J. Virol.* **91**, (2017).

57. Piedade, D. & Azevedo-Pereira, J. M. The role of microRNAs in the pathogenesis of herpesvirus infection. *Viruses* **8**, (2016).

58. Cui, C. *et al.* Prediction and Identification of Herpes Simplex Virus 1-Encoded MicroRNAs. *J. Virol.* **80**, 5499–5508 (2006).

59. Jurak, I. *et al.* Numerous Conserved and Divergent MicroRNAs Expressed by Herpes Simplex Viruses 1 and 2. *J. Virol.* **84**, 4659–4672 (2010).

60. Singaravelu, R. *et al.* A conserved miRNA-183 cluster regulates the innate antiviral response. *J.*

Biol. Chem. **294**, 19785–19794 (2019).

61. El Sobky, S. A. *et al.* Contradicting roles of miR-182 in both NK cells and their host target hepatocytes in HCV. *Immunol. Lett.* **169**, 52–60 (2016).

62. Singaravelu, R. *et al.* MicroRNAs regulate the immunometabolic response to viral infection in the liver. *Nat. Chem. Biol.* **11**, 988–993 (2015).

63. Zhang, T., Yang, Z., Kusumanchi, P., Han, S. & Liangpunsakul, S. Critical Role of microRNA-21 in the Pathogenesis of Liver Diseases. *Front. Med.* **7**, 1–7 (2020).

64. Chen, Y., Dong, X., Yu, D. & Wang, X. Serum miR-96 is a promising biomarker for hepatocellular carcinoma in patients with chronic hepatitis B virus infection. *Int. J. Clin. Exp. Med.* **8**, 18462–18468 (2015).

65. Shaw, T. A. *et al.* MicroRNA-124 Regulates Fatty Acid and Triglyceride Homeostasis. *iScience* **10**, 149–157 (2018).

66. Singaravelu, R. *et al.* MicroRNA-7 mediates cross-talk between metabolic signaling pathways in the liver. *Sci. Rep.* **8**, 1–10 (2018).

67. Brubaker, S. W., Bonham, K. S., Zanoni, I. & Kagan, J. C. *Innate Immune Pattern Recognition: A Cell Biological Perspective*. *Annual Review of Immunology* vol. 33 (2015).

68. Kobayashi, K. S. & Flavell, R. A. Shielding the double-edged sword: negative regulation of the innate immune system. *J. Leukoc. Biol.* **75**, 428–433 (2003).

69. Vallabhapurapu, S. & Karin, M. Regulation and Function of NF-κB Transcription Factors in the Immune System. *Annu. Rev. Immunol.* **27**, 693–733 (2009).

70. Honda, K., Takaoka, A. & Taniguchi, T. Type I Inteferon Gene Induction by the Interferon Regulatory Factor Family of Transcription Factors. *Immunity* **25**, 349–360 (2006).

71. Yoneyama, M. *et al.* The RNA helicase RIG-I has an essential function in double-stranded RNA-induced innate antiviral responses. *Nat. Immunol.* **5**, 730–737 (2004).

72. Medzhitov, R. & Janeway, C. A. Decoding the patterns of self and nonself by the innate immune system. *Science (80-.).* **296**, 298–300 (2002).

73. Honda, K., Yanai, H., Takaoka, A. & Taniguchi, T. Regulation of the type I IFN induction: A current view. *Int. Immunol.* **17**, 1367–1378 (2005).

74. Pestka, S., Krause, C. D. & Walter, M. R. Interferons, interferon-like cytokines, and their receptors. *Immunol. Rev.* **202**, 8-32 (2004).

75. Schoenborn, J. R. & Wilson, C. B. Regulation of Interferon-γ During Innate and Adaptive Immune Responses. *Adv. Immunol.* **96**, 41–101 (2007).

76. Pestka, S. *et al.* The interferon gamma (IFN-γ) receptor: A paradigm for the multichain cytokine receptor. *Cytokine Growth Factor Rev.* **8**, 189–206 (1997).

77. Schijns, V. E., Wierda, C. M., van Hoeij, M. & Horzinek, M. C. Exacerbated viral hepatitis in IFN-gamma receptor-deficient mice is not suppressed by IL-12. *J. Immunol.* **157**, 815–21 (1996).

78. Emmanuelle Jouanguy, Rainer Doffinger, Stephanie Dupuis, Annaick Pallier Altare, F. & Casanova, J. IL-12 and IFN-yin host defense against mycobacteria and salmonella in mice and men Emmanuelle Jouanguy , Rainer Ddffinger , Stephanie Dupuis , Anndick. *Curr. Opin. Immunol.* **11**, 346–351 (1999).

79. Donnelly, R. P. & Kotenko, S. V. Interferon-lambda: A new addition to an old family. *J. Interf.*

Cytokine Res. **30**, 555–564 (2010).

80. Kotenko, S. V. *et al.* IFN-λs mediate antiviral protection through a distinct class II cytokine receptor complex. *Nat. Immunol.* **4**, 69–77 (2003).

81. Platanias, L. C. Mechanisms of type-I- and type-II-interferon-mediated signalling. *Nat. Rev. Immunol.* **5**, 375–386 (2005).

82. Kotenko, S. V. & Durbin, J. E. Contribution of type III interferons to antiviral immunity: Location, location, location. *J. Biol. Chem.* **292**, 7295–7303 (2017).

83. Yan, N. & Chen, Z. J. Intrinsic antiviral immunity. *Nat. Immunol.* **13**, 214–222 (2012).

84. Al-khatib, K., Williams, B. R. G., Silverman, R. H., Halford, W. & Carr, D. J. J. Distinctive Roles for 2′,5′-Oligoadenylate Synthetases and Double-Stranded RNA-Dependent Protein Kinase R in the In Vivo Antiviral Effect of an Adenoviral Vector Expressing Murine IFN-β. *J. Immunol.* **172**, 5638–5647 (2004).

85. Trépo, C., Chan, H. L. Y. & Lok, A. Hepatitis B virus infection. *Lancet* **384**, 2053–2063 (2014).

86. Ward, R. P. & Kugelmas, M. Using pegylated interferon and ribavirin to treat patients with chronic hepatitis C. *Am. Fam. Physician* **72**, 655–662 (2005).

87. Sallard, E., Lescure, F. X., Yazdanpanah, Y., Mentre, F. & Peiffer-Smadja, N. Type 1 interferons as a potential treatment against COVID-19. *Antiviral Res.* **178**, (2020).

88. Wang, B. *et al.* Subcutaneous injection of IFN alpha-2b for COVID-19: An observational study. *BMC Infect. Dis.* **20**, 1–6 (2020).

89. Daffis, S. *et al.* Interferon Regulatory Factor IRF-7 Induces the Antiviral Alpha Interferon Response and Protects against Lethal West Nile Virus Infection. *J. Virol.* **82**, 8465–8475 (2008).

90. Amarante-Mendes, G. P. *et al.* Pattern recognition receptors and the host cell death molecular machinery. *Front. Immunol.* **9**, 1–19 (2018).

91. Akira, S., Uematsu, S. & Takeuchi, O. Pathogen recognition and innate immunity. *Cell* **124**, 783–801 (2006).

92. Cai, X., Chiu, Y. H. & Chen, Z. J. The cGAS-cGAMP-STING pathway of cytosolic DNA sensing and signaling. *Mol. Cell* **54**, 289–296 (2014).

93. Kawai, T. & Akira, S. The role of pattern-recognition receptors in innate immunity: Update on toll-like receptors. *Nat. Immunol.* **11**, 373–384 (2010).

94. Celhar, T., Magalhães, R. & Fairhurst, A. M. TLR7 and TLR9 in SLE: When sensing self goes wrong. *Immunol. Res.* **53**, 58–77 (2012).

95. Lin, S. C., Lo, Y. C. & Wu, H. Helical assembly in the MyD88-IRAK4-IRAK2 complex in TLR/IL-1R signalling. *Nature* **465**, 885–890 (2010).

96. Yamamoto, M., Sato, S. & Hemmi, H. Role of Adaptor TRIF in the the MyD88-independent toll-like receptor signaling pathway. *Science.* **301**, 640–643 (2003).

97. Pfeffer, L. M. The role of nuclear factor κb in the interferon response. *J. Interf. Cytokine Res.* **31**, 553–559 (2011).

98. tenOever, B. R. *et al.* Multiple Functions of the IKK-Related Kinase IKKε in Interferon-Mediated Antiviral Immunity. *Science (80-.).* **315**, 1274–1278 (2007).

99. Paun, A. & Pitha, P. M. The IRF family, revisited. *Biochimie* **89**, 744–753 (2007).

100. Goubau, D., Deddouche, S. & Reis, C. Review Cytosolic Sensing of Viruses. *Immunity* **38**, 855–869 (2013).

101. Kowalinski, E. *et al.* Structural basis for the activation of innate immune pattern-recognition receptor RIG-I by viral RNA. *Cell* **147**, 423–435 (2011).

102. Jin, J. *et al.* Noncanonical NF-κB pathway controls the production of type I interferons in antiviral innate immunity. *Immunity* **40**, 342–354 (2014).

103. Kato, H. *et al.* Cell type-specific involvement of RIG-I in antiviral response. *Immunity* **23**, 19–28 (2005).

104. Yamada, T. *et al.* RIG-I triggers a signaling-abortive anti-SARS-CoV-2 defense in human lung cells. *Nat. Immunol.* **22**, 820–828 (2021).

105. Sprokholt, J. K. *et al.* RIG-I–like Receptor Triggering by Dengue Virus Drives Dendritic Cell Immune Activation and T H 1 Differentiation . *J. Immunol.* **198**, 4764–4771 (2017).

106. Jiang, Y. *et al.* Genome-wide analysis of protein–protein interactions and involvement of viral proteins in SARS-CoV-2 replication. *Cell Biosci.* **11**, 1–16 (2021).

107. Ning, S., Pagano, J. S. & Barber, G. N. IRF7: Activation, regulation, modification and function. *Genes Immun.* **12**, 399–414 (2011).

108. Mori, M. *et al.* Identification of Ser-386 of Interferon Regulatory Factor 3 as Critical Target for Inducible Phosphorylation That Determines Activation. *J. Biol. Chem.* **279**, 9698–9702 (2004).

109. Chen, W. *et al.* Contribution of Ser386 and Ser396 to Activation of Interferon Regulatory Factor 3. *J. Mol. Biol.* **379**, 251–260 (2008).

110. Lin, R., Mamane, Y. & Hiscott, J. Multiple regulatory domains control IRF-7 activity in response to virus infection. *J. Biol. Chem.* **275**, 34320–34327 (2000).

111. Sato, M. *et al.* Distinct and essential roles of transcription factors IRF-3 and IRF-7 in response to viruses for IFN-α/β gene induction. *Immunity* **13**, 539–548 (2000).

112. Au, W. C., Moore, P. A., LaFleur, D. W., Tombal, B. & Pitha, P. M. Characterization of the interferon regulatory factor-7 and its potential role in the transcription activation of interferon A genes. *J. Biol. Chem.* **273**, 29210–29217 (1998).

113. Dalrymple, N. A., Cimica, V. & Mackow, E. R. Dengue virus NS proteins inhibit RIG-I/MAVS signaling by blocking TBK1/IRF3 phosphorylation: Dengue virus serotype 1 NS4A is a unique interferon-regulating virulence determinant. *MBio* **6**, 1–12 (2015).

114. Zhang, Q. *et al.* Severe Acute Respiratory Syndrome Coronavirus 2 (SARS-CoV-2) Membrane (M) and Spike (S) Proteins Antagonize Host Type I Interferon Response. *Front. Cell. Infect. Microbiol.* **11**, 1–13 (2021).

115. Darnell, J. E., Kerr, I. M. & Stark, G. R. Jak-STAT pathways and transcriptional activation in response to IFNs and other extracellular signaling proteins. *Science* **264**, 1415–1421 (1994).

116. Decker, T., Kovarik, P. & Meinke, A. GAS elements: A few nucleotides with a major impact on cytokine-induced gene expression. *J. Interf. Cytokine Res.* **17**, 121–134 (1997).

117. Sadzak, I. *et al.* Recruitment of Stat1 to chromatin is required for interferon-induced serine phosphorylation of Stat1 transactivation domain. *Proc. Natl. Acad. Sci. U. S. A.* **105**, 8944–8949 (2008).

118. Sohn, S.-Y. & Hearing, P. Adenovirus Sequesters Phosphorylated STAT1 at Viral Replication Centers and Inhibits STAT Dephosphorylation. *J. Virol.* **85**, 7555–7562 (2011).

119. Kumthip, K. *et al.* Hepatitis C Virus NS5A Disrupts STAT1 Phosphorylation and Suppresses Type I Interferon Signaling. *J. Virol.* **86**, 8581–8591 (2012).

120. Tang, Y. *et al.* MicroRNA-146a contributes to abnormal activation of the type I interferon pathway in human lupus by targeting the key signaling proteins. *Arthritis Rheum.* **60**, 1065–1075 (2009).

121. Zheng, Q. *et al.* Siglec1 suppresses antiviral innate immune response by inducing TBK1 degradation via the ubiquitin ligase TRIM27. *Cell Res.* **25**, 1121–1136 (2015).

122. Zheng, Q., Hou, J., Zhou, Y., Yang, Y. & Cao, X. Type I IFN–Inducible Downregulation of MicroRNA-27a Feedback Inhibits Antiviral Innate Response by Upregulating Siglec1/TRIM27. *J. Immunol.* **196**, 1317–1326 (2016).

123. Wang, P. *et al.* Inducible microRNA-155 Feedback Promotes Type I IFN Signaling in Antiviral Innate Immunity by Targeting Suppressor of Cytokine Signaling 1. *J. Immunol.* **185**, 6226–6233 (2010).

124. Li, H. *et al.* The metabolic responses to hepatitis B virus infection shed new light on pathogenesis and targets for treatment. *Sci. Rep.* **5**, 8421 (2015).

125. Vastag, L., Koyuncu, E., Grady, S. L., Shenk, T. E. & Rabinowitz, J. D. Divergent effects of human cytomegalovirus and herpes simplex virus-1 on cellular metabolism. *PLoS Pathog.* **7**, (2011).

126. Heaton, N. S. & Randall, G. Dengue virus-induced autophagy regulates lipid metabolism. *Cell Host Microbe* **8**, 422–432 (2010).

127. Perera, R. *et al.* Dengue virus infection perturbs lipid homeostasis in infected mosquito cells. *PLoS Pathog.* **8**, (2012).

128. Paul, D. & Bartenschlager, R. Flaviviridae Replication Organelles: Oh, What a Tangled Web We Weave. *Annu. Rev. Virol.* **2**, 289–310 (2015).

129. Neufeldt, C. J., Cortese, M., Acosta, E. G. & Bartenschlager, R. Rewiring cellular networks by members of the Flaviviridae family. *Nat. Rev. Microbiol.* **16**, 125–142 (2018).

130. Zhang, Z. *et al.* Host lipids in positive-strand RNA virus genome replication. *Front. Microbiol.* **10**, 1–18 (2019).

131. Harak, C. & Lohmann, V. Ultrastructure of the replication sites of positive-strand RNA viruses. *Virology* **479**–**480**, 418–433 (2015).

132. Levy, G. *et al.* Nuclear receptors control pro-viral and antiviral metabolic responses to hepatitis C virus infection. *Nat. Chem. Biol.* **12**, 1037–1045 (2016).

133. Lin, S. *et al.* GC/MS-based metabolomics reveals fatty acid biosynthesis and cholesterol metabolism in cell lines infected with influenza A virus. *Talanta* **83**, 262–268 (2010).

134. Nasheri, N. *et al.* Modulation of fatty acid synthase enzyme activity and expression during hepatitis C virus replication. *Chem. Biol.* **20**, 570–582 (2013).

135. Park, C. Y., Jun, H. J., Wakita, T., Cheong, J. H. & Hwang, S. B. Hepatitis C virus nonstructural 4B protein modulates sterol regulatory element-binding protein signaling via the AKT pathway. *J. Biol. Chem.* **284**, 9237–9246 (2009).

136. Gosert, R. *et al.* Identification of the Hepatitis C Virus RNA Replication Complex in Huh-7 Cells Harboring Subgenomic Replicons. *J. Virol.* **77**, 5487–5492 (2003).

137. Romero-Brey, I. *et al.* Three-Dimensional Architecture and Biogenesis of Membrane Structures

Associated with Hepatitis C Virus Replication. *PLoS Pathog.* **8**, (2012).

138. Welsch, S. *et al.* Composition and Three-Dimensional Architecture of the Dengue Virus Replication and Assembly Sites. *Cell Host Microbe* **5**, 365–375 (2009).

139. Aizaki, H., Lee, K. J., Sung, V. M. H., Ishiko, H. & Lai, M. M. C. Characterization of the hepatitis C virus RNA replication complex associated with lipid rafts. *Virology* **324**, 450–461 (2004).

140. Heaton, N. S. *et al.* Dengue virus nonstructural protein 3 redistributes fatty acid synthase to sites of viral replication and increases cellular fatty acid synthesis. *Proc. Natl. Acad. Sci. U. S. A.* **107**, 17345–17350 (2010).

141. Soto-Acosta, R., Bautista-Carbajal, P., Cervantes-Salazar, M., Angel-Ambrocio, A. H. & del Angel, R. M. DENV up-regulates the HMG-CoA reductase activity through the impairment of AMPK phosphorylation: A potential antiviral target. *PLoS Pathog.* **13**, (2017).

142. Soto-Acosta, R. *et al.* The increase in cholesterol levels at early stages after dengue virus infection correlates with an augment in LDL particle uptake and HMG-CoA reductase activity. *Virology* **442**, 132–147 (2013).

143. Sun, X. & Whittaker, G. R. Role for Influenza Virus Envelope Cholesterol in Virus Entry and Infection. *J. Virol.* **77**, 12543–12551 (2003).

144. Huang, H. *et al.* Human herpesvirus 6 envelope cholesterol is required for virus entry. *J. Gen. Virol.* **87**, 277–285 (2006).

145. Campbell, S. M., Crowe, S. M. & Mak, J. Lipid rafts and HIV-1: From viral entry to assembly of progeny virions. *J. Clin. Virol.* **22**, 217–227 (2001).

146. Aizaki, H. *et al.* Critical Role of Virion-Associated Cholesterol and Sphingolipid in Hepatitis C Virus Infection. *J. Virol.* **82**, 5715–5724 (2008).

147. Sanders, D. W. *et al.* Sars-cov-2 requires cholesterol for viral entry and pathological syncytia formation. *Elife* **10**, (2021).

148. Wang, S. *et al.* Cholesterol 25-Hydroxylase inhibits SARS -CoV-2 and other coronaviruses by depleting membrane cholesterol . *EMBO J.* **39**, (2020).

149. Hotta, K. *et al.* Effect of cellular cholesterol depletion on rabies virus infection. *Virus Res.* **139**, 85–90 (2009).

150. Singaravelu, R. *et al.* Soraphen A: A Probe for Investigating the Role of de Novo Lipogenesis during Viral Infection. *ACS Infect. Dis.* **1**, 130–134 (2016).

151. Hua, X. *et al.* SREBP-2, a second basic-helix-loop-helix-leucine zipper protein that stimulates transcription by binding to a sterol regulatory element. *Proc. Natl. Acad. Sci. U. S. A.* **90**, 11603–11607 (1993).

152. Yokoyama, C. *et al.* SREBP-1, a basic-helix-loop-helix-leucine zipper protein that controls transcription of the low density lipoprotein receptor gene. *Cell* **75**, 187–197 (1993).

153. Brown, M. S. & Goldstein, J. L. The SREBP pathway: Regulation of cholesterol metabolism by proteolysis of a membrane-bound transcription factor. *Cell* **89**, 331–340 (1997).

154. Shimano, H. *et al.* Isoform 1c of sterol regulatory element binding protein is less active than isoform 1a in livers of transgenic mice and in cultured cells. *J. Clin. Invest.* **99**, 846–854 (1997).

155. Horton, J. D., Goldstein, J. L. & Brown, M. S. SREBPs: Activators of the complete program of cholesterol and fatty acid synthesis in the liver. *J. Clin. Invest.* **109**, 1125–1131 (2002).

156. Wang, Y., Viscarra, J., Kim, S. J. & Sul, H. S. Transcriptional regulation of hepatic lipogenesis. *Nat. Rev. Mol. Cell Biol.* **16**, 678–689 (2015).

157. Madison, B. B. Srebp2: A master regulator of sterol and fatty acid synthesis1. *J. Lipid Res.* **57**, 333–335 (2016).

158. Zelenski, N. G., Rawson, R. B., Brown, M. S. & Goldstein, J. L. Membrane topology of S2P, a protein required for intramembranous cleavage of sterol regulatory element-binding proteins. *J. Biol. Chem.* **274**, 21973–21980 (1999).

159. Rawson, R. B., DeBose-Boyd, R., Goldstein, J. L. & Brown, M. S. Failure to cleave sterol regulatory element-binding proteins (SREBPs) causes cholesterol auxotrophy in Chinese hamster ovary cells with genetic absence of SREBP cleavage-activating protein. *J. Biol. Chem.* **274**, 28549–28556 (1999).

160. Bengoechea-Alonso, M. T. & Ericsson, J. SREBP in signal transduction: cholesterol metabolism and beyond. *Curr. Opin. Cell Biol.* **19**, 215–222 (2007).

161. Goldstein, J. L., DeBose-Boyd, R. A. & Brown, M. S. Protein sensors for membrane sterols. *Cell* **124**, 35–46 (2006).

162. Geelen, M. H., Gibson, D. & Rodwell, V. Hydroxymethylglutaryl-CoA reductase - the rate-limiting enzyme of cholesterol biosynthesis. *FEBS Lett.* **201**, 183–186 (1986).

163. Yu, Y., Maguire, T. G. & Alwine, J. C. Human Cytomegalovirus Infection Induces Adipocyte-Like Lipogenesis through Activation of Sterol Regulatory Element Binding Protein 1. *J. Virol.* **86**, 2942–2949 (2012).

164. Waris, G., Felmlee, D. J., Negro, F. & Siddiqui, A. Hepatitis C Virus Induces Proteolytic Cleavage of Sterol Regulatory Element Binding Proteins and Stimulates Their Phosphorylation via Oxidative Stress. *J. Virol.* **81**, 8122–8130 (2007).

165. Qiao, L. *et al.* SREBP-1a activation by HBx and the effect on hepatitis B virus enhancer II/core promoter. *Biochem. Biophys. Res. Commun.* **432**, 643–649 (2013).

166. Mackenzie, J. M., Khromykh, A. A. & Parton, R. G. Cholesterol Manipulation by West Nile Virus Perturbs the Cellular Immune Response. *Cell Host Microbe* **2**, 229–239 (2007).

167. Hyrina, A. *et al.* Human Subtilisin Kexin Isozyme-1 (SKI-1)/Site-1 Protease (S1P) regulates cytoplasmic lipid droplet abundance: A potential target for indirect-acting anti-dengue virus agents. *PLoS One* **12**, 1–22 (2017).

168. Liu, H. *et al.* Endoplasmic Reticulum Protein SCAP Inhibits Dengue Virus NS2B3 Protease by Suppressing Its K27-Linked Polyubiquitylation. *J. Virol.* **91**, 1–16 (2017).

169. Meng, Z., Liu, Q., Sun, F. & Qiao, L. Hepatitis C virus nonstructural protein 5A perturbs lipid metabolism by modulating AMPK/SREBP-1c signaling. *Lipids Health Dis.* **18**, 1–13 (2019).

170. Yuan, S. *et al.* SREBP-dependent lipidomic reprogramming as a broad-spectrum antiviral target. *Nat. Commun.* **10**, (2019).

171. Abu-Farha, M. *et al.* The role of lipid metabolism in COVID-19 virus infection and as a drug target. *Int. J. Mol. Sci.* **21**, (2020).

172. Cao, X., Yin, R., Albrecht, H., Fan, D. & Tan, W. Cholesterol: A new game player accelerating vasculopathy caused by SARS-CoV-2? *Am. J. Physiol. - Endocrinol. Metab.* **319**, E197–E202 (2020).

173. Lu, T. T., Repa, J. J. & Mangelsdorf, D. J. Orphan Nuclear Receptors as eLiXiRs and FiXeRs of

Sterol Metabolism. *J. Biol. Chem.* **276**, 37735–37738 (2001).

174. P. T. Lange, C. N. Jondle, E. J. Darrah, K. E. Johnson, V. L. T. crossm LXR Alpha Restricts Gammaherpesvirus Reactivation from. *J. Virol.* 1–16 (2019).

175. Janowski, B. A., Willy, P. J., Devi, T. R., Falckt, J. R. & Mangelsdorf, D. J. An oxysterol signalling pathway mediated by the nuclear receptor LXRa. *Lett. to Nat.* **96**, 266–271 (1996).

176. Lehmann, J. M. *et al.* Activation of the nuclear receptor LXR by oxysterols defines a new hormone response pathway. *J. Biol. Chem.* **272**, 3137–3140 (1997).

177. Berrodin, T. J. *et al.* Identification of 5α,6α-epoxycholesterol as a novel modulator of liver X receptor activity. *Mol. Pharmacol.* **78**, 1046–1058 (2010).

178. Repa, J. J. & Mangelsdorf, D. J. The role of orphan nuclear receptors in the regulation of cholesterol homeostasis. *Annu. Rev. Cell Dev. Biol.* **16**, 459–481 (2000).

179. Sheng, X. xiang *et al.* The LXR ligand GW3965 inhibits Newcastle disease virus infection by affecting cholesterol homeostasis. *Arch. Virol.* **161**, 2491–2501 (2016).

180. Liu, Y. *et al.* Activation of liver X receptor plays a central role in antiviral actions of 25-hydroxycholesterol. *J. Lipid Res.* **59**, 2287–2296 (2018).

181. Bocchetta, S. *et al.* Up-regulation of the ATP-binding cassette transporter A1 inhibits hepatitis C virus infection. *PLoS One* **9**, (2014).

182. Zeng, J. *et al.* Liver X receptors agonists impede hepatitis C virus infection in an Idol-dependent manner. *Antiviral Res.* **95**, 245–256 (2012).

183. Nakajima, S. *et al.* Fungus-Derived Neoechinulin B as a Novel Antagonist of Liver X Receptor, Identified by Chemical Genetics Using a Hepatitis C Virus Cell Culture System. *J. Virol.* **90**, 9058–9074 (2016).

184. Zhao, C. & Dahlman-Wright, K. Liver X receptor in cholesterol metabolism. *J. Endocrinol.* **204**, 233–240 (2010).

185. Repa, J. J. *et al.* Regulation of ATP-binding cassette sterol transporters ABCG5 and ABCG8 by the liver X receptors α and β. *J. Biol. Chem.* **277**, 18793–18800 (2002).

186. Gupta, S., Pandak, W. M. & Hylemon, P. B. Lxrα is the dominant regulator of CYP7A1 transcription. *Biochem. Biophys. Res. Commun.* **293**, 338–343 (2002).

187. Shimano, H. *et al.* Isoform 1c of sterol regulatory element binding protein is less active than isoform 1a in livers of transgenic mice and in cultured cells. *J. Clin. Invest.* **99**, 846–854 (1997).

188. Joseph, S. B. *et al.* Direct and indirect mechanisms for regulation of fatty acid synthase gene expression by liver X receptors. *J. Biol. Chem.* **277**, 11019–11025 (2002).

189. Yoshikawa, T. *et al.* Identification of Liver X Receptor-Retinoid X Receptor as an Activator of the Sterol Regulatory Element-Binding Protein 1c Gene Promoter. *Mol. Cell. Biol.* **21**, 2991–3000 (2001).

190. Repa, J. J. *et al.* Regulation of mouse sterol regulatory element-binding protein-1c gene (SREBP-1c) by oxysterol receptors, LXRα and LXRβ. *Genes Dev.* **14**, 2819–2830 (2000).

191. Sparrow, C. P. *et al.* A potent synthetic LXR agonist is more effective than cholesterol loading at inducing ABCA1 mRNA and stimulating cholesterol efflux. *J. Biol. Chem.* **277**, 10021–10027 (2002).

192. Korach-André, M. *et al.* Liver x receptors regulate de novo lipogenesis in a tissue-specific manner

in c57bl/6 female mice. *Am. J. Physiol. - Endocrinol. Metab.* **301**, 210–222 (2011).

193. Bong, S., Kiseok, A., Dae, J. & Jun, W. Expression of Liver X Receptor Correlates with Intrahepatic Inflammation and Fibrosis in Patients with Nonalcoholic Fatty Liver Disease. *Dig. Dis. Sci.* **59**, 2975–2982 (2014).

194. Levin, N. *et al.* Macrophage Liver X Receptor Is Required for Antiatherogenic Activity of LXR Agonists. *Arterioscler. Thromb. Vasc. Biol.* **25**, 135–142 (2005).

195. Zelcer, N., Hong, C., Boyadjian, R., Tontonoz, P. & Mev, S. LXR Regulates Cholesterol Uptake Through Idol-Dependent Ubiquitination of the LDL Receptor Cellular. *Life Sci.* **325**, 100–104 (2009).

196. Morrow, M. P. *et al.* Stimulation of the liver X receptor pathway inhibits HIV-1 replication via induction of ATP-binding cassette transporter A1. *Mol. Pharmacol.* **78**, 215–225 (2010).

197. Ramezani, A. *et al.* Stimulation of liver X receptor has potent anti-HIV effects in a humanized mouse model of HIV infection. *J. Pharmacol. Exp. Ther.* **354**, 376–383 (2015).

198. Mujawar, Z., Morrow, M., Sviridov, D. & Bukrinsky, M. Human immunodeficiency virus impairs reverse cholesterol transport from macrophages. *Retrovirology* **3**, S82 (2006).

199. Brügger, B. *et al.* The HIV lipidome: A raft with an unusual composition. *Proc. Natl. Acad. Sci. U. S. A.* **103**, 2641–2646 (2006).

200. Ono, A. & Freed, E. O. Plasma membrane rafts play a critical role in HIV-1 assembly and release. *Proc. Natl. Acad. Sci. U. S. A.* **98**, 13925–13930 (2001).

201. Zheng, Y. H., Plemenitas, A., Linnemann, T., Fackler, O. T. & Peterlin, B. M. Nef increases infectivity of HIV via lipid rafts. *Curr. Biol.* **11**, 875–879 (2001).

202. Najafi-Shoushtari, S. H. *et al.* MicroRNA-33 and the SREBP host genes cooperate to control cholesterol homeostasis. *Science* **328**, 1566–1569 (2010).

203. Ru, P. *et al.* Feedback Loop Regulation of SCAP/SREBP-1 by miR-29 Modulates EGFR Signaling-Driven Glioblastoma Growth. *Cell Rep.* **16**, 1527–1535 (2016).

204. Horie, T. *et al.* MicroRNA-33 regulates sterol regulatory element-binding protein 1 expression in mice. *Nat. Commun.* **4**, (2013).

205. Cheng, J. *et al.* MicroRNA-144 silencing protects against atherosclerosis in male, but not female mice. *Arterioscler. Thromb. Vasc. Biol.* 412–425 (2020).

206. Goedeke, L. *et al.* MicroRNA-148a regulates LDL receptor and ABCA1 expression to control circulating lipoprotein levels. *Nat. Med.* **21**, 1280–1288 (2015).

207. Chandra, A., Sharma, K., Pratap, K., Singh, V. & Saini, N. Inhibition of microRNA-128-3p attenuates hypercholesterolemia in mouse model. *Life Sci.* **264**, 118633 (2021).

208. Deng, Y. *et al.* Inhibition of miR-148a-3p resists hepatocellular carcinoma progress of hepatitis C virus infection through suppressing c-Jun and MAPK pathway. *J. Cell. Mol. Med.* **23**, 1415–1426 (2019).

209. Liu, D. *et al.* MicroRNA-33/33* inhibit the activation of MAVS through AMPK in antiviral innate immunity. *Cell. Mol. Immunol.* **18**, 1450–1462 (2021).

210. Hyrina, A. *et al.* Treatment-Induced Viral Cure of Hepatitis C Virus-Infected Patients Involves a Dynamic Interplay among three Important Molecular Players in Lipid Homeostasis: Circulating microRNA (miR)-24, miR-223, and Proprotein Convertase Subtilisin/Kexin Type 9. *EBioMedicine* **23**, 68–78 (2017).

211. Peng, S. *et al.* Endogenous Cellular MicroRNAs Mediate Antiviral Defense against Influenza A Virus. *Mol. Ther. - Nucleic Acids* **10**, 361–375 (2018).

212. Ahmed, N., Ahmed, N. & Pezacki, J. P. miR-383 Regulates Hepatic Lipid Homeostasis and Response to Dengue Virus Infection. *ACS Infect. Dis.* **8**, 928-941 (2022)

213. Scheller, N. *et al.* Proviral MicroRNAs Detected in Extracellular Vesicles from Bronchoalveolar Lavage Fluid of Patients with Influenza Virus-Induced Acute Respiratory Distress Syndrome. *J. Infect. Dis.* **219**, 540–543 (2019).

Chapter 2

A conserved miRNA-183 cluster regulates the innate antiviral response

2.1 Preface

This chapter contains data and text previously published in the Journal of Biological Chemistry as "Singaravelu, R.; Ahmed, N.; Quan, C.; Srinivasan, P.; Ablenas, C. J.; Roy, D. G.; Pezacki, J. P. A Conserved MiRNA-183 Cluster Regulates the Innate Antiviral Response. J. Biol. Chem. 2019, 294 (51), 19785–19794. https://doi.org/10.1074/jbc.RA119.010858." This article was authored by R.Singaravelu*, N. Ahmed*, C. Quan, P. Srinivasan, C.J. Ablenas, D.G. Roy and J.P.Pezacki. R.Singaravelu, and N. Ahmed are co-first authors and contributed equally to this published work. The individual contributions are detailed below:

As a co-first author of this publication, I made significant experimental and intellectual contributions to this article. R.Singaravelu, myself and J. P. Pezacki have conceived the research and experimental plan for this study. I have performed the majority of the cell culture work, RNA isolations, qRT-PCR experiments, western blot sample preparation and analysis, virus experiments, ISRE luciferase assay and CRISPRa cell line preparation and downstream analysis. C. Quan, P. Srinivasan, C.J. Ablenas, D.G. Roy aided with qPCR, 3'UTR assays, immunofluorescence, and western blot analysis. R.Singaravelu, myself and J. P. Pezacki wrote the initial manuscript, and editing was performed by all authors.

2.2 Abstract

Upon immune recognition of viruses, the mammalian innate immune response activates a complex signal transduction network to combat infection. This activation requires phosphorylation of key transcription factors regulating interferon (IFN) production and signaling, including IFN regulatory factor 3 (IRF3) and signal transducers and activators of transcription protein 1 (STAT1). The mechanisms regulating these STAT1 and IRF3 phosphorylation events remain unclear. Herein, using human and mouse cell lines, along with gene microarrays, quantitative RT-PCR (qPCR), viral infection and plaque assays, and reporter gene assays, we demonstrate that a bilaterian conserved microRNA (miRNA) cluster conserved among bilaterian animals, encoding miR-96, miR-182, and miR-183, regulates IFN signaling. In particular, we observed that the miR-183 cluster promotes IFN production and signaling, mediated through enhancing IRF3 and STAT1 phosphorylation. We also found that the miR-183 cluster activates the IFN pathway and inhibits vesicular stomatitis virus (VSV) infection through direct targeting of several negative regulators of IRF3 and STAT1 activities, including protein phosphatase 2A (PPP2CA) and tripartite motif containing 27 (TRIM27). Overall, the findings of our work reveal an important role for the evolutionarily conserved miR-183 cluster in the regulation of mammalian innate immunity.

2.3 Introduction

The innate immune system represents the immediate and non-specific response to pathogens in almost all multicellular organisms[1]. This first line of defense coordinates protection against a variety of both single-stranded (ss) and double-stranded (ds) DNA and RNA viruses as well as intracellular bacteria and parasites via the action of a class of cytokines called interferons (IFNs). Interferons induce the expression of numerous antiviral effector proteins, and IFN production relies on multiple phosphorylation events, including C-terminal phosphorylation of IFN regulatory factor 3 (IRF3)[2,3], a transcription factor that regulates the expression of both type I and III IFNs[4]. An integrated gene network of both positive and negative regulators is crucial for the proper dynamic activation and resolution of IFN signaling.

Recent work has highlighted a group of small RNAs, called microRNAs (miRNAs) as a key regulatory layer in cell-intrinsic immunity and the inflammatory response[5]. Generally, miRNAs post-transcriptionally regulate gene expression relevant to diverse cellular processes by base pairing with the 3'UTR of mRNAs and mediating mRNA destabilization and translational repression[6]. MicroRNA expression can be modulated during viral infection or the innate immune response[5,7], and can serve to either potentiate or dampen the immune response[8–10] . The functional relevance of microRNAs in shaping the innate antiviral response isn't completely understood.

In examining miRNA signatures associated with a viral infection, we identified that the highly conserved miR-183 cluster (miR-96, miR-182, and miR-183; Fig. 2.1A) is dysregulated in the context of different viral infections, including both DNA and RNA viruses[11–15]. Furthermore, genetic variation in this miRNA cluster is associated with increased susceptibility to inflammatory and auto-immune disease[16]. Despite these connections, the role of miR-183 cluster in innate immunity is unclear.

Here, we examined the role of miR-183 cluster in the innate immune response. We found that all three miRNAs encoded in the cluster promoted IFN signaling and production through repression of key negative regulators of the IRF3 and STAT1 signaling. Our work demonstrates a novel role for this miRNA cluster in co-operative regulation of the IFN pathway.

2.4 Results and discussion

2.4.1 miR-183 Cluster Suppresses Viral Replication

To characterize the miR-183 cluster's role in the innate antiviral response, we first examined the influence of the cluster on virus production. As previous work had shown dysregulation of the cluster's expression in the context of viral infections of the liver[13,14,17],we performed our initial studies in the IFN signaling competent HepG2 hepatoma cells[18]. We transfected HepG2 cells with mimics of each miRNA in the cluster and subsequently infected the cells with GFP-encoding vesicular stomatitis virus (VSV-GFP). miR-183 mimic transfection elicited the most potent antiviral effect, inducing an over 2-log drop in virus production (Fig. 2.1B). Fluorescence microscopy confirmed decreased GFP production in miR-183 transfected cells infected with the VSV reporter virus (Fig. 2.1C). We also observed an analogous antiviral effect in MCF7 breast cancer cells (Fig. 2.1D) and immortalized mouse embryonic fibroblasts (Fig. S2.1), suggesting the cluster's antiviral effects are conserved across mice and humans. A comparison of the cluster's inhibitory effects against VSV in the three tested models revealed miR-183 was consistently the most potent anti-viral microRNA. In order to further confirm the miR-183 cluster's antiviral effects, we examined VSV virus production in miRNA inhibitor treated MCF7 cells, as breast cancer cells are known to express upregulated levels of the miR-183 family[19]. Consistent with our mimic experiments, inhibition of each miRNA individually during VSV infection produced an approximately one log increase in viral titer (Fig. 2.1E) – reinforcing a shared function for the miR-183, miR-182, and miR-96 in antiviral defense.

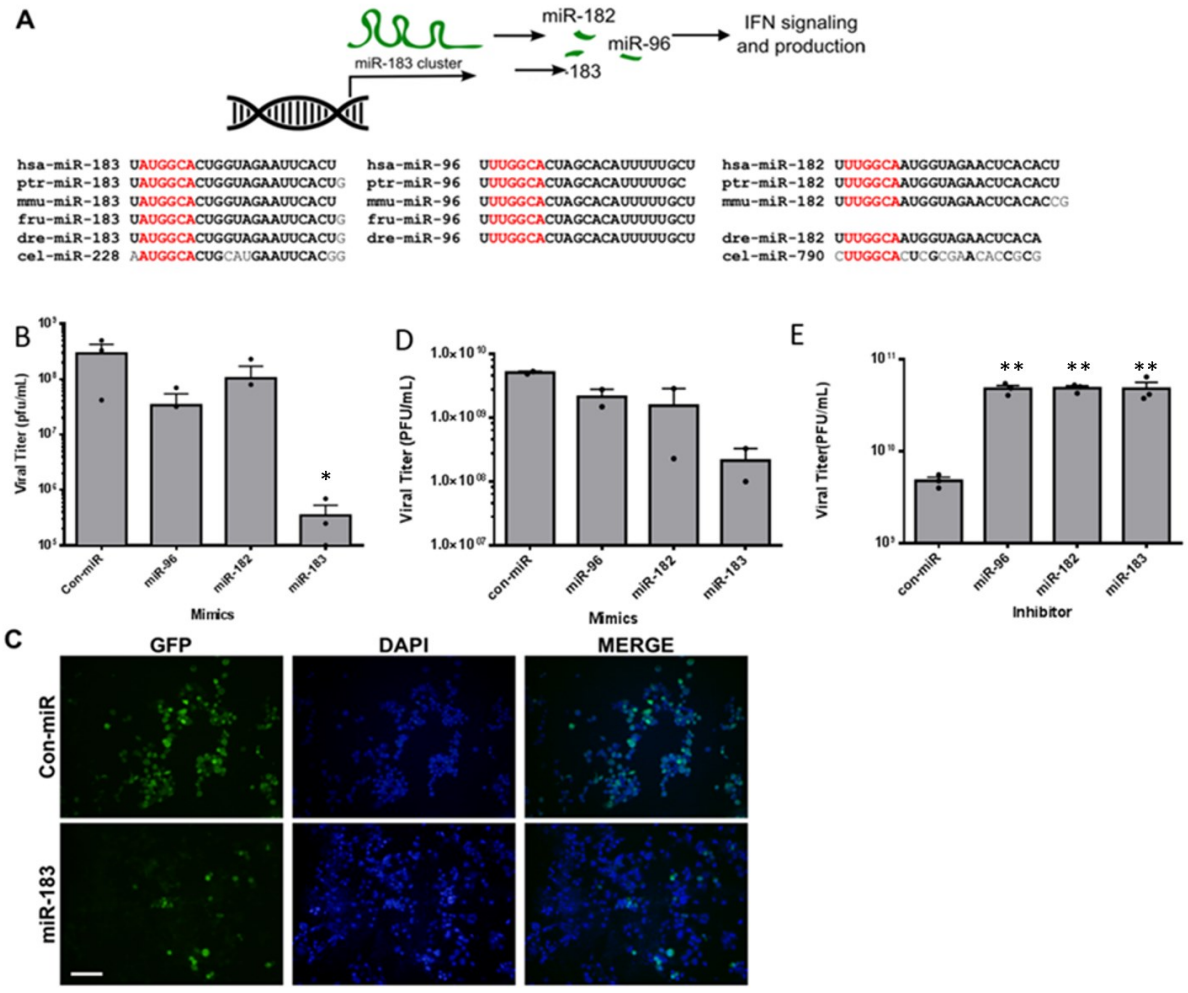

Figure 2.1. Immune-regulated miRNA cluster inhibits viral infection. (A) Schematic depicting immunoregulatory role of miR-183 cluster. Conservation of miR-96, miR-182, and miR-183 shown below. (B)-(C), HepG2 cells were transfected with mimics for miR-96, miR-182, or miR-183, along with a negative control mimic (Con-miR) at a final concentration of 50nM. 48 hours post-transfection, cells were infected with VSV-GFP (MOI = 0.01) for 24h. The effects of miRNAs on virus production was assessed by plaque assays for (B) VSV-GFP and (C) VSV-GFP infected cells were visualized 72 hours post-transfection and 24h post-infection using fluorescence microscopy and representative images are shown for Con-miR and miR-183 transfected cells. Scale bar = 100 µm. (D)-(E), Plaque assay results showing the influence of miR-183 cluster (D) mimics and (E) inhibitors on VSV-GFP production in MCF7 breast cancer cells 72 hours post-transfection with miRNA mimics/or inhibitors and 24 hours post infection. (B) And (E) Error bars represent mean± SEM from 3 independent experiments. (D) Data represents the means ±SEM of two biological replicates. .*P<0.05, **P<0.01.

2.4.2 miR-183 Cluster Promotes IFN Signaling

In order to delineate the mechanism by which the miR-183 cluster mediates its anti-viral effects, we performed gene expression profiling on HepG2 cells treated with miR-183 cluster mimics and subsequently immunostimulated with polyinosine-polycytidylic acid (poly(I:C), a viral dsRNA analog) complexed with transfection reagent LyoVec. This poly(I:C)/LyoVec complex acts as an agonist of the cytoplasmic sensor of viral RNA, retinoic acid-inducible gene I (RIG-I). Among the genes activated by over 8-fold by each miR-96/182/183 mimic independently were several well-established interferon-stimulated genes (ISGs), including OAS2, RSAD2, DDX60, and IFITM1 (Fig. 2.2A).

Gene ontology enrichment analysis of genes upregulated greater than 1.5-fold in expression revealed that biological processes related to type I IFN signaling were activated by each miRNA of the cluster (Fig. 2.2B; Tables S2.1-S2.3). Data from qPCR experiments of type I and III IFNs (IFNB1 and IFNL1) as well as ISGs' (STAT1, DDX58, and RSAD2) expression levels in poly(I:C) stimulated HepG2s confirmed enhanced IFN signaling and production in miR-183 cluster treated cells (Fig. 2.2C-D). Additionally, similar activation of IFN and ISG expression was observed in VSV-infected MCF7 breast cancer cells treated with miR-183 mimic (Fig. S2.2A-B). Conversely, inhibition of the miR-183 cluster produced the opposite effect, decreasing IFNB1 and RSAD2 expression (Fig. S2.3). Analogous levels of ISG expression were observed in HepG2 cells following VSV infection (Fig. S2.4). These data strongly validate the regulatory role of the miR-183 cluster in IFN signaling.

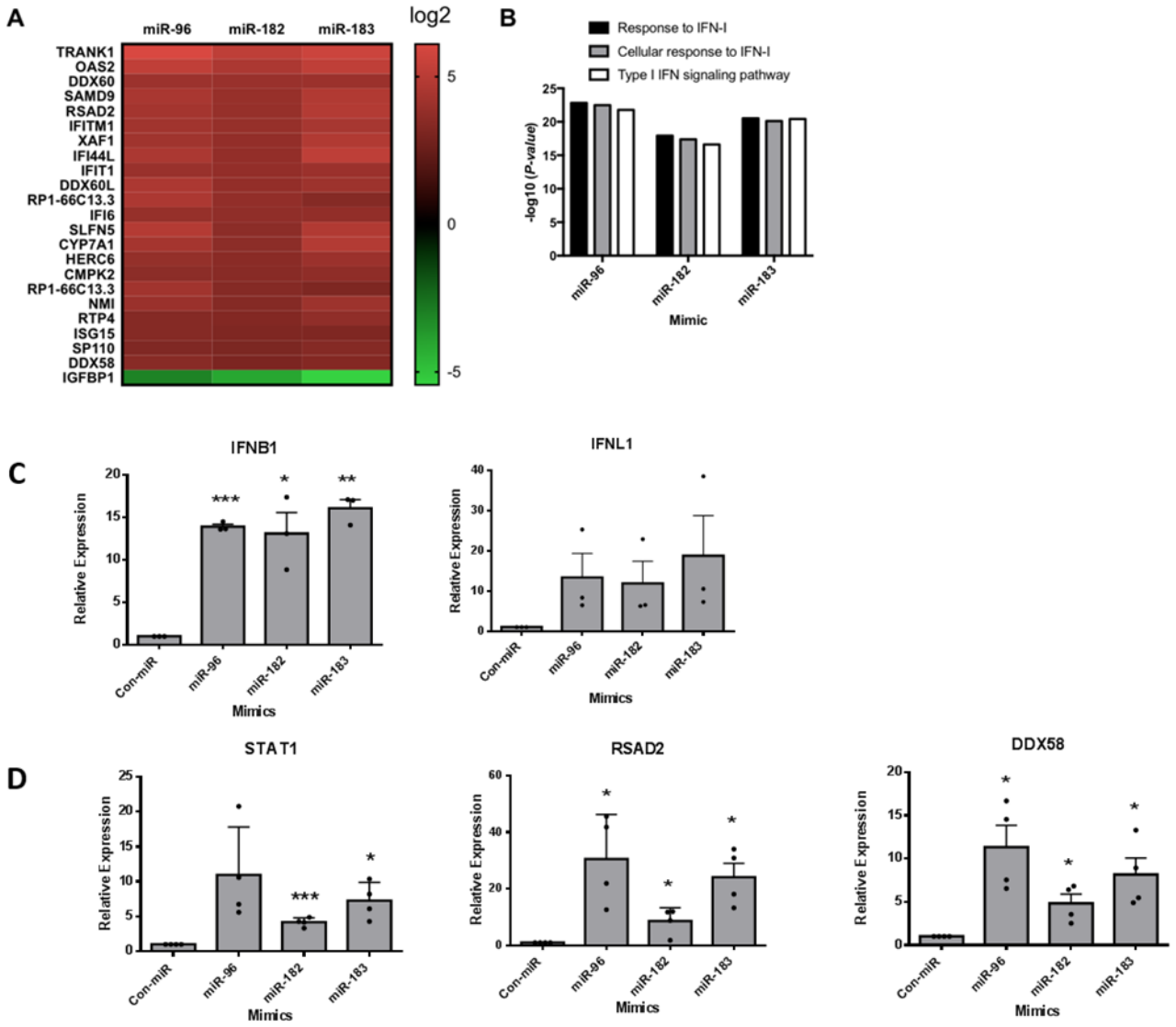

Figure 2.2 miR-183 cluster regulates IFN signaling. (A) HepG2 cells were transfected with control miRNA (Con-miR), miR-96, miR-182, or miR-183 mimics independently at 50nM final concentration. 48h post transfection, cells were immunostimulated with poly(I:C)/LyoVec (500ng/mL) for 24h. Heat map of genes differentially expressed by over 8 fold (up or down) in each treatment condition relative to Con-miR transfected HepG2 cells. Fold changes in gene expression relative to control are shown. (B) Gene ontology analysis classifying activated genes (≥ 1.5 fold increase) in miR-183 cluster treated HepG2 cells by biological process. Top 3 GO terms, all type I IFN (IFN-I) related processes, are shown for each examined condition. (C) qRT-PCR analysis of relative IFN expression (IFNB1 and IFNL1) and (D) ISG expression (RSAD2, STAT1, and DDX58) in HepG2 cells transfected with miR-183 cluster at 50nM final concentration and subsequently stimulated with poly(I:C)/LyoVec at a final concentration of 500ng/mL for 24h. Data represents the means ±SEM of four biological replicates.*P<0.05, **P<0.01, ***P<0.001. IFNL1 data represents the means ±SEM of three biological replicates.

2.4.3 miR-183 Promotes Jak/STAT Signaling

Type I and III IFN stimulation activates the JAK/STAT pathway[20], which yields phosphorylation-dependent activation of STAT1, a transcription factor required for ISG induction. Interestingly, we observed increased STAT1 mRNA expression in miR-183–treated cells, suggesting that miR-183 activates constitutive Jak/STAT signaling in the absence of immune stimulation (Fig. S2.5). Activation of STAT1 depends on phosphorylation at a C-terminal tyrosine residue (Tyr-701), whereas additional phosphorylation at Ser-727 is thought to be required for maximal activation of the transcription factor[21]. We examined the miR-183 cluster's effect on these two STAT1 phosphorylation sites. As miR-183 exhibited the most potent antiviral effect (Fig. 2.1, B–D, and Fig. S2.1), we focused our efforts on characterizing this miRNA's effects on Jak/STAT signaling. miR-183–transfected HepG2 cells showed increased STAT1 phosphorylation at Tyr-701 and Ser-727 during poly(I:C)/LyoVec and IFN-α immunostimulation at various time points (Fig. 2.3, A–C), consistent with enhanced Jak/STAT signaling. We performed short pulses of IFN-α to distinguish changes in phosphorylation status from overall increases in STAT1 expression levels. The results showed that the increase in phosphorylation by miR-183 occurred prior to any change in the expression of STAT1 (Fig. 2.3B). Consistent with this, miR-183 was shown to be able to enhance IFN-stimulated response element (ISRE)-driven reporter activity during TBK1 and IKKε overexpression in HEK293T cells (Fig. S2.6). Measurements by qPCR also confirmed that the miRNA cluster activated ISG expression during IFN- α stimulation, with DDX58, RSAD2, and STAT1 expression increasing over 4-fold in cells transfected with each mimic independently (Fig. 2.3D). Increased STAT1 Tyr-701 phosphorylation was also observed in the context of VSV-GFP infection; however, no significant difference in phosphorylation at the Ser-727 site was seen (Fig. 2.3E). The use of an attenuated VSV strain, defective in its capacity to evade IFN signaling because

of a deletion in the matrix (M) protein (22), rescued the miR-183–mediated effect on Ser-727 phosphorylation. This suggests that WT VSV M protein partially impairs miR-183's effect on STAT1; however, because it has been shown that it is possible to achieve STAT1 activation independent of the phosphorylation at Ser-727[21], there is only partial impairment. Maximal activation of STAT1 is achieved when phosphorylation at Ser-727 is also maximized[21]. Furthermore, similar results were observed in poly(I:C)/ LyoVec-treated A549 lung cancer cells (Fig. S2.7). Collectively, our observations revealed that miR-183 enhances Jak/STAT signaling under both basal and virus-stimulated conditions. Viral RNA can also be sensed by Toll-like receptors (TLRs) 3, 7, and 8 in the endosomal compartment, and ligand engagement of these TLRs results in downstream IFN production and signaling. We examined whether the cluster could influence TLR3 signaling in MCF7 cells by treating miR-183 cluster mimic–transfected cells with naked poly(I:C) and probing STAT1 phosphorylation levels. Our immunoblot analyses revealed that miR-96 and miR-183 promoted TLR3 agonist– induced STAT1 phosphorylation (Fig. S2.8). Taken together, these results demonstrate that the miR-183 cluster activates both TLR and RIG-I–induced Jak/STAT signaling.

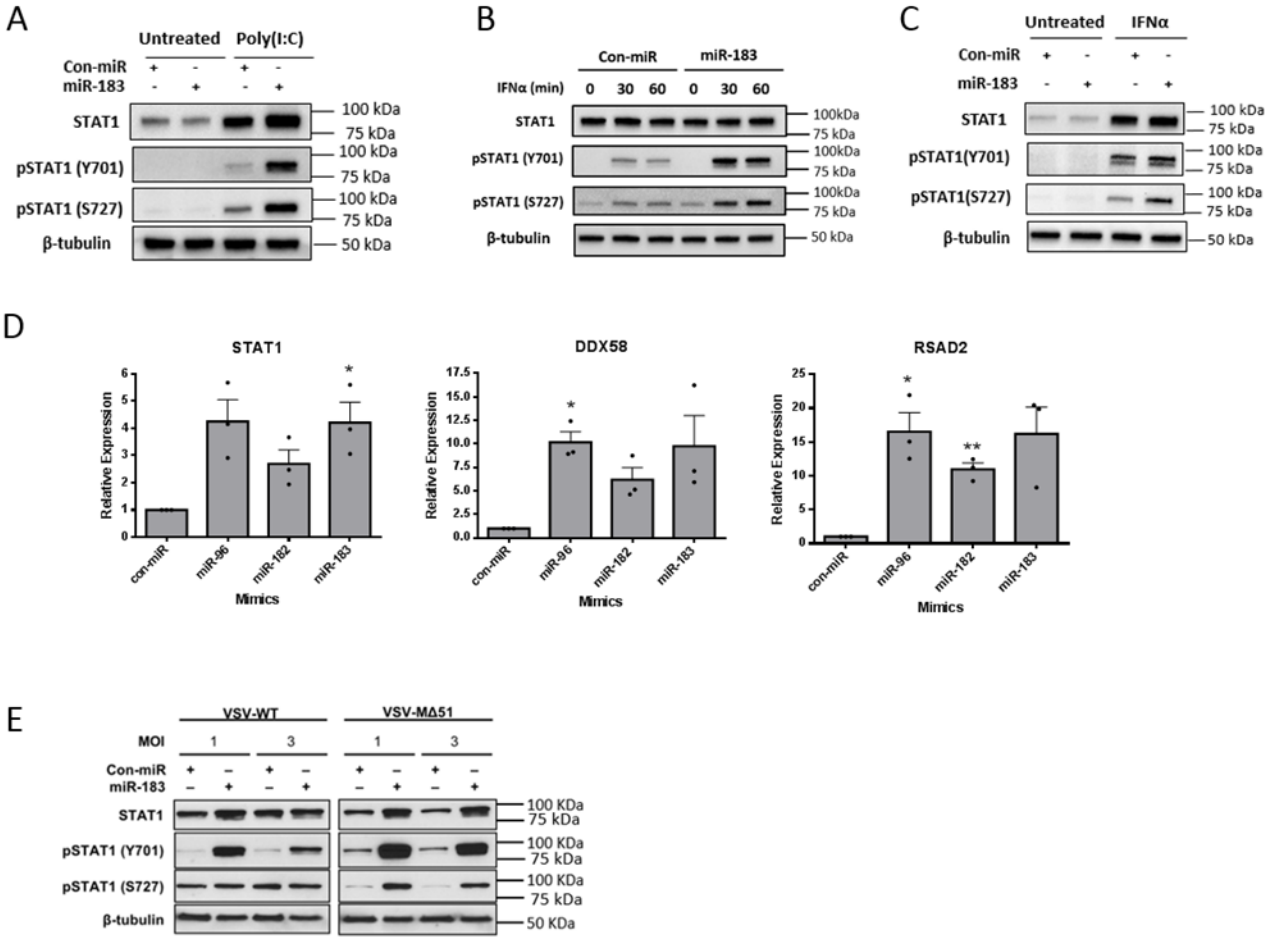

Figure 2.3 miR-183 activates Jak/STAT signaling. (A) HepG2 cells were transfected with either control mimic (Con-miR) or miR-183 at 50nM final concentration for 48h and then treated with poly(I:C)/LyoVec (500ng/ mL) for 24h. Western blot analysis of total STAT1 and phosphorylated STAT1 (pSTAT1 Y701 and S727) are shown. β-tubulin levels serve as loading control. (B) HepG2 cells were transfected with either control mimic (Con-miR) or miR-183 at 50nM final concentration for 48h and subsequently treated with IFN-α (1000U) for 30 mins and 60 mins. (C) HepG2 cells were transfected with either control mimic (Con-miR) or miR-183 at 50nM final concentration for 48h and subsequently treated with IFN-α (1000U) for 24 Western blot analysis of total STAT1 and phosphorylated STAT1 (pSTAT1 Y701 and S727) are shown. β-tubulin levels serve as loading control. (D) qRT-PCR analysis of relative ISG expression (RSAD2, STAT1, and DDX58) in HepG2 cells transfected with miR-183 cluster mimics at 50nM final concentration, and subsequently stimulated with 1000U/mL IFN-α for 24h. Data represents the means ±SEM of three biological replicates. *P<0.05, **P<0.01. (E) HepG2 cells were transfected with either control mimic (Con-miR) or miR-183 at final concentration of 50nM and 48h post-transfection, cells were infected with VSV-GFP or an attenuated VSV-GFP strain (MΔ51) at two different MOIs (1 and 3) for 24h. Western blot analysis was then performed as in (A).

2.4.4 miR-183 represses negative regulators of IFN production

To characterize the direct targets of miR-183 contributing to its stimulatory effects on IFN signaling/production and antiviral effects, we utilized the gene expression profiling data to identify potential miR-183 targets. To do this, we examined the overlap between miR-183 predicted targets from TargetSca[22] and genes whose expression was down-regulated by miR-183 mimic transfection in poly(I:C)/LyoVec–stimulated HepG2 cells (>1.5-fold) (Fig. 2.4A). This produced a list of 413 genes, and we examined this list for genes described previously to be negative regulators of IFN production and signaling. miR183 repressed the expression of serine/threonine protein phosphatase 2A catalytic subunit α isoform (PPP2CA)[23] and tripartite motif– containing 27 (TRIM27)[24], genes shown previously to inhibit IFN production with putative miR-183 binding sites in their 3 UTRs (Fig. 2.4B). We then validated repression of miR-183 regulated genes in poly(I:C)/LyoVec-immunostimulated HepG2 cells transfected with mimics of the miR-183 cluster. qPCR confirmed that miR183 inhibited mRNA levels of these predicted targets by over 50% in poly(I:C)/LyoVec-treated HepG2 cells (Fig. 2.4C). In parallel, decreased protein phosphatase 2A (PP2A) catalytic subunit protein abundance was confirmed by Western blot analysis (Fig. 2.4D) and PPP2CA was validated as a direct target of miR-183 (Fig. S2.9). These results suggest that the miR-183 cluster represses the expression of negative regulators of IRF3 phosphorylation to mediate their inhibitory effects on IFN production. PP2A and TRIM27 inhibit interferon production by decreasing IRF3 phosphorylation[23,24]. Phosphorylation of IRF3 at the C terminus is required for the transcription factor to homo/ heterodimerize and translocate to the nucleus to mediate transcriptional activation of IFN genes and ISGs. Therefore, we hypothesized that miR-183 activates IFN production and signaling through increased IRF3 activation and examined the phosphorylation status of IRF3 in miR-183–transfected cells. Western blot analyses

confirmed increased IRF3 phosphorylation and down-regulated expression of PPP2CA in miR-183–transfected HepG2 cells during poly(I:C) treatment or VSV infection (Fig. 2.4, D and E). This miR-183– enhanced IRF3 phosphorylation was also observed in RIG-I agonist–treated A549 cells (Fig. S2.6) and TLR3 agonist–treated MCF7 cells (Fig. S2.7). PP2A has also been proposed previously to impair IFN-induced STAT1 phosphorylation[25]; miR-183 targeting of the phosphatase would contribute to its effects on Jak/STAT signaling (Fig. 2.3). Furthermore, knockdown of PPP2CA in HepG2 cells resulted in the dampening of the miR-183-mediated effect on STAT1 phosphorylation following poly(I:C) stimulation (Fig. S2.10). As predicted, both miR-183 and specific siRNA targeting PPP2CA led to lower levels of protein expression and a commensurate increase in phosphorylation of STAT1. Treatment with PPP2CA siRNA dampens the effects of miR183 by lowering the mRNA levels of the key miRNA target (Fig. S2.10). Additionally, it is evident that, with siRNA knockdown of PPP2CA, the magnitude of difference in STAT1 phosphorylation (Tyr-701 and Ser-727) between Con-miR– and miR-183– transfected HepG2 cells is not as significant relative to what is observed in naïve Con-siRNA–transfected HepG2 cells (Fig. S2.10, lanes 1 and 2 versus lanes 3 and 4). This further validates that miR-183's effect on Jak–STAT signaling depends on PPP2CA repression. Overall, this confirms that miR-183- driven enhancement of IFN signaling and the accompanying antiviral response are mediated through PPP2CA targeting. In addition, specific induction of the miR-183 cluster by the CRISPR activation system[26] in HepG2 cells produced consistent increases in IRF3 and STAT1 phosphorylation and ISG expression as well as concomitant down-regulation of PPP2CA expression during poly(I:C)/LyoVec stimulation (Fig. S2.11). Therefore, our data demonstrate that the miR-183 cluster mediates its antiviral effects through repression of negative regulators of IRF3 and STAT1 phosphorylation (Fig. 2.5).

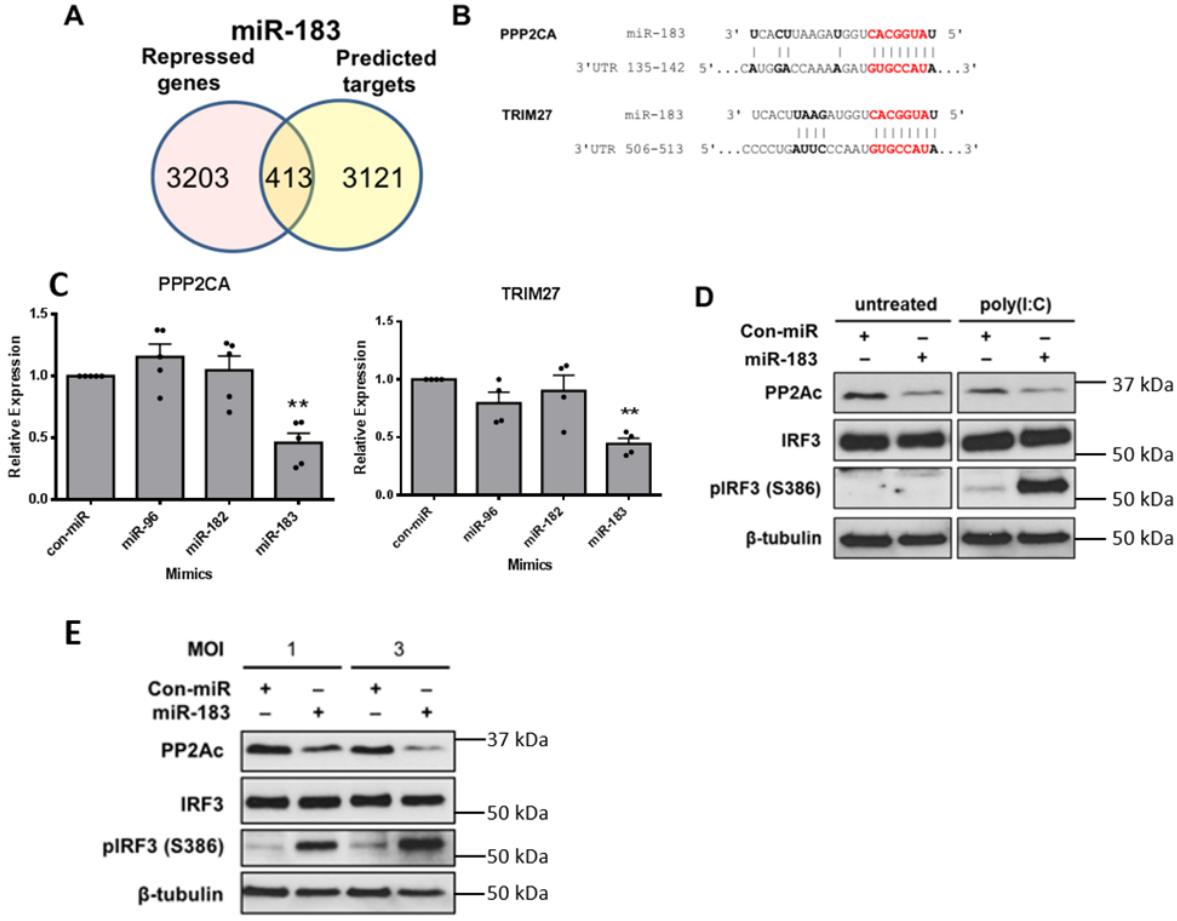

Figure 2.4. miR-183 activates IRF3 phosphorylation. (A) Venn diagram visualizes overlap between miR-183 predicted targets and genes repressed in miR-183 mimic transfected HepG2 cells at a concentration of 50nM and immunostimulated with poly(I:C) at a concentration of 500ng/mL for 24h. (B) The predicted miR-183 binding sites in the 3'UTRs of three negative regulators of IRF3 signaling (PPP2CA and TRIM27). Sites were taken from Targetscan [22]. (C) qRT-PCR analysis of miR-183 target expression levels in miR-183 mimics transfected (50nM) and poly(I:C) (500ng/mL) treated HepG2 cells. Poly (I:C) treatment was done for 24h.Treatment PPP2CA data represents the means ±SEM of five biological replicates. TRIM27 data represents the means ±SEM of four biological replicates **P<0.01, ***P<0.001 (D)-(E) Western blot analysis of PP2A catalytic subunit alpha (PP2Ac), total IRF3 and phosphorylated IRF3 (pIRF3 S386) levels in control (Con-miR) or miR-183 mimic transfected HepG2s at 50nM final concentration (D) treated with poly(I:C) (500ng/mL) 48h post-transfection or (E) infected with different MOIs of VSV-GFP 48h post-transfection. β-tubulin levels serve as loading control.

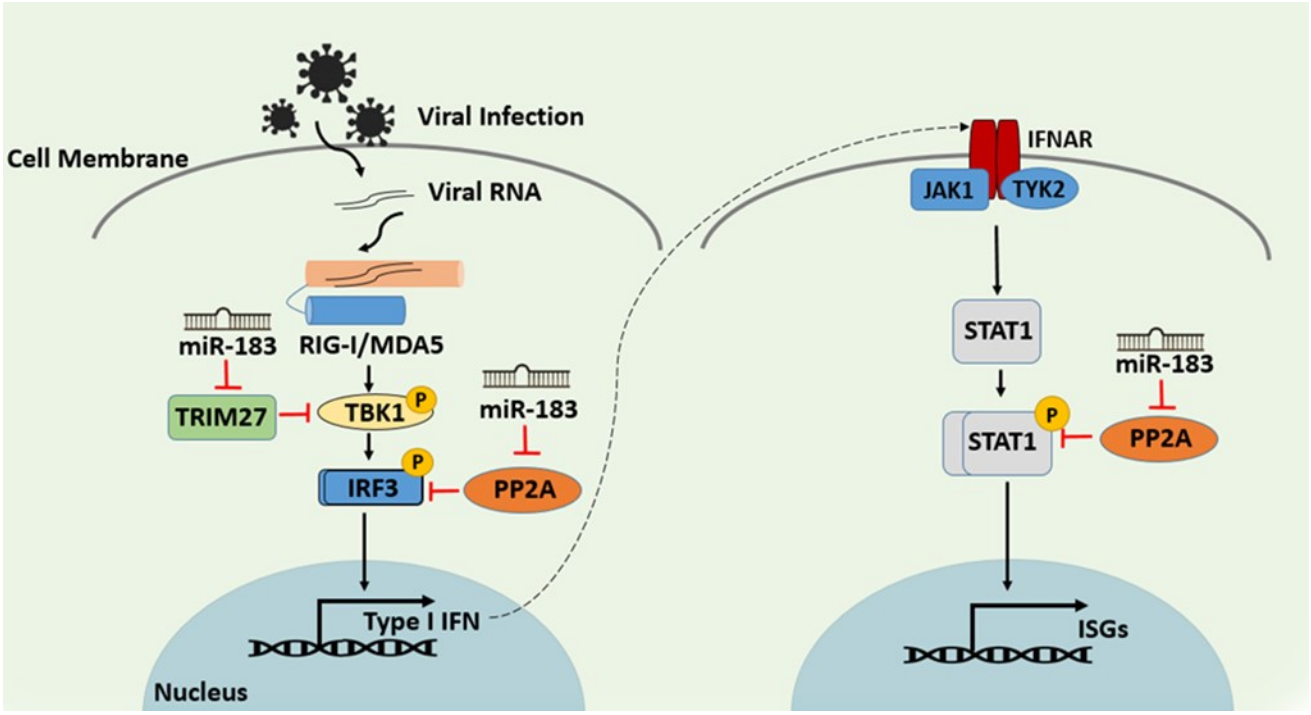

Figure 2.5. A schematic representation of the proposed model for the mechanism by which miR-183 regulates the innate antiviral immune response. The miR-183 cluster positively regulates type I Interferon and ISG production by repressing negative regulators of the antiviral response. Specifically, mir-183 targets PPP2CA, which is known to negatively regulate IRF3 and STAT1 phosphorylation[24,26] ,and miR-183 also targets TRIM27 and as a result impair the degradation of TBK1 and enhance IRF3 signaling in the initiation of type I IFN production[25] . This establishes a model by which miR-183's repression of PPP2CA and TRIM27 enhances the activation of IFN and ISG production.

2.5 Conclusion

Overall, our work elucidates a novel role for the miR-183 cluster in the regulation of the innate antiviral response through activation of IFN production and signaling. Whereas previous studies have highlighted functional roles for miRNAs encoded in the miR-183 cluster in helper T lymphocyte clonal expansion[27] and natural killer cell function[28], our work highlights a novel function for this highly conserved miRNA cluster in the cell-intrinsic defense against pathogens. Furthermore, miR-183's regulation of tonic IFN signaling could also play an important role in immune homeostasis as increased constitutive IFN signaling has been linked to autoimmunity[29]. This provides a potential explanation for the previously reported association between increased miR-183 cluster expression and lupus disease in mice[30]. The identification of the miR-183 family as a primary regulator of IFN signaling opens novel avenues for immunomodulatory strategies to treat interferonopathies and other immune disorders. This is, to the best of our knowledge, the only known example of a miRNA cluster shaping the innate immune response through cooperative regulation of the IFN pathway.

2.6 Experimental Procedures

2.6.1 Reagents

The HepG2 hepatoma cells (HB-8065), MCF7 breast cancer cells (HTB-22), A549 lung epithelial cancer cells (CCL-185), and HEK293 human embryonic kidney cells (CRL-1573) were procured from the ATCC. Mouse embryonic fibroblast cells [31] were kindly provided by Dr. Marc Servant (Université de Montreal, Montreal, QC, Canada). VSV-GFP WT and mutant viruses were kindly provided by Dr. John C. Bell (Ottawa Hospital Research Institute, Ottawa, ON, Canada)[32]. All mirVana miRNA mimics and inhibitors, along with controls, were purchased from Ambion. PPP2CA-targeting siRNA (4390824) and the negative control (4390843, Silencer Select) were purchased from Ambion. The PPP2CA 3 UTR luciferase construct was purchased from Genecopoeia. Low-molecular-weight (LMW) poly(I:C) complexed with LyoVec and LMW poly(I:C) alone were purchased from Invivogen. IFN-α was procured from PBL Assay Science. The pISRE-Luc plasmid was a kind gift from Dr. Katherine Fitzgerald (University of Massachusetts Medical School, Worcester, MA). pcDNA3.1-TBK1-FLAG, pcDNA3.1- FLAG-IKBKE, and empty pcDNA3.1 were a kind gift from Dr. Daniel Lamarre (Centre hospitalier de l' Université de Montréal, Montreal, QC,Canada)[33]. The lentiviral vectors encoding MS2- p65-HSF1 (61426) and dCas9-VP64 (61425) fusion proteins and the lenti sgRNA(MS2)_puro-optimized backbone (73797) were gifts from Feng Zhang (Broad Institute, Cambridge, MA), obtained from Addgene [26].

2.6.2 Cell culture and transfections

Adherent HepG2 cells were cultured in DMEM (Invitrogen) supplemented with 10% FBS (PAA Laboratories), 1X nonessential amino acids (NEAAs; Gibco), 50 units/ml penicillin, and 50 mg/ml streptomycin. Adherent HEK293 cells were cultured in minimum essential medium (Invitrogen)

supplemented with 10% FBS, 1 mM sodium pyruvate (Gibco), 1X NEAAs, 50 units/ml penicillin, and 50 mg/ml streptomycin. Adherent mouse embryonic fibroblasts, A549 cells, and Vero cells were cultured in DMEM supplemented with 10% FBS. Adherent MCF7 cells were cultured in minimum essential medium containing 10% FBS, 1% NEAAs, 1% sodium pyruvate, and 0.01 mg/ml recombinant insulin (Sigma-Aldrich). All cell culture maintenance and experiments were performed at 37 °C and 5% CO2. IFN-α was used at a working concentration of 1000 units/ ml. LMW poly(I:C) complexed with LyoVec was used at 500 ng/ml, whereas LMW poly(I:C) for TLR3 agonism was used at 50 g/ml. Transfections for miRNA mimics and inhibitors were performed using Lipofectamine RNAiMax (Life Technologies). Transfections were performed according to the manufacturer's protocol, using 2.5 l μL of RNAiMAx/1 l μL of 100 M of miRNA mimic. Transfection of plasmid DNA was performed using Lipofectamine 2000 (Life Technologies) according to the manufacturer's protocol.

2.6.3 mRNA microarray analysis

RNA isolation from HepG2 cells was performed with the RNeasy kit (Qiagen). Gene expression profiling was performed using Affymetrix Human Gene ST.2.0 arrays. Data were normalized and analyzed using the Affymetrix Expression Console and Transcriptome Analysis Console (v3.0), according to the manufacturer's protocols. Gene ontology analysis was performed using the ToppGene Suite[34]. For ToppGene analysis, P values were adjusted with Bonferroni correction. Heatmap visualization of expression data was done on data set filtered for genes activated over 8 fold under all conditions (HepG2s transfected with mimics of miR-96, miR-182, or miR-183 individually at 50 nM). Since multiple transcript cluster IDs corresponded to TRANK1, we have shown the fold change corresponding to ID 17123262, the probe showing the highest magnitude of fold change in expression. Gene expression profiling data from the miR-183 cluster and control

mimic transfected HepG2 cells immunostimulated with poly(I:C) have been deposited to NCBI Gene Expression Omnibus under the following accession number: GEO: GSE 139027

2.6.4 Quantitative RT-PCR

RNA isolation from hepatocytes was performed using TriZol (Life Technologies), RNeasy kits (Qiagen), or NucleoSpin miRNA (Macherey-Nagel), according to the manufacturer's protocol. RNA integrity was confirmed by 0.8% agarose gel electrophoresis in 1X TBE (Ambion). For mRNA profiling, 250 ng of total RNA was reverse transcribed using the Superscript II RT kit (Life Technologies) following the manufacturer's instructions. qPCR was subsequently performed on an iCycler (Bio-Rad) using iQ SYBR Green SSO Advanced Supermix (Bio-Rad), according to the manufacturer's protocol. Primer sequences are listed in Table S4. Relative miRNA levels were quantified using the Taqman miRNA Assay (Applied Biosystems), with 10 ng of total RNA used for reverse transcription using the TaqMan MicroRNA Reverse Transcription Kit (Applied Biosystems). For both mRNA and miRNA quantification, the $2^{-\Delta\Delta Ct}$ method was used to calculate fold changes in expression relative to mock or control-treated samples[35], with 18S rRNA or RNU6B levels being used for normalization.

2.6.5 Viral infections

HepG2 cells and MCF7 cells were seeded at 5 x 105 cells/well in six-well plates and simultaneously reverse-transfected with 50 nM control, miR-96, miR-182, miR-183 mimics or inhibitors. Forty-eight hours post-transfection, media was removed and cells were incubated at 37°C in serum-free DMEM containing VSV-GFP particles at the appropriate MOIs. One hour post-infection, cells were washed with 1X PBS, and media was replaced with DMEM supplemented with 10% FBS. Twenty-four hours post-infection (VSV), cell supernatants (for plaque assays) were collected and clarified via centrifugation at 1,700g for 10 min to remove cells

and cellular debris. Adherent cells were washed once with PBS and then lysed for subsequent cellular RNA and protein analyses.

2.6.6 Viral plaque assays

Vero cells were seeded at 7.5 x 105 cells/well in six-well plates. Twenty-four hours after seeding, ten-fold serial dilutions ($1:10^1$ to $1:10^9$) of the supernatants collected from VSV-infected HepG2 cells were prepared in DMEM. Media was removed from Vero cells and replaced with 100 µL of virus-containing supernatant (one dilution per well). Cells were incubated in virus-containing supernatant at 37°C for one hour. One-hour post-infection, 2 mL of warm (37-40°C) agarose media (1X DMEM, 10% FBS, 1% w/v agarose) was added to each well and allowed to solidify. After 24 hours (VSV), plaques were counted by visual examination. Viral titers in supernatants were back-calculated based on serial dilutions and expressed as plaque-forming units (pfu) per mL of supernatant.

2.6.7 VSV-GFP fluorescence imaging

HepG2 cells were seeded at 2 x 105 cells/well in twelve-well plates and simultaneously reverse-transfected with Con-miR, miR-96, miR-182, and miR-183 mimics as previously described. Forty-eight hours post-transfection, cells were infected with VSV-GFP. 24h post-infection, cells were washed twice with PBS and fixed with a solution of 4% v/v formaldehyde and 4% w/v sucrose in water for 15 min at room temperature. Fixed cells were washed twice with PBS for 3 min and stored in PBS at 4°C until imaging. Fixed cells were mounted with ProLong Diamond Antifade Mountant with DAPI (Life Technologies). Imaging was performed using an Axiophot fluorescence microscope (Zeiss) attached to a DP-70 Colour CCD camera (Olympus) with a 50 W mercury fluorescence excitation light source using either a blue or green filter cube for DAPI or

GFP respectively. Images were acquired using ImagePro 6 software suite (MediaCybernetics) and analyzed using ImageJ (NIH).

2.6.8 3'UTR luciferase reporter assay

The miR-183 binding site in a dual luciferase reporter containing the 3'UTR of protein phosphatase 2A catalytic subunit α was mutated using the QuikChange Lightning kit (Stratagene) as per the manufacturer's protocol with a primer designed to introduce a point mutation in the first nucleotide of the miR-183 seed sequence (FWD 5'-GGACCAAAAGATGTGCCTAATAAAAATACAAAGCC-3' and REV 5'-GGCTTTGTATTTTTATTAGGCACATCTTTTGGTCC-3'). Hek293 cells were seeded at 4 x 104 cells/well in 24-well plates and transfected 24 hours later with 500 ng/mL of either the wild-type or mutant 3'UTR construct as previously described. Twenty-four hours post-transfection, cells were transfected with Con-miR, miR-96, miR-182, miR-183 mimics as previously described. Forty-eight hours post-mimic transfection, cells were lysed in 1X passive lysis buffer (Promega) and the dual luciferase assay was carried out as previously described[36], using a SpectraMax L luminometer (Molecular Devices).

2.6.9 PPP2CA knockdown

HepG2 cells were reverse transfected in 10cm dish with 50nM control or miR-183 mimic. 24h post-transfection, cells were reseeded in a 12-well plate and then reverse transfected with 50nM siRNA targeting PPP2CA or control siRNA. 24h post siRNA transfection, cells were stimulated with Poly(I:C) Lyovec at 500ng/mL final concentration. 24h post-stimulation, cells were lysed in 1X SDS lysis buffer and prepared for immunoblotting.

2.6.10 Immunoblotting

After transfections, cells were washed twice with PBS and lysed with an SDS lysis buffer consisting of 50 mM Tris-HCl (pH 6.8), 2% SDS, and 10% glycerol. A protease inhibitor cocktail mix (Roche Diagnostics) was added to each extract. The protein concentration of each sample was quantified using the DC Protein Assay (Bio-Rad) according to the manufacturer's protocol. Prior to loading, 10% v/v of DTT and bromophenol blue (1:1) were added to each sample, and 40–60 μg/well was loaded onto an SDS–PAGE gel (10% resolving, 4% stacking gel). The resolved proteins were transferred to a Hybond-P PVDF membrane (Amersham Biosciences). The membrane was probed using the following primary antibodies and corresponding volume dilutions (in 3% w/vBSA); rabbit anti-STAT1, 1:1000 (Cell Signaling Technology, Beverly, MA, #9172); rabbit anti-phospho-STAT1 (Tyr701), 1:1000 (Cell Signaling Technology, #7649); rabbit anti-phospho-STAT1 (Ser727), 1:1000 (Cell Signalling Technology, #9177); rabbit anti-IRF3, 1:1000 (Santa Cruz Biotechnology, Dallas, TX, sc-9082) and anti-IRF3, 1:1000 (Cell signaling, #10949S) ; rabbit anti-phospho-IRF3 (Ser386), 1:1000 (EMD Millipore, Etobicoke, ON, ABE501) and rabbit anti-phospho-IRF3 (Ser386), 1:1000 (Abcam, ab76493) ; rabbit anti-PP2A (α/β catalytic subunit), 1:5000 (Abcam, ab32141); or rabbit anti-β-tubulin, 1:1000 (Santa Cruz Biotechnology, sc-9104) and anti- β-tubulin, 1:5000 (Abcam, ab6046). β-tubulin expression levels were used as loading controls. Membranes were then incubated with horseradish peroxidase (HRP)-conjugated goat anti-mouse or donkey anti-rabbit secondary antibodies (Jackson ImmunoResearch Laboratories, Westgrove, PA). Protein bands were visualized using either Amersham ECL Prime Western Blotting Detection Reagent (GE Healthcare, Ottawa, ON) or Clarity ECL Western Blotting Substrate (Bio-Rad) according to the respective manufacturer’s protocols, depending on antibody strength and background signal.

2.6.11 ISRE-Luciferase assay

Hek293T cells were reverse transfected with 50 nM control or miR-183 mimic in 10 cm dishes. 24 hours post-transfection with miRNA mimics, cells were reseeded in a 24-well plate and reverse transfected with 100 ng ISRE promoter-driven firefly luciferase reporter plasmid (ISRE-Luc), 50 ng of Renilla luciferase-expressing plasmid (pGL4, Promega), and 100 ng overexpression plasmids pcDNA3.1-TBK1-FLAG, pcDNA3.1-FLAG-IKBKE, or empty pcDNA3.1 as a negative control. 24 hours post-transfection, the cells were lysed with 1X passive lysis buffer (Promega) and dual-luciferase reporter assays were performed as previously described [36].

2.6.12 CRISPR activation and lentivirus generation

Hek293T cells in 10 cm dishes were transfected with packaging vectors pMD2.G (2 μg), psPAX2 (4 μg), and 6 μg transfer vector. Viral supernatant was collected 72 hours post-transfection, filtered (0.45μm), and used for transduction of HepG2 cells. HepG2 cells were lentivirally infected with dCas9-VP64 and MS2-p65-HSF1, and selected using blasticidin and hygromycin for >2 weeks; subsequently, cells were lentivirally infected with a non-targeting guide (NTC) or guides targeting the promoter of miR-183. Guides were annealed and cloned into lenti-sgRNA(MS2)_puro optimized backbone via the BsmBI sites. Five guides were tested for capacity to activate CRISPR activation-induced miR-183 cluster expression, and the top tested guide was identified using Taqman miRNA qPCR assays (cloned with oligos: FWD-CACCGAGGGCCTCCGTCCAGCCGCG and REV-AAACCGCGGCTGGACGGAGGCCCTC) was used for functional analysis of miR-183 cluster GOF. Non-targeting guide sequences (FWD: CACCGGCGAGGTATTCGGCTCCGCG; REV–AAACCGCGGAGCCGAATACCTCGCC) were used as a control.

2.6.13 Statistical analysis

Data are presented as the mean of replicates, with error bars representing the standard error of the mean. Unless otherwise stated, statistical significance was evaluated using a two-tailed Student's t-test, and P-values less than 0.05 were deemed significant.

2.7 Acknowledgments

We thank Dr. M.H. Powdrill (uOttawa) for useful discussions and help throughout the course of this work. mRNA microarray profiling was performed by The Centre for Applied Genomics (TCAG), The Hospital for Sick Children, Toronto, Ontario, Canada. R.S. is a recipient of training and funding from the Canadian Network on Hepatitis C (CanHepC), and funding from Vanier Canadian Graduate Scholarship and Ontario Graduate Scholarship. N.A. is supported by a NSERC Postgraduate Scholarship-Doctoral. C.Q. and P.S. were supported by NSERC Undergraduate Student Research Awards.

2.8 Conflict of interest

University of Ottawa has filed a patent on the miR-183 cluster's immunomodulatory properties in the name of John Paul Pezacki and Ragunath Singaravelu.

2.9 References

1. Kimbrell, G. A. & Beutler, B. The evolution and genetics of innate immunity. **2**, 256–267 (2001).
2. Fitzgerald, K. A. *et al.* IKKE and TBKI are essential components of the IRF3 signalling pathway. *Nat. Immunol.* **4**, 491–496 (2003).
3. Sharma, S. *et al.* Triggering the interferon antiviral response through an IKK-related pathway. *Science (80-.).* **300**, 1148–1151 (2003).
4. Onoguchi, K. *et al.* Viral infections activate types I and III interferon genes through a common mechanism. *J. Biol. Chem.* **282**, 7576–7581 (2007).
5. Forster, S. C., Tate, M. D. & Hertzog, P. J. MicroRNA as type I interferon-regulated transcripts and modulators of the innate immune response. *Front. Immunol.* **6**, 1–9 (2015).
6. Jonas, S. & Izaurralde, E. Towards a molecular understanding of microRNA-mediated gene silencing. *Nat. Rev. Genet.* **16**, 421–433 (2015).
7. Powdrill, M. H., Desrochers, G. F., Singaravelu, R. & Pezacki, J. P. The role of microRNAs in metabolic interactions between viruses and their hosts. *Curr. Opin. Virol.* **19**, 71–76 (2016).
8. O'Connell, R. M., Taganov, K. D., Boldin, M. P., Cheng, G. & Baltimore, D. MicroRNA-155 is induced during the macrophage inflammatory response. *Proc. Natl. Acad. Sci. U. S. A.* **104**, 1604–1609 (2007).
9. Sheedy, F. J. *et al.* Negative regulation of TLR4 via targeting of the proinflammatory tumor suppressor PDCD4 by the microRNA miR-21. *Nat. Immunol.* **11**, 141–147 (2010).
10. Taganov, K. D., Boldin, M. P., Chang, K. & Baltimore, D. NF-kappaB-dependent induction of microRNA miR-146, an inhibitor targeted to signaling proteins of innate immune responses. **103**, 12481–12486 (2006).
11. Oussaief, L. *et al.* Modulation of MicroRNA Cluster miR-183-96-182 Expression by. **89**, 12178–12188 (2015).
12. Singaravelu, R. *et al.* MicroRNAs regulate the immunometabolic response to viral infection in the liver. *Nat. Chem. Biol.* **11**, 988–993 (2015).
13. El Sobky, S. A. *et al.* Contradicting roles of miR-182 in both NK cells and their host target hepatocytes in HCV. *Immunol. Lett.* **169**, 52–60 (2016).
14. Chen, Y., Dong, X., Yu, D. & Wang, X. Serum miR-96 is a promising biomarker for hepatocellular carcinoma in patients with chronic hepatitis B virus infection. *Int. J. Clin. Exp. Med.* **8**, 18462–18468 (2015).
15. Stark, T. J., Arnold, J. D., Spector, D. H. & Yeo, G. W. High-Resolution Profiling and Analysis of Viral and Host Small RNAs during Human Cytomegalovirus Infection. *J. Virol.* **86**, 226–235 (2012).
16. Yu, H., Liu, Y., Bai, L., Kijlstra, A. & Yang, P. Predisposition to Behçet's disease and VKH syndrome by genetic variants of miR-182. *J. Mol. Med.* **92**, 961–967 (2014).

17. Singaravelu, R. *et al.* MicroRNA-7 mediates cross-talk between metabolic signaling pathways in the liver. *Sci. Rep.* **8**, 1–10 (2018).

18. Mitchell, A. M. *et al.* Transmitted hepatitis c viruses induce cell-type- and genotype-specific differences in innate signaling within the liver. *MBio* **6**, 1–11 (2015).

19. Li, P. *et al.* MiR-183/-96/-182 cluster is up-regulated in most breast cancers and increases cell proliferation and migration. *Breast Cancer Res.* **16**, 1–17 (2014).

20. Au-Yeung, N., Mandhana, R. & Horvath, C. M. Transcriptional regulation by STAT1 and STAT2 in the interferon JAK-STAT pathway. *Jak-Stat* **2**, e23931 (2013).

21. Wen, Z., Zhong, Z. & Darnell, J. E. Maximal activation of transcription by statl and stat3 requires both tyrosine and serine phosphorylation. *Cell* **82**, 241–250 (1995).

22. Agarwal, V., Bell, G. W., Nam, J.-W. & Bartel, D. P. Predicting effective microRNA target sites in mammalian mRNAs. *Elife* **4**, 1–38 (2015).

23. Long, L. *et al.* Recruitment of phosphatase PP2A by RACK1 adaptor protein deactivates transcription factor IRF3 and limits Type I interferon signaling. *Immunity* **40**, 515–529 (2014).

24. Zheng, Q. *et al.* Siglec1 suppresses antiviral innate immune response by inducing TBK1 degradation via the ubiquitin ligase TRIM27. *Cell Res.* **25**, 1121–1136 (2015).

25. Shanker, V., Trincucci, G., Heim, H. M. & Duong, H. T. F. Protein phosphatase 2A impairs IFNα-induced antiviral activity against the hepatitis C virus through the inhibition of STAT1 tyrosine phosphorylation. *J. Viral Hepat.* **20**, 612–621 (2013).

26. Joung, J. *et al.* Genome-scale CRISPR-Cas9 knockout and transcriptional activation screening. *Nat. Protoc.* **12**, 828–863 (2017).

27. Stittrich, A. B. *et al.* The microRNA miR-182 is induced by IL-2 and promotes clonal expansion of activated helper T lymphocytes. *Nat. Immunol.* **11**, 1057–1062 (2010).

28. Donatelli, S. S. *et al.* TGF-β-inducible microRNA-183 silences tumor-associated natural killer cells. *Proc. Natl. Acad. Sci. U. S. A.* **111**, 4203–4208 (2014).

29. Gough, D. J., Messina, N. L., Clarke, C. J. P., Johnstone, R. W. & Levy, D. E. Constitutive Type I Interferon Modulates Homeostatic Balance through Tonic Signaling. *Immunity* **36**, 166–174 (2012).

30. Dai, R. *et al.* Identification of a common lupus disease-associated microRNA expression pattern in three different murine models of lupus. *PLoS One* **5**, 1–8 (2010).

31. Clement, J.-F. *et al.* Phosphorylation of IRF-3 on Ser 339 Generates a Hyperactive Form of IRF-3 through Regulation of Dimerization and CBP Association. *J. Virol.* **82**, 3984–3996 (2008).

32. Stojdl, D. F. *et al.* VSV strains with defects in their ability to shutdown innate immunity are potent systemic anti-cancer agents. *Cancer Cell* **4**, 263–275 (2003).

33. Tremblay, N. *et al.* Spliceosome SNRNP200 Promotes Viral RNA Sensing and IRF3 Activation of Antiviral Response. *PLoS Pathog.* **12**, (2016).

34. Chen, J., Bardes, E. E., Aronow, B. J. & Jegga, A. G. ToppGene Suite for gene list

enrichment analysis and candidate gene prioritization. *Nucleic Acids Res.* **37**, 305–311 (2009).

35. Livak, K. J. & Schmittgen, T. D. Analysis of relative gene expression data using real-time quantitative PCR and the 2-ΔΔCT method. *Methods* **25**, 402–408 (2001).

36. Dyer, B. W., Ferrer, F. A., Klinedinst, D. K. & Rodriguez, R. A noncommercial dual luciferase enzyme assay system for reporter gene analysis. *Anal. Biochem.* **282**, 158–161 (2000).

Chapter 3

miR-383 regulates hepatic lipid homeostasis and response to Dengue virus infection

3.1 Preface

This chapter contains data and text previously published in ACS infectious disease as "Ahmed, N., Ahmed, N. & Pezacki, J. P. miR-383 Regulates Hepatic Lipid Homeostasis and Response to Dengue Virus Infection. ACS Infect. Dis. (2021) doi:10.1021/acsinfecdis.1c00470". This article was authored by Nadine Ahmed, Noreen Ahmed, and John Pezacki. The individual contributions are detailed below:

As the first author of this publication, I made significant experimental and intellectual contributions to this article. I as well as J. P. Pezacki have conceived the research and experimental plan for this study. I have performed the majority of the cell culture work, RNA isolations, qRT-PCR experiments, western blot sample preparation and analysis, virus experiments, ELISA assay, and microarray sample preparation and analysis. Noreen Ahmed aided with qRT-PCR experiments, 3'UTR assays, and western blot sample preparation and analysis. I wrote the initial manuscript and editing was performed by all authors.

3.2 Abstract

Recently, microRNAs (miRNAs), as endogenous non-coding RNAs that inhibit mRNA translation, have been identified to broadly possess functional roles in regulating cellular signaling and metabolic processes due to their chemical and biological properties. In addition, they have emerged to be of critical importance in modulating host-virus interactions, especially for RNA viruses. Herein, we discovered that miR-383-5p targets certain lipid and cholesterol biosynthetic pathways and restricts Dengue virus (DENV) infection in hepatic cells. Global transcriptomics analysis of Huh7 human hepatoma cells over-expressing miR-383-5p revealed enrichment of lipid and cholesterol metabolic processes. Bioinformatic analysis of genes repressed in miR-383-5p overexpressing cells divulged the repression of a key target PLA2G4A, a pro-viral host factor essential for the production of infectious DENV particles. Our study demonstrated the effectiveness of miRNA mimics as tools to study cellular signaling pathways that contribute to viral pathogenesis. Overall, our study identifies miR-383-5p as an interesting host factor during DENV propagation and highlights its role in the regulation of hepatic lipid metabolism response to DENV infection.

3.3 Introduction

Increasing evidence has highlighted the integral roles that microRNAs (miRNAs) play in modulating a wide range of cellular signaling and metabolic processes[1–3]. miRNAs are a class of highly conserved and abundant, small non-coding RNAs involved in post-transcriptional regulation of gene expression[4,5]. Generally, they perform their function by binding to the 3′untranslated region of target mRNAs to induce degradation and suppress translation [4,6]. These small molecules have been shown to regulate lipid metabolism, hepatic microenvironments, cancer-cell proliferation, innate immunity, and host-viral interactions[1,7–10]. Unlike small interfering RNAs (siRNAs), which are developed to target an individual gene, miRNAs have evolved to cooperatively target multiple genes, consequentially resulting in pronounced effects over a given pathway and acting as an additional regulatory layer[6]. Recently, several reports have revealed the involvement of miRNAs in modulating lipid metabolism in healthy and diseased livers[8,11–14]. Hepatic cells have been established as the site for *de novo* lipid synthesis and fatty acid oxidation and uptake[15]. Dysregulation and disruptions in such processes have been associated with pathological states such as non-alcoholic fatty liver disease, hepatic steatosis, and hepatocellular carcinoma development [16,17].

Many viruses, including Dengue viruses (DENV), have evolved to manipulate the host's metabolic processes and hepatic cellular microenvironments to promote and facilitate their life cycle and production of viral progeny[18–20]. For example, as an enveloped virus, DENV has evolved to rely on the host's lipid membranes and metabolome to promote their life cycle[21,22]. DENV is a member of the *Flaviviridae* family and it is the etiological agent for dengue hemorrhagic fever[23]. This RNA virus has been found to target the host's lipids and lipid metabolism to promote viral propagation. Thus, targeting lipid metabolic pathways has been highlighted as a potential antiviral and

therapeutic strategy against DENV[23]. In particular, DENV has been found to induce structural rearrangement of intracellular membrane compartments in human cells or Aedes Aegypti mosquitos' cells to promote viral replication and the eventual production of viral progeny[21,22]. Recent metabolomics studies in DENV-infected mosquito cells provide an example of metabolic alterations induced by DENV infection where infected mosquito cells have shown alterations in their phospholipid cellular profiles. In this case, lysophospholipids were found to be upregulated as a response to DENV infection[24]. This alteration in the metabolic profile was attributed to the virus-induced downregulation of AGPAT1, which is a rate-limiting enzyme of lysophospholipid synthesis[24]. Virus-induced alterations in the lipid metabolic states of the infected host cell can contribute to the establishment of a virus-favorable environment. Since miRNAs can play a role in regulating these pathways in a virus-dependent manner, a thorough understanding of the probable functions of miRNA in modulating the metabolic states of infected cells may aid in defining the etiology of viral infection and virus-induced metabolic modifications.

miR-383-5p (miR-383) is a miRNA that has been shown to inhibit hepatocellular carcinoma development, and this tumor suppressor function is correlated with the observed low abundance in carcinoma cells[25,26]. In addition to its known role in modulating carcinogenesis, miR-383 expression levels have been found to be dysregulated as a response to free fatty acid treatment of primary mouse hepatocytes and additionally have been implicated in insulin signaling[27]. Moreover, previous work has revealed the dysregulation of miR-383 in the blood of patients with mild dengue infections relative to severe infections[28]. Taken together, these observations suggest an important role for miR-383 during DENV infection in humans. Thus, we sought to investigate the potential role of miR-383 in modulating hepatic homeostasis and its role in regulating DENV pathogenesis.

Herein, we show that DENV infection upregulates the expression of miR-383 and miR-383 overexpression impairs DENV infection in hepatic cells. Interestingly, genome-wide gene expression profiling of miR-383 expressing Huh7 cells reveals enrichment of lipid and cholesterol metabolic processes. However, we were able to identify key targets for miR-383 that include PLA2G4A, which offers an explanation for miR-383's role in DENV infection. Thus, miR-383 mimics have the potential as a therapeutic option for DENV and aid in the identification of regulatory nodes that can be therapeutically targeted for antiviral properties.

3.4 Results

3.4.1 miR-383 modulates DENV infection in hepatic.

DENV infection in human cells appears to correlate with dysregulation of miR-383 in clinical samples from patients with DENV infection [28]. Given this, we hypothesize that miR-383 may have a functional role in modulating cellular processes during DENV infection. Thus, we sought to investigate the effects of DENV infection on the transcriptional levels of miR-383. This allows us to evaluate whether miR-383 plays a functional role in the liver during viral infection and virus-induced metabolic stress. We first evaluated the levels of the miR-383 following infection with DENV serotype 2 strain (DENV-2) in Huh7 hepatoma cell line. In order to examine this, we infected Huh7 cells with DENV at an MOI of 0.1. Consistent with the clinical findings, 48h post-infection we observed an approximately 4-fold increase in the level of miR-383 (Figure 3.1A). Next, we sought to investigate the effects of miR-383 overexpression on DENV replication and infectivity. Thus, we transfected Huh7 with miR-383 mimics, 24h post-transfection, cells were infected DENV-2 at an MOI 0.1. qRT-PCR analysis of intracellular DENV-2 revealed an approximately 50% decrease in viral RNA levels in miR-383 transfected cells relative to con-miR transfected cells, and a consequential decrease in infectivity and viral titers were as well observed (Figure 3.1B, S3.1). Conversely, inhibition of endogenous levels of miR-383 results in a statistically significant increase in the levels of intracellular levels of the virus (Figure 3.1B). Taken together, these findings suggest that miR-383 overexpression may act to restrict DENV levels, possibly by repressing one or more host factors that are needed by the virus to successfully propagate in the host cell. To further examine whether the antiviral effects exerted by miR-383 are selective, we transfected huh7 cells with miR-383 mimics and subsequently infected the cells with Vesicular Stomatitis Virus (VSV). Interestingly, miR-383 did not inhibit the intracellular levels of

VSV relative to con-miR transfected cells (Figure S3.2), suggesting there is a degree of selectivity to the antiviral potential of miR-383. Taken together, these findings suggest that miR-383 overexpression may act selectively to restrict DENV levels, possibly by repressing one or more host factors that are essential to its propagation in the host cells.

3.4.2 miR-383 regulates the Hepatic lipid microenvironment

In order to gain insight into the effects of miR-383 on regulating hepatic pathways and antiviral DENV restriction mechanisms in hepatic cells, we performed microarray gene expression profiling analysis in Huh7 cells transfected with con-miR or miR-383 mimics. Bioinformatics analysis via ToppGeneSuite [29] was performed to identify pathways enriched by miR-383. Genome-wide expression profiling reveals that miR-383 overexpression modulates the expression of several genes associated with cholesterol and fatty acid metabolic processes. Interestingly, gene ontology enrichment analysis of genes up-regulated ≥1.5 folds revealed the enrichment of biological processes involved in lipid and sterol metabolic processes in cells overexpressing miR-383 in infected and uninfected conditions (Figure 3.1C and S3.3), respectively and (Table S3.1 and S3.2), respectively. In order to further validate that miR-383 was upregulating lipid metabolism and consequently lipid accumulation, we performed microscopy studies. Consistent with gene expression profiles, Oil-Red O staining of Huh7 cells overexpressing miR-383 further confirmed hepatic lipid accumulation (Figure 3.1D). Collectively, these data confirm that miR-383 has a functional role in controlling hepatic cellular metabolism and homeostasis and this effect on metabolism may be related to its misregulation observed in these cells.

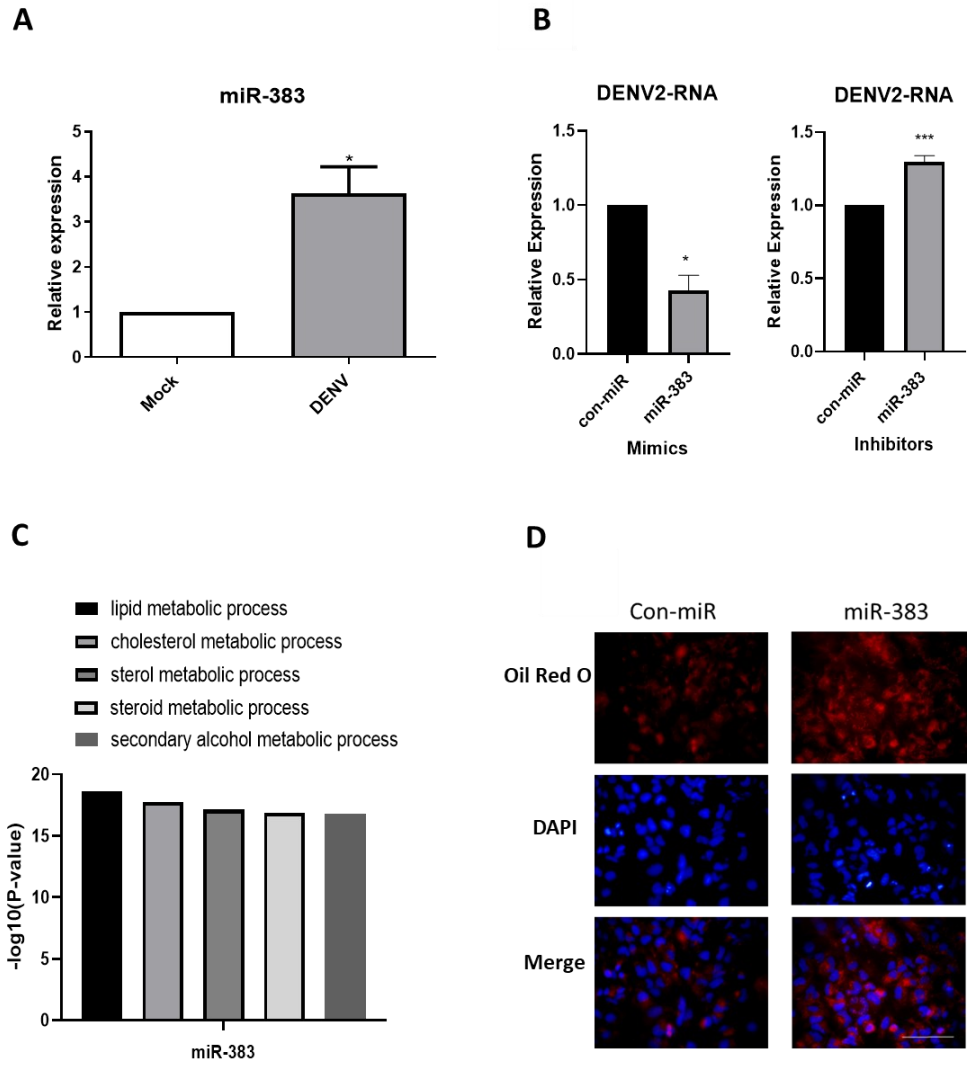

Figure 3.1. miR-383 overexpression modulates DENV life cycle and metabolic processes in hepatoma cells. (A) Huh7 cells were either mock-infected or DNEV-2 infected, 48h post infection cells were lysed and levels of mature miR-383 were evaluated. (B) Huh7 cells were either transfected with con-miR or miR-383 mimics or inhibitors, 24h post-transfection cells were infected with DENV at an MOI of 0.1. 48h post infection cells were lysed and RNA analysis on intracellular DENV levels was performed C) Gene ontology analysis classifying activated genes (≥1.5-fold increase) in miR-383 transfected and non-infected Huh7 cells. The top five gene ontology terms are all related to lipid and cholesterol metabolic processes. D) Oil red O staining of cellular lipid content in con-miR and miR-383-mimic-transfected Huh7 cells. Cells were visualized using fluorescence microscopy. (Oil Red O-Red, DAPI-Blue) Scale bar, 100 μm.

3.4.3 miR-383 enhances SREBP2 signaling

Next, we sought to investigate miR-383-enriched pathways due to their relevant role in the modulation of host-virus interaction, and dysregulation in enzymes involved in these pathways has been reported to affect DENV pathogenesis[30,31]. According to our transcriptomics analysis, miR-383 enhances sterol metabolic processes. Based on this, we hypothesize that miR-383 enhances the activation of sterol regulatory element-binding protein 2 (SREBP2) regulated pathways. SREBP2 is primarily responsible for the activation of genes involved in cholesterol biosynthesis[32]. Therefore, we sought to examine the list of upregulated genes from our microarray experiments for genes known to be regulated by SREBP2. SREBPs expression has been shown to be autoregulated[33–35], therefore we hypothesize that an increase in the levels of SREBP2 mRNA transcripts and its targets should be observed with the miR-383-directed augmentation of SREBP2 signaling pathway. SREBP2 activates the expression of HMG-CoA reductase (HMGCR), Lanosterol synthase (LSS), and mevalonate kinase (MVK) all of which are genes essential for the biosynthesis of cholesterol, and as expected these genes were upregulated by miR-383. RT-qPCR confirmed the upregulation of SREBP2 and SREBP2-regulated genes (SREBP2, HMGCR, LSS, MVK and SQLE) in miR-383 transfected cells in non-infected and infected cells (Figure 3.2A and Figure S3.4A). Furthermore, we were able to show a consistent increase in the protein levels of SREBP2 and several SREBP2 targets in miR-383 transfected cells relative to con-miR transfected cells (Figure 3.2B, Figure S3.5). Interestingly, DENV infection does not significantly alter the transcriptional levels of SREBP2-regulated genes (Figure S3.6), suggesting that DENV modulates cholesterol cellular microenvironments through primarily altering the activity of the involved enzyme as previously documented[30,31]. Previous *in vitro* studies have suggested that DENV infection primarily induces cholesterol synthesis by upregulation of the enzymatic activity of

HMG-CoA reductase activity[30]. In addition, it is important to note that although DENV induces approximately 4-fold upregulation of miR-383 expression (Fig 3.1A), these levels are relatively lower than the amounts of miRNA present post-transfection of exogenous miRNA mimics[36–38]. Thus, it is not surprising that miR-383-specific changes in cholesterol metabolism post-mimic transfection are enhanced relative to the effects observed as a response to miR-383 level changes induced by DENV infection. Furthermore, DENV infection results in alteration in the transcriptional profile of a multitude of host factors in the infected cells[39,40], which may dilute or counteract the effects of miR-383 on the affected pathways, as a mechanism to evade the anti-viral host responses, in comparison to direct transient transfection of miR-383 mimics in the cells.

To evaluate the effects of endogenous miR-383 on the SREBP2-modulated pathway, we utilized miR-383 inhibitors to suppress the endogenous functional miRNAs. Interestingly, upon transfection of Huh7 cells with miR-383 inhibitors, we observed a decrease in the levels of SREBP2 and SREBP2-regulated genes (Figure 3.2C). Collectively, these findings confirm that miR-383-induced activation of SREBP2 signaling contributes to the observed enrichment of sterol metabolic processes in miR-383 overexpressing cells, and conversely suppressing the endogenous levels of miR-383 antagonizes these processes. To determine how miR-383 affects SREBP2, we examined the list of genes that are downregulated ≥ 1.5-fold in the microarray for negative regulators of SREBP2 signaling, since miRNAs function generally as repressors of mRNA translation. Interestingly, we identified RNF145, a ubiquitin E3 ligase that inhibits SREBP2 processing and function[41]. To further validate the functional role of RNF145 in negatively regulating the SREBP2-modulated pathway, we transfected Huh7 cells with siRNA targeting RNF45 and subsequently tested the effect of the knock-down on the transcription of SREBP2 and SREBP2-modulated genes. As expected and consistent with previous reports, with the knockdown

of RNF145, we observed a statistically significant increase in the levels of SREBP2 transcriptional levels and SREBP2 targets (Figure S3.7A and S3.7B)[41]. Given this, we next evaluated the effect of miR-383 overexpression on the levels of RNF145. RT-qPCR confirmed the downregulation of RNF145 levels in miR-383 transfected cells in non-infected and infected cells (Figure 3.2 D and Figure S3.4B). Conversely, treating the cells with miR-383 inhibitors resulted in a modest but statistically significant increase in the levels of endogenous RNF145 levels (Figure 3.2E). Furthermore, DENV infection in naïve cells results in modest but statistically significant downregulation of RNF145 levels (Figure S3.7C). To examine the mechanism by which miR-383 regulates RNF145 levels, we sought to evaluate whether miR-383 directly targets RNF145 for degradation and translational repression. Although RNF145 3'UTR lacks seed site complementarity with miR-383, we have shown that miR-383 targets RNF145 3'UTR using a 3'UTR assay (Figure 3.2F). These findings suggest that miR-383 likely represses RNF145 through non-canonical interactions to suppress its expression. Therefore, miR-383-induced suppression of RNF145 levels likely contributes to the observed upregulation of SREBP2 activity.

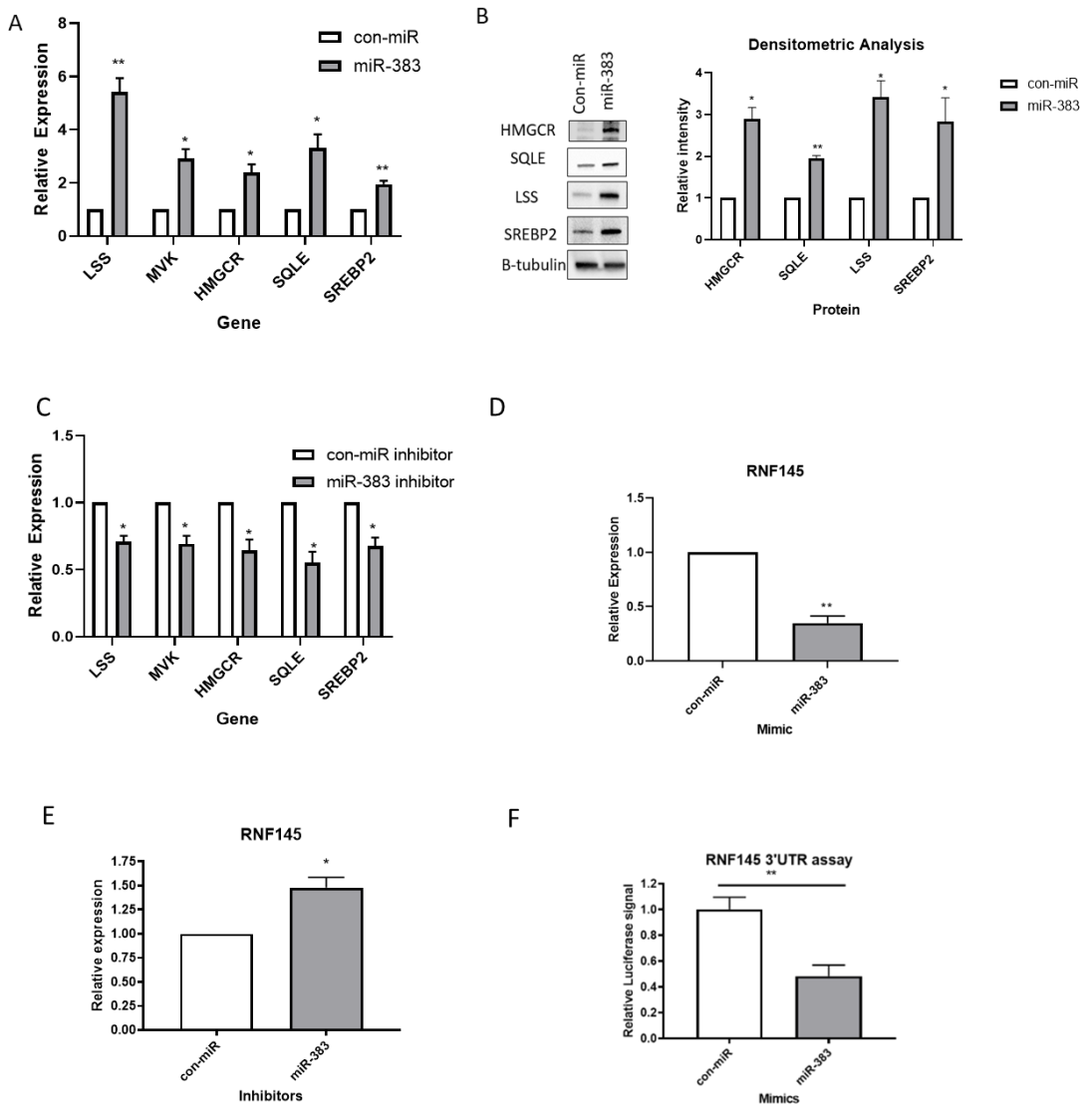

Figure 3.2. miR-383 regulates SREBP2-activated signaling. A) Huh7 cells were either transfected with con-miR or miR-383, 72h post-transfection, cells were lysed for RNA analysis. RT-qPCR was performed on SREBP2 target genes. B) Western blot and densitometric analysis of SREBP2 and SREBP-2 target protein levels in con-miR or miR-383 transfected Huh7 cells. C) Huh7 cells were either transfected with con-miR or miR-383 inhibitors. 72h post-transfection, cells were lysed for RNA analysis. RT-qPCR was performed on SREBP2 target genes. D) levels of RNF145 are reduced in miR-383 mimics transfected cells relative to con-miR mimics transfected cells. E) levels of RNF145 are increases in miR-383 inhibitors transfected cells relative to con-miR inhibitor transfected cells. F) 3'UTR assay validating RNF145 as a miR-383 target. Error bars represent the means ±SEM of three biological replicates and five independent biological replicates for MVK and SREBP2 in figure A *P<0.05 and **P<0.01.

3.4.4 miR-383 modulates the expression of lipid metabolism-associated genes

Since lipid accumulation is another phenotype observed with miR-383 overexpression, we sought to uncover the mechanism by which miR-383 results in the enhancement of lipid and triglyceride accumulation in hepatic cells. Given that sterol regulatory element–binding protein-1c (SREBP-1c) is a master regulator of lipogenesis, we hypothesize that miR-383 enhances the activity of SREBP1c to transcriptionally regulate lipogenic and lipid metabolism-associated genes to promote cellular lipid and triglyceride accumulation. SREBP1c is known to regulate the expression of various enzyme that catalyzes various steps in fatty acid and triglyceride synthesis pathways[42–44]. RT-qPCR analysis confirmed the upregulation of SREBP1c regulated genes which include fatty acid synthase (FASN), Acetyl-coA carboxylase (ACACA) and glycerol-3-phosphate acyltransferase 1 (GPAT1 or GPAM), a rate-limiting enzyme of triglyceride biosynthesis in non-infected and infected cells (figure 3.3A and 3.3B, respectively). Interestingly, SREBP1c transcriptional levels were as well upregulated, which suggests that the upregulation of SREBP1c levels induced by miR-383 overexpression is potentially the molecular mechanism that contributes to the accumulation of cellular lipids and triglycerides in hepatic cells. Additionally, as previously discussed, SREBPs have been found to be autoregulated[34,35], thus an increase in SREBP1c activity will increase the levels of mRNA as well. Western blot analysis of cells treated with miR-383 mimics confirmed upregulation of SREBP1c targets (GPAM, ACACA and FASN) relative to con-miR-treated cells (Figure 3.3C and Figure S3.8). Interestingly, qRT-PCR analysis of DENV-infected cells was found to modestly upregulate the expression of FASN and SREBP1c (Figure S3.9). Furthermore, in order to evaluate the effects of endogenous miR-383 on the regulation of SREBP1c-regulated genes, we utilized miR-383 inhibitors. Upon transfection of the cells with miR-383 inhibitors, we observed a statistically significant decrease in the levels of SREBP1c,

FASN, ACACA, and GPAM (Figure 3.3D). Overall, these findings highlight that miR-383-induced activation of SREBP1c signaling contributes to the observed enrichment of lipid metabolic processes in miR-383 overexpressing cells.

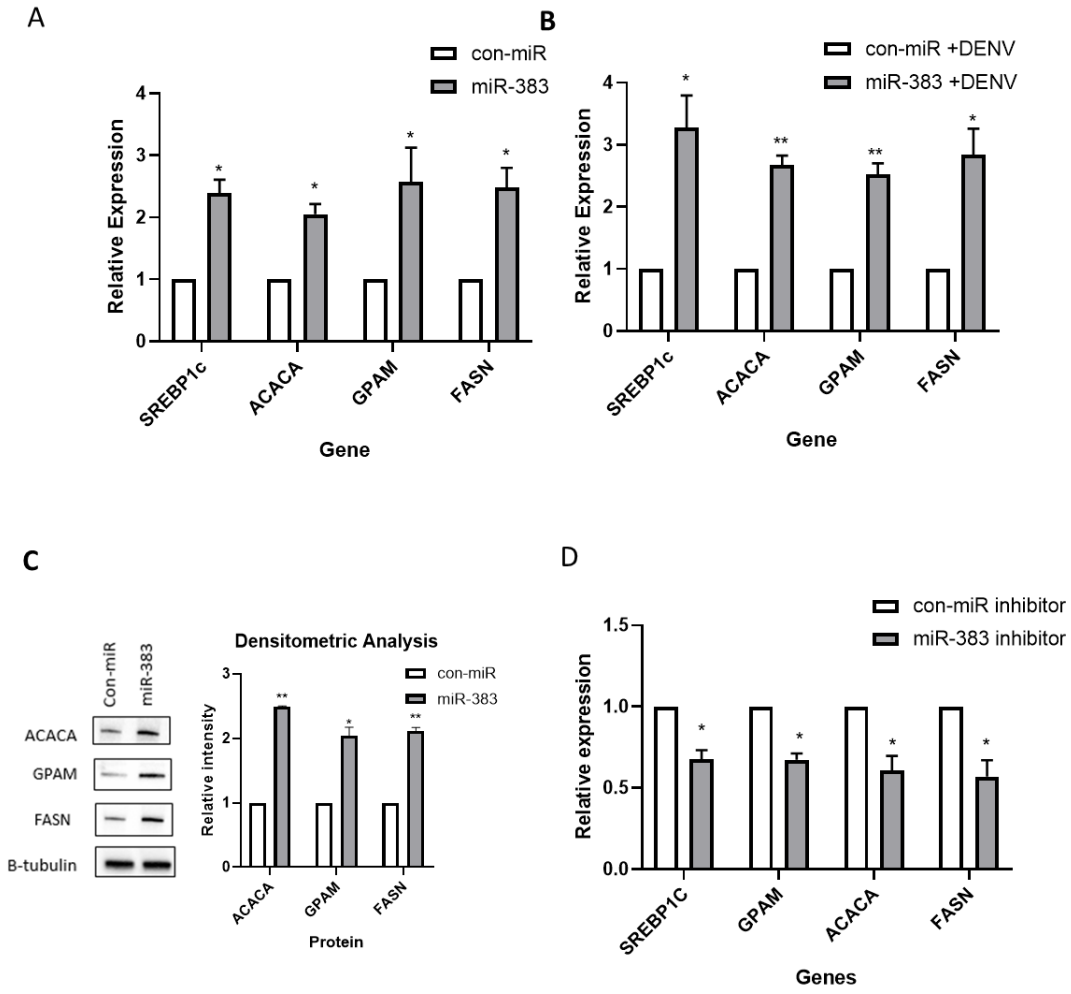

Figure 3.3 miR-383 enhances cellular lipid accumulation and modulates the expression of lipid metabolism associated genes. A) Huh7 cells were either transfected with con-miR or miR-383, 72h post-transfection, cells were lysed for RNA analysis. RT-qPCR was performed on lipid metabolism associated genes. B) Huh7 cells were either transfected with con-miR or miR-383. 24h post-transfection cells were infected with DENV at MOI of 0.1. 48h post infection cells were lysed for RNA analysis and RT-qPCR was performed on lipid metabolism associated genes. c) Western blot and densitometric analysis of ACACA, GPAM and FASN protein levels in con-miR or miR-383 transfected Huh7 cells. D) Huh7 cells were either transfected with con-miR or miR-383 inhibitors. 72h post-transfection, cells were lysed for RNA analysis SREBP1C and SREBP1C target genes levels were evaluated. Error bars represent the means ±SEM of three independent biological replicates and five independent biological replicate for GPAM in figure A *P<0.05, **P<0.01.

3.4.5 miR-383 represses PLA2G4A to elicit an antiviral phenotype

Confounding our analysis is the fact that lipid accumulation usually gives rise to an enhanced cellular environment for DENV and related viruses[45,46]. To elucidate the mechanism by which miR-383 enhances the lipid cellular microenvironment yet still restricts DENV infection, we sought to identify direct targets of miR-383 in Huh7 cells that may act to restrict DENV infection. Firstly, we again examined our global transcriptomics analysis and assessed the overlap between miR-383 predicted targets from the target scan and the genes whose expression was downregulated by miR-383 mimic transfection in Huh7 cells (≥1.5 folds) [47]. This produced a list of around 382 genes (Figure 3.4A and Table S3.3). We further examined the list of genes to identify genes and host factors previously described to be exploited DENV to promote pathogenesis (Table S3.3). Among the genes identified, miR-383 repressed the levels of PLA2G4A by around 3-fold in the global transcriptomics PLA2G4A encodes cytosolic phospholipase A2 (cPLA2) which is an enzyme that catalyzes the hydrolysis of the sn-2 acyl bond of glycerolipids to release arachidonic acid (Figure 4B) [48,49]. This enzyme has been found to be essential for the modulation of cellular membrane functions and interestingly has been identified as a crucial Hepatitis C virus (HCV) and DENV host dependency factor which is essential for the production of infectious viral progeny[48]. Interestingly, DENV infection results in a decrease in the levels of PLA2G4A, which might suggest that this decrease is a host's response to infection (Figure S3.10).

To validate that PLA2G4A mRNA levels are altered during miR-383 overexpression, we performed RT-qPCR. RT-qPCR analysis of the levels of PLA2G4A in lysates obtained from Huh7 cells overexpressing miR-383 validated the repression of PLA2G4A in miR-383 over-expressing cells (figure 3.4C). Conversely, an increase in the levels of PLA2G4A was observed in miR-383 inhibitor-treated cells (figure 3.4D). In conjunction with the changes in the transcriptional levels

of PLA2G4A, we observed a decrease in the abundance cPLA2 protein levels in lysates obtained from cells over-expressing miR-383 (figure 3.4E and Figure S3.11). Additionally, we evaluated the levels of active cPLA2 in miR-383 over-expressing huh7 cells. As expected, we confirmed that miR-383 decreases both the abundance and activity of cPLA2 (Figure 3.4E and 3.4F). Since phosphorylation of cPLA2 by MAPK at Ser505 stimulates its catalytic activity[50,51], we sought to evaluate the phosphorylation state of cPLA2 to report on the levels of active cPLA2 in miR-383 over-expressing cells. Western blot analysis revealed a downregulation of the levels of phosph-cPLA2 in miR-383 expression cells relative to con-miR transfected cells in infected and non-infected cells (Figure 3.4E). These data provide key mechanistic information regarding how miR-383 may be giving rise to an antiviral effect against DENV and possibly modulating an antiviral response against other flaviviruses as well.

Next, we sought to evaluate whether miR-383 directly targets PLA2G4A for degradation and translational repression. We examined the 3'UTR for a potential miR-383 putative site, and we were able to identify a potential binding site in PLA2G4A 3' UTR (Figure 3.5A). We then validated PLA2G4A, using a 3` UTR assay, as a direct target of miR-383 (Figure 3.5B and 3.5C), where 2 nucleotides in the 3'UTR binding site were mutated. When the cells were co-transfected with miR-383 mimics and the WT 3'UTR plasmid, a decrease in luciferase signal was observed and a rescue of the signal was detected in cells transfected with the mutated 3'UTR plasmid (Figure 3.5B). Conversely, when miRNA inhibitors were co-transfected with the WT 3'UTR PLA2G4A plasmid, an increase in the luciferase signal was observed and no observed change when the 3'UTR complementary site is mutated (Figure 3.5C). Overall, these results reveal that miR-383 represses the levels of PLA2G4A by directly targeting its 3'UTR. Finally, we quantified the levels of intracellular arachidonic acid in cells overexpressing miR-383, and as expected, a decrease in the

levels of arachidonic acid was observed (Figure 3.5D). collectively, these findings further confirm that miR-383 modulates the anti-DENV effects by targeting a viral dependency factor, PLA2G4A, which has been confirmed to be essential for DENV infection.

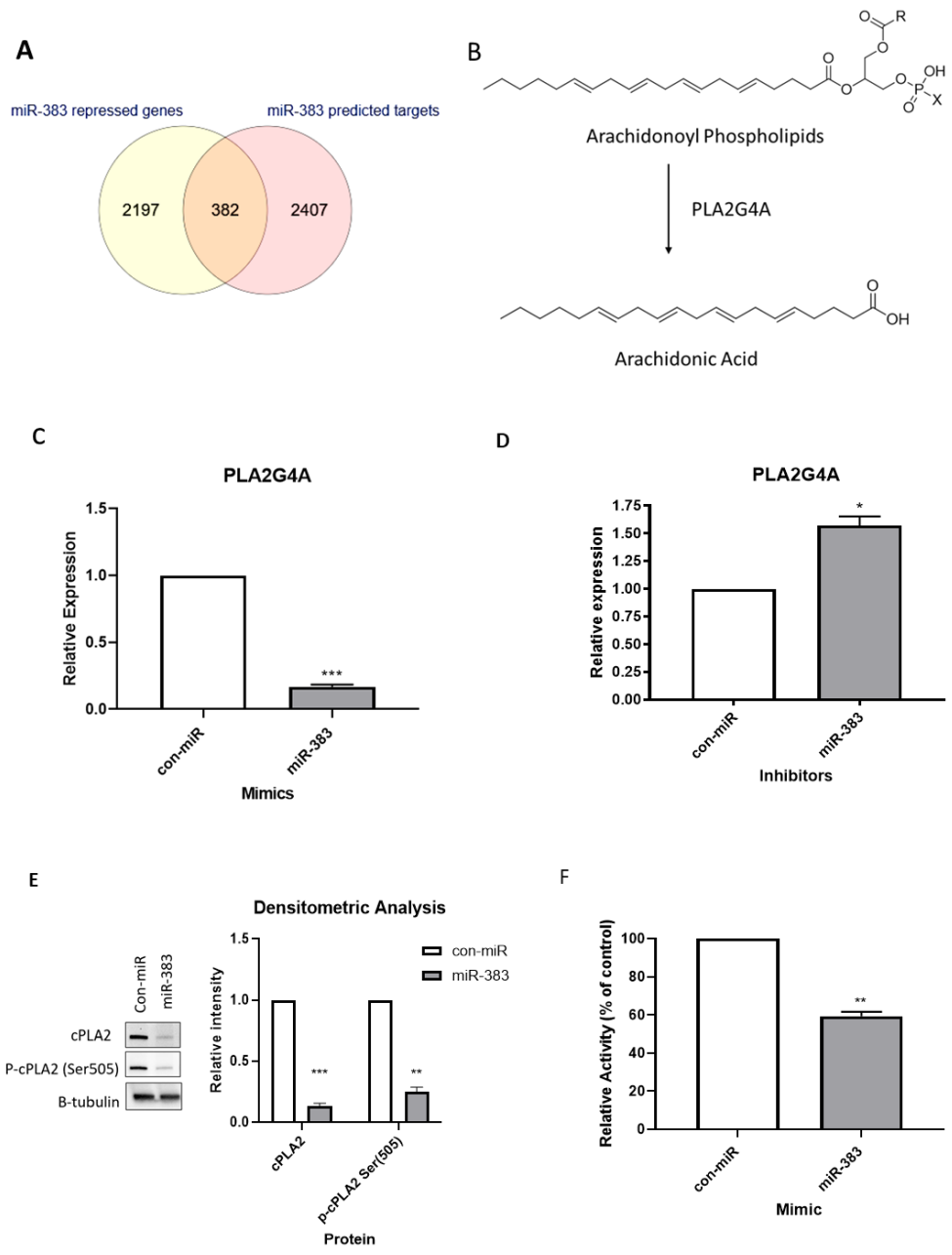

Figure 3.4. miR-383 represses PLA2G4A to elicit antiviral phenotype. (A) Venn diagram visualizes overlap between miR-383 predicted targets and genes repressed in miR-383 mimic transfected Huh7 cells (B) a representation of the reaction catalyzed by PLA2G4A (cPLA2).(c) qRT-PCR analysis of PLA2G4A levels in miR-383 and con-miR transfected cells. (D) qRT-PCR analysis of PLA2G4A levels in miR-383 and con-miR inhibitor transfected cells. (E) Western blot analysis and densitometric of PLA2G4A (cPLA2) and phspho-PLA2G4A Ser(505) (p-cPLA2) in con-miR and miR-383 transfected huh7 cells.(F) relative cPLA2 enzyme activity in con-miR and miR-383 transfected Huh7 cells. Error bars represent the means ±SEM *P<0.05, **P<0.01, ***P<0.001.

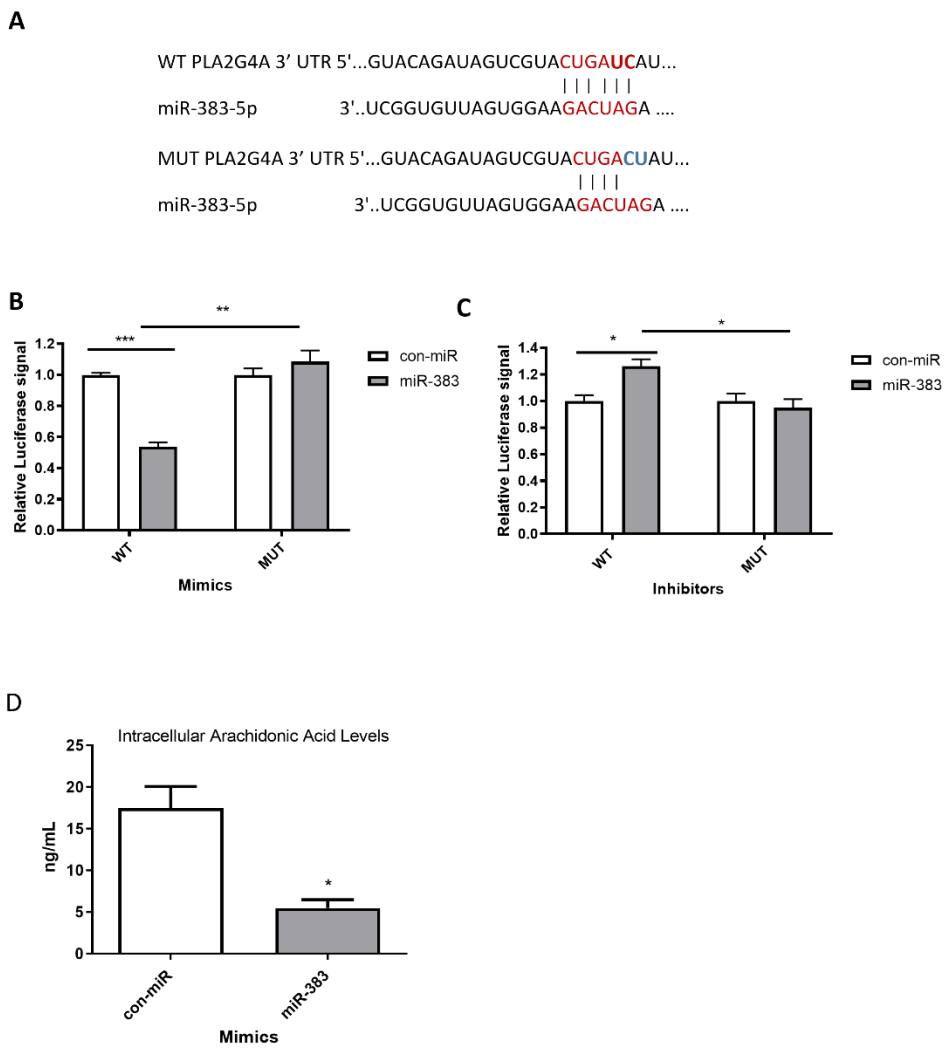

Figure 3.5. miR-383 directly targets PLA2G4A and results in decrease in intracellular Arachidonic acid Levels. A) 3'UTR of PLA2G4A and complementary sequences in miR-383 seed sites indicating the mutated nucleotides in the MUT PLA2G4A 3'UTR sequence. B) 3'UTR assay validating PLA2G4A as a miR-383 target using miR-383 mimics C)3'UTR assay validating PLA2G4A as a miR-383 target using miR-383 inhibitors. D) ELISA assay quantifying the levels of intracellular Arachidonic acid in cells transfected with con-miR or miR-383 mimics. Error bars represent the means ±SEM *P<0.05, **P<0.01, ***P<0.001.

3.4.6 Arachidonic acid (AA) restores DENV levels in miR-383 over-expressing cells.

Arachidonic acid has been previously implicated in DENV and flavivirus pathogenesis [48]. In order to further validate whether the anti-viral effects observed in miR-383 overexpressing is due to the suppression of PLA2G4A levels and consequential decrease in the endogenous levels of cellular arachidonic acid, we supplemented the media of miR-383 or con-miR transfected cells with 50uM arachidonic acid following DENV infection. Interestingly, DENV levels were restored in miR-383 transfected cells supplemented with arachidonic acid (Figure 3.6A). qRT-PCR analysis confirmed the repression of PLA2G4A levels in miR-383 transfected cells, treated and non-treated with arachidonic acid (Figure 3.6B). To validate the involvement of PLA2G4A in modulating the antiviral effects in miR-383 overexpressing cells, we performed siRNA knockdown experiments to suppress the endogenous levels of PLA2G4A in huh7 cells during DENV-2 infection. We first validated the successful knock-down of PLA2G4A levels using RT-qPCR (Figure 3.6C). Next, we confirmed a decrease in the levels of intracellular DENV-2 levels in knockdown cells relative to control-siRNA transfected cells (Figure 3.6D). These data further confirm that the antiviral effects of miR-383 overexpression are mediated by the repression of the levels of PLA2G4A and arachidonic acid.

3.4.7 miR-383-directed decrease in the levels of unsaturated fatty acids (AA) and PLA2G4A contributes to the enhancement of SREBP1c-dependent gene transcription.

Next, we sought to evaluate the effects of arachidonic acid depletion mediated by the decrease of PLA2G4A levels and activity in miR-383 over-expressing cells. Previous studies have confirmed the negative regulatory and inhibitory effects of unsaturated fatty acids, in particular arachidonic acid, on the levels and function of SREBP1c in cultured rat hepatoma cells[52]. Consistent with this, western blot analysis of miR-383 transfected cells confirmed the decrease in the levels of PLA2G4A, as we have previously demonstrated in (Figure 3.4E). Additionally, in miR-383 transfected samples, we confirmed the upregulation of FASN and ACACA and GPAM, SREBP1c-regulated genes (Figure 3.3C). To further validate the involvement of PLA2G4A in the modulation of SREBP1c-modulated signaling, we evaluated the expression levels of SREBP1C and FASN in PLA2G4A siRNA-transfected cells relative to control siRNA-transfected cells. As expected, FASN and SREBP1C expression is enhanced in PLA2G4A-siRNA transfected cells (Figure S3.12). Collectively, these findings suggest that a decrease in PLA2G4A abundance likely contributes to the enrichment of lipogenesis and SREBP1C-regulated signaling in miR-383 over-expressing Huh7 cells.

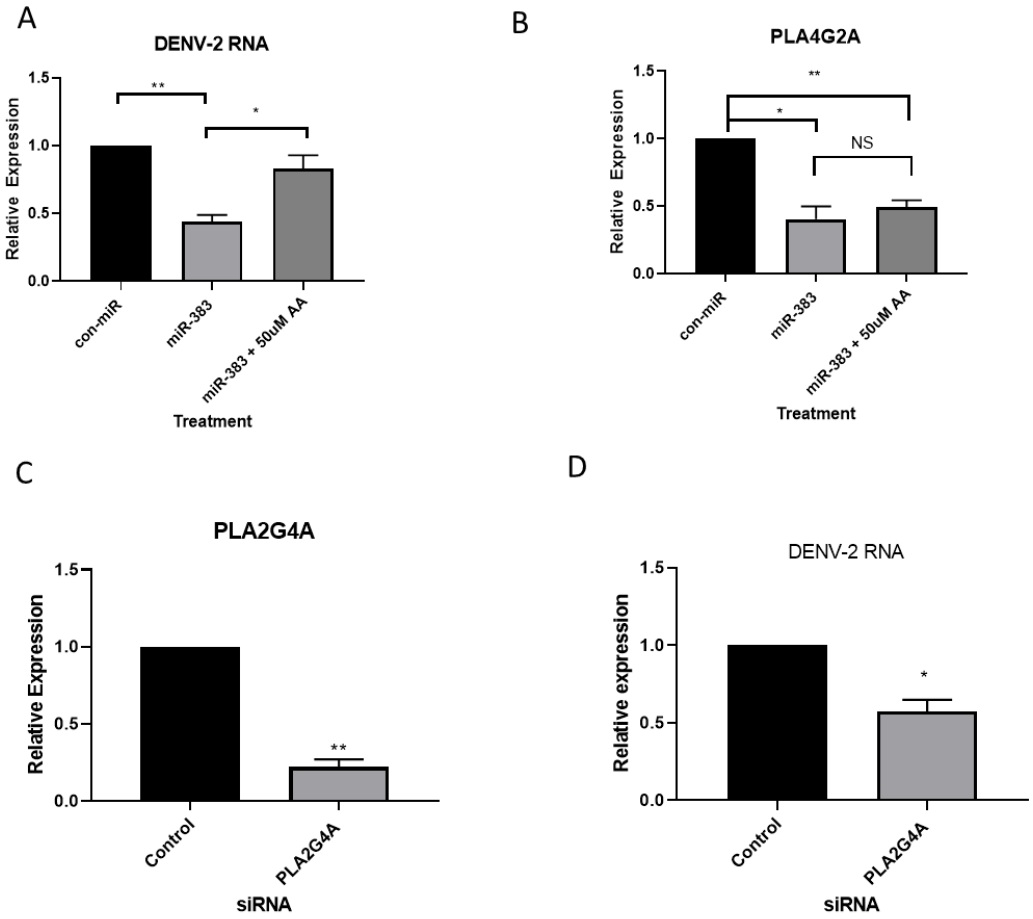

Figure 3.6 miR-383-directed decrease in the levels of unsaturated fatty acids (AA) and PLA2G4A levels contributes to the decrease in DENV levels. (A) qRT-PCR analysis of DENV-2 levels (B) and PLA2G4A levels in con-miR or miR-383 transfected huh7 cells following AA or vehicle treatment (c) qRT-PCR analysis of PLA2G4A in PLA2G4A siRNA and control siRNA treated cells (D) qRT-PCR analysis of DENV2 levels in PLA2G4A siRNA and control siRNA treated. Error bars represent the means ±SEM of at least 3 independent biological replicates. *P<0.05, **P<0.01.

3.5 Discussion

Recent advances in noncoding RNA research have uncovered the importance of the additional regulatory layer that miRNAs introduce to biological processes and cellular functions[53]. Several miRNAs have been found to possess regulatory importance in modulating metabolic pathways and antiviral mechanisms[7,54]. A significant example is underlined by the discovery of miR-122 and its role in regulating HCV replication[9,55]. In addition to its known importance in HCV life cycle, it has been as well found to regulate hepatic lipid metabolism and cholesterol biosynthesis[13]. Several studies have also uncovered the dysregulation in the human miRNA profiles in DENV-infected patients[28,56]. For example, Tambyah *et al*. identified 348 miRNAs that are differentially expressed in different cohorts of DENV patients. Interestingly, they highlighted a few miRNAs differentially dysregulated among patients displaying mild and severe secondary complications related to the infection. These miRNAs could potentially be utilized to distinguish mild DENV from severe DENV complications[28]. Furthermore, several other miRNAs have been shown to regulate different metabolic processes such as fatty acid oxidation, lipid biosynthesis, and lipid excretion which are essential for the maintenance of hepatic homeostatic balance[2,12].

In our study, we have shown that miR-383 plays a significant role in modulating hepatic lipid homeostasis and response to DENV infection. We firstly evaluated the effects of infection on the expression of miR-383. Interestingly, we have shown that miR-383 expression is induced by DENV infection. Thus, we assessed the effects of miR-383 overexpression on DENV infection, and interestingly miR-383 decreases the levels of intracellular viral RNA load and modestly affects viral titer. We, additionally, sought to evaluate whether the miR-383-induced antiviral effects observed are selective towards DENV. To address this, we infected miR-383 transfected Huh7 cells with VSV and found that miR-383 does not restrict the levels of VSV relative to con-miR-

transfected cells (Figure S3.2). This suggests that miR-383 is a host factor that is induced upon infection and selectively acts on restricting DENV viral infection. Secondly, to gain insight into the mechanism by which miR-383 restricts DENV pathogenesis, we performed a global transcriptomics analysis to evaluate the effects of miR-383 on gene expression.

Based on gene ontology analysis of miR-383 over-expressing cell profiles, there was an enrichment of cholesterol and lipid metabolic processes. Given that cholesterol and lipid metabolism is implicated in DENV pathogenesis, we decided to further investigate these pathways and their modulation by miR-383. In our study, we show that enhancement of cholesterol metabolic processes is attributed to the miR-383-induced reduction in the levels of RNF145, a ubiquitin ligase found to negatively regulate the cholesterol biogenesis pathway[41]. We as well have shown that SREBP1c targets are upregulated by miR-383 overexpression, and this contributes to hepatic lipid accumulation. Although in our study we focus on SREBP2 and SREBP1c regulated processes, due to their known role in the regulation of metabolic processes in the liver[32], it is essential to note that miR-383 potentially affects pathways that could be regulated by other factors known to regulate lipogenesis in the hepatic cells [57]. These factors could be of interest for future investigations.

In addition to miR-383-modulated changes in metabolic pathways, we have shown that miR-383 directly targets PLA2G4A, a gene expressing a MAP-K regulated phospholipase (cPLA2) which is a pro-viral host factor that contributes to HCV and DENV pathogenesis[48]. cPLA2 catalyzes the hydrolysis of the sn-2 acyl bond of glycerolipids to produce lysophospholipids and release arachidonic acid; a mechanism that has been previously reported to promote flavivirus pathogenesis [48,49]. Previous reports have shown that arachidonic acid results in an increase in membrane fluidity[58]. This could alter several stages of the viral life cycle, which include the

budding and trafficking of viral proteins essential for propagation. Thus, we further examined the functional consequences of arachidonic acid depletion mediated by a miR-383-directed decrease in the levels of PLA2G4A on DENV levels. Upon supplementation of miR-383 over-expressing cells with arachidonic acid, DENV levels in infected cells were restored. In addition to this, we showed that PLA2G4A-knockdown results in a decrease in DENV viral levels. Thus, these findings validated that the antiviral effects of miR-383 overexpression are mediated by the repression of the levels of PLA2G4A and endogenous levels of arachidonic acid.

In our study, we also assessed the selectivity of miR-383 modulated antiviral effects by evaluating the levels of VSV in miR-383 transfected cells. We observed no change in VSV levels during miR-383 transfection relative to con-miR-transfected Huh7 cells (figure S3.2). It has been previously demonstrated that PLA2G4A does not contribute to the pathogenesis of VSV[48], thus it is expected to observe little or no repression in the levels of VSV. Taken together, these findings suggest that miR-383 antiviral effects are at least somewhat selective for DENV.

Future work to evaluate whether other enveloped viruses including flaviviruses and coronaviruses, whose propagation is dependent on PLA2G4A[59,60], are negatively regulated by miR-383 will shed more light on the role of miR-383. As part of future studies, a panel of viruses with dependence on lipid metabolism as well as those known to be less dependent or unaffected by the host metabolic changes should be examined in the context of miR-383 overexpression. These studies should shed light on the specificity and selectivity of miR-383 in modulating antiviral responses. Depending on the virus being investigated and pathways being hijacked by the virus, other targets of miR-383 may have a stronger contribution to the biological phenotype. Uncovering the role of miR-383 in the modulation of the host response to other related viruses is a topic for future investigations.

Finally, we examined the effects of miR-383-mediated knockdown of PLA2G4A on SREBP1C-modulated signaling. We showed that knockdown of PLA2G4A results in the upregulation of SREBP1C and its target (FASN). This supports previous reports which suggest that arachidonic acid treatments inhibit the transcriptional activation of SREBP1c and its targets in cultured rat hepatoma cells[52].

Overall, our study reveals that miR-383 regulates hepatic lipid homeostasis and DENV infection in hepatic cells. This uncovers a novel mechanism where a miR-383-directed decrease in the abundance of a metabolic lipase may have pronounced effects on hepatic cell metabolic state and antiviral responses against DENV and potentially other enveloped viruses with displayed dependence on the host metabolic states. Our findings uncover novel roles of miR-383, specifically highlighting its controversial function as a lipogenic miRNA that possesses antiviral effects on a virus that highly depends on the host's cellular metabolism. Our study as well underscores the possibility of the utilization of miRNAs as tools to uncover pathways that could be targeted for antiviral therapies. Recent advancement in RNA therapeutics highlights the utility of miRNA mimics as tools to interrogate the function of miRNAs[61]. In the case of this study, miR-383 mimics could potentially be utilized as an approach to alleviate the burden of DENV infection. Generally, miRNA mimics are utilized to restore and enhance the function of endogenous miRNA with therapeutic potential[62]. The utility of miRNA mimics in cancer therapeutics has been recently investigated. In these studies, targeted delivery and administration of antitumorigenic miRNA mimics resulted in suppression of cancer proliferation and reduction in tumour size[62,63]. To date, miRNA-based antiviral therapies and strategies has been focused on HCV[64,65], however, with advancement in RNA therapeutics, an interest in investigating the therapeutic potential of antiviral miRNAs in modulating host-viral interactions is increasing[10,66]. Therefore, our study provides

novel ideas for exploring miR-383 as a potential therapeutic miRNA that may aid in managing DENV viral infection.

3.6 Conclusion

We have found that mi-383 acts as an important regulator of gene expression during DENV infection. The effects of miR-383 in modulating host-virus interactions appear to occur through the regulation of host cellular processes and signaling pathways to create an antiviral cellular state, rather than through direct interactions with the viral genome. Also, we found that miR-383 overexpression regulates hepatic cellular lipid microenvironments and restricts Dengue virus replication and life cycle. We identified PLA2G4A as a key miR-383 target, which has previously been shown to be a pro-viral host factor. Downregulation of PLA2G4A by miR-383 results in an antiviral state against DENV in human liver cells.

3.7 Methods

3.7.1 Reagents and cell culture

Huh7 human hepatoma cell lines were kindly gifted by Dr. Charles M. Rice (Rockefeller University, New York, NY). DENV-2 strain 16681 was kindly gifted by Dr. Tom Hobman (University of Alberta, Alberta, Canada). VSV was kindly provided by Dr. John C. Bell (Ottawa Hospital Research Institute, Ottawa, ON, Canada). Huh7 were cultured and maintained in Dulbecco's Modified Eagle Medium (DMEM; Invitrogen) supplemented with 10% fetal bovine serum (FBS; PAA Laboratories) and 100 nM non-essential amino acids. HEK293T cells (CRL-3216) were purchased from ATCC and they were cultured and maintained in DMEM 10% FBS. Vero cells (CCL-81) were purchased from ATCC and they were cultured and maintained in DMEM 10% FBS. miR-383 mimics and inhibitors as well as negative control mimics or inhibitors (con-miR) were purchased from *mirVana* (Ambion, Austin, TX). PLA2G4A (assay id 144379) and RNF145 (assay id 142228) siRNAs (silencer predesigned siRNAs) were purchased from Thermofisher scientific. Transfections for miRNA mimics and siRNAs were performed using Lipofectamine RNAiMAX (Life Technologies, Carlsbad, CA). Transfections were performed according to the manufacturer's protocol, a ratio of 2.5 µL of RNAiMAx per 1 µL of 100 µM of miRNA mimic was utilized for miRNA transfections. Transfection of plasmid DNA was performed using Lipofectamine 2000 (Life Technologies, Carlsbad, CA), as per manufacturer's protocol.

3.7.2 Transfections and infections

Generally, for non-infected cells, transfections were conducted in 6-well plates. On day one, cells were seeded at 200,000 cells/ well. The following day, cells were forward transfected with 100nM con-miR mimic or miR-383 mimics final concentration or con-miR or miR-383 inhibitors at a final

concentration of 50nM. For siRNA transfections, cells were transfected at a final concentration of 50nM. Transfections were conducted in OptiMEM using RNAiMAX reagent according to the manufacturer's protocol. 72h post-transfection, cells were lysed for RNA or protein analysis. For DENV infections, Huh7 cells were used and infected with the DENV-2 strain 16681. Cells were initially seeded at 200,000 cells per well in a 6-well plate. The next day, the cells were forward transfected, as previously described with con-miR or miR-383 mimic at a 100nM final concentration or PLA2G4A siRNA at a 50nM final concentration. The following day, the cells were infected with DENV at an MOI of 0.1 in minimal serum-free media for 2h. The medium was then replaced with complete medium following the 2h incubation. For arachidonic acid treatments, 2h post-infections medium was replaced with medium containing either vehicle (EtOH) or medium containing arachidonic acid at a final concentration of 50 μM (Cayman chemicals, Ann Arbor, Michigan). Forty-eight hours post-infection, cells were lysed using RLT Plus lysis buffer (RNeasyPluskit, Qiagen, Mississauga, ON) or Norgen total RNA isolation kit (Norgen Biotek, Thorold, ON) for total RNA analysis or lysed with 1X SDS lysis buffer (50 mM Tris-HCl [pH 6.8], 2% SDS, and 10% glycerol) for western blot analysis. For RNF145 siRNA transfection, cells were seeded as previously described, 24 hours post-seeding, cells were transfected with RNF145-siRNA or control-siRNA at a final concentration of 50nM. 72 hours post transfection, cells were lysed for RNA analysis as previously described. For VSV infections, Huh7 cells were used. Cells were initially seeded at 200,000 cells per well in a 6-well plate. The next day, the cells were forward transfected, as previously described with con-miR or miR-383 mimic at a 100nM final concentration. The 48h post transfection, the cells were infected with VSV at an MOI of 0.01 in minimal serum-free media for 1h.24h post-infection, the medium was replaced with complete medium, and cells were lysed for RNA analysis as previously described.

3.7.3 Quantitative real-time PCR

For the RNA analysis, RNA isolations were performed using RNA RNeasyPluskit, (Qiagen, Mississauga, ON) or Norgen total RNA isolation kit (Norgen Biotek, Thorold, ON). For the RT-qPCR analysis, the isolated RNA was quantified using a NanoDrop (Thermo Fisher Scientific). RNA integrity was evaluated using a 0.8% agarose RNA integrity gel in 1X Tris borste-EDTA (Ambion). 500ng of isolated RNA was reversed transcribed using the iScript reverse transcription kit (BioRad) according to the manufacturer's protocol. qPCR was then performed using SSOAdvanced Universal SYBR GreenSupermix (Bio-Rad) according to the manufacturer's instructions. The runs were analysed using a CFX Connect Real-Time PCR Detection System (Bio-Rad, Hercules, CA). Final concentration of 500nM of each evaluated primer was used in a final reaction volume of 10 µL. A list of the primers used in this study can be found in Table S1. $2^{-\Delta\Delta Ct}$ was utilized for the analysis of the levels of mRNA and to evaluate the relative fold changes in mRNA expression[67], with 18S rRNA levels being used for normalization. Relative expression was calculated to evaluate the expression changes between con-miR transfected samples and miR-383 transfected samples.

3.7.4 Plaque assay

Vero cells were seeded at 7.5 × 105 cells/well in 6-well plates. The next day, the supernatants collected from DENV-infected Huh7 cells were 10-fold serially diluted (1:10 to $1:10^9$). The media on Vero cells was replaced with 100 µl of serially diluted virus. Vero cells were incubated in virus-containing supernatant at 37 °C for 2 h. Following the 2h infection, 2 ml of warm DMEM 1%((Carboxymethylcellulose) DMEM medium was added to each well and allowed to solidify. After 6-7days, 2mL 10% formaldehyde was added to each well and incubated for 30 mins. Following formaldehyde fixation, media containing fixing solution was removed and staining solution (10%

ethanol, 0.1% crystal violet) was added to each well and incubated for 15-30 mins, excess stain was then washed with water and dried. Plaque forming units per milliliter of supernatant were calculated considering the dilution factor to report on the viral titers.

3.7.5 Immunoblotting

Cells for immunoblotting were lysed in 1X SDS lysis buffer (50 mM Tris-HCl [pH 6.8], 2% SDS, and 10% glycerol). Following lysis, the lysates were sheared using 21 G needle (BDBiosciences). DC assay (Bio-Rad) was used to determine the protein concentration. SDS-PAGE was performed with the protein lysates and 30ug of lysates were separated on the 10% TGX stain-free gel (BioRad). The migrated proteins were visualized on a ChemiDoc MP (Bio-Rad). Trans-Blot turbo (Bio-Rad) was utilized to transfer proteins on a PVDF membrane. Following the transfer, the membranes were blocked using 5% BSA in TBS-T or 5% milk in TBS-T. Subsequently, the membranes were incubated with primary antibodies overnight at various dilutions depending on the identity of the antibody.

Following primary incubation, the membranes with secondary donkey anti-rabbit or goat anti-mouse antibody conjugated with horseradish peroxidase (1:20000; Jackson ImmunoResearch Laboratories, Inc., 115-035-062). ChemiDoc MP (Bio-Rad) with clarity ECL solution reagent (Bio-Rad) was used to visualize the blots. Image Lab (Bio-Rad) was used to adjust and crop the blots for presentation. List of primary antibodies used in this study is found in Table S4.

3.7.6 Oil red O lipid staining

Initially, Huh7 were seeded 20,000 cells / well in a 4-well chamber slides. 24 hours post seeding, the cells were transfected with con-miR or miR-383 at 100nM final concentration. 48 hours post transfection, the cells were washed 1X with PBS and fixed for 10 minutes using 10% formaldehyde. Fresh 10% formaldehyde was added and incubated for 1 hour. Chambers were

subsequently washed with water and incubated in 60% isopropanol for 20 mins. 60% isopropanol containing 0.35% oil Red O (Sigma) was added and incubated for 10 minutes. Cells were then washed 5X with water and Prolong™ Gold Antifade Mountant with DAPI (Thermofisher) was used to mount the chamber slides. Axiophot fluorescence microscope (Zeiss) attached to a DP-70 Colour CCD camera (Olympus) with a 50W mercury fluorescence excitation light source was utilized to acquire Images. Images were obtained using ImagePro 6 software suite (mediaCybernetics) and image analysis was done using ImageJ (NIH).

3.7.7 mRNA microarray

RNA isolation from con-miR and miR-383 transfected cells was performed using Norgen total RNA isolation kit (Norgen Biotek, Thorold, ON). For the microarray gene profiling, Affymetrix Human Gene ST.2.0 arrays were utilized. Affymetrix Expression Console and Transcriptome Analysis Console (v3.0) was used to analyze and normalize the obtained data. Pathway enrichment and gene ontology analysis were conducted using ToppGene Suite[29]. Bonferroni correction was utilized to adjust P values. Gene expression profiling data from miR-383 and con-miR transfected non-infected and DENV infected Huh7 have been deposited to NCBI Gene Expression Omnibus under the following accession number: GEO: GSE196763.

3.7.8 cPLA2 Activity assay

Huh7 cells were seeded in 10 cm plates. The next day cells were transfected with either control mimic or miR-383 mimics as previously described. 72h post transfection cells were harvested and assayed for cPLA2 activity using cPLA2 activity kit (Cayman chemicals, Ann Arbor, MI) as described in the manufacturer's protocol.

3.7.9 Arachidonic Acid ELISA assay

200,000 Huh7 cells were seeded on day 1, the next day, cells were transfected with either con-miR or miR-383, 72h post transfection, cells were collected and lysed as per manufacturer's protocol (Novus Biological, Toronto, CA). For the assay 1000,000 cells were resuspended in 250ul of PBS. The assay was conducted as per manufacturer's instructions (Novus Biological).

3.7.10 3′UTR luciferase reporter assay

miR-383 putative binding sites were mutated in dual luciferase reporters containing 3'UTR of PLA2G4A and RNF145 purchased from (Genecopoeia). Site-directed mutagenesis was performed using Quick-change Lightning kit (Agilent) as per the manufacturer's protocol with primers designed to introduce a point mutation in 2 nucleotides of the miR-383 seed complementary sequence in PLA2G4A 3'UTR. Primer sequences are as follows: FWD: 5'-gagtatcagccagtctctcatagtcagtacgactatctgtactg-3'and REV: 5'-cagtacagatagtcgtactgactatgagagactggctgatactc-3'. To perform the assay, HEK293T cells were initially seeded in a 12-well plate. The following day, the cells were transfected with the 500ng/mL of either wild-type or mutant 3'UTR construct using lipofectamine 2000. 24h post plasmid transfection, the cells were transfected with either miR-383 mimic or con-miR as previously described[68]. 48h post mimic transfection, the cells were lysed using 1X passive lysis buffer (Promega), readings were obtained using a SpectraMax L luminometer (Molecular Devices).

3.7.11 Statistical analysis

In this study, data is presented as the mean of replicates, with error bars representing the standard error of the mean. One-sample t-test or Two-tailed Student's t-test was used to report on statistical significance where P-values less than 0.05 are deemed significant.

3.8 Acknowledgements

mRNA microarray profiling was performed by The Centre for Applied Genomics (TCAG), The Hospital for Sick Children, Toronto, Ontario, Canada. N.A. and N.A. are supported by a NSERC Postgraduate Scholarship-Doctoral (PGS-D). This work is supported by funding from a Natural Sciences and Engineering Research Council (NSERC) grant (298496) and a Canadian Institutes of Health Research (CIHR) grant (136807).

3.9 References

1. Esau, C. *et al.* miR-122 regulation of lipid metabolism revealed by in vivo antisense targeting. *Cell Metab.* **3**, 87–98 (2006).
2. Rottiers, V. & Näär, A. M. MicroRNAs in metabolism and metabolic disorders. *Nat. Rev. Mol. Cell Biol.* **13**, 239–251 (2012).
3. Osada, H. & Takahashi, T. MicroRNAs in biological processes and carcinogenesis. *Carcinogenesis* **28**, 2–12 (2007).
4. Pasquinelli, A. E. MicroRNAs and their targets: Recognition, regulation and an emerging reciprocal relationship. *Nat. Rev. Genet.* **13**, 271–282 (2012).
5. Vidigal, J. A. & Ventura, A. The biological functions of miRNAs: Lessons from in vivo studies. *Trends Cell Biol.* **25**, 137–147 (2015).
6. Ben-Hamo, R. & Efroni, S. MicroRNA regulation of molecular pathways as a generic mechanism and as a core disease phenotype. *Oncotarget* **6**, 1594–1604 (2015).
7. Singaravelu, R. *et al.* MicroRNAs regulate the immunometabolic response to viral infection in the liver. *Nat. Chem. Biol.* **11**, 988–993 (2015).
8. Singaravelu, R. *et al.* MicroRNA-7 mediates cross-talk between metabolic signaling pathways in the liver. *Sci. Rep.* **8**, 1–10 (2018).
9. Elmén, J. *et al.* Antagonism of microRNA-122 in mice by systemically administered LNA-antimiR leads to up-regulation of a large set of predicted target mRNAs in the liver. *Nucleic Acids Res.* **36**, 1153–1162 (2008).
10. Singaravelu, R. *et al.* A conserved miRNA-183 cluster regulates the innate antiviral response. *J. Biol. Chem.* **294**, 19785–19794 (2019).
11. Hsu, S. hao & Ghoshal, K. MicroRNAs in Liver Health and Disease. *Curr. Pathobiol. Rep.* **1**, 53–62 (2013).
12. Zhang, T., Yang, Z., Kusumanchi, P., Han, S. & Liangpunsakul, S. Critical Role of microRNA-21 in the Pathogenesis of Liver Diseases. *Front. Med.* **7**, 1–7 (2020).
13. Long, J. K., Dai, W., Zheng, Y. W. & Zhao, S. P. MiR-122 promotes hepatic lipogenesis via inhibiting the LKB1/AMPK pathway by targeting Sirt1 in non-alcoholic fatty liver disease. *Mol. Med.* **25**, 1–13 (2019).
14. Chen, Y., Dong, X., Yu, D. & Wang, X. Serum miR-96 is a promising biomarker for hepatocellular carcinoma in patients with chronic hepatitis B virus infection. *Int. J. Clin. Exp. Med.* **8**, 18462–18468 (2015).
15. Mashek, D. G. Hepatic Fatty Acid Trafficking : Multiple Forks in the road. *Adv. Nutr.* **6**,97–710 (2013).
16. Ipsen, D. H., Lykkesfeldt, J. & Tveden-Nyborg, P. Molecular mechanisms of hepatic lipid accumulation in non-alcoholic fatty liver disease. *Cell. Mol. Life Sci.* **75**, 3313–3327 (2018).
17. Sangineto, M. *et al.* Lipid metabolism in development and progression of hepatocellular

carcinoma. *Cancers (Basel).* **12**, 1–19 (2020).

18. Yang, W. *et al.* Fatty acid synthase is up-regulated during hepatitis C virus infection and regulates hepatitis C virus entry and production. *Hepatology* **48**, 1396–1403 (2008).

19. Tardif, K. D., Waris, G. & Siddiqui, A. Hepatitis C virus, ER stress, and oxidative stress. *Trends Microbiol.* **13**, 159–163 (2005).

20. Martin-Acebes, M. A. *et al.* The Composition of West Nile Virus Lipid Envelope Unveils a Role of Sphingolipid Metabolism in Flavivirus Biogenesis. *J. Virol.* **88**, 12041–12054 (2014).

21. Neufeldt, C. J., Cortese, M., Acosta, E. G. & Bartenschlager, R. Rewiring cellular networks by members of the Flaviviridae family. *Nat. Rev. Microbiol.* **16**, 125–142 (2018).

22. Paul, D. & Bartenschlager, R. Flaviviridae Replication Organelles: Oh, What a Tangled Web We Weave. *Annu. Rev. Virol.* **2**, 289–310 (2015).

23. Villareal, V. A., Rodgers, M. A., Costello, D. A. & Yang, P. L. Targeting host lipid synthesis and metabolism to inhibit dengue and hepatitis C viruses. *Antiviral Res.* **124**, 110–121 (2015).

24. Vial, T. *et al.* Dengue virus reduces AGPAT1 expression to alter phospholipids and enhance infection in Aedes aegypti. *PLoS Pathog.* **15**, 1–23 (2019).

25. Chen, L. *et al.* miR-383 inhibits hepatocellular carcinoma cell proliferation via targeting APRIL. *Tumor Biol.* **37**, 2497–2507 (2016).

26. Wang, J. *et al.* miR-383 inhibits cell growth and promotes cell apoptosis in hepatocellular carcinoma by targeting IL-17 via STAT3 signaling pathway. *Biomed. Pharmacother.* **120**, 109551 (2019).

27. Chakraborty, C., Doss, C. G. P., Bandyopadhyay, S. & Agoramoorthy, G. Influence of miRNA in insulin signaling pathway and insulin resistance: Micro-molecules with a major role in type-2 diabetes. *Wiley Interdiscip. Rev. RNA* **5**, 697–712 (2014).

28. Tambyah, P. A. *et al.* microRNA expression in blood of dengue patients. *Ann. Clin. Biochem.* **53**, 466–476 (2015).

29. Chen, J., Bardes, E. E., Aronow, B. J. & Jegga, A. G. ToppGene Suite for gene list enrichment analysis and candidate gene prioritization. *Nucleic Acids Res.* **37**, 305–311 (2009).

30. Soto-Acosta, R., Bautista-Carbajal, P., Cervantes-Salazar, M., Angel-Ambrocio, A. H. & del Angel, R. M. DENV up-regulates the HMG-CoA reductase activity through the impairment of AMPK phosphorylation: A potential antiviral target. *PLoS Pathog.* **13**, (2017).

31. Soto-Acosta, R. *et al.* The increase in cholesterol levels at early stages after dengue virus infection correlates with an augment in LDL particle uptake and HMG-CoA reductase activity. *Virology* **442**, 132–147 (2013).

32. Madison, B. B. Srebp2: A master regulator of sterol and fatty acid synthesis1. *J. Lipid Res.* **57**, 333–335 (2016).

33. Shin, D. J. & Osborne, T. F. Thyroid Hormone Regulation and Cholesterol Metabolism Are Connected through Sterol Regulatory Element-binding Protein-2 (SREBP-2). *J. Biol. Chem.* **278**, 34114–34118 (2003).

34. Sato, R. *et al.* Sterol-dependent transcriptional regulation of sterol regulatory element-binding protein-2. *J. Biol. Chem.* **271**, 26461–26464 (1996).

35. Amemiya-Kudo, M. *et al.* Promoter analysis of the mouse sterol regulatory element-binding protein-1c gene. *J. Biol. Chem.* **275**, 31078–31085 (2000).

36. Lou, W. *et al.* Identification of potential miRNA-mRNA regulatory network contributing to pathogenesis of HBV-related HCC 11 Medical and Health Sciences 1112 Oncology and Carcinogenesis 06 Biological Sciences 0604 Genetics. *J. Transl. Med.* **17**, 1–14 (2019).

37. Kim, D. H., Sætrom, P., Snøve, O. & Rossi, J. J. MicroRNA-directed transcriptional gene silencing in mammalian cells. *Proc. Natl. Acad. Sci. U. S. A.* **105**, 16230–16235 (2008).

38. Montgomery, R. L. *et al.* Micro RNA mimicry blocks pulmonary fibrosis . *EMBO Mol. Med.* **6**, 1347–1356 (2014).

39. Hanley, J. P. *et al.* Immunotranscriptomic profiling the acute and clearance phases of a human challenge dengue virus serotype 2 infection model. *Nat. Commun.* **12**, 1–14 (2021).

40. Sessions, O. M. *et al.* Host Cell Transcriptome Profile during Wild-Type and Attenuated Dengue Virus Infection. *PLoS Negl. Trop. Dis.* **7**, 1–12 (2013).

41. Zhang, L. *et al.* Inhibition of cholesterol biosynthesis through RNF145-dependent ubiquitination of SCAP. *Elife* **6**, 1–20 (2017).

42. Horton, J. D. *et al.* Combined analysis of oligonucleotide microarray data from transgenic and knockout mice identifies direct SREBP target genes. *Proc. Natl. Acad. Sci. U. S. A.* **100**, 12027–12032 (2003).

43. Horton, J. D., Bashmakov, Y., Shimomura, I. & Shimano, H. Regulation of sterol regulatory element binding proteins in livers of fasted and refed mice. *Proc. Natl. Acad. Sci. U. S. A.* **95**, 5987–5992 (1998).

44. Liang, G. *et al.* Diminished hepatic response to fasting/refeeding and liver X receptor agonists in mice with selective deficiency of sterol regulatory element-binding protein-1c. *J. Biol. Chem.* **277**, 9520–9528 (2002).

45. Peña, J. & Harris, E. Early dengue virus protein synthesis induces extensive rearrangement of the endoplasmic reticulum independent of the UPR and SREBP-2 pathway. *PLoS One* **7**, 1–15 (2012).

46. Melo, C. F. O. R. *et al.* The role of lipids in the inception, maintenance and complications of dengue virus infection. *Sci. Rep.* **8**, 1–9 (2018).

47. Agarwal, V., Bell, G. W., Nam, J. W. & Bartel, D. P. Predicting effective microRNA target sites in mammalian mRNAs. *Elife* **4**, 1–38 (2015).

48. Menzel, N. *et al.* MAP-kinase regulated cytosolic phospholipase A2 activity is essential for production of infectious Hepatitis C virus particles. *PLoS Pathog.* **8**, 21 (2012).

49. Leslie, C. C. Properties and regulation of cytosolic phospholipase A2. *J. Biol. Chem.* **272**, 16709–16712 (1997).

50. Lin, L. L. *et al.* cPLA2 is phosphorylated and activated by MAP kinase. *Cell* **72**, 269–278 (1993).

51. Kramer, R. M. *et al.* p38 Mitogen-activated Protein Kinase Phosphorylates Cytosolic Phospholipase A2 (cPLA2) in Thrombin-stimulated Platelets. *J. Biol. Chem.* **271**, 27723–27729 (1996).

52. Ou, J. *et al.* Unsaturated fatty acids inhibit transcription of the sterol regulatory element-binding protein-1c (SREBP-1c) gene by antagonizing ligand-dependent activation of the LXR. *Proc. Natl. Acad. Sci. U. S. A.* **98**, 6027–6032 (2001).

53. Christopher, A. *et al.* MicroRNA therapeutics: Discovering novel targets and developing specific therapy. *Perspect. Clin. Res.* **7**, 68 (2016).

54. Shaw, T. A. *et al.* MicroRNA-124 Regulates Fatty Acid and Triglyceride Homeostasis. *iScience* **10**, 149–157 (2018).

55. Jopling, C. L., Yi, M., Lancaster, A. M., Lemon, S. M. & Sarnow, P. Modulation of Hepatitis C Virus RNA Abundance by a Liver-Specific MicroRNA. *Science* **1**, 1577–1581 (2005).

56. Ouyang, X. *et al.* Dysregulated serum miRNA profile and promising biomarkers in dengue-infected patients. *Int. J. Med. Sci.* **13**, 195–205 (2016).

57. Wang, Y., Viscarra, J., Kim, S. J. & Sul, H. S. Transcriptional regulation of hepatic lipogenesis. *Nat. Rev. Mol. Cell Biol.* **16**, 678–689 (2015).

58. Yang, X., Sheng, W., Sun, G. Y. & Lee, J. C. M. Effects of fatty acid unsaturation numbers on membrane fluidity and α-secretase-dependent amyloid precursor protein processing. *Neurochem. Int.* **58**, 321–329 (2011).

59. Müller, C. *et al.* Inhibition of Cytosolic Phospholipase A 2 α Impairs an Early Step of Coronavirus Replication in Cell Culture . *J. Virol.* **92**, (2018).

60. Liebscher, S. *et al.* Phospholipase A2 activity during the replication cycle of the flavivirus West Nile virus. *PLoS Pathog.* **14**, (2018).

61. Damase, T. R. *et al.* The Limitless Future of RNA Therapeutics. *Front. Bioeng. Biotechnol.* **9**, 1–24 (2021).

62. To, K. K. W. *et al.* Advances in the discovery of microRNA-based anticancer therapeutics: latest tools and developments. *Expert Opin. Drug Discov.* **15**, 63–83 (2020).

63. Trang, P. *et al.* Systemic delivery of tumor suppressor microRNA mimics using a neutral lipid emulsion inhibits lung tumors in mice. *Mol. Ther.* **19**, 1116–1122 (2011).

64. van der Ree, M. H. *et al.* Safety, tolerability, and antiviral effect of RG-101 in patients with chronic hepatitis C: a phase 1B, double-blind, randomised controlled trial. *Lancet* **389**, 709–717 (2017).

65. Van Der Ree, M. H. *et al.* Miravirsen dosing in chronic hepatitis C patients results in decreased microRNA-122 levels without affecting other microRNAs in plasma. *Aliment.*

Pharmacol. Ther. **43**, 102–113 (2016).

66. Hum, C. *et al.* MicroRNA Mimics or Inhibitors as Antiviral Therapeutic Approaches Against COVID-19. *Drugs* **81**, 517–531 (2021).

67. Livak, K. J. & Schmittgen, T. D. Analysis of relative gene expression data using real-time quantitative PCR and the 2-ΔΔCT method. *Methods* **25**, 402–408 (2001).

68. Dyer, B. W., Ferrer, F. A., Klinedinst, D. K. & Rodriguez, R. A noncommercial dual luciferase enzyme assay system for reporter gene analysis. *Anal. Biochem.* **282**, 158–161 (2000).

Chapter 4

microRNA-185 inhibits SARS-CoV-2 infection through the modulation of the host's lipid microenvironment

4.1 Preface

As a primary author of this chapter, I made significant experimental and intellectual contributions. J. P. Pezacki and I have conceived the research and experimental plan for this study. I have performed the majority of the cell culture work, RNA isolations, qRT-PCR experiments, western blot sample preparation, pseudotype virus preparation, entry assays, HCoV-229E virus experiments, and downstream analysis. Magen E. Francis and Alyson Kelvin performed SARS-CoV-2 infections and Noreen Ahmed generated D614G and N501Y mutants as well as assisted with luciferase assays. I wrote the manuscript/chapter and editing was performed by Noreen Ahmed and J.P Pezacki.

4.2 Abstract

With the emergence of the novel *betacoronavirus*, Severe Acute Respiratory Syndrome Coronavirus 2 (SARS-CoV-2), there has been an urgent need for the development of fast-acting antivirals particularly in dealing with different variants of concern (VOC). SARS-CoV-2, like other RNA viruses, depends on host cell machinery to propagate and misregulate metabolic pathways for its advantage. Herein we discovered that the immunometabolic microRNA-185 (miR-185) restricts SARS-CoV-2 propagation by affecting its entry and infectivity. The antiviral effects of miR-185 were studied in SARS-CoV-2 Spike protein pseudotyped virus, surrogate virus (HCoV-229E), as well as live SARS-CoV-2 virus in Huh7, A549, and Calu3 cells. In each model, we consistently observed microRNA-induced reduction in lipid metabolism pathways-associated genes including SREBP2, SQLE, PPARg, AGPAT3, and SCARB1. Interestingly, we also observed changes in angiotensin-converting enzyme 2 (ACE2) levels, the entry receptor for SARS-CoV-2. Taken together these data show that miR-185 significantly restricts host metabolic and other pathways that appear to be essential to SAR-CoV-2 replication and propagation. Overall, this study highlights an important link between non-coding RNAs, immunometabolic pathways, and viral infection. miR-185 mimics alone or in combination with other antiviral therapeutics represent possible future fast-acting antiviral strategies that are likely to be broadly antiviral against multiple variants as well as different virus types of pandemic potential.

4.3 Introduction

Severe Acute Respiratory Syndrome Coronavirus 2 (SARS-CoV-2) is the etiological agent which results in the development of COVID-19 [1]. SARS-CoV-2 has been a global concern over the past few years and therefore international efforts were put in place to rapidly address viral spread and dissemination to limit complications associated with the infection[2]. This disease of concern is characterized by several severe clinical outcomes, which include acute respiratory distress syndrome, septic shock, and multiple organ dysfunction syndromes[3]. Thus, unprecedented efforts were established for rapid drug discovery and development of potent antiviral therapeutic strategies[4]. Some of these strategies include convalescent plasma, neutralizing antibodies, vaccines, and therapeutic antiviral drugs[4–7]. Fortunately, effective vaccine development and production rapidly evolved over the past year aiding in curbing the spread of the virus globally[2,8]. However, with the emergence of other SARS-CoV-2 variants of concern (VOC), which are more resistant to the neutralization effects of the developed vaccines[9–11], there is a constant need for the development and the identification of potent therapeutic antivirals to aid in the suppression of the severe consequences of the infection. Hence, further understanding of SARS-CoV-2-host interactions at a superior level would aid in delineating molecular pathways and mechanisms essential for SARS-CoV-2 life cycle.

Both SARS-CoV and SARS-CoV-2 share similar cellular tropisms where they preferentially infect the lower respiratory tract while utilizing angiotensin-converting enzyme 2 (ACE2) as their receptor[12]. It has been found that the ACE2 receptor is localized in lipid rafts[12], which may indicate the involvement of cholesterol and glycosphingolipids in modulating SARS-CoV-2 and ACE2 interactions since these lipid components are enriched in these lipid micordomains[13,14]. SARS-

CoV-2 also has been shown to be highly dependent on host-cell metabolic pathways that provide components and energy needed for the creation of progeny viruses[15].

Recently, microRNAs (miRNAs) have emerged as essential regulators of these pathways and even have direct antiviral activity[16]. We have previously shown that miR-185 possesses antiviral properties against hepatitis C and Dengue viruses and the antiviral effects are mediated by miR-185's alterations in the host's lipid microenvironment which is essential for these viruses, some of these pathways include cholesterol and triglyceride biosynthesis[17].In this study, we focus on investigating the effects of miR-185 on the modulation of SARS-CoV-2 entry and replication, delineating the effects of miR-185 on SARS-CoV-2 life cycle. Specifically, we used coronavirus cell culture models to evaluate the functional effects of miR-185 overexpression on viral replication and propagation. Initially, we investigated the role of miR-185 in modulating the entry of SARS-CoV2 using a spike protein pseudotyped virus model. To further evaluate the impact of this miRNA on the SARS-CoV-2 VOC, we utilized the same model to assess the impact of the miRNA on spike harboring mutations of interest such as D614G and N501Y and the Alpha, Beta, Delta, and Omicron VOCs. Next, we investigated the role of the miRNA in low pathogenicity coronavirus 229E infection (HCoV-229E). Finally, we validated our findings in the SARS-CoV-2 cell culture model. Our study highlights the impact of miR-185 in antagonizing SARS-CoV-2 infection and underscores the therapeutic potential of miRNAs in decreasing the burden of SARS-CoV-2 and COVID-19.

4.4 Results

4.4.1 Expression of SARS-CoV-2 spike protein and pseudovirus incorporation of SARS-CoV-2 Spike (S) protein.

To examine the effects of miR-185 overexpression on viral entry, we sought to utilize the lentiviral pseudovirus system expressing SARS-CoV-2 Spike (S) protein. To ensure optimal production of our engineered particles, a plasmid expressing SARS-CoV-2 Spike protein lacking the terminal 19 amino acids containing the endoplasmic reticulum retention signal was utilized[18]. The HIV-based retroviral system was used to produce the engineered pseudovirus (Fig 4.1A). The HIV-based system consisting of HIV-1 NL4-3 ΔEnv Vpr Luciferase Reporter Vector (pNL4-3.Luc.R-E-) conveniently expresses a luciferase gene that allows for the detection of viral entry upon infection[19]. Initially, to confirm the successful production of the engineered particles, we validated the expression of the SARS-CoV-2 Spike protein in Hek293T producer cells and the incorporation of the protein into pseudovirus using western blotting. As expected, the S protein was readily detected using the anti-Spike antibody in cells transfected with the S encoding vector and engineered pseudovirus (Fig 4.1B). Consequently, this system is utilized in our study to report on Spike-based entry of SARS-CoV-2.

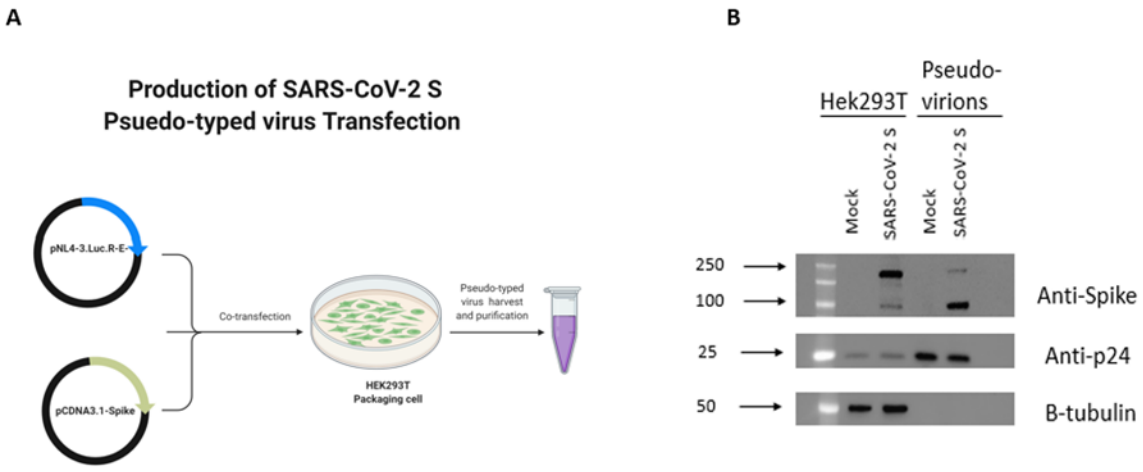

Figure 4.1 Detection of SARS-CoV2 S protein in Hek293T cell lysates and on pseudo-typed virus. (A) schematic representation of methodology utilized to produce Spike protein pseudo-typed virus. (B) Western blot analysis of Spike protein in HEK293T lysates used for virus production and in virus particles. Anti-spike was used to verify expression of spike protein in cell lysates and pseudo-typed virus. HIV anti-p24 and B-tubulin antibody were used as loading control for virions and cell lysates, respectively.

4.4.2 miR-185 antagonizes SARS-CoV-2 S protein pseudotyped virus entry in Huh7 and Calu-3 cell lines.

In order to assess the impact of miR-185 overexpression on the entry of SARS-CoV-2 pseudovirions incorporating SARS-CoV-2 S protein, we transfected miR-185 or con-miR mimics or inhibitors in Calu-3 and Huh7 cells, which were previously validated to endogenously expresses sufficient levels of ACE2[20]. Following transfection, the cells were infected with equal amounts of pseudovirus for 48h. Cells were lysed, and a luciferase assay was performed to examine the levels of luciferase signal in con-miR and miR-185 transfected cells. Interestingly, miR-185 overexpressing cells displayed a significant decrease in luciferase signal relative to con-miR transfected cells, suggesting a decrease in pseudovirus entry in both cell lines (Fig 4.2A,4.2B). Additionally, we sought to investigate the effects of inhibition of the endogenous levels of miR-185 on viral entry. Interestingly, in miR-185 inhibitor transfected Huh7 cells, an increase in viral entry was observed (Fig 4.2B). Overall, these findings suggest that miR-185 likely alters endogenous mechanisms essential for vial entry to antagonize SARS-CoV-2 Spike-based entry into these cells.

Accumulation of mutations in the SARS-CoV2 spike protein has led to the emergence of VOCs, displaying higher disease severity, resistance to neutralizing antibodies elicited by current vaccines or from previous infection, and reduced efficacy of treatment[21,22]. VOCs accumulate mutations in the Spike protein and some of these mutations were found to enhance the Spike binding to its receptor and SARS-CoV-2 fitness. Thus, we sought to investigate the effects of miR-185 mimic transfection on the entry of virions engineered to express S protein harboring some of the Spike mutations known to enhance Spike-based entry into host cells.

The D614G and N501Y mutations are found to be responsible for the increased transmissibility and fitness of the B.1.1.7 and the B.1.351 variants[21,22]; thus entry assays were performed with

pseudovirus harboring these mutations. Western blot analysis validated the successful expression of these mutants on pseudotyped particles (Fig 4.2C). Interestingly, miR-185 is found to suppress the entry of the D614G and N501Y mutants in both Calu-3 and A549 cells expressing ACE2 (Fig 4.2D-4.2G). Finally, we aimed to evaluate whether miR-185 inhibitory effects are extended to some of the current VOCs. To examine the effects of miR-185 on the cellular entry of these VOCs, we similarly produced and validated the expression of Alpha, Beta, Delta, and Omicron variants S proteins on the pseudo-typed virus (Fig 4.3A). Interestingly, miR-185 overexpression ubiquitously suppresses SARS-CoV-2 entry despite variations in S sequence in Calu-3(Fig 4.3B, 4.3C, 4.3D, and 4.3E) and Huh7 cells (Fig S4.1A, S4.1B, and S4.1C). Overall, these findings suggest that miR-185 may play a role in SARS-CoV-2 pathogenesis, potentially by altering the cellular microenvironment to impede binding and entry.

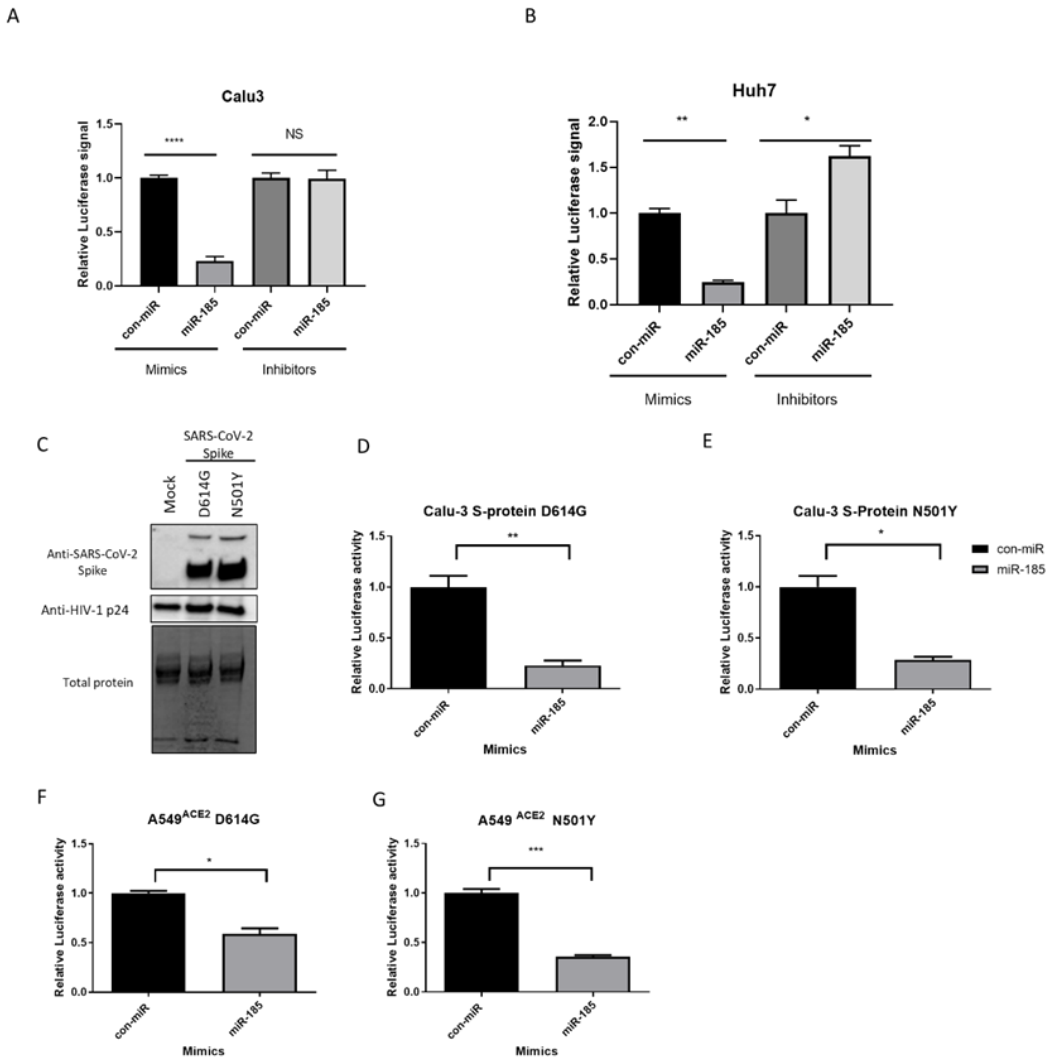

Figure 4.2 miR-185 inhibits pseudovirions entry in Huh7 hepatoma cell line and Calu-3 lung carcinoma cell line. (A) Huh7 cells were forward transfected with miR-185 mimics/inhibitors or con-miR mimics/inhibitors and (B)Calu-3 cells were reverse transfected with miR-185 mimics/inhibitors or con-miR mimics/inhibitors. 24h post transfection, the cells were infected with 100ul of media containing Sars-CoV-2 S pseudo-typed virus. C) Western blot analysis of Spike protein on pseudo-typed virus particles. Anti-spike was used to verify expression of spike pseudo-typed virus and HIV anti-p24 for virions was used as loading control for virions. D) Calu-3 cells infected with S-protein D614G pseudo-typed virus E) Calu-3 cells infected with S-protein N501Ypseudotyped virus F) A549 ^{ACE2} cells infected with with S-protein D614G pseudo-typed virus G) A549 ^{ACE2} cells infected with S-protein N501Y pseudo-typed virus. 48h post infection, cells were lysed in 1X passive lysis buffer and Luciferase activity was measured using a microplate reader. All experiments were read in technical triplicates for at least three biological replicates. Two-tailed Student's t-test was used to report on statistical significance. Error bars represent the means ±SEM of at least three biological replicates. *P<0.05, **P<0.01, ***P<0.001.

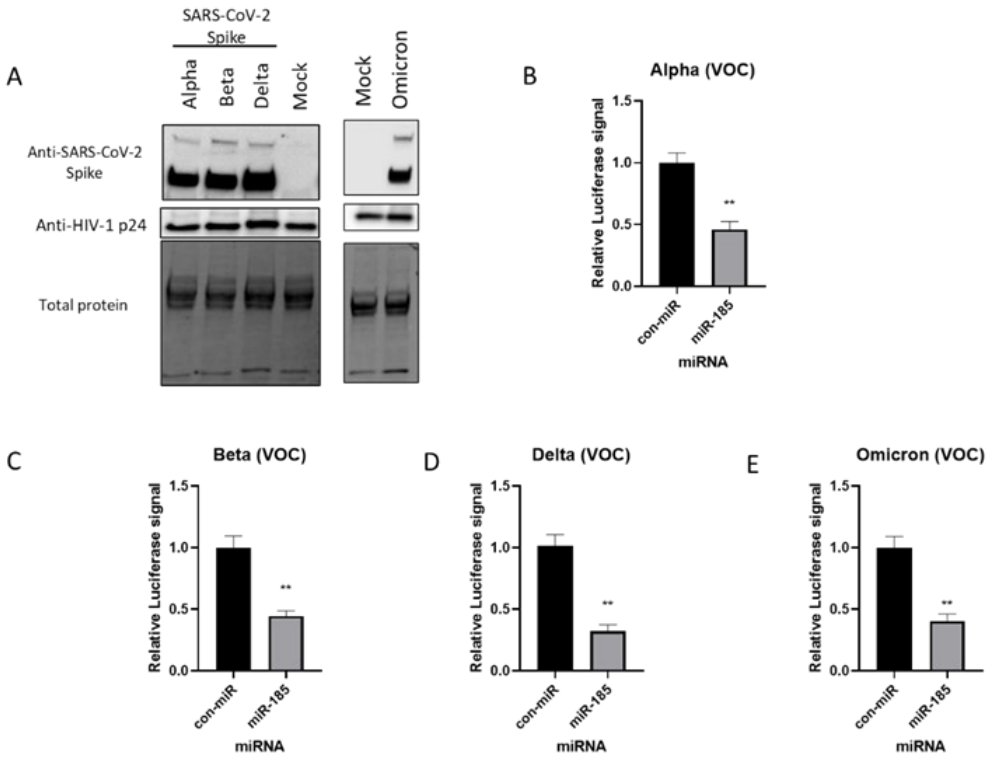

Figure 4.3 miR-185 inhibits entry of SARS-CoV-2 alpha, beta, and delta spike variants pseudo-typed virus in cell culture. A) Western blot analysis of Spike protein on pseudo-typed virus particles. Anti-spike was used to verify expression of spike pseudo-typed virus and HIV anti-p24 for virions was used as loading control for virions. D) Calu-3 cells infected with S-protein D614G pseudo-typed virus Calu3 cells were transfected with miR-185 mimics or con-miR mimics and 24h post transfection, the cells were infected with 100ul of media containing Sars-CoV-2 S pseudo-typed virus (B) Alpha (C)Beta and (D) delta variants of concern (E) Omicron variant of concern. 48h post infection, cells were lysed in 1X passive lysis buffer and Luciferase activity was measured using a microplate reader. All experiments were read in technical triplicates for at least three biological replicates. Error bars represent the means ±SEM of at least three biological replicates. Two-tailed Student's t-test was used to report on statistical significance. *P<0.05, **P<0.01, ***P<0.001

4.4.3 Inhibition of SREBP2-modulated signaling antagonizes SARS-CoV-2 Spike pseudotyped viral entry

We have previously shown that miR-185 expression is induced by 25-Hydroxycholesterol (25-HC)[17]. 25-HC is an oxysterol that displays broad antiviral properties against various families of enveloped viruses, which includes coronaviruses[23–26]. This lipid effector synthesis from cholesterol is catalyzed by cholesterol-25-hydroxylase whose expression is induced by interferon (IFN) in macrophages as an innate response to viral infection[27]. Interestingly, 25-HC has been as well shown to have antagonizing effects on viral-cell fusion and viral entry[28,29]. Furthermore, 25-HC has been found to inhibit cholesterol synthesis by targeting the activity of sterol regulatory element-binding proteins (SREBPs), which are membrane-bound transcription factors that modulate the synthesis and expression of genes involved in lipid and cholesterol biosynthesis[30]. Thus, we sought to validate the effects of cholesterol depletion on viral entry using our model by treating Huh7 cells with cholesterol-depleting small molecules such as 25-HC and Fluvastatin, an HMG-CoA reductase inhibitor that suppresses cholesterol synthesis. We treated cells with varying concentrations of both 25-HC and Fluvastatin and we found a dose-dependent decrease in the levels of pseudovirus entry, with the most potent inhibition at 5μM for 25-HC and 10μM for Fluvastatin (Fig S4.2A and 4.2B, respectively). These findings suggest that dysregulation of cholesterol levels mediated by 25-HC and Fluvastatin treatments antagonizes SARS-CoV-2 S pseudotyped virus entry and overall suggest that the antiviral effects mediated by these compounds likely affect early stages of the viral life cycle.

Membrane cholesterol and lipid composition have been found to be indispensable for enveloped viral entry and attachment. It was shown that ACE2 is localized to cholesterol-rich lipid rafts, suggesting that cholesterol may play an essential role in modulating several steps in the SARS-CoV-2 life cycle since cholesterol was found to play extensive roles in the life cycles of other

pathogens including SARS-CoV[13,31,32]. Additionally, cholesterol depletion has been found to disrupt virion membrane and binding affinity to the host cell, while cholesterol-rich regions in the host's membrane have been found to be instrumental for spike-mediated fusion and viral entry [33]. Moreover, a decrease in the levels of membrane-bound cholesterol in host cells results in a reduction in spike binding to ACE2 and a decrease in infectivity[34]. Our data with 25-HC and Fluvastatin support an important role for *de novo* cholesterol biosynthesis in the SARS-CoV-2 life cycle, particularly important for cell entry mechanisms.

4.4.4 miR-185 inhibits SARS-CoV-2 entry by modulating lipid metabolism and repression of ACE2 expression in Calu-3 cells

Given that miR-185 is a 25-HC regulated miRNA, we sought to evaluate the mechanism by which this miRNA inhibits viral entry. We have previously shown that miR-185 is an immunometabolic miRNA that strongly regulates lipid and cellular metabolism and thus alters the lipid microenvironment[17]. Specifically, overexpression of miR-185 in Huh7 cells was shown to decrease lipid droplet formation, cellular triglyceride levels, and cholesterol biosynthesis[17]. Given this, we sought to evaluate the levels of genes involved in these processes following miR-185 overexpression. miR-185 directly targets SREBP2, a transcription factor that modulates the expression of cholesterol biosynthetic genes and is a master regulator of these processes[35]. Thus, we first aimed to evaluate the levels of SREBP2 mRNA using qPCR following miR-185 transfection in Calu-3 cells. A significant decrease in the levels of SREBP2 was observed in cells overexpressing miR-185 relative to con-miR transfected cells. This suggests that miR-185 likely alters cholesterol metabolism by targeting and suppressing a master regulator of this process.

To further confirm miR-185 inhibitory effects on cholesterol biosynthesis, we evaluated the levels of squalene epoxidase (SQLE) which encodes an enzyme that catalyzes cholesterol synthesis and

whose expression is regulated by SREBP2. SQLE was significantly downregulated in cells overexpressing miR-185 (Figure 4.4A). We have further confirmed the decrease in the protein levels of SREBP2 and SQLE in miR-185 overexpressing Calu-3 cells relative to con-miR transfected cells (Figure 4.4B). Additionally, we show that miR-185 suppresses the levels of another lipogenic direct target, HDL-scavenger receptor B type 1 (SACRB1). This protein is known to facilitate the ACE2-dependent entry of SARS-CoV2[36], contributing to miR-185 suppressive effects on entry. In fact, treatment of cultured cells with pharmacological SACRB1 inhibitors inhibits SARS-CoV-2 infection[36]. Overall, these findings suggest that miR-185 inhibitory effects are modulated by the direct or indirect repression of cholesterol metabolism-associated genes, such as SREBP2, SQLE, and SCARB1.

In addition to repressing genes involved in cholesterol biosynthesis and metabolism, miR-185 suppresses the levels of other target genes and lipogenic transcription factors involved in fatty acid and triglyceride biosynthesis and regulation; for example, we show that AGPAT3, an enzyme that catalyzes steps in the biosynthesis of triglycerides from glycerol-3-phosphate (G3P))[37], is significantly downregulated in miR-185 overexpressing cells relative to con-miR transfected cells (Figure 4A). Although ACE2 is not a predicted target of miR-185, we observed a decrease in the levels of ACE2 mRNA in miR-185 overexpressing cells (Figure 4.4C). Interestingly, PPAR-gamma, a lipogenic transcription factor, was previously found to regulate ACE2 expression[38]. In Calu-3 cells overexpressing miR-185, PPAR-gamma expression is downregulated (Figure 4.4A), and we hypothesize dysregulations in the levels of PPAR-gamma may result in the observed decrease in the levels of ACE2 and ultimately contributes to miR-185 ability to suppress SARS-CoV-2 entry into host cells. Overall, these finding confirms miR-185 function in modulating lipid

metabolic processes in Calu-3 cells and points towards a mechanism by which miR-185 potentially regulates the anti-SARS-CoV-2 response observed in cells overexpressing the miRNA.

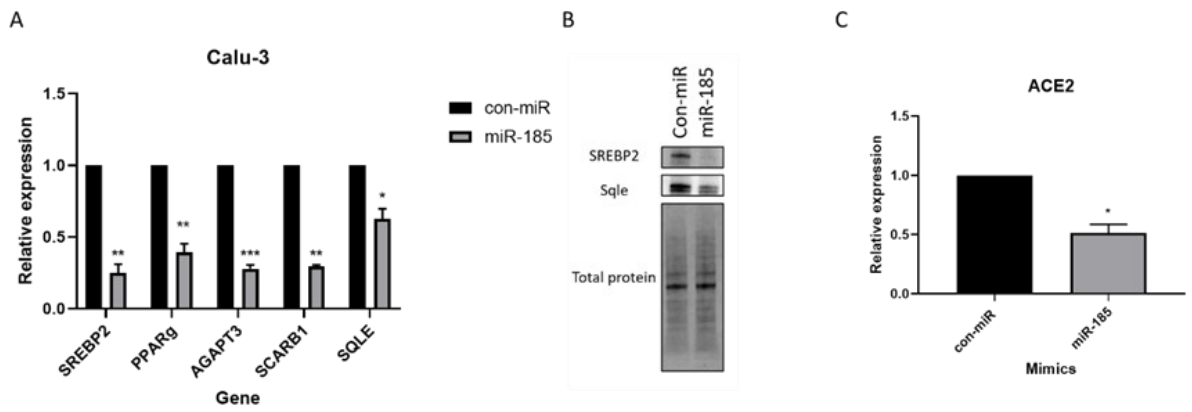

Figure 4.4 miR-185 inhibits entry by modulating lipid metabolism and repression of ACE2 expression in Calu-3 cells. Calu-3 cells were reverse transfected with miR-185 mimics/inhibitors or con-miR mimics/inhibitors.72 h post-transfection, cells were lysed for RNA analysis. (A) qRT-PCR analysis of lipogenic genes in con-miR and miR-185 transfected cells. (B) Western blot analysis of SREBP2 and SREBP2 target, SQLE (C) ACE2 levels in con-miR and miR-185 transfected cells. one-sample t-test was used to determine statistical significance. Error bars represent the means ±SEM of at least three biological replicates. *P<0.05, **P<0.01, ***P<0.001

4.4.5 miR-185 inhibits HCoV-229E replication and infectivity

Next, we sought to evaluate the effects of miR-185 overexpression on the replication and the life cycle of live coronavirus infection. We First sought to evaluate the effects of a low pathogenic human coronavirus 229E (HCoV-229). Initially, we assessed the effects on viral replication by quantifying the levels of intracellular viral RNA levels in Huh7 cells overexpressing the miR-185. Interestingly, a significant decrease in the levels of the intracellular virus was observed (Figure 4.5A). Consistent with that, a decrease in infectivity was observed (Figure 4.5B). A decrease in viral replication was as well reflected in A549, lung carcinoma cell line, which confirms that miR-185 suppressive effect on HCoV is observed in cells that represents a primary site of infection (Figure S4.3).

Next, we pursued to examine miR-185 effect on cholesterol biosynthesis in Huh7 cells during HCoV-229E infection. Consistent with previous findings observed in Calu3 cells, a decrease in SREBP2 levels was observed along with a decrease in SREBP2 target, SQLE (Figure 4.5C). Additionally, a decrease in metabolic targets of miR-185 was observed, with a significant decrease in the levels of AGPAT3 and SCARB1(Figure 4.5C). Overall, these findings validate the suppressive antiviral effects of miR-185 in an infectious model, and these effects are likely modulated through miR-185's inhibitory effects on metabolic pathways that are found to enhance viral entry, replication, and infectivity.

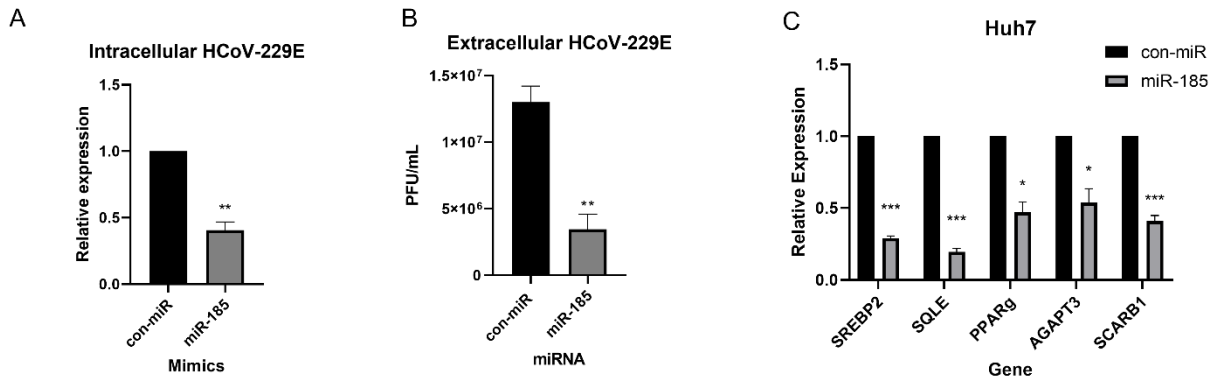

Figure 4.5 miR-185 inhibits HCoV-229E replication and infectivity. Huh7 cells were transfected with miR-185 mimics or con-miR mimics.24 h post-transfection, cells were infected with HCoV-229E at an MOI of 0.05. (A)48h post-infection cells lysed for RNA analysis of intracellular levels of virus. (B) plaque assay of extracellular levels of virus from con-miR and miR-185 transfected cells. (C) qRT-PCR analysis of lipogenic genes in con-miR and miR-185 transfected cells. One-sample t-test was used to determine statistical significance (A and C), Two-tailed Student's t-test was used to report on statistical significance in B. Error bars represent the means ±SEM of at least three biological replicates. *P<0.05, **P<0.01, ***P<0.001.

4.4.6 miR-185 overexpression inhibits SARS-CoV-2 pathogenesis in Calu-3 cells

Finally, to investigate whether miR-185 could modulate SARS-CoV-2 infection. We transfected Calu-3 cells with con-miR or miR-185 mimics and 24h post-transfection we infected the cells with SARS-CoV-2 at an MOI of 0.01. Intracellular and Extracellular viral levels were investigated at 24h, 48h and 72h post-infection. 2-3 $\log_{10}$ fold changes (TCID50/mL) were observed in intracellular and extracellular virus levels at all investigated time points (Figure 4.6A and 4.6B). Further confirming the inhibitory effects of miR-185 on the coronavirus entry and infection *in vitro*. The suppression of SREBP2 and AGPAT3, which are predicted and validated direct targets of miR-185, were confirmed to be downregulated in miR-185 overexpressing cells in all tested time points (Figure S4.4). These findings further validate that miR-185 attenuates SARS-CoV-2 viral infection through inhibiting lipid and sterol metabolic pathways which promote coronavirus infection in human cells.

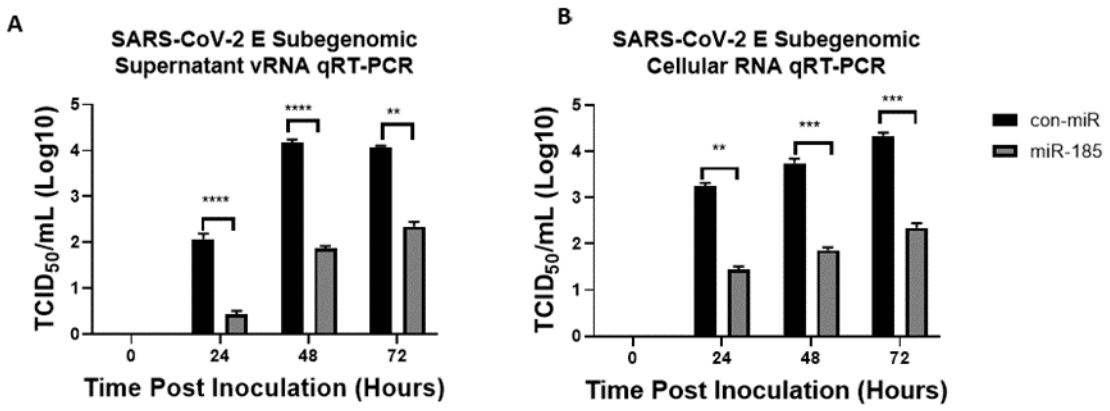

Figure 4.6 miR-185 results in significant inhibition in SARS-CoV-2 intracellular and extracellular levels at various timepoints post inoculation. (A) quantification of extracellular SARS-CoV-2 subgenomic levels from Calu-3 transfected with either con-miR or miR-185 at 24h, 48h and 72h post-inoculation. (B) quantification of intracellular SARS-CoV-2 subgenomic levels from Calu-3 transfected with either con-miR or miR-185 at 24h, 48h and 72h post-inoculation. Error bars represent the means ±SEM of at least three biological replicates. *P<0.05, **P<0.01, ***P<0.001, ****P<0.0001.

4.5 Discussion

microRNAs are non-coding RNAs that have been found to extensively regulate diverse aspects of cellular pathways and mechanisms[39–41]. They are considered to be master regulators of gene expression and they can modulate diverse pathways, thus it is not surprising to observe dysregulated miRNA profiles in altered cellular states as a result of disease or infection[41–43]. Several miRNAs have emerged of critical importance in the modulation of viral infections and therefore miRNAs may represent a target for therapeutic investigation[17,43–45]. For example, miR-122 is a miRNA that has been found to play an integral role in promoting HCV replication, and therefore miR-122 represents a potential therapeutic target for attenuating HCV pathogenesis. In fact, miravirsen and RG-101 , experimental anti-miR-122 oligonucleotides were developed for clinical use and were found to decrease HCV RNA levels in chronic HCV patients through Phase 1 and phase 2 trials[46,47]. Therefore, it is of critical importance to evaluate the role of miRNAs in the modulation of virus infection since they may represent pro or antiviral host factors that may be utilized to control viral pathogenesis.

In this study, we evaluate the role of miR-185 in the modulation of SARS-CoV2 pathogenesis and examine the potential mechanism by which the miRNA act to inhibit viral entry, replication, and infectivity. We have previously shown that miR-185's expression is regulated by 25-HC, 25-HC is an antiviral molecule produced by cholesterol 25-hydroxylase, an enzyme that catalyzes the oxidation of cholesterol to 25-HC[17,48,49]. Broad antiviral properties of this molecule have been demonstrated with recent reports highlighting the potency of 25-HC in inhibiting SARS-CoV-2 infection *in vitro* and *in vivo*[50].

In this study, we initially generate SARS-CoV-2 Spike pseudotyped viral particles to examine the effects of miR-185 on viral entry. The entry mechanism of SARS-CoV-2 has been extensively

studied. Generally, on mature viruses, the spike protein responsible for binding to the cellular receptor, is present in a trimeric form, containing an S1 head and an S2 stalk. S1 contains the receptor binding domain (RBD) and recognizes the cellular receptor, ACE2[12]. Upon recognition, a subsequent viral entry where eventually viral and lysosomal membrane fusion takes place. In addition to ACE2, other host cellular proteases such as TMPRSS2 have been identified to aid in the viral entry process[12]. Interestingly, cholesterol and other lipid species significantly affect the SARS-CoV-2 entry process. As a modulator of lipid metabolism[17], we sought to investigate the effects of miR-185 on SARS-CoV-2 entry and pathogenesis.

We show that miR-185 suppresses entry of pseudotyped virus expressing WT Spike, D614G, and N501Y mutants, and the Alpha, Beta, Delta, and Omicron Spike. This has led us to believe that miR-185 dysregulates pathways that are essential for the entry of SARS-CoV-2 despite of the nature of the Spike protein and thus represents a pan-antiviral mechanism against current and potential SARS-CoV-2 variants. We show that miR-185 dysregulates the entry of viral particles by modulating lipid metabolic pathways, which include pathways involved in cholesterol and triglyceride biosynthesis. This was evidenced by miR-185's significant suppressive effects on the expression of genes regulating these processes. Specifically, we show that miR-185 targets and decreases the levels of endogenous SREBP2, a transcriptional regulator of cholesterol biosynthesis, and its targets thereby dysregulating the levels of cholesterol in the cells and influencing SARS-CoV-2 entry and infectivity.

Lipids' involvement in SARS-CoV-2 pathogenesis is now being extensively investigated. Several studies have revealed that during human coronavirus infection the cell's lipid profile is significantly dysregulated[34,51]. A recent study showed that similar to other (+)RNA viruses, SARS-CoV-2 induces lipid droplet formation, a phenotype not observed during SARS-CoV

infection[52]. These lipid droplets are usually exploited by RNA viruses to obtain energy to support their replication or acquire lipids for particle formation. This phenotype was consistently observed *in vivo* and *in vitro* during SARS-CoV-2 infection similar to observations in hepatocytes following HCV infection [53]. Additionally, it has been shown that cholesterol localized in the lipid rafts is an essential entry factor for coronaviruses, both *in vitro* and *in vivo* [34,54], and a determinant of the SARS-CoV-2 pathogenesis and replication. Sterols and oxysterols significantly influence the mechanisms of viral infections and cellular response to infections[55]. Lipid rafts are indispensable for the entry and internalization of coronaviruses, where cholesterol depletion from cellular membranes was found to decrease viral entry[56–58]. Specifically for SARS-CoV-2, it was shown that localization of cholesterol in lipid rafts is crucial for infectivity and entry which suggests that metabolic remodeling in the host cell is an essential factor and a determinant of viral pathogenesis[58]. Thus, our study shows that a miR-185-mediated decrease in the levels of endogenous cholesterol contributes to a decrease in viral entry and infectivity. Furthermore, we show that miR-185 overexpression significantly suppresses HCoV-229 and SARS-CoV-2 replication and infectivity.

Our study highlights the therapeutic potential of miRNAs in regulating virus infections. Generally, miRNAs with antiviral properties can be utilized as an antiviral strategy in combination with current therapies to antagonize viral infectivity and propagation. Additionally, with information obtained from this study, small molecular modulators of miRNA function may be used to recapitulate miRNA antiviral function. Overall, our work highlights the role of miR-185 as a potential therapeutic miRNA that shows potent suppressive antiviral effects against SARS-CoV-2 infection.

4.6 Methods

4.6.1 Reagents and cell culture

Huh7 human hepatoma cell lines were kindly gifted by Dr. Charles M. Rice (Rockefeller University, New York, NY). Huh7 were cultured and maintained in Dulbecco's Modified Eagle Medium (DMEM; Invitrogen) supplemented with 10% fetal bovine serum (FBS; PAA Laboratories) and 100 nM non-essential amino acids. HEK293T cells (CRL-3216) were purchased from ATCC and they were cultured and maintained in DMEM 10% FBS. Calu-3 cells were purchased from ATCC (HTB-55) and they were cultured and maintained in DMEM 10% FBS. pCMV14-3X-Flag-SARS-CoV-2 S was a gift from Zhaohui Qian (Addgene plasmid # 145780; http://n2t.net/addgene:145780 ; RRID:Addgene_145780). pCDNA3.3_CoV2_B.1.1.7 was a gift from David Nemazee (Addgene plasmid # 170451; http://n2t.net/addgene:170451; RRID:Addgene_170451). pcDNA3.3_CoV2_501V2 was a gift from David Nemazee (Addgene plasmid # 170449 ; http://n2t.net/addgene:170449 ; RRID:Addgene_170449). pcDNA3.3-SARS2-B.1.617.1 was a gift from David Nemazee (Addgene plasmid # 172319; http://n2t.net/addgene:172319; RRID:Addgene_172319). pcDNA3.3_SARS2_omicron_BA.1 was a gift from David Nemazee (Addgene plasmid # 180375 ; http://n2t.net/addgene:180375 ; RRID:Addgene_180375). SARS-CoV-2 isolate /Canada/ON/VIDO-01-2020 was used for SARS-CoV-2 infections. This virus was isolated from a patient at a Toronto hospital who had returned from Wuhan, China[59]. The second passage viral stock was sequenced (GISAID – EPI_ISL_425177) to confirm stability of the virus after culture in vDMEM on Vero-76 cells. All work with infectious SARS-CoV-2 virus was performed in a Containment Level 3 (CL3) facility at the Vaccine and Infectious Disease Organization (VIDO) (Saskatoon, Saskatchewan, Canada). HCoV-229E was a kind gift from Dr. Maxim Berezovski (University of Ottawa, ON, CA) and was

originally obtained from ATCC (VR-740). miR-185 mimics and inhibitors as well as negative control mimics and inhibitors (con-miR) were purchased from *mirVana* (Ambion, Austin, TX). Lipofectamine RNAiMAX (Life Technologies, Carlsbad, CA) was utilized to perform miRNA mimics and inhibitor transfections. Transfections were performed according to the manufacturer's protocol with a ratio of 2.5 µL of RNAiMAx per 1 µL of 100 µM of miRNA mimic or inhibitors. Transfection of plasmid DNA was performed using Lipofectamine 2000 (Life Technologies, Carlsbad, CA), as per manufacturer's protocol. Fluvastatin was purchased from Sigma (SML0038) and 25-Hydroxycholesterol was purchased from Cayman Chemicals (11097).

4.6.2 Generation of D614G and N501Y mutants

Site-directed mutagenesis was performed using Quick-change Lightning kit (Agilent) as per the manufacturer's protocol with primers designed to introduce a point mutation which results in D614G and N501Y mutations in the pCMV14-3X-Flag-SARS-CoV-2 S plasmid. Primer sequences are as follows: for the N501Y mutation: Forward: 5' GGATTCCAGCCAACCTACGGCGTGGGTTACCAAC 3' Reverse: 5' GTTGGTAACCCACGCCGTAGGTTGGCTGGAATCC 3' and for the D614G mutation Forward: 5' GTGCTGTACCAAGGCGTGAATTGCACAG 3' Reverse: 5' CTGTGCAATTCACGCCTTGGTACAGCAC 3'.

4.6.3 Production of pseudo-typed viral particles

Hek293T cells in 10cm culture dishes were transfected with 2ug of plasmid containing SARS-CoV-2 S glycoprotein (original spike, Alpha, Beta or delta variant) or mock plasmid and 4ug HIV-1 NL4-3 ΔEnv Vpr Luciferase Reporter Vector (pNL4-3. Luc.R-E-). pNL4-3. Luc.R-E- was a kind gift from Dr Benoit Barbeau from University of Quebec in Montreal. 72h post transfection

supernatants containing viral particles were harvested, centrifuged at 800 × g for 5 min to remove cell debris and passed through 0.45 μm filter.

4.6.4 Detection of S protein of SARS-CoV-2 by western blot

Spike protein in cells or on pseudovirions were detected by western blot using anti-SARS-CoV-2 S Monoclonal antibody (GeneTEX, GTX632604). Hek293T transfected with SARS-CoV-2 expressing plasmid and pNL4-3.Luc.R-E or mock were lysed using 1X SDS lysis buffer (50 mM Tris-HCl [pH 6.8], 2% SDS, and 10% glycerol). To pellet down pseudovirus, the viral supernatants were centrifuged at 27800 rpm for 3 h in a AH-629 swinging bucket rotor at 4 °C through a 30% sucrose cushion, and virus pellets were resuspended into 100 μl SDS lysis buffer. Following lysis, the lysates were passed through a 21 G needle (BDBiosciences). Lysates were separated on the 10% TGX stain-free gel (BioRad). The migrated proteins were visualized and activated on a ChemiDoc MP (Bio-Rad). The proteins were then transferred onto a PVDF membranes using the Trans-Blot turbo (Bio-Rad). Following the transfer, the membranes were blocked using 5% BSA in TBS-T. Subsequently, the membranes were incubated with primary antibodies overnight at various dilutions depending on the identity of the antibody. Following primary incubation, the membranes with secondary donkey anti-rabbit antibody conjugated with horseradish peroxidase (1:20000; Jackson ImmunoResearch Laboratories, Inc., 115-035-062). The blots were visualized on the ChemiDoc MP (Bio-Rad) with clarity ECL solution reagent (Bio-Rad). Blot images were cropped and adjusted for contrast using Image Lab (Bio-Rad).

4.6.5 Entry assays

Huh7 or $A549^{ACE2}$ cells were seeded in 24 well plates and the next day the cells were transfected with either 100nM con-miR 50nM con-inhibitor or 100nM miR-185 mimic or 50nM inhibitor. Conversely, Calu-3 were reverse transfected with mimics and inhibitors. On the following day,

cells were transduced with 100ul of media containing pseudovirions. Spinfection at 800xg for 1h was performed to ensure efficient viral attachment. Cells were lysed 48h post transduction using 1X passive lysis buffer (Promega). Luciferase activity was measured using a microplate reader. All experiments were read in technical triplicates for at least three biological replicates.

4.6.6 Fluvastatin and 25-Hydroxychlesterol treatments

Huh7 cells were seeded in 24-well plates and the next day, cells were pre-treated for 24 hours with varying concentrations of Fluvastatin, 25-HC or vehicle. Following pre-treatment, cells were transduced with equal amounts of pseudovirus. Spinfection at 800xg for 1h was performed to ensure efficient viral attachment. Cells were lysed 48h post transduction using 1X passive lysis buffer (Promega). Luciferase activity was measured using a microplate reader. All experiments were read in technical triplicates for at least three biological replicates.

4.6.7 Transfections and infections

Generally, for non-infected cells, transfections were conducted in 6-well plates. On day one, cells were reverse transfected with con-miR or miR-185 mimics or inhibitors at a 100nM final concentration for mimics or 50nM final concentration for inhibitors. Transfections were conducted in OptiMEM using RNAiMAX reagent according to the manufacturer's protocol. 72h post-transfection, cells were lysed for RNA analysis. For 229E infections, Huh7 cells or A549 Cells were used and infected with the HCoV-229E. Cells were initially seeded at 200,000 cells per well in a 6-well plate. The next day, the cells were forward transfected, as previously described with con-miR or miR-185 mimic at a 100nM final concentration. The following day, the cells were infected with HCoV-229E at an MOI of 0.05 in minimal serum-free media for 2h. The Medium was then replaced with complete medium following the 2h incubation. Forty-eight hours post-

infection, cells were lysed using Norgen total RNA isolation kit (Norgen Biotek, Thorold, ON) fro Total RNA isolation.

4.6.8 HCoV-229E Plaque assay

Huh7 cells were seeded at 6.5×10^5 cells/well in 6-well plates. The next day, the supernatants collected from HcoV-229E-infected cells were 10-fold serially diluted (1:10 to $1:10^6$). The media on Huh7 cells was replaced with 100 µl of serially diluted virus. Huh7 cells cells were incubated in virus-containing supernatant at 37 °C for 2 h. Following the 2h infection, 2 ml of warm DMEM 1% Carboxymethylcellulose DMEM medium was added to each well and allowed to solidify. After2-3 days, 2mL 10% formaldehyde was added to each well and incubated for 30 mins. Following formaldehyde fixation, media containing fixing solution was removed and staining solution (10% ethanol, 0.1% crystal violet) was added to each well and incubated for 15-30 mins, excess stain was then washed with water and dried. Plaque forming units per milliliter of supernatant were calculated considering the dilution factor to report on the viral titers.

4.6.9 Quantitative real-time PCR

For the RNA analysis, RNA isolations were performed using RNA RNeasyPluskit, (Qiagen, Mississauga, ON) or Norgen total RNA isolation kit (Norgen Biotek, Thorold, ON). For the RT-qPCR analysis, the isolated RNA was initially quantified using a NanoDrop (Thermo Fisher Scientific). RNA integrity was evaluated using a 0.8% agarose RNA integrity gel in 1X Tris borste-EDTA (Ambion). 500ng of isolated RNA was reverse transcribed using the iScript reverse transcription kit (BioRad) according to the manufacturer's protocol. qPCR was subsequently performed using SSOAdvanced Universal SYBR GreenSupermix (Bio-Rad) according to the manufacturer's instructions. CFX Connect Real-Time PCR Detection System (Bio-Rad, Hercules, CA) was utilized for the analysis of the qPCR runs. Final concentration of 500nM of each

evaluated primer was used in a final reaction volume of 10 µL. $2^{-\Delta\Delta Ct}$ method was utilized to analyze the relative levels of mRNA and relative fold change in mRNA levels[60]. 18sRNA was utilized to normalize samples.

4.6.10 Transfections of miRNAs for SARS-CoV-2 inoculation

Calu-3 Cells (ATCC) were grown in complete DMEM prior to transfections. Cells were transfected in 6-well plates with miRNA-185 miRNA mimic or control miRNA (miRVana, ThermoFisher Scientific) via Lipofectamine RNAiMAX transfection reagent (ThermoFisher Scientific) in Optimem (Gibco, Life Technologies) medium. The transfection reagents were added to the growth media of cells for a final concentration of 100 nM of miRNA. Calu-3 cells were also plated with no transfection reagent as a control. At 24-hours post-transfection, media was removed from the cells. Cells were washed twice with 1X PBS before adding 100 µl of SARS-CoV-2/Canada/ON/VIDO-01/2020 at an MOI of 0.01. Supernatant and cellular RNA were collected for downstream analyses at 0-, 24-, 48- and 72 hours post-inoculation.

4.6.11 RNA extraction from SARS-CoV-2 infected cells and quantitative Real-Time PCR (qRT-PCR)

Cellular RNA was extracted using the Qiagen© RNeasy Mini kit (Qiagen) according to the manufacturer's instructions. vRNA was extracted supernatant using the Qiagen© QIAamp Viral RNA Mini Kit (Qiagen). All cellular qRT-PCR was performed in triplicate on cDNA synthesized as previously described[61]. vRNA was quantified by Qiagen© Quanti-fast RT probe master mix (Qiagen) using primer/probe sets specific for the SARS-CoV-2 subgenomic E gene. The reactions were performed on a StepOnePlusTM Real-Time PCR System in a 96-well plate (Thermo Fisher) as previously described[62].

4.6.12 Statistical analysis

Data is presented as the mean of replicates, with error bars representing the standard error of the mean. Unless otherwise stated, statistical significance was evaluated using Student's t-test, and P-values less than 0.05 were deemed significant.

4.7 Acknowledgments

N.A. and N.A. are supported by a NSERC Postgraduate Scholarship-Doctoral (PGS-D). This work is supported by funding from a Natural Sciences and Engineering Research Council (NSERC) grant (298496) and a Canadian Institutes of Health Research (CIHR) grant (136807).

4.8 References

1. Harvey, W. T. *et al.* SARS-CoV-2 variants, spike mutations and immune escape. *Nat. Rev. Microbiol.* **19**, 409–424 (2021).
2. Awadasseid, A., Wu, Y., Tanaka, Y. & Zhang, W. Effective drugs used to combat SARS-CoV-2 infection and the current status of vaccines. *Biomed. Pharmacother.* **137**, 111330 (2021).
3. Ebrahimi, M., Malehi, A. S. & Rahim, F. COVID-19 patients: A systematic review and meta-analysis of laboratory findings, comorbidities, and clinical outcomes comparing medical staff versus the general population. *Osong Public Heal. Res. Perspect.* **11**, 269–279 (2020).
4. Liu, C. H., Lu, C. H., Wong, S. H. & Lin, L. T. Update on Antiviral Strategies Against COVID-19: Unmet Needs and Prospects. *Front. Immunol.* **11**, 1–13 (2021).
5. Kyriakidis, N. C., López-Cortés, A., González, E. V., Grimaldos, A. B. & Prado, E. O. SARS-CoV-2 vaccines strategies: a comprehensive review of phase 3 candidates. *npj Vaccines* **6**, (2021).
6. Peng, X.-L. *et al.* Advances in the design and development of SARS-CoV-2 vaccines. *Mil. Med. Res.* **8**, 1–31 (2021).
7. Barone, P. & DeSimone, R. A. Convalescent plasma to treat coronavirus disease 2019 (COVID-19): considerations for clinical trial design. *Transfusion* **60**, 1123–1127 (2020).
8. Polack, F. P. *et al.* Safety and Efficacy of the BNT162b2 mRNA Covid-19 Vaccine. *N. Engl. J. Med.* **383**, 2603–2615 (2020).
9. Liu, L. *et al.* Striking Antibody Evasion Manifested by the Omicron Variant of SARS-CoV-2. *Nature* **202**,676-681 (2021)
10. Arora, P. *et al.* The spike protein of SARS-CoV-2 variant A.30 is heavily mutated and evades vaccine-induced antibodies with high efficiency. *Cell. Mol. Immunol.* **18**, 2673–2675 (2021).
11. Chen, R. E. *et al.* Resistance of SARS-CoV-2 variants to neutralization by monoclonal and serum-derived polyclonal antibodies. *Nat. Med.* **27**, 717–726 (2021).
12. Hoffmann, M. *et al.* SARS-CoV-2 Cell Entry Depends on ACE2 and TMPRSS2 and Is Blocked by a Clinically Proven Protease Inhibitor. *Cell* **181**, 271-280.e8 (2020).
13. Lu, Y., Liu, D. X. & Tam, J. P. Lipid rafts are involved in SARS-CoV entry into Vero E6 cells. *Biochem. Biophys. Res. Commun.* **369**, 344–349 (2008).
14. Radenkovic, D., Chawla, S., Pirro, M., Sahebkar, A. & Banach, M. Cholesterol in relation to covid-19: Should we care about it? *J. Clin. Med.* **9**, 1–9 (2020).
15. Krishnan, S. *et al.* Metabolic perturbation associated with COVID-19 disease severity and SARS-CoV-2 replication. *Mol. Cell. Proteomics* **20**, 0–14 (2021).
16. Mohr, A. M. & Mott, J. L. Overview of microRNA biology. *Semin. Liver Dis.* **35**, 3–11 (2015).

17. Singaravelu, R. *et al.* MicroRNAs regulate the immunometabolic response to viral infection in the liver. *Nat. Chem. Biol.* **11**, 988–993 (2015).

18. Ou, X. *et al.* Characterization of spike glycoprotein of SARS-CoV-2 on virus entry and its immune cross-reactivity with SARS-CoV. *Nat. Commun.* **11**, (2020).

19. Deng, H. K. *et al.* Identification of a major co-receptor for primary isolates of HIV-1. *Nature* **381**, 661–666 (1996).

20. Sherman, E. J. & Emmer, B. T. ACE2 protein expression within isogenic cell lines is heterogeneous and associated with distinct transcriptomes. *Sci. Rep.* **11**, 1–13 (2021).

21. Hou, Y. J. *et al.* SARS-CoV-2 D614G variant exhibits efficient replication ex vivo and transmission in vivo. *Science* **370**, 1464–1468 (2020).

22. Liu, Y. *et al.* The N501Y spike substitution enhances SARS-CoV-2 infection and transmission. *Nature* **602**, 294–299 (2021)

23. Zang, R. *et al.* Cholesterol 25-hydroxylase suppresses SARS-CoV-2 replication by blocking membrane fusion. *Proc. Natl. Acad. Sci. U. S. A.* **117**, 32105–32113 (2020).

24. Zu, S. *et al.* 25-Hydroxycholesterol is a potent SARS-CoV-2 inhibitor. *Cell Res.* **30**, 1043–1045 (2020).

25. Li, C. *et al.* 25-Hydroxycholesterol Protects Host against Zika Virus Infection and Its Associated Microcephaly in a Mouse Model. *Immunity* **46**, 446–456 (2017).

26. Anggakusuma *et al.* Interferon-inducible cholesterol-25-hydroxylase restricts hepatitis C virus replication through blockage of membranous web formation. *Hepatology* **62**, 702–714 (2015).

27. Liu, S. Y., Sanchez, D. J., Aliyari, R., Lu, S. & Cheng, G. Systematic identification of type I and type II interferon-induced antiviral factors. *Proc. Natl. Acad. Sci. U. S. A.* **109**, 4239–4244 (2012).

28. Gomes, B., Gonçalves, S., Disalvo, A., Hollmann, A. & Santos, N. C. Effect of 25-hydroxycholesterol in viral membrane fusion: Insights on HIV inhibition. *Biochim. Biophys. Acta - Biomembr.* **1860**, 1171–1178 (2018).

29. Liu, S. Y. *et al.* Interferon-Inducible Cholesterol-25-Hydroxylase Broadly Inhibits Viral Entry by Production of 25-Hydroxycholesterol. *Immunity* **38**, 92–105 (2013).

30. Adams, C. M. *et al.* Cholesterol and 25-hydroxycholesterol inhibit activation of SREBPs by different mechanisms, both involving SCAP and insigs. *J. Biol. Chem.* **279**, 52772–52780 (2004).

31. Ahn, A., Gibbons, D. L. & Kielian, M. The Fusion Peptide of Semliki Forest Virus Associates with Sterol-Rich Membrane Domains. *J. Virol.* **76**, 3267–3275 (2002).

32. Li, G. M., Li, Y. G., Yamate, M., Li, S. M. & Ikuta, K. Lipid rafts play an important role in the early stage of severe acute respiratory syndrome-coronavirus life cycle. *Microbes Infect.* **9**, 96–102 (2007).

33. Sanders, D. W. *et al.* Sars-cov-2 requires cholesterol for viral entry and pathological syncytia formation. *Elife* **10**, (2021).

34. Glende, J. *et al.* Importance of cholesterol-rich membrane microdomains in the interaction of the S protein of SARS-coronavirus with the cellular receptor angiotensin-converting enzyme 2. *Virology* **381**, 215–221 (2008).

35. Madison, B. B. Srebp2: A master regulator of sterol and fatty acid synthesis1. *J. Lipid Res.* **57**, 333–335 (2016).

36. Wei, C. *et al.* HDL-scavenger receptor B type 1 facilitates SARS-CoV-2 entry. *Nat. Metab.* **2**, 1391–1400 (2020).

37. Teissier, É. & Pécheur, E. I. Lipids as modulators of membrane fusion mediated by viral fusion proteins. *European Biophysics Journal* vol. 36 887–899 (2007).

38. de Carvalho, M. V., Gonçalves-De-albuquerque, C. F. & Silva, A. R. PPAR gamma: From definition to molecular targets and therapy of lung diseases. *Int. J. Mol. Sci.* **22**,1–20 (2021).

39. Ebert, M. S. & Sharp, P. A. Roles for MicroRNAs in conferring robustness to biological processes. *Cell* **149**, 515–524 (2012).

40. Jonas, S. & Izaurralde, E. Towards a molecular understanding of microRNA-mediated gene silencing. *Nat. Rev. Genet.* **16**, 421–433 (2015).

41. O'Brien, J., Hayder, H., Zayed, Y. & Peng, C. Overview of microRNA biogenesis, mechanisms of actions, and circulation. *Front. Endocrinol. (Lausanne).* **9**, 1–12 (2018).

42. Tambyah, P. A. *et al.* microRNA expression in blood of dengue patients. *Ann. Clin. Biochem.* **53**, 466–476 (2015).

43. Ouyang, X. *et al.* Dysregulated serum miRNA profile and promising biomarkers in dengue-infected patients. *Int. J. Med. Sci.* **13**, 195–205 (2016).

44. Jopling, C. L., Yi, M., Lancaster, A. M., Lemon, S. M. & Sarnow, P. Modulation of Hepatitis C Virus RNA Abundance by a Liver-specific MicroRNA. *Science* **1**, 1577–1581 (2005).

45. Singaravelu, R. *et al.* A conserved miRNA-183 cluster regulates the innate antiviral response. J. Biol. Chem. 294, 19785–19794 (2019).

46. Van Der Ree, M. H. *et al.* Miravirsen dosing in chronic hepatitis C patients results in decreased microRNA-122 levels without affecting other microRNAs in plasma. *Aliment. Pharmacol. Ther.* **43**, 102–113 (2016).

47. van der Ree, M. H. *et al.* Safety, tolerability, and antiviral effect of RG-101 in patients with chronic hepatitis C: a phase 1B, double-blind, randomised controlled trial. *Lancet* **389**, 709–717 (2017).

48. Cagno, V. *et al.* Inhibition of herpes simplex-1 virus replication by 25-hydroxycholesterol and 27-hydroxycholesterol. *Redox Biol.* **12**, 522–527 (2017).

49. Liu, Y. *et al.* Activation of liver X receptor plays a central role in antiviral actions of 25-hydroxycholesterol. *J. Lipid Res.* **59**, 2287–2296 (2018).

50. Wang, S. *et al.* Cholesterol 25-Hydroxylase inhibits SARS -CoV-2 and other coronaviruses by depleting membrane cholesterol . *EMBO J.* **39**, (2020).

51. Yan, B. *et al.* Characterization of the lipidomic profile of human coronavirus-infected cells: Implications for lipid metabolism remodeling upon coronavirus replication. *Viruses* **11**, (2019).

52. Nardacci, R. *et al.* Evidences for lipid involvement in SARS-CoV-2 cytopathogenesis. *Cell Death Dis.* **12**, (2021).

53. Sagan, S. M. *et al.* The influence of cholesterol and lipid metabolism on host cell structure and hepatitis C virus replication. *Biochem. Cell Biol.* **84**, 67–79 (2006).

54. Lu, Y., Liu, D. X. & Tam, J. P. Lipid rafts are involved in SARS-CoV entry into Vero E6 cells. *Biochem. Biophys. Res. Commun.* **369**, 344–349 (2008).

55. Spann, N. J. & Glass, C. K. Sterols and oxysterols in immune cell function. *Nat. Immunol.* **14**, 893–900 (2013).

56. Nomura, R. *et al.* Human Coronavirus 229E Binds to CD13 in Rafts and Enters the Cell through Caveolae. *J. Virol.* **78**, 8701–8708 (2004).

57. Guo, H. *et al.* The important role of lipid raft-mediated attachment in the infection of cultured cells by coronavirus infectious bronchitis virus beaudette strain. *PLoS One* **12**, 1–12 (2017).

58. Li, X. *et al.* Dependence of SARS-CoV-2 infection on cholesterol-rich lipid raft and endosomal acidification. *Comput. Struct. Biotechnol. J.* **19**, 1933–1943 (2021).

59. Marchand-Senécal, X. *et al.* Diagnosis and Management of First Case of COVID-19 in Canada: Lessons Applied from SARS-CoV-1. *Clin. Infect. Dis.* **71**, 2207–2210 (2020).

60. Livak, K. J. & Schmittgen, T. D. Analysis of relative gene expression data using real-time quantitative PCR and the 2-ΔΔCT method. *Methods* **25**, 402–408 (2001).

61. Paquette, S. G. *et al.* Influenza Transmission in the Mother-Infant Dyad Leads to Severe Disease, Mammary Gland Infection, and Pathogenesis by Regulating Host Responses. *PLoS Pathog.* **11**, 1–34 (2015).

62. Corman, V. M. *et al.* Detection of 2019 novel coronavirus (2019-nCoV) by real-time RT-PCR. *Eurosurveillance* **25**, (2020).

Chapter 5

Discussion and future perspectives

5.1 Investigating miRNA/mRNA regulatory nodes which modulate host-virus interactions and fine-tune viral pathogenesis.

The work presented in this thesis aims to identify novel miRNAs with unique functional roles in regulating host-virus interactions. In the presented studies in chapters (2-4), we identify three miRNA groups (miR-183 cluster, miR-383, and miR-185) with novel roles in regulating innate immune antiviral responses and host metabolic responses to antagonize viral pathogenesis. In these studies, we delineate the mechanism of actions of each miRNA by identifying their mRNA targets that contribute to the associated antiviral phenotypes. Our studies highlight the critical regulatory layer that miRNAs add to the intrinsic antiviral host responses to viral infections. In fact, a miRbase release identified more than 2000 miRNA precursors in the human genome, each of which possesses the potential to regulate hundreds of mRNA targets with downstream impacts on viral lifecycles[1]. Thus, identifying miRNAs that may regulate host-virus interactions may aid in identifying targetable regulatory nodes to therapeutically modulate viral propagation and viral pathogenesis.

Two approaches may be utilized to identify miRNAs with roles in regulating viral infection. One of the possible means is profiling endogenous miRNAs following viral infection and identifying miRNAs that are strongly dysregulated as a response to infection[2–5]. These identified miRNAs may have an impact on the viral life cycle, or their dysregulation could be associated with the host's response to the infection. The other potential approach is a loss-of-function or gain-of-function phenotypic screen to evaluate the contribution of a specific miRNA of interest on viral

accumulation and pathogenesis[6,7]. These two methods are widely utilized to identify miRNAs with potential functional roles in modulating host-virus interactions.

Prior to my thesis, miRNAs have been shown in multiple instances to be predictive biomarkers for human infection, suggesting that perturbations of miRNA expression and function are maintained in the clinical disease [8–11]. In my thesis, we identify miRNAs with relevant roles in modulating host-virus interplay. Additionally, my thesis aims to evaluate their potential involvement in regulating virus pathogenesis by uncovering their mechanism of action. Overall, my work examines the emerging role of miRNAs as tools that allow for the identification of targetable host factors and pathways that may influence viral pathogenesis.

5.2 miR-183 cluster

In the context of antiviral signaling and IFN-regulated cellular networks, miRNAs have been identified to play a crucial regulatory function[12]. As previously discussed, miRNAs have the potential to influence viral pathogenesis either through direct interactions with the viral genome or indirect interactions through the regulation of host-associated networks. Identifying these interactions hold potential in therapy and this was highlighted by miRNA-targeted treatments which recently reached the clinical setting with potential antiviral therapeutic outcome[8,13]. For example, miR-122 inhibitors were developed to suppress HCV infection and reached phase 2 clinical trials and thus highlighting the potential of miRNA-based targeted antiviral therapeutics[8,13]. Additionally, fine-tuning the expression of miRNAs known to regulate innate immune responses may act as an effective molecular strategy for the development of antiviral immunotherapeutics with broad efficacy.

In chapter 2, we identified a cluster with novel roles in modulating type-I interferon signaling to suppress viral infection[14]. We initially identified this highly conserved miRNA cluster (miR-96, miR-182, and miR-183) to be dysregulated while examining miRNA patterns during viral infections. The cluster was found to be dysregulated in expression during various DNA and RNA viral infections, pointing towards a potential role in the modulation of viral pathogenesis[15–19]. In our study, we show that the miR-183 cluster enhances type I signaling and production by targeting two negative regulators of these processes. We show that miR-183 enhances IRF3 and STAT1 phosphorylation by targeting PPP2CA and TRIM27. Specifically, TRIM27 functions as an E3 ligase to induce K48-linked ubiquitination at both Lys251 and Lys372 residues of TBK1, this results in the proteasomal degradation of TBK1 to consequently suppress IRF3 phosphorylation, and thus inhibiting type I IFN production[20]. Additionally, we show that miR-183 directly targets

PPP2CA, a phosphatase shown to dephosphorylate and deactivates IRF3 and STAT1; subsequently inhibiting type I interferon-mediated signaling and production[21,22]. It is essential to note that it is as well possible that the miR-183 cluster may target other currently unidentified genes or signaling networks that regulate the host antiviral response to viral infections and other pathogens. This presumption may lead to interesting future work to reveal precisely how the miR-183 cluster functions in different ways to regulate immune responses.

Future work should as well systemically interrogate the different downregulated genes in the miR-183 cluster's profiles obtained from the microarray analysis. For example, upon further investigation of downregulated genes in miR-183 transfected microarray samples, additional negative regulators of the antiviral innate immune response can be identified and are predicted direct targets of miR-183. Thus, future investigations to fully characterize the list of down-regulated genes from our microarray may reveal novel mechanisms of innate immune regulation mediated by the miR-183 cluster. Some possible targets which may contribute to miR-183's antiviral properties and warrant further exploration include Dihydroorotate dehydrogenase (DHODH), Forkhead box protein O1 (FOXO1), and Nuclear Receptor Subfamily 0 Group B Member 2 (NR0B2).

DHODH is an enzyme that catalyzes the rate-limiting step in the *de novo* pyrimidine synthesis pathway and is found to oxidize dihydroorotate (DHO) acid to orotate (ORO)[23]. DHODH has been found to be implicated in viral pathogenesis with several studies providing evidence to support the antiviral potential of inhibiting DHODH which depletes pyrimidine pools essential for efficient viral replication[24,25]. Thus, future examination of miR-183's potential in inhibiting and targeting DHODH may reveal a novel mechanism contributing to miR-183's antiviral potential.

Another miR-183 predicted target that warrants future investigation is FOXO1. FOXO1 is a highly conserved transcription factor that has regulatory functions in a wide variety of processes including cell cycle progression, arrest, and apoptosis[26]. Studies have validated FOXO1 to be a potential target of the miRNA cluster in mesothelioma cells and T-lymphocytes[27,28], suggesting a potential regulatory function of the cluster on FOXO1. Interestingly, a more recent study revealed the inhibitory effects of FOXO1 overexpression on virus-triggered ISRE activation, and IFN-β induction suggesting an inhibitory role in innate antiviral responses[29]. The same study revealed that FOXO1 mediates this effect by inducing the degradation of IRF3[29]. Given this, it would be of interest to investigate and validate the contribution of miR-183 cluster's potential targeting of FOXO1to the observed antiviral phenotype.

Finally, although not a predicted target of the cluster, NR0B2 was found to be downregulated in miR-183-transfected microarray samples relative to con-miR transfected samples. NR0B2 is an orphan nuclear hormone receptor that has been found to be implicated in the regulation of various metabolic processes including glucose, bile acid, cholesterol, and fatty acid homeostasis[30]. Interestingly, this nuclear receptor has been found to negatively regulate NF-κB p65 modulated signaling and consequential activation of the NLRP3 inflammasome[31]. Thus, future work should examine the influence of the miR-183 cluster on the regulation of the NLRP3 inflammasome through the NR0B2 regulatory axis and examine how the cluster negatively regulates the expression of NR0B2.

Additionally, future work should aim to expand the cell lines used in this study to include immune cells such as macrophages and aim to validate the finding in primary cells mimicking more physiologically relevant conditions. It would also be beneficial to ultimately investigate the immunomodulatory effects of the cluster *in vivo*. The findings from such experiments would

further solidify the significance and the physiological relevance of the cluster in modulating the innate immune responses and evaluate its relevance in the development of antiviral therapeutics. Additionally, it would be of interest to evaluate the antiviral impact of the cluster on pathogens of different origins that are known to activate the innate immune response such as DNA viruses, retroviruses, and bacterial infections. Examining the expression profile during miR-183 cluster overexpression and stimulation during diverse pathogens may point toward novel cluster-modulatory mechanisms and evaluate the cluster's potential of having broad immunomodulatory functions.

Our study focused on identifying potential direct targets of the miR-183 cluster that may be contributing to its antiviral properties. However, the indirect effects of miRNAs may contribute to their functionality. Thus, future work will aim to expand on our abundance-based genomics and transcriptomics approaches to include functional and activity-based proteomics approaches such as activity-based protein profiling (ABPP) to further characterize the cluster's function in the modulation of antiviral responses. Previous ABPP work in the Pezacki lab utilized functionally characterized the changes in the active proteome during HCV infection using activity-based probes targeting various classes of enzymes, including serine hydrolases and kinases[32–34]. More recently, our lab utilized ABPP to characterize the functional effects of miRNAs in the modulation of antiviral responses during HCV infection[35,36]. Thus, future work should employ a similar approach to characterize the contributions of the cluster to the functional proteome and assess their effect on immune and antiviral function.

5.3 miR-383

In chapter 3, we have identified a miRNA with novel roles in the modulation of hepatic lipid metabolism and response to DENV infection. Previous reports point to a potential functional role of the miRNA in lipid metabolism, where misregulation of miR-383 levels was observed in primary mouse hepatocytes as a response to fatty acid treatment[37].

In our study, to further examine and elucidate the effects and functional role of miR-383 in hepatic cells, we perform transcriptomic and pathway enrichment analysis which uncovered the enhancement and enrichment of lipid and cholesterol metabolic pathways and mechanisms. We attributed these observed effects to the enhancement of SREBP2 and SREBP1c-modulated signaling and transcription, where we observed enhanced levels of the transcription factors and their targets in cells over-expressing the miRNA and conversely observed a decrease in cells with repressed levels of the miRNA. Although these findings confirm the mechanism by which miR-383 likely upregulated cholesterol and hepatic lipid metabolism, it is essential to note that there is a possibility that miR-383 may be modulating other metabolic pathways to give rise to this phenotype.

LXR receptors α and β have been found to play pivotal roles in the transcriptional control of lipid metabolism, with evidence supporting their role in maintaining cholesterol and lipid homeostasis[38,39]. For example, it has been shown that mice lacking LXRα accumulate significant amounts of cholesterol in the liver when fed a high-cholesterol diet[38]. Additionally, it has been shown that LXR acts as a regulator of SREBP-1C expression, thus affecting fatty acid metabolism by influencing the expression of FASN and ACACA[40]. Given this, it would be of interest to examine whether the lipogenic phenotype observed in miR-383 overexpressing cells could be attributed as well to miR-383-directed misregulation in LXR-dependent signaling.

In our study, we attribute the cholesterol accumulation to miR-383-directed downregulation of a negative regulator of SREBP-2 signaling, RNF145. Although this gene does not possess a site in its 3'UTR complementary to the miR-383 seed site, we still observe significant downregulation in RNF145. We attributed this to a potential non-canonical interaction. However, future studies should further investigate the mode of interaction between miR-383 and the 3'UTR to further validate the potential binding of miR-383 to the target's 3'UTR. Interestingly, previous reports identified RNF145 to be transcriptionally controlled by LXR[41]. Thus, future investigations should further examine miR-383's effects on LXR signaling and downstream effects on RNF145 levels.

In this study, we examine miR-383's role in modulating DENV infection. Previous work has revealed the dysregulation of miR-383 in the blood of patients with mild dengue infections relative to severe infections[11]. Taken together, these observations suggest an important role for miR-383 during DENV infection in humans. Thus, we sought to investigate the potential role of miR-383 in modulating and regulating DENV pathogenesis. Our study revealed that miR-383 inhibits DENV pathogenesis by targeting PLA2G4A, an enzyme that catalyzes the hydrolysis of membrane phospholipids to release arachidonic acid. This enzyme has been found to act as a host dependency factor for several viruses such as HCV and DENV[42]. More recently, PLA2G4A was found to be dysregulated during SARS-CoV-2 infection, suggesting a potential involvement in SARS-CoV-2 pathogenesis[43]. Thus, future work should examine the effects of miR-383 on SARS-CoV-2 among other viruses with potential dependency on the action of PLA2G4A. Some of the viruses which displayed dependencies on the activity of PLA2G4A include HCV, WNV, and coronaviruses[42,44,45]. This should further reveal the therapeutic potential of miR-383 and its utility as a tool for broad antiviral applications.

Although in this study we identified a pro-viral host factor that contributes to miR-383 observed antiviral potential, future studies should still systemically evaluate other downregulated genes from our transcriptomics studies. Interrogation of these downregulated genes should reveal other novel targets of miR-383 which may have pro-viral propensities and can be therapeutically targeted for antiviral properties.

Future studies as well should examine miR-383's involvement in arachidonic acid metabolism and its downstream effects on arachidonic acid depletion through the targeting of PLA2G4A. Arachidonic acids are converted via the action of cyclooxygenase enzymes to generate arachidonic acid-derived inflammatory intermediates such as prostaglandins[46]. Thus, investigating the effects of miR-383 on these downstream processes may uncover a novel role of miR-383 in regulating intracellular pro-inflammatory responses. Additionally, arachidonic acid was found to transcriptionally regulate COX-2 expression [47].COX-2 has been found to act as a pro-viral host factor that facilitates DENV replication[48]. Thus, future work should evaluate miR-383's impact on COX-2 levels. This should uncover an additional potential mechanism by which miR-383 may be modulating its antiviral effects which could be an interesting basis for future investigation.

Finally, our work should be validated in other cell lines to evaluate the applicability of this miRNA's antiviral potential in a broader context. Moreover, to evaluate and confirm the physiological relevance of this miRNA, analogous studies in primary cells and *in* vivo should be conducted. Overall, these studies should further confirm miR-383's contribution to the antiviral therapeutic potential of miRNAs.

5.4 miR-185

In chapter 4, we identify miR-185 to possess antiviral properties against coronaviruses, HCoV-229E, and SARS-CoV-2. In particular, we demonstrated that miR-185 represses the expression of several host genes that are found to positively regulate various stages of the viral life cycle. We have previously shown that miR-185 possesses antiviral properties against hepatitis C and Dengue viruses and the antiviral effects are mediated by miR-185's alterations in the host's lipid microenvironment which is essential for these viruses[16].

In this study, we confirmed the downregulation of SREBP2 and its targets to affect cholesterol biosynthesis, which has been previously shown to be implicated in SARS-CoV-2 entry. In addition to targeting SREBP2, we show that miR-185 negatively regulates the expression of another lipogenic direct target, HDL-scavenger receptor B type 1 (SACRB1). This protein is known to facilitate the ACE2-dependent entry of SARS-CoV2[49], contributing to miR-185 suppressive effects on entry. Interestingly, ACE2 expression is downregulated in miR-185 expressing cells, contributing to the observed miR-185-directed suppressive effects on entry even though miR-185 is not predicted to directly target ACE2. Although we attribute the observed suppressive effects to miR-185 targeting of PPAR-gamma, a lipogenic transcription factor that was previously found to regulate ACE2 expression[50], future work should aim to further investigate the mode of regulation by which miR-185 suppresses the expression of ACE2. Evaluation of miR-185 effects on ACE2 expression in cells lacking PPAR-gamma should shed light to validate miR-185's mechanism of regulation. Overall, future work should aim to assess each target's contribution to distinct stages of the SARS-CoV-2 lifecycle and contribution to the overall observed antiviral phenotype.

In this study, we show that miR-185 suppresses the entry of various VOCs which includes Alpha, Beta, Delta, and Omicron using the Spike pseudotyped virus model. Although the results from

these experiments point towards an antiviral functional role due to the observed suppression of viral entry, future work should aim to validate the inhibitory effects of miR-185 in a live virus models for each of the tested variants. These experiments should solidify miR-185 inhibitory effects on SARS-CoV-2 pathogenesis and validate miR-185's role as a potential therapeutic tool with broad antiviral applications.

Additionally, future investigations should aim to expand on the cellular models utilized in this study. In this study, we primarily utilized Calu-3 and Huh7 cell lines for the entry assays and live virus experiments. Although these cell lines are permissive to the virus and SARS-CoV-2 infection, they do not necessarily mimic human physiological conditions. Thus, it would be invaluable to replicate some of the experiments in primary human airway epithelial cells to validate the relevance of the findings in a more physiologically relevant model. Another model that has been proven to be versatile and useful for the study of SARS-CoV-2 pathogenesis is the organoids model. Organoids are generally composed of multiple cell types to model the physiological conditions of human organs. These structures can self-replicate and are suitable for studying the antiviral properties of therapeutic compounds and large-scale screening experiments[51]. SARS-CoV-2 has been found to affect several organs such as the kidneys[52], liver[53], and the cardiovascular system[54]. Thus, utilizing organoids to assess the antiviral properties of miR-185 will allow us to reproduce the pathology of COVID-19 in specific tissues on which they are modeled and evaluate the suppressive effects of miR-185 on SARS-CoV-2 in organoids of different origins. Finally, due to the complexity of the pathophysiology of the disease, it would be ideal to evaluate miR-185 suppressive effects on SARS-CoV-2 infection *in vivo* and in animal models of the disease. A transgenic mouse model expressing human ACE2 would be ideal for the validation of miR-185's

effects in a more complex system that more accurately represents the pathophysiology of the disease[55].

In addition to miR-185 the antiviral effects mediated by manipulation of the lipid microenvironment through the suppression of SREBP2 modulated signaling, it would be of interest to evaluate miR-185's effect on interleukin (IL)-1β driven inflammation and the downstream effects on COVID-19 pathology. Recent studies highlighted the crosstalk between SREBP2 signaling and activation of the inflammatory response[56]. Several studies revealed that (IL)-1β levels are elevated during COVID-19 infection contributing to the induction of cytokine storm due to uncontrolled immune responses in COVID-19 infection[57]. Thus, it would be invaluable to evaluate whether miR-185-directed suppression of SREBP2 signaling may consequentially dampen (IL)-1β release to control the inflammatory outcomes during SARS-CoV-2 infection.

miR-185 was identified by our lab using a systematic approach to identify miRNAs regulating virus-associated host pathways [16]. In this study, our lab utilized the Small Molecule-mediated annotation of miRNAs targets (SMART) approach to identify 25-HC modulated miRNAs that are capable to suppress HCV infection by modulating metabolic pathways. This method allowed for the identification of miR-185 and validated its regulation by 25-HC[16]. Future work should utilize the same method to identify other miRNAs that are modulated by diverse classes of antiviral therapeutic small molecules to regulate SARS-CoV-2 pathogenesis. This will allow for the systemic identification of novel and pathway-specific miRNA profiles with antiviral potential against SARS-CoV-2 and its variants.

5.5 General conclusions

In this presented thesis, we identify miRNAs with novel roles in modulating the pathogenesis of different viruses. This thesis highlights the therapeutic potential of miRNAs and uncovers the mechanism of action of each of the investigated miRNA in regulating the observed antiviral phenotype. Recent advancements in RNA delivery methods highlight the potential of utilizing miRNAs as therapeutic tools against various viral infections. Our work identified a novel miRNA cluster, miR-183 cluster, to have intrinsic antiviral capabilities by enhancing innate immune responses. Additionally, we identify miR-383 to possess antiviral roles against DENV infection my targeting a pro-viral host factor, PLA2G4A. Targeting this factor not only suppresses viral propagation but also modulates lipid homeostasis in the liver. This highlights the diversity in miRNA function and examines the complexity of regulatory layers that miRNAs add to host-virus interactions. Finally, in chapter 4, we examine the role of an immunomodulatory miRNA, miR-185, in regulating SARS-CoV-2 infection. In this chapter, we show that regulating metabolic regulatory nodes may impact several stages of the viral life cycle, impacting SARS-CoV-2 entry and pathogenesis. Overall, our work not only highlights the antiviral capabilities of the miRNAs examined in this thesis but also reveals the potential use of miRNAs as tools to identify novel targetable pathways and mechanisms for broader antiviral effects.

5.6 References

1. Kozomara, A. & Griffiths-Jones, S. MiRBase: Annotating high confidence microRNAs using deep sequencing data. *Nucleic Acids Res.* **42**, 68–73 (2014).
2. Makkoch, J. *et al.* Human microRNAs profiling in response to influenza A viruses (subtypes pH1N1, H3N2, and H5N1). *Exp. Biol. Med.* **241**, 409–420 (2016).
3. Farr, R. J. *et al.* Detection of SARS-CoV-2 infection by microRNA profiling of the upper respiratory tract. *PLoS One* **17**, 1–10 (2022).
4. Tambyah, P. A. *et al.* microRNA expression in blood of dengue patients. *Ann. Clin. Biochem.* **53**, 466–476 (2016).
5. Powdrill, M. H., Desrochers, G. F., Singaravelu, R. & Pezacki, J. P. The role of microRNAs in metabolic interactions between viruses and their hosts. *Curr. Opin. Virol.* **19**, 71–76 (2016).
6. Smith, J. L., Jeng, S., McWeeney, S. K. & Hirsch, A. J. A MicroRNA Screen Identifies the Wnt Signaling Pathway as a Regulator of the Interferon Response during Flavivirus Infection. *J. Virol.* **91**, (2017).
7. Santhakumar, D. *et al.* Combined agonist-antagonist genome-wide functional screening identifies broadly active antiviral microRNAs. *Proc. Natl. Acad. Sci. U. S. A.* **107**, 13830–13835 (2010).
8. Lanford, R. E. *et al.* Therapeutic silencing of microRNA-122 in primates with chronic hepatitis C virus infection. *Science (80-.).* **327**, 198–201 (2010).
9. Hu, W. Z. *et al.* Functional miRNAs in breast cancer drug resistance. *Onco. Targets. Ther.* **11**, 1529–1541 (2018).
10. Li, Y. J. *et al.* Alterations of Serum Levels of BDNF-Related miRNAs in Patients with Depression. *PLoS One* **8**, 1–7 (2013).
11. Tambyah, P. A. *et al.* microRNA expression in blood of dengue patients. *Ann. Clin. Biochem.* **53**, 466–476 (2015).
12. Forster, S. C., Tate, M. D. & Hertzog, P. J. MicroRNA as type I interferon-regulated transcripts and modulators of the innate immune response. *Front. Immunol.* **6**, 1–9 (2015).
13. van der Ree, M. H. *et al.* Safety, tolerability, and antiviral effect of RG-101 in patients with chronic hepatitis C: a phase 1B, double-blind, randomised controlled trial. *Lancet* **389**, 709–717 (2017).
14. Singaravelu, R. *et al.* A conserved miRNA-183 cluster regulates the innate antiviral response. *J. Biol. Chem.* **294**, 19785–19794 (2019).
15. Oussaief, L. *et al.* Modulation of MicroRNA Cluster miR-183-96-182 Expression by. **89**, 12178–12188 (2015).
16. Singaravelu, R. *et al.* MicroRNAs regulate the immunometabolic response to viral infection in the liver. *Nat. Chem. Biol.* **11**, 988–993 (2015).
17. El Sobky, S. A. *et al.* Contradicting roles of miR-182 in both NK cells and their host

target hepatocytes in HCV. *Immunol. Lett.* **169**, 52–60 (2016).

18. Chen, Y., Dong, X., Yu, D. & Wang, X. Serum miR-96 is a promising biomarker for hepatocellular carcinoma in patients with chronic hepatitis B virus infection. *Int. J. Clin. Exp. Med.* **8**, 18462–18468 (2015).

19. Stark, T. J., Arnold, J. D., Spector, D. H. & Yeo, G. W. High-Resolution Profiling and Analysis of Viral and Host Small RNAs during Human Cytomegalovirus Infection. *J. Virol.* **86**, 226–235 (2012).

20. Zheng, Q. *et al.* Siglec1 suppresses antiviral innate immune response by inducing TBK1 degradation via the ubiquitin ligase TRIM27. *Cell Res.* **25**, 1121–1136 (2015).

21. Long, L. *et al.* Recruitment of phosphatase PP2A by RACK1 adaptor protein deactivates transcription factor IRF3 and limits Type I interferon signaling. *Immunity* **40**, 515–529 (2014).

22. Shanker, V., Trincucci, G., Heim, H. M. & Duong, H. T. F. Protein phosphatase 2A impairs IFNα-induced antiviral activity against the hepatitis C virus through the inhibition of STAT1 tyrosine phosphorylation. *J. Viral Hepat.* **20**, 612–621 (2013).

23. Munier-Lehmann, H., Vidalain, P. O., Tangy, F. & Janin, Y. L. On dihydroorotate dehydrogenases and their inhibitors and uses. *J. Med. Chem.* **56**, 3148–3167 (2013).

24. Hoffmann, H. H., Kunz, A., Simon, V. A., Palese, P. & Shaw, M. L. Broad-spectrum antiviral that interferes with de novo pyrimidine biosynthesis. *Proc. Natl. Acad. Sci. U. S. A.* **108**, 5777–5782 (2011).

25. Cheung, N. N. *et al.* Broad-spectrum inhibition of common respiratory RNA viruses by a pyrimidine synthesis inhibitor with involvement of the host antiviral response. *J. Gen. Virol.* **98**, 946–954 (2017).

26. Yuan, C., Wang, L., Zhou, L. & Fu, Z. The function of FOXO1 in the late phases of the cell cycle is suppressed by PLK1-mediated phosphorylation. *Cell Cycle* **13**, 807–819 (2014).

27. Suzuki, R. *et al.* miR-182 and miR-183 promote cell proliferation and invasion by targeting FOXO1 in mesothelioma. *Front. Oncol.* **8**, 1–9 (2018).

28. Ichiyama, K. *et al.* The MicroRNA-183-96-182 Cluster Promotes T Helper 17 Cell Pathogenicity by Negatively Regulating Transcription Factor Foxo1 Expression. *Immunity* **44**, 1284–1298 (2016).

29. Lei, C. Q. *et al.* FoxO1 negatively regulates cellular antiviral response by promoting degredation of IRF3. *J. Biol. Chem.* **288**, 12596–12604 (2013).

30. Zhang, Y., Hagedorn, C. H. & Wang, L. Role of nuclear receptor SHP in metabolism and cancer. *Biochim. Biophys. Acta - Mol. Basis Dis.* **1812**, 893–908 (2011).

31. Yang, C. S. *et al.* Small heterodimer partner interacts with NLRP3 and negatively regulates activation of the NLRP3 inflammasome. *Nat. Commun.* **6**, 1–11 (2015).

32. Singaravelu, R., Blais, D. R., McKay, C. S. & Pezacki, J. P. Activity-based protein profiling of the hepatitis C virus replication in Huh-7 hepatoma cells using a non-directed active site probe. *Proteome Sci.* **8**, 1–15 (2010).

33. Blais, D. R. *et al.* Activity-based protein profiling identifies a host enzyme, carboxylesterase 1, which is differentially active during hepatitis C virus replication. *J. Biol. Chem.* **285**, 25602–25612 (2010).

34. Desrochers, G. F., Cornacchia, C., McKay, C. S. & Pezacki, J. P. Activity-Based Phosphatidylinositol Kinase Probes Detect Changes to Protein-Protein Interactions during Hepatitis C Virus Replication. *ACS Infect. Dis.* **4**, 752–757 (2018).

35. Filip, R. *et al.* Profiling of MicroRNA Targets Using Activity-Based Protein Profiling: Linking Enzyme Activity to MicroRNA-185 Function. *Cell Chem. Biol.* **28**, 202-212.e6 (2021).

36. Desrochers, G. F., Filip, R., Bastianelli, M., Stern, T. & Pezacki, J. P. microRNA-27b regulates hepatic lipase enzyme LIPC and reduces triglyceride degradation during hepatitis C virus infection. *J. Biol. Chem.* **298**, 101983 (2022).

37. Xia, S. F. *et al.* Role of miR-383 and miR-146b in different propensities to obesity in male mice. *J. Endocrinol.* **234**, 201–216 (2017).

38. Peet, D. J. *et al.* Cholesterol and bile acid metabolism are impaired in mice lacking the nuclear oxysterol receptor LXRα. *Cell* **93**, 693–704 (1998).

39. Janowski, B. A., Willy, P. J., Devi, T. R., Falckt, J. R. & Mangelsdorf, D. J. An oxysterol signalling pathway mediated by the nuclear receptor LXRa. *Lett. to Nat.* **96**, 266–271 (1996).

40. Higuchi, N. *et al.* Liver X receptor in cooperation with SREBP-1c is a major lipid synthesis regulator in nonalcoholic fatty liver disease. *Hepatol. Res.* **38**, 1122–1129 (2008).

41. Cook, E. C. L. *et al.* Identification of the ER-resident E3 ubiquitin ligase RNF145 as a novel LXR-regulated gene. *PLoS One* **12**, 1–18 (2017).

42. Menzel, N. *et al.* MAP-kinase regulated cytosolic phospholipase A2 activity is essential for production of infectious Hepatitis C virus particles. *PLoS Pathog.* **8**, 21 (2012).

43. Bock, J. O. & Ortea, I. Re-analysis of SARS-CoV-2-infected host cell proteomics time-course data by impact pathway analysis and network analysis: A potential link with inflammatory response. *Aging (Albany. NY).* **12**, 11277–11286 (2020).

44. Liebscher, S. *et al.* Phospholipase A2 activity during the replication cycle of the flavivirus West Nile virus. *PLoS Pathog.* **14**, (2018).

45. Müller, C. *et al.* Inhibition of Cytosolic Phospholipase A 2 α Impairs an Early Step of Coronavirus Replication in Cell Culture . *J. Virol.* **92**, (2018).

46. Jang, Y., Kim, M. & Hwang, S. W. Molecular mechanisms underlying the actions of arachidonic acid-derived prostaglandins on peripheral nociception. *J. Neuroinflammation* **17**, 1–27 (2020).

47. Hughes-Fulford, M., Li, C. F., Boonyaratanakornkit, J. & Sayyah, S. Arachidonic acid activates phosphatidylinositol 3-kinase signaling and induces gene expression in prostate cancer. *Cancer Res.* **66**, 1427–1433 (2006).

48. Lin, C. K. *et al.* Cyclooxygenase-2 facilitates dengue virus replication and serves as a

potential target for developing antiviral agents. *Sci. Rep.* **7**, 1–15 (2017).

49. Wei, C. *et al.* HDL-scavenger receptor B type 1 facilitates SARS-CoV-2 entry. *Nat. Metab.* **2**, 1391–1400 (2020).

50. de Carvalho, M. V., Gonçalves-De-albuquerque, C. F. & Silva, A. R. PPAR gamma: From definition to molecular targets and therapy of lung diseases. *International Journal of Molecular Sciences* vol. 22 1–20 (2021).

51. Ranga, A., Gjorevski, N. & Lutolf, M. P. Drug discovery through stem cell-based organoid models. *Adv. Drug Deliv. Rev.* **69**–**70**, 19–28 (2014).

52. Li, Z. *et al.* Caution on Kidney Dysfunctions of COVID-19 Patients. *SSRN Electron. J.* 1–25 (2020) doi:10.2139/ssrn.3559601.

53. Fan, Z. *et al.* Clinical Features of COVID-19-Related Liver Functional Abnormality. *Clin. Gastroenterol. Hepatol.* **18**, 1561–1566 (2020).

54. Zheng, Y. Y., Ma, Y. T., Zhang, J. Y. & Xie, X. COVID-19 and the cardiovascular system. *Nat. Rev. Cardiol.* **17**, 259–260 (2020).

55. Bao, L. *et al.* The pathogenicity of SARS-CoV-2 in hACE2 transgenic mice. *Nature* **583**, 830–833 (2020).

56. Kusnadi, A. *et al.* The Cytokine TNF Promotes Transcription Factor SREBP Activity and Binding to Inflammatory Genes to Activate Macrophages and Limit Tissue Repair. *Immunity* **51**, 241-257.e9 (2019).

57. Cavalli, G. & Dagna, L. The right place for IL-1 inhibition in COVID-19. *Lancet Respir. Med.* **9**, 223–224 (2021).

Chapter 6

Appendices

6.1 Supplemental information for Chapter 2 "Conserved miRNA-183 cluster regulates the innate antiviral response"

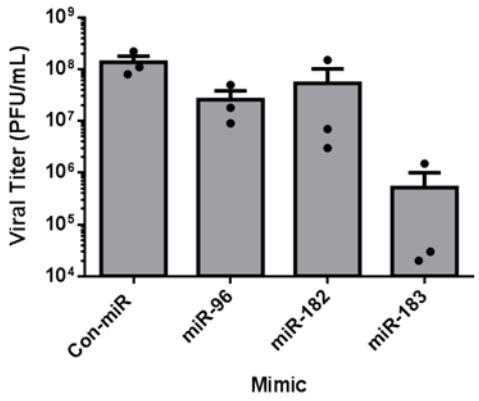

Figure S2. 1miR-183 inhibits VSV replication in mouse embryonic fibroblasts. Mouse embryonic fibroblasts (iMEFs) were transfected with 50nM miR-183 cluster mimics, independently**.** 48h post-transfection, cells were infected with VSV-GFP at an MOI of 0.01 for 24h. Supernatants were collected and the influence of miR-183 cluster mimics on VSV-GFP production in iMEFs was analysed by plaque assay. Data represents the means ±SEM of four biological replicates.

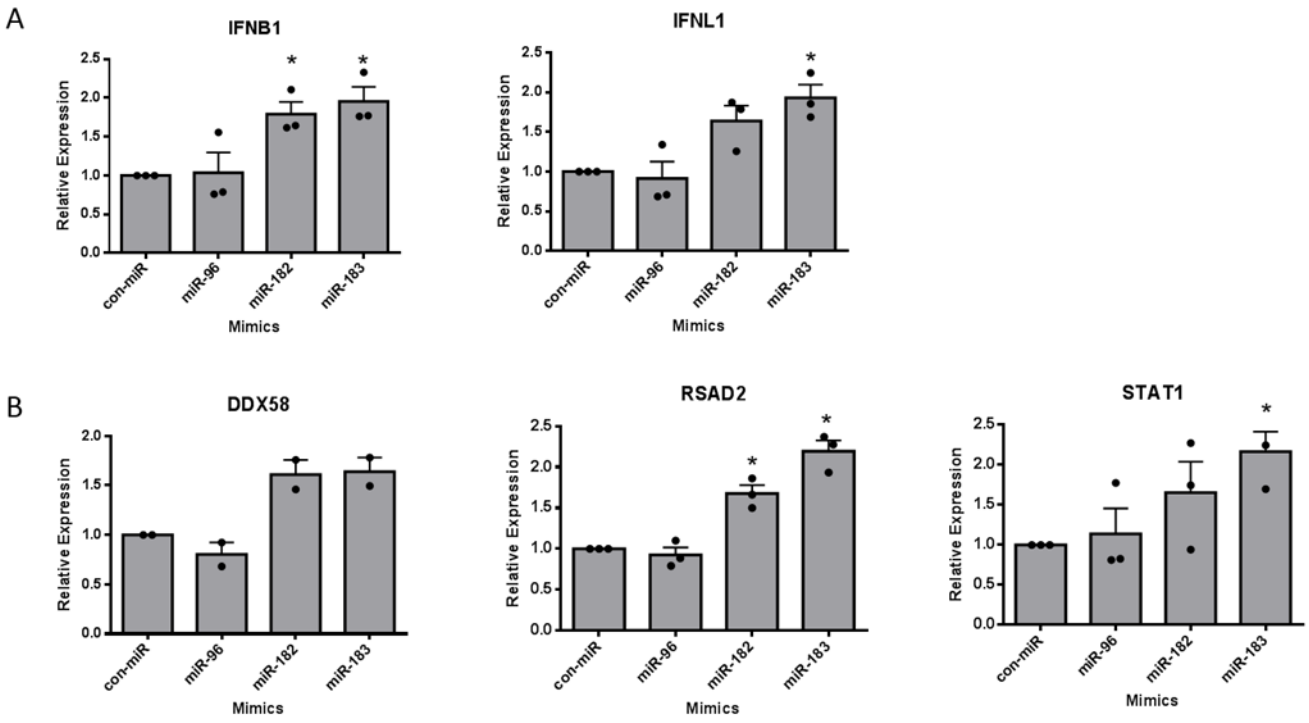

Figure S2. 2miR-183 activates innate antiviral response in MCF7 cells. (A)-(B) qRT-PCR analysis of relative (A) IFN expression (IFNB1 and IFNL1) and (B) ISG expression (RSAD2, STAT1, and DDX58) in MCF7 cells transfected with miR-183 cluster mimics or negative control (Con-miR) at a concentration of 50nM, and 48h post-transfection, infected with VSV-GFP at MOI of 0.01 for 24h. Data represents the means ±SEM of three biological replicates. *P<0.05.

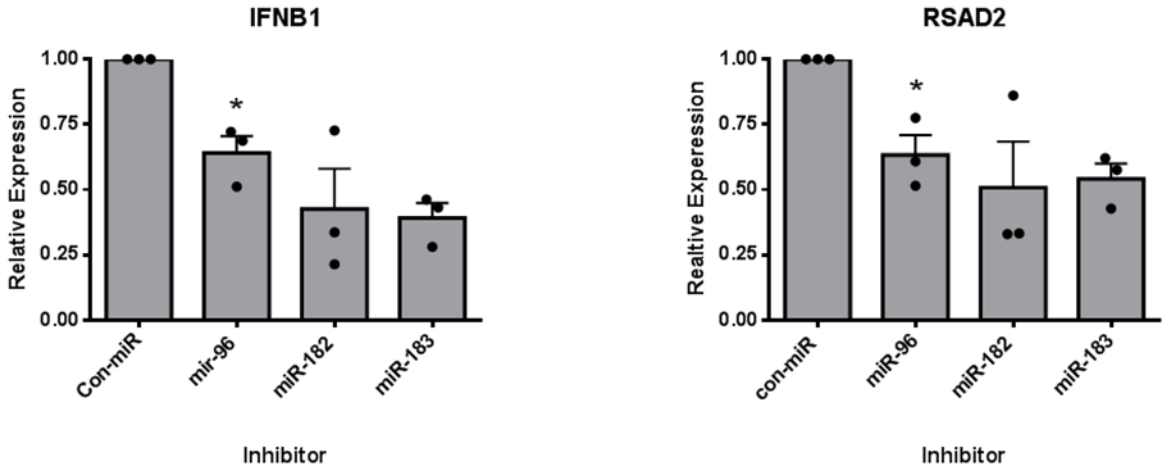

Figure S2. 3 miR-183 cluster inhibition impairs innate immune signaling. qRT-PCR analysis of relative IFNB1 and RSAD2 expression in VSV-GFP infected MCF7 cells transfected with inhibitors of the miR-183 cluster or negative control (Con-miR) at a concentration of 50nM, and 48h post-transfection, infected with VSV-GFP at MOI of 0.01 for 24h. Data represents the means ±SEM of three biological replicates.*P<0.05, and **P<0.01.

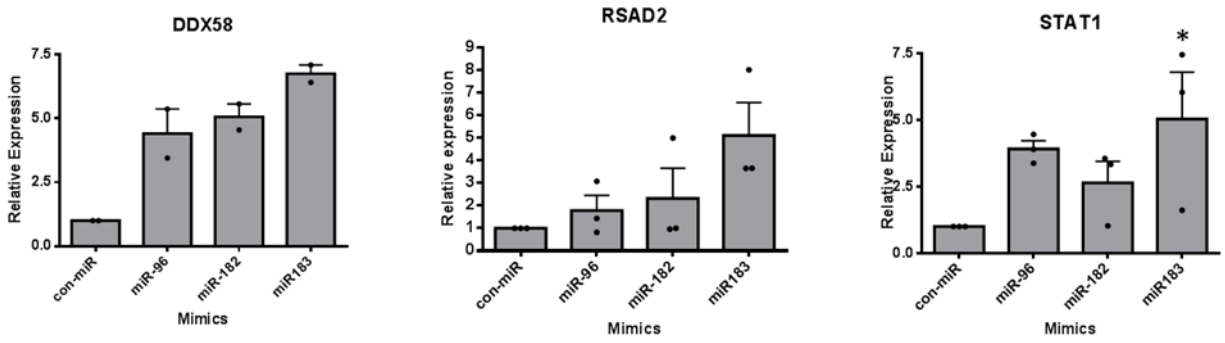

Figure S2. 4 miR-183 activates innate antiviral response in HepG2 cells. qRT-PCR analysis of relative ISG expression (RSAD2, STAT1, and DDX58) in HepG2 cells transfected with miR-183 cluster mimics or negative control (Con-miR) at a concentration of 50nM, and 48h post-transfection, infected with VSV-GFP at MOI of 0.01 for 24h. Error bars represent ±SEM .*P<0.05.

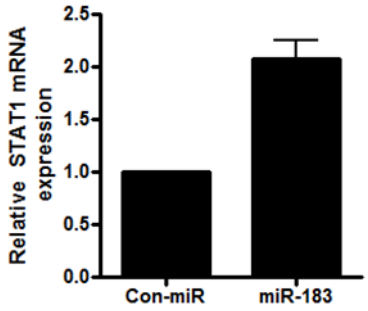

Figure S2. 5 miR-183 activates STAT1 expression. HepG2 cells were transfected with mimics for miR-183 or a negative control (Con-miR) at 50nM final concentration. The effects of miR-183 on STAT1 mRNA expression were measured via qRT-PCR 72 hours post-transfection.

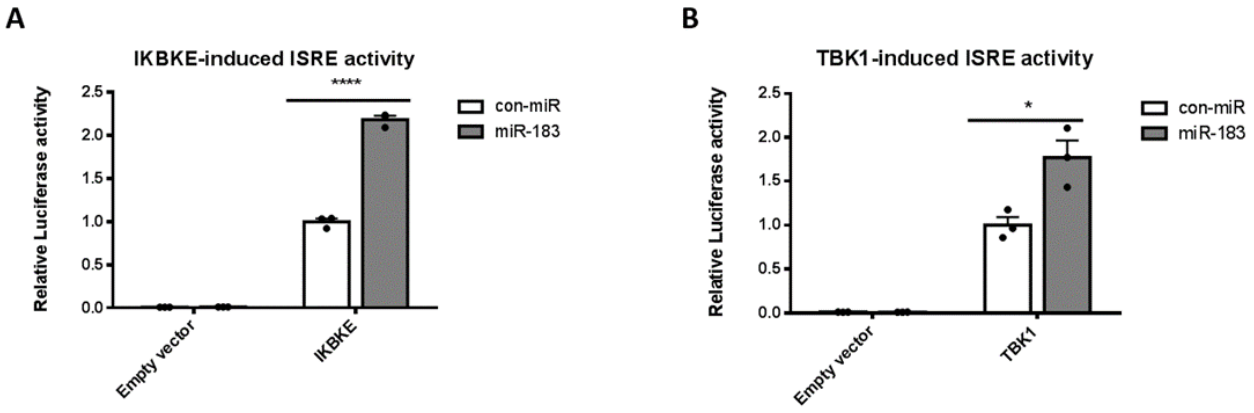

Figure S2. 6 miR-183 activates interferon-stimulated response element-driven gene expression. Hek293T cells were co-transfected with either miR-183 or control mimic (50nM), (A) IKBKE (100ng) or (B) TBK1 expression plasmids (100ng) or Empty vector (100ng), pISRE-Luc (100ng) and Renilla expression plasmid (transfection control) (50ng). Luciferase levels were normalized to Renilla luciferase levels and then control mimics (n = 3, mean ± SEM.).

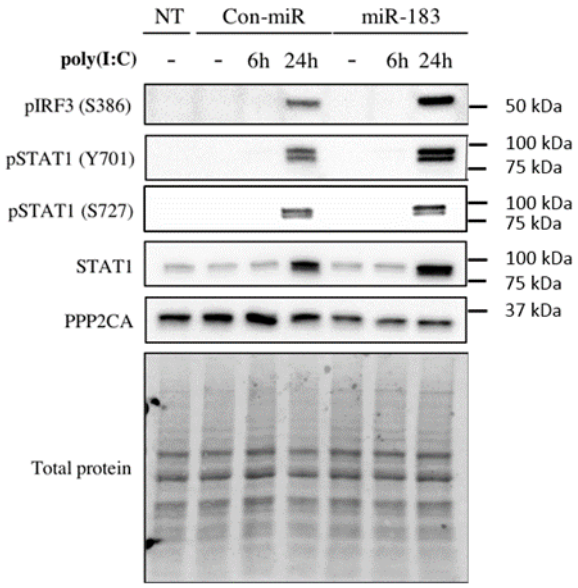

Figure S2. 7 miR-183 induces IRF3 and STAT1 phosphorylation in A549 cells. A549 cells were transfected with mimics for miR-183 or a negative control (Con-miR) at 50nM final concentration, and then immunostimulated with poly(I:C) at 500ng/mL for either 6 or 24 hours. Western blot analysis of PP2A catalytic subunit alpha (PPP2CA), phosphorylated IRF3 (pIRF3 S386), phosphorylated STAT1 (pSTAT1 Y701 and S727), and total STAT1 was performed. No treatment (NT) was also performed, and total protein loading serves as loading control.

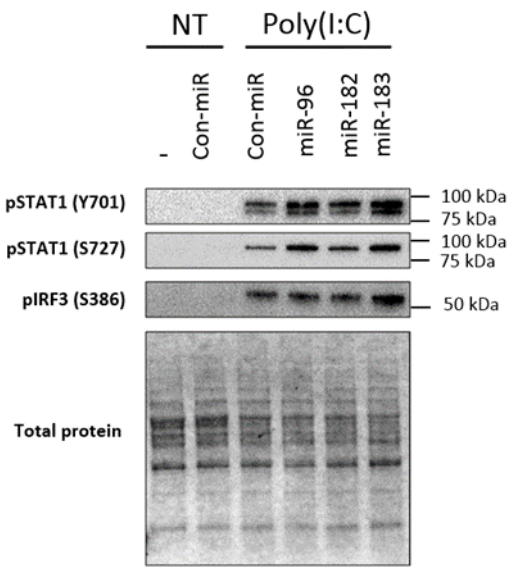

Figure S2. 8 miR-183 cluster regulates IRF3 and STAT1 phosphorylation in TLR3 agonist treated MCF7 cells. MCF7 cells were transfected with miR-183 cluster mimics or a negative control mimic (Con-miR), and then treated with naked poly(I:C) at a concentration of 50μg/mL for 24 hours. Western blot analysis of phosphorylated IRF3 (pIRF3 S386) and phosphorylated STAT1 (pSTAT1 Y701 and S727) was performed. No treatment (NT) was also performed, and total protein loading serves as loading control.

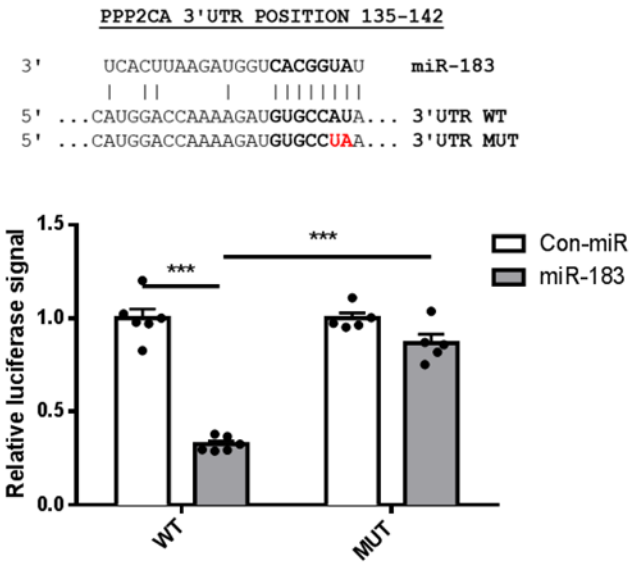

Figure S2. 9 miR-183 directly regulates PPP2CA. Relative luciferase reporter activity in Hek293 cells transfected with bicistronic vectors encoding firefly luciferase with the 3'UTR of PPP2CA bearing the wildtype (WT) or mutated (MUT) miR-183 binding sites and treated with control mimic (Con-miR) or miR-183. Dual luciferase assay activity was analyzed and Renilla luciferase signal was used to normalize for transfection efficiency. Results shown are normalized to respective control mimic. Mutated sequence of miR-183 binding site is shown. Data represents the means ±SEM of six biological replicates, ***P<0.001.

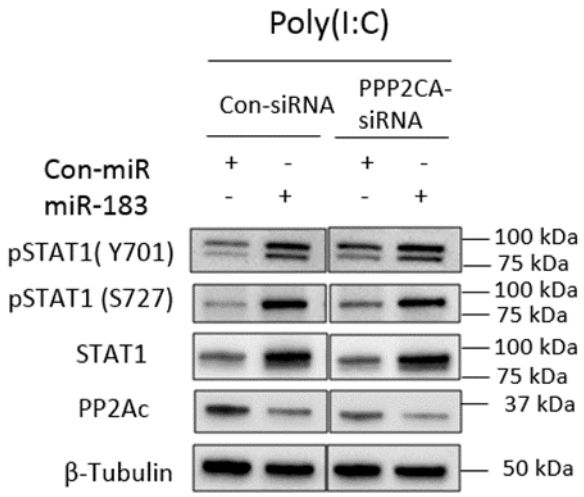

Figure S2. 10 siRNA-mediated knockdown of PPP2CA dampens miR-183 effect on STAT1 phosphorylation. HepG2 cells were first transfected with con-miR or miR-183 mimics (50nM), 24h post mimic transfection cells were transfected control siRNA (con-siRNA) or siRNA targeting (PPP2CA-siRNA) (50nM). 48h post mimic transfection, cells were stimulated poly(I:C) (500ng/mL) for 24h. Dampening of miR-183 effect on STAT1 phosphorylation (pSTAT1 Y701 and S727) is observed in PPP2CA-siRNA treated cells relative to con-siRNA. Immunoblot analysis on PP2Ac levels were performed to confirm PPP2CA knockdown and β-tubulin levels serve as loading control.

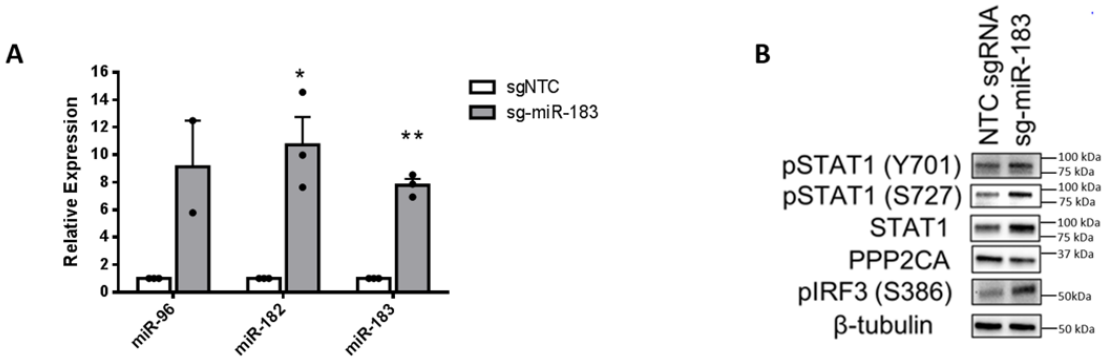

Figure S2. 11 CRISPR activation of miR-183 activates STAT1 expression. HepG2 cells stably expressing dCas9-VP64 and MS2-p65-HSF1 were transduced with either a non-target control guide NTC) or an optimized guide targeting the miR-183 cluster promoter (miR-183). (**A**) qPCR analysis of relative expression of miR-183 cluster is shown for each guide during CRISPR-activation induced expression of the miRNA cluster. Data represents the means ± SEM of three biological replicates. (**B**) CRISPRa-mediated miR-183 cluster induced HepG2 cells were stimulated with 500 ng/mL of poly(I:C)/LyoVec for 24h and immunoblot analysis of phosphorylated STAT1 (Y701 and S727), total STAT1, PPP2CA, phosphorylated IRF3 (S386) was performed. Non-targeting control guide expressing cells were also analyzed, and β-tubulin levels serve as loading control.

Table S2. 1 Gene ontology biological process analysis classifying miR-96 activated genes in immunostimulated cells.

ID	Name*	P-value
GO:0034340	response to type I interferon	1.511E-23
GO:0071357	cellular response to type I interferon	3.178E-23
GO:0060337	type I interferon signaling pathway	1.670E-22
GO:0006955	immune response	1.543E-17
GO:0045087	innate immune response	7.453E-17
GO:0006952	defense response	2.954E-16
GO:0034341	response to interferon-gamma	1.944E-15
GO:0034097	response to cytokine	1.734E-14
GO:0048525	negative regulation of viral process	2.923E-14
GO:0051607	defense response to virus	3.865E-14

Top ten overrepresented processes are listed among genes activated by greater than 1.5 fold in miR-96 mimic transfected HepG2 cells immunostimulated with poly(I:C)/LyoVec by biological process.

Table S2. 2 Gene ontology biological process analysis classifying miR-182 activated genes in immunostimulated cells.

ID	Name*	P-value
GO:0034340	response to type I interferon	1.201E-18
GO:0071357	cellular response to type I interferon	4.113E-18
GO:0060337	type I interferon signaling pathway	2.477E-17
GO:0051607	defense response to virus	5.282E-13
GO:0034341	response to interferon-gamma	1.570E-12
GO:0009615	response to virus	1.793E-11
GO:0048525	negative regulation of viral process	2.196E-11
GO:0098542	defense response to other organism	3.335E-11
GO:1903901	negative regulation of viral life cycle	4.787E-11
GO:0045071	negative regulation of viral genome replication	4.647E-10

Top ten overrepresented processes are listed among genes activated by greater than 1.5 fold in miR-182 mimic transfected HepG2 cells immunostimulated with poly(I:C)/LyoVec by biological process.

Table S2. 3 Gene ontology biological process analysis classifying miR-183 activated genes in immunostimulated cells.

ID	Name	P-value
GO:0034340	response to type I interferon	2.888E-21
GO:0060337	type I interferon signaling pathway	3.714E-21
GO:0071357	cellular response to type I interferon	7.691E-21
GO:0098542	defense response to other organism	1.238E-14
GO:0006955	immune response	1.427E-14
GO:0051607	defense response to virus	4.501E-14
GO:0009615	response to virus	1.112E-13
GO:0045087	innate immune response	6.650E-13
GO:0006952	defense response	1.162E-12
GO:0051707	response to other organism	4.653E-12

Top ten overrepresented processes are listed among genes activated by greater than 1.5 fold in miR-183 mimic transfected HepG2 cells immunostimulated with poly(I:C)/LyoVec by biological process.

Table S2. 4 List of qPCR primers used in this study.

Oligonucleotide	Sequence
RNA18S5	FWD: GCGATGCGGCGGCGTTATTC
	REV: CAATCTGTCAATCCTGTCCGTGTCC
DDX58	FWD: CTGGACCCTACCTACATCCTG
	REV: GGCATCCAAAAAGCCACGG
IFNB1	FWD: TCTGGCACAACAGGTACTAGGC
	REV: GAGAAGCACAACAGGAGAGCAA
IFNL1	FWD: TTCCAAGCCCACCACAAC
	REV: TCCCTCACCTGGAGAAGC
PPP2CA	FWD: GGTGGTCTCTCGCCATCTATAG
	REV: CTGGATCTGACCACAGCAAGTC
RSAD2	FWD: TGGGTGCTTACACCTGCTG
	REV: GAAGTGATAGTTGACGCTGGTT
STAT1	FWD: ATGGCAGTCTGGCGGCTGAATT
	REV: CCAAACCAGGCTGGCACAATTG
TRIM27	FWD: AGCCTGATCGCTCAGCTAGAAG
	REV: GGAGGTGTATCCAAGGTTCAG

6.2 Supplemental information for Chapter 3 "miR-383 regulates hepatic lipid homeostasis and response to Dengue virus infection"

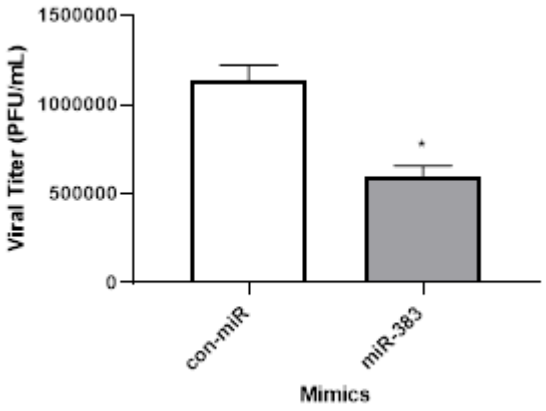

Figure S3. 1 miR-383 overexpression antagonizes DENV2 infectivity. Huh7 cells were either transfected with con-miR or miR-383. 24h post transfection, cells were infected with DENV-2 at an MOI 0.1. 48h post-transfection, supernatants were collected, and plaque assay was performed on vero cells as described in methods section. Titer represented as Plaque forming units/ mL (PFU/mL). Error bars represent the means ±SEM of three biological replicates. *P<0.05.

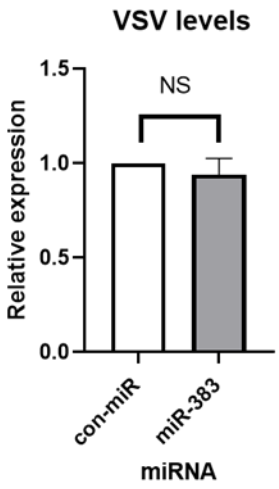

Figure S3. 2 miR-383 does not affect VSV pathogenesis. Huh7 cells were either transfected with con-miR or miR-383. 48h post transfection, cells were infected with VSV at an MOI 0.01. 24h post-transfection, **c**ells were lysed for qPCR analysis of intracellular levels of VSV. Error bars represent the means ±SEM of three biological replicates. NS. Not significant.

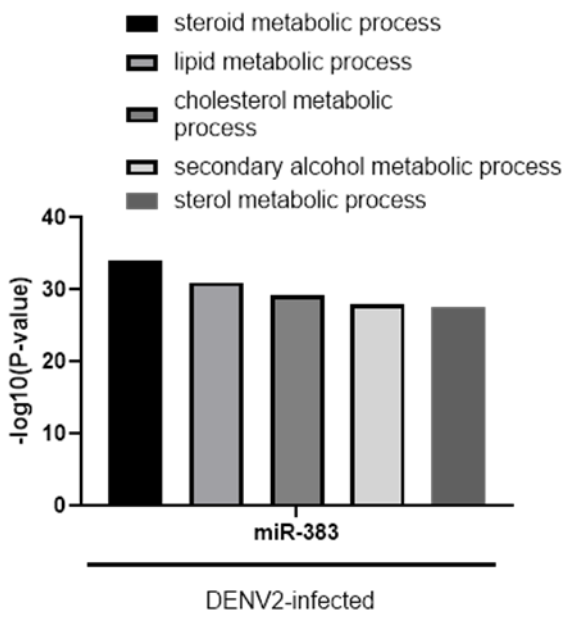

Figure S3. 3 Gene ontology analysis of miR-383 overexpressing cells relative to control transfected cell during DENV-2 infection. Huh7 cells were transfected with either con-miR or miR-383, 24h post-transfection cells were infected with DENV-2 for 48h. Gene ontology analysis classifying activated genes (≥1.5-fold increase) in miR-383 transfected and DENV infected Huh7 cells. The top five gene ontology terms are all related to lipid and cholesterol metabolic processes.

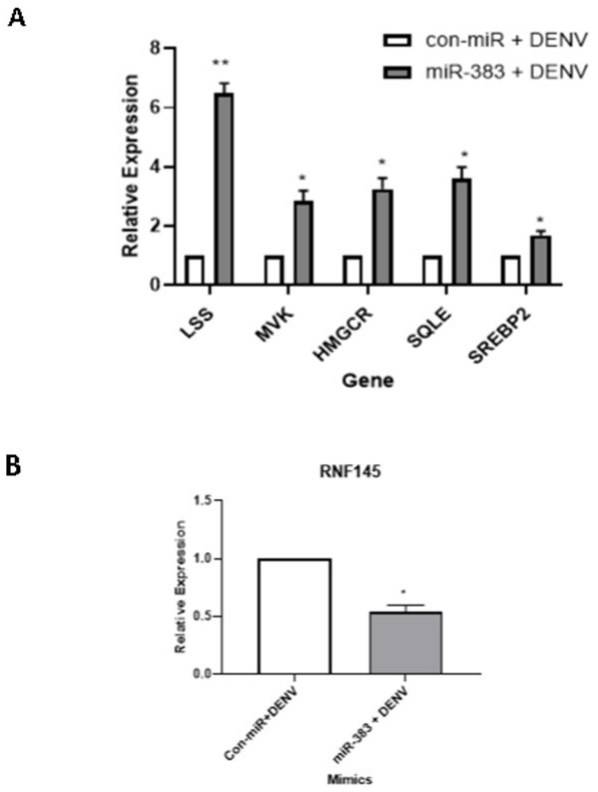

Figure S3. 4 miR-383 regulates SREBP2-activated signaling during DENV infection. A) Huh7 cells were either transfected with con-miR or miR-383. 24h post transfection, cells were infected with DENV-2 at an MOI 0.1. 48h post-transfection, cells were lysed for RNA analysis. RT-qPCR was performed on SREBP2 target genes. B) levels of RNF145 are reduced in miR-383 transfected cells relative to con-miR transfected cells. Error bars represent the means ±SEM of at least three independent biological replicates.*P<0.05 and **P<0.01.

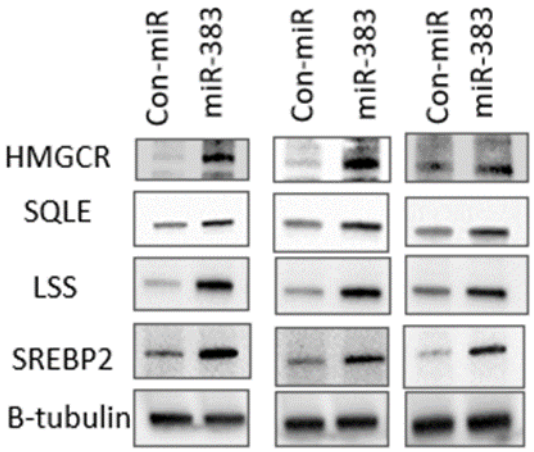

Figure S3. 5 Western blot analysis of independent replicates of SREBP2 and target levels in miR-383 and con-miR transfected cells. Huh7 cells were either transfected with con-miR or miR-383. 72h post transfection, cells were lysed, and western analysis were performed for SREBP2 and SREBP2-target genes.

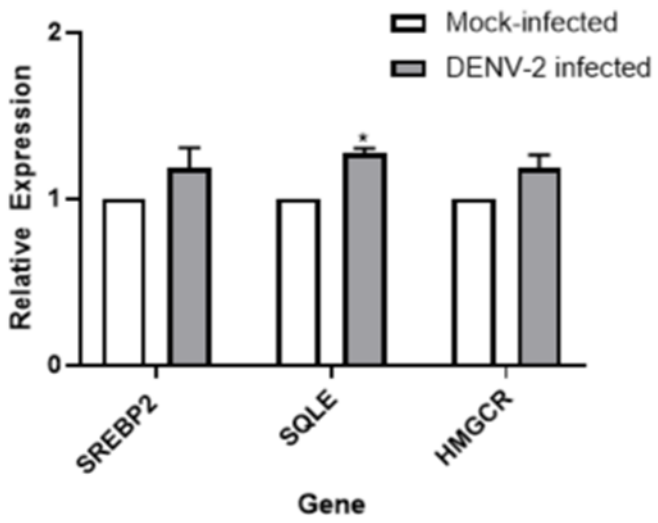

Figure S3. 6 SREBP2 and SREBP2-target levels in DENV-2 infected cells. Huh7 cells were either mock-infected or DENV-2 infected at an MOI of 0.1. 48h-post infection cells were lysed and RT-qPCR analysis were performed on SREBP2, SQLE and HMGCR. Error bars represent the means ±SEM of three biological replicates. *P<0.05.

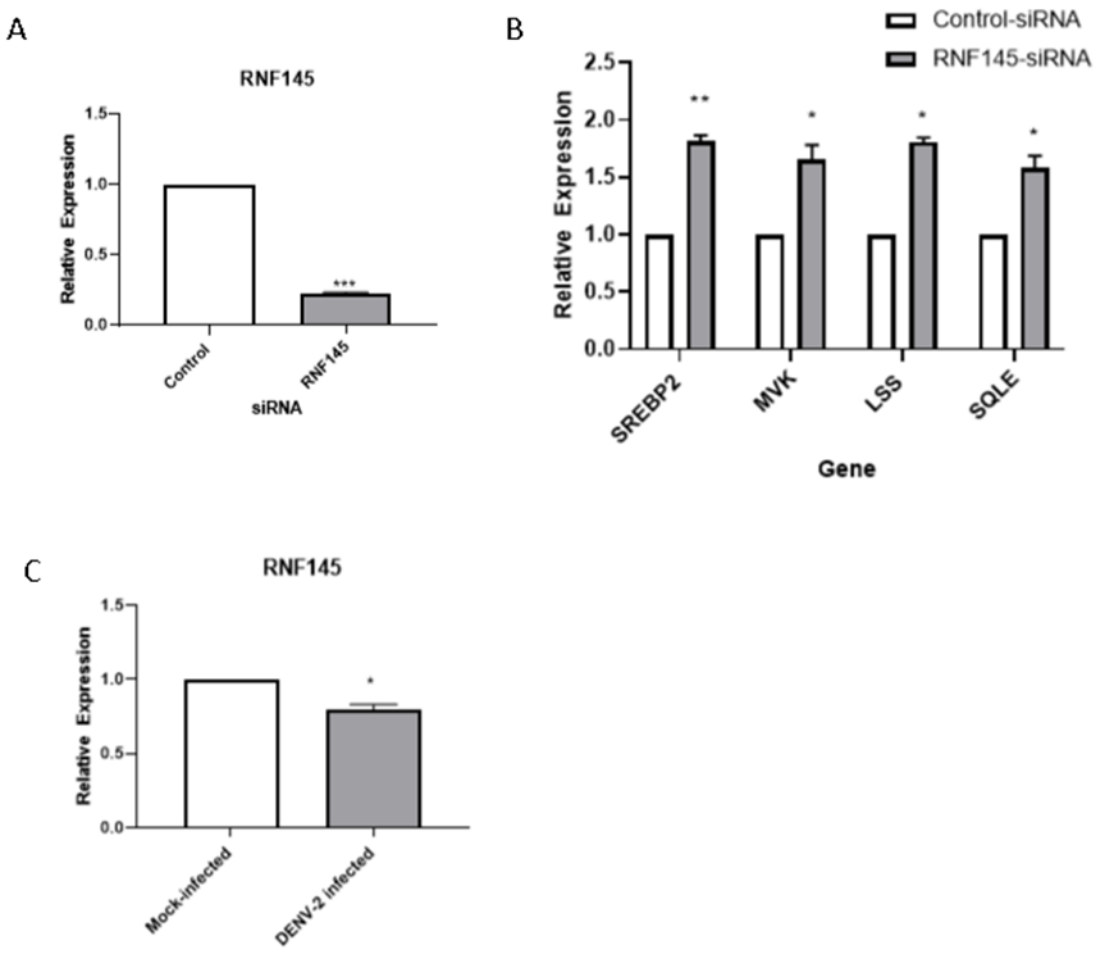

Figure S3. 7 RNF145 knock down upregulated SREBP2-modulated transcription in huh7 cells. Huh7 cells were either transfected with con-siRNA or RNF145-siRNA. 48h post-transfection, cells were lysed and RT-qPCR analysis was performed on A) RNF145 B)SREBP2 and SREBP2 target genes. C) Huh7 cells were either mock-infected or DENV-2 infected at an MOI of 0.1. 48h-post infection cells were lysed, and RT-qPCR analysis were performed onRNF145. Error bars represent the means ±SEM of three biological replicates. *P<0.05, **P<0.01, ***P<0.001.

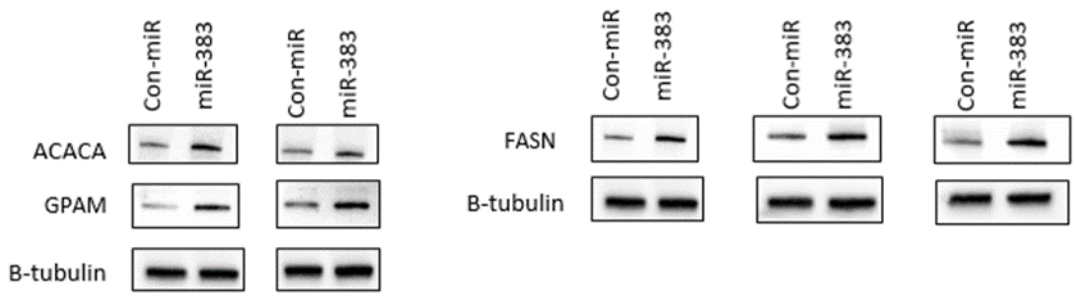

Figure S3. 8 Western blot analysis of independent replicates of SREBP1C targets levels in miR-383 and con-miR transfected cells. Huh7 cells were either transfected with con-miR or miR-383. 72h post transfection, cells were lysed and western analysis were performed for SREBP1C-target genes.

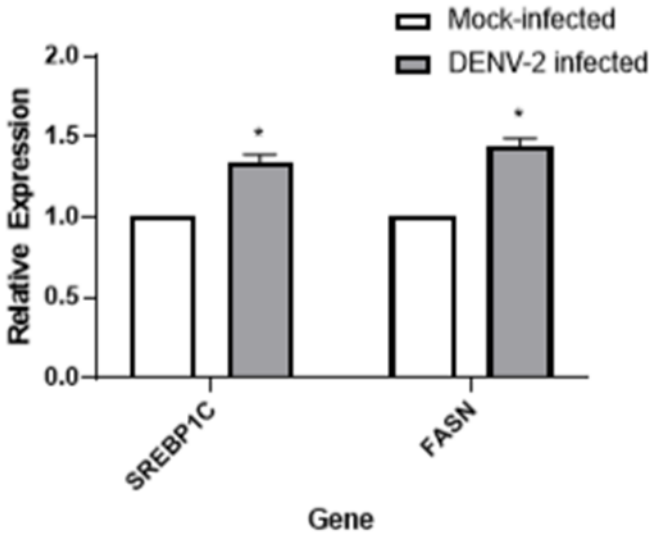

Figure S3. 9 SREBP1C and targets genes (FASN) levels in DENV-2 infected cells. Huh7 cells were either mock-infected or DENV-2 infected at an MOI of 0.1. 48h-post infection cells were lysed, and RT-qPCR analysis were performed on SREBP1C and FASN. Error bars represent the means ±SEM of three biological replicates. *P<0.05.

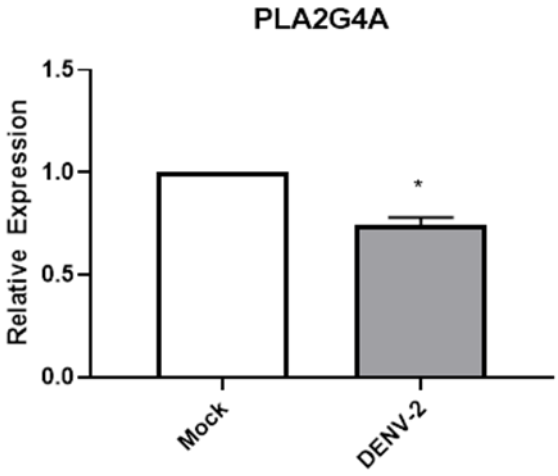

Figure S3. 10 DENV infection modulates the levels of PLA2G4A . Huh7 cells were either transfected with con-miR or miR-383. 72h post transfection, cells were lysed and q-RT-PCR analysis were performed. Error bars represent the means ±SEM of three biological replicates. *P<0.05.

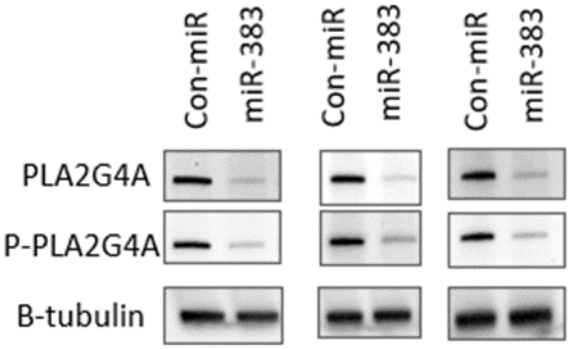

Figure S3. 11 Western blot analysis of independent replicates of PLA2G4A and phospho-PLA2G4A levels in miR-383 and con-miR transfected cells. Huh7 cells were either transfected with con-miR or miR-383. 72h post transfection, cells were lysed and western analysis were performed for PLA2G4A and phospho-PLA2G4A.

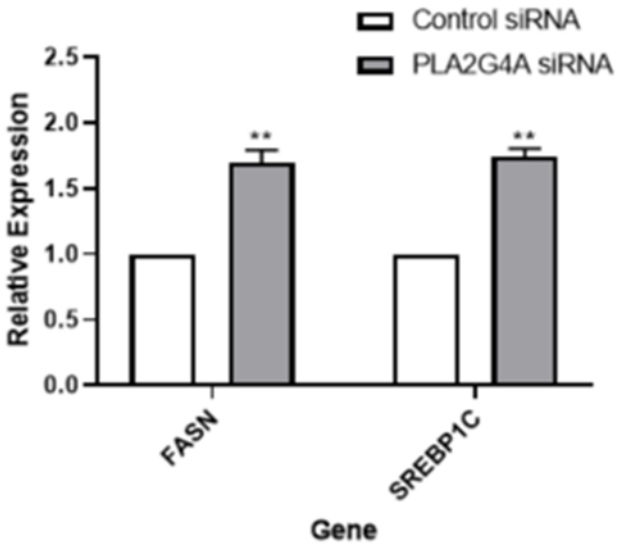

Figure S3. 12 Decrease in the levels of PLA2G4A enhances SREBP1C-mediated transcription. Huh7 cells were either transfected with PLA2G4A siRNA or control siRNA. 72h post transfection, cells were lysed and RT-qPCR was performed. qRT-PCR analysis of SREBP1C and FASN levels in PLA2G4A siRNA and control siRNA treated were assessed. Error bars represent the means ±SEM of at least 3 independent biological replicates. **P<0.01.

Table S3. 1 Gene ontology biological process analysis classifying miR-383 activated genes in Huh7 hepatoma cells.

ID	Name*	P-value
GO:0006629	lipid metabolic process	2.57E-19
GO:0008203	cholesterol metabolic process	1.89E-18
GO:0016125	sterol metabolic process	7.43E-18
GO:0008202	steroid metabolic process	1.26E-17
GO:1902652	secondary alcohol metabolic process	1.58E-17
GO:1901615	organic hydroxy compound metabolic process	9.79E-17
GO:0006066	alcohol metabolic process	1.47E-14
GO:1901700	response to oxygen-containing compound	7.87E-13
GO:0044283	small molecule biosynthetic process	1.61E-12
GO:0010876	lipid localization	2.21E-12

Top ten overrepresented processes are listed among genes activated by greater than 1.5 fold in miR-383 mimic transfected Huh7 cells by biological process.

Table S3. 2 Gene ontology biological process analysis classifying miR-383 activated genes in Huh7 hepatoma cells during DENV2 infection.

ID	Name*	P-value
GO:0008202	steroid metabolic process	1.05E-34
GO:0006629	lipid metabolic process	9.29E-32
GO:0008203	cholesterol metabolic process	6.51E-30
GO:1902652	secondary alcohol metabolic process	8.81E-29
GO:0016125	sterol metabolic process	2.48E-28
GO:1901615	organic hydroxy compound metabolic	8.24E-27
GO:0006066	alcohol metabolic process	2.07E-24
GO:0006082	organic acid metabolic process	7.06E-24
GO:0044255	cellular lipid metabolic process	3.97E-23
GO:0043436	oxoacid metabolic process	1.37E-22

Top ten overrepresented processes are listed among genes activated by greater than 1.5-fold in miR-383 mimic transfected Huh7 cells by biological process.

Table S3. 3 List of 382 genes which represent the overlap between miR-383 predicted targets and genes repressed in miR-383 mimic transfected Huh7 cells

Gene symbol	Description
ABHD10	abhydrolase domain containing 10
ABT1	activator of basal transcription 1
ACER2	alkaline ceramidase 2
ADCY3	adenylate cyclase 3
ADPGK	ADP-dependent glucokinase
ADRBK2	adrenergic, beta, receptor kinase 2
ADSS	adenylosuccinate synthase
AKAP10	A kinase (PRKA) anchor protein 10
AKAP5	A kinase (PRKA) anchor protein 5
AKAP7	A kinase (PRKA) anchor protein 7
ALDH1L2	aldehyde dehydrogenase 1 family, member L2
ALG6	ALG6, alpha-1,3-glucosyltransferase
AMN1	antagonist of mitotic exit network 1 homolog (S. cerevisiae)
ATG5	autophagy related 5
ATP8A1	ATPase, aminophospholipid transporter (APLT), class I, type 8A, member 1
ATR	ataxia telangiectasia and Rad3 related
ATXN1L	ataxin 1-like
ATXN3	ataxin 3
AZI2	5-azacytidine induced 2
BBX	bobby sox homolog (Drosophila)
BCAS2	breast carcinoma amplified sequence 2
BCAS3	breast carcinoma amplified sequence 3
BTN3A1	butyrophilin, subfamily 3, member A1
BTN3A2	butyrophilin, subfamily 3, member A2
BUB1	BUB1 mitotic checkpoint serine/threonine kinase
C12orf45	chromosome 12 open reading frame 45
C12orf66	chromosome 12 open reading frame 66
C14orf37	chromosome 14 open reading frame 37
C1orf27	chromosome 1 open reading frame 27
C1orf52	chromosome 1 open reading frame 52
C4orf33	chromosome 4 open reading frame 33
C8orf37	chromosome 8 open reading frame 37
C8orf4	chromosome 8 open reading frame 4
CA5B	carbonic anhydrase VB, mitochondrial
CAMLG	calcium modulating ligand
CASP2	caspase 2, apoptosis-related cysteine peptidase

CBWD2	COBW domain containing 2
CCDC15	coiled-coil domain containing 15
CCDC177	Homo sapiens coiled-coil domain containing 177 (CCDC177), mRNA.
CCDC25	coiled-coil domain containing 25
CCNDBP1	cyclin D-type binding-protein 1
CDC14B	cell division cycle 14B
CDC42SE1	CDC42 small effector 1
CDC42SE2	CDC42 small effector 2
CDIPT	CDP-diacylglycerol--inositol 3-phosphatidyltransferase
CDK6	cyclin-dependent kinase 6
CENPF	centromere protein F, 350/400kDa
CENPP	centromere protein P
CEP97	centrosomal protein 97kDa
CHST14	carbohydrate (N-acetylgalactosamine 4-0) sulfotransferase 14
CLDN12	claudin 12
CMSS1	cms1 ribosomal small subunit homolog (yeast)
CNIH1	cornichon family AMPA receptor auxiliary protein 1
CNTNAP3	contactin associated protein-like 3
COA5	cytochrome c oxidase assembly factor 5
COL4A3BP	collagen, type IV, alpha 3 (Goodpasture antigen) binding protein
COX7B	cytochrome c oxidase subunit VIIb
CRBN	cereblon
CRLS1	cardiolipin synthase 1
CTGF	connective tissue growth factor
CTNNAL1	catenin (cadherin-associated protein), alpha-like 1
CXCL16	chemokine (C-X-C motif) ligand 16
DBF4	DBF4 homolog (S. cerevisiae)
DBR1	debranching RNA lariats 1
DCAF17	DDB1 and CUL4 associated factor 17
DCTN3	dynactin 3 (p22)
DDIT4	DNA-damage-inducible transcript 4
DDX21	DEAD (Asp-Glu-Ala-Asp) box helicase 21
DFFA	DNA fragmentation factor, 45kDa, alpha polypeptide
DHRS12	dehydrogenase/reductase (SDR family) member 12
DHRS13	dehydrogenase/reductase (SDR family) member 13
DHX36	DEAH (Asp-Glu-Ala-His) box polypeptide 36
DIAPH3	diaphanous-related formin 3
DIMT1	DIM1 dimethyladenosine transferase 1 homolog (S. cerevisiae)
DMTF1	cyclin D binding myb-like transcription factor 1
DNAJC10	DnaJ (Hsp40) homolog, subfamily C, member 10
DNAL1	dynein, axonemal, light chain 1

DPY19L3	dpy-19-like 3 (C. elegans)
DPYSL5	dihydropyrimidinase-like 5
DR1	down-regulator of transcription 1, TBP-binding (negative cofactor 2)
DSG3	desmoglein 3
DSN1	DSN1, MIS12 kinetochore complex component
DUSP5	dual specificity phosphatase 5
E2F7	E2F transcription factor 7
EDARADD	EDAR-associated death domain
EEF2K	eukaryotic elongation factor-2 kinase
EFHC1	EF-hand domain (C-terminal) containing 1
EHD3	EH-domain containing 3
EIF4EBP1	eukaryotic translation initiation factor 4E binding protein 1
EIF4G2	eukaryotic translation initiation factor 4 gamma, 2
ELMOD2	ELMO/CED-12 domain containing 2
EMB	embigin
EPB41L4B	erythrocyte membrane protein band 4.1 like 4B
EXO1	exonuclease 1
FAM126B	family with sequence similarity 126, member B
FAM174A	family with sequence similarity 174, member A
FAM76B	family with sequence similarity 76, member B
FBXO5	F-box protein 5
FGF19	fibroblast growth factor 19
FIG4	FIG4 homolog, SAC1 lipid phosphatase domain containing (S. cerevisiae)
FKBP4	FK506 binding protein 4, 59kDa
FUT8	fucosyltransferase 8 (alpha (1,6) fucosyltransferase)
G2E3	G2/M-phase specific E3 ubiquitin protein ligase
GABRA2	gamma-aminobutyric acid (GABA) A receptor, alpha 2
GALNT11	UDP-N-acetyl-alpha-D-galactosamine:polypeptide N-acetylgalactosaminyltransferase 11 (GalNAc-T11)
GALNT7	UDP-N-acetyl-alpha-D-galactosamine:polypeptide N-acetylgalactosaminyltransferase 7 (GalNAc-T7)
GAS2L3	growth arrest-specific 2 like 3
GDE1	glycerophosphodiester phosphodiesterase 1
GEMIN5	gem (nuclear organelle) associated protein 5
GINS1	GINS complex subunit 1 (Psf1 homolog)
GLRX3	glutaredoxin 3
GMCL1	germ cell-less, spermatogenesis associated 1
GNL3L	guanine nucleotide binding protein-like 3 (nucleolar)-like
GNPDA2	glucosamine-6-phosphate deaminase 2
GPALPP1	GPALPP motifs containing 1
GPD1L	glycerol-3-phosphate dehydrogenase 1-like

GPR89A	G protein-coupled receptor 89A
GPRASP2	G protein-coupled receptor associated sorting protein 2
GPX8	glutathione peroxidase 8 (putative)
GRAP2	GRB2-related adaptor protein 2
GRM6	glutamate receptor, metabotropic 6
GRWD1	glutamate-rich WD repeat containing 1
GSTCD	glutathione S-transferase, C-terminal domain containing
HDAC2	histone deacetylase 2
HDAC9	histone deacetylase 9
HELLS	helicase, lymphoid-specific
HHLA2	HERV-H LTR-associating 2
HIST3H2A	histone cluster 3, H2a
HMGN2	high mobility group nucleosomal binding domain 2
HNRNPA1	heterogeneous nuclear ribonucleoprotein A1
HPGD	hydroxyprostaglandin dehydrogenase 15-(NAD)
HSPA13	heat shock protein 70kDa family, member 13
HTR3E	5-hydroxytryptamine (serotonin) receptor 3E, ionotropic
HUS1	HUS1 checkpoint homolog (S. pombe)
IARS	isoleucyl-tRNA synthetase
ICAM1	intercellular adhesion molecule 1
IDS	Iduronate 2-sulfatase (Hunter syndrome), isoform CRA_e; Iduronate 2-sulfatase 14 kDa chain; cDNA FLJ42669 fis, clone BRAMY2022168, highly similar to IDURONATE 2-SULFATASE
IFI30	interferon, gamma-inducible protein 30
IFIT1	interferon-induced protein with tetratricopeptide repeats 1
IMPACT	impact RWD domain protein
IPO5	importin 5
IPO7	importin 7
ITGB1BP1	integrin beta 1 binding protein 1
ITGB3BP	integrin beta 3 binding protein (beta3-endonexin)
ITPK1	inositol-tetrakisphosphate 1-kinase
KANSL2	KAT8 regulatory NSL complex subunit 2
KAT2A	K(lysine) acetyltransferase 2A
KBTBD4	kelch repeat and BTB (POZ) domain containing 4
KCTD2	potassium channel tetramerization domain containing 2
KIAA0100	KIAA0100
KIAA0101	KIAA0101
KIAA0825	KIAA0825
KIF18B	kinesin family member 18B
KIF3B	kinesin family member 3B
KLHDC10	kelch domain containing 10

KLRC3	killer cell lectin-like receptor subfamily C, member 3
KNTC1	kinetochore associated 1
KPNB1	karyopherin (importin) beta 1
KRTAP2-1	keratin associated protein 2-1
KRTAP9-4	keratin associated protein 9-4
LAYN	layilin
LDHA	lactate dehydrogenase A
LGMN	legumain
LIG4	ligase IV, DNA, ATP-dependent
LRRC34	leucine rich repeat containing 34
LYPLA1	lysophospholipase I
LYRM7	LYR motif containing 7
MAL2	mal, T-cell differentiation protein 2 (gene/pseudogene)
MAN2A1	mannosidase, alpha, class 2A, member 1
MANEA	mannosidase, endo-alpha
MAPK12	mitogen-activated protein kinase 12
MBTD1	mbt domain containing 1
MCM8	minichromosome maintenance complex component 8
MCMBP	minichromosome maintenance complex binding protein
MDM2	MDM2 oncogene, E3 ubiquitin protein ligase
MEAF6	MYST/Esa1-associated factor 6
MED19	mediator complex subunit 19
MEF2C	myocyte enhancer factor 2C
MEST	mesoderm specific transcript
MFN1	mitofusin 1
MFSD1	major facilitator superfamily domain containing 1
MID1	midline 1 (Opitz/BBB syndrome)
MLLT11	myeloid/lymphoid or mixed-lineage leukemia (trithorax homolog, Drosophila); translocated to, 11
MOB1A	MOB kinase activator 1A
MOB1B	MOB kinase activator 1B
MOB4	MOB family member 4, phocein
MORN4	MORN repeat containing 4
MOSPD1	motile sperm domain containing 1
MRPL17	mitochondrial ribosomal protein L17
MRPS18C	mitochondrial ribosomal protein S18C
MRPS23	mitochondrial ribosomal protein S23
MRTO4	mRNA turnover 4 homolog (S. cerevisiae)
MTHFD1L	methylenetetrahydrofolate dehydrogenase (NADP+ dependent) 1-like
MTHFD2	methylenetetrahydrofolate dehydrogenase (NADP+ dependent) 2, methenyltetrahydrofolate cyclohydrolase

MTMR6	myotubularin related protein 6
MTUS1	microtubule associated tumor suppressor 1
NABP1	nucleic acid binding protein 1
NCAM2	neural cell adhesion molecule 2
NCKAP1	NCK-associated protein 1
NDUFA2	NADH dehydrogenase (ubiquinone) 1 alpha subcomplex, 2, 8kDa
NFKBID	nuclear factor of kappa light polypeptide gene enhancer in B-cells inhibitor, delta
NID2	nidogen 2 (osteonidogen)
NIP7	NIP7, nucleolar pre-rRNA processing protein
NOC3L	nucleolar complex associated 3 homolog (S. cerevisiae)
NPAT	nuclear protein, ataxia-telangiectasia locus
NR2C1	nuclear receptor subfamily 2, group C, member 1
NR2F6	nuclear receptor subfamily 2, group F, member 6
NSL1	NSL1, MIS12 kinetochore complex component
NUDCD2	NudC domain containing 2
OIP5	Opa interacting protein 5
OPN3	opsin 3
ORC1	origin recognition complex, subunit 1
OTUD4	OTU domain containing 4
PAK2	p21 protein (Cdc42/Rac)-activated kinase 2
PAPD7	PAP associated domain containing 7
PARP2	poly (ADP-ribose) polymerase 2
PAX6	paired box 6
PDE4A	phosphodiesterase 4A, cAMP-specific
PDE6A	phosphodiesterase 6A, cGMP-specific, rod, alpha
PEX19	peroxisomal biogenesis factor 19
PFKM	phosphofructokinase, muscle
PFN2	profilin 2
PGAM5	phosphoglycerate mutase family member 5
PGM5	phosphoglucomutase 5
PHKG2	phosphorylase kinase, gamma 2 (testis)
PIAS3	protein inhibitor of activated STAT, 3
PIP4K2C	phosphatidylinositol-5-phosphate 4-kinase, type II, gamma
PITPNC1	phosphatidylinositol transfer protein, cytoplasmic 1
PKIA	protein kinase (cAMP-dependent, catalytic) inhibitor alpha
PLA2G4A	phospholipase A2, group IVA (cytosolic, calcium-dependent)
PLAC8	placenta-specific 8
PLCG2	phospholipase C, gamma 2 (phosphatidylinositol-specific)
PLEKHB2	pleckstrin homology domain containing, family B (evectins) member 2
POLE3	polymerase (DNA directed), epsilon 3, accessory subunit
POLR2C	polymerase (RNA) II (DNA directed) polypeptide C, 33kDa

POLR2H	polymerase (RNA) II (DNA directed) polypeptide H
POT1	protection of telomeres 1
PPIL6	peptidylprolyl isomerase (cyclophilin)-like 6
PPM1E	protein phosphatase, Mg2+/Mn2+ dependent, 1E
PPP1R3D	protein phosphatase 1, regulatory subunit 3D
PRC1	protein regulator of cytokinesis 1
PRDM5	PR domain containing 5
PRDX3	peroxiredoxin 3
PRRT1	proline-rich transmembrane protein 1
PRTFDC1	phosphoribosyl transferase domain containing 1
PRUNE	prune exopolyphosphatase
PSME4	proteasome (prosome, macropain) activator subunit 4
PSTPIP2	proline-serine-threonine phosphatase interacting protein 2
PTGES3L-AARSD1	PTGES3L-AARSD1 readthrough
PTPN4	protein tyrosine phosphatase, non-receptor type 4 (megakaryocyte)
PYCR1	pyrroline-5-carboxylate reductase 1
PYGO1	pygopus homolog 1 (Drosophila)
RAB17	RAB17, member RAS oncogene family
RAB27B	RAB27B, member RAS oncogene family
RAD51	RAD51 recombinase
RAD51AP1	RAD51 associated protein 1
RAD54B	RAD54 homolog B (S. cerevisiae)
RASA2	RAS p21 protein activator 2
RASEF	RAS and EF-hand domain containing
RASL10B	RAS-like, family 10, member B
RBBP8	retinoblastoma binding protein 8
RBBP9	retinoblastoma binding protein 9
RBM3	RNA binding motif (RNP1, RRM) protein 3
RBMS1	RNA binding motif, single stranded interacting protein 1
RFC2	replication factor C (activator 1) 2, 40kDa
RFT1	RFT1 homolog (S. cerevisiae)
RNF141	ring finger protein 141
RNF41	ring finger protein 41
ROGDI	rogdi homolog (Drosophila)
RPL22L1	ribosomal protein L22-like 1
RPL41	ribosomal protein L41
RPP30	ribonuclease P/MRP 30kDa subunit
RPRD1B	regulation of nuclear pre-mRNA domain containing 1B
RTKN2	rhotekin 2
SASS6	spindle assembly 6 homolog (C. elegans)

SCOC	short coiled-coil protein
SDE2	SDE2 telomere maintenance homolog (S. pombe)
SENP1	SUMO1/sentrin specific peptidase 1
SERINC5	serine incorporator 5
SERPINB9	serpin peptidase inhibitor, clade B (ovalbumin), member 9
SETD9	SET domain containing 9
SFRP1	secreted frizzled-related protein 1
SGOL1	shugoshin-like 1 (S. pombe)
SHMT2	serine hydroxymethyltransferase 2 (mitochondrial)
SLC25A12	solute carrier family 25 (aspartate/glutamate carrier), member 12
SLC25A23	solute carrier family 25 (mitochondrial carrier; phosphate carrier), member 23
SLC25A40	solute carrier family 25, member 40
SLC29A1	solute carrier family 29 (equilibrative nucleoside transporter), member 1
SLC30A6	solute carrier family 30 (zinc transporter), member 6
SLC35A3	solute carrier family 35 (UDP-N-acetylglucosamine (UDP-GlcNAc) transporter), member A3
SLC36A4	solute carrier family 36 (proton/amino acid symporter), member 4
SLC37A3	solute carrier family 37, member 3
SLC41A1	solute carrier family 41 (magnesium transporter), member 1
SLC7A1	solute carrier family 7 (cationic amino acid transporter, y+ system), member 1
SLC7A11	solute carrier family 7 (anionic amino acid transporter light chain, xc- system), member 11
SLFN13	schlafen family member 13
SLMAP	sarcolemma associated protein
SMC2	structural maintenance of chromosomes 2
SPDL1	spindle apparatus coiled-coil protein 1
SPRY1	sprouty homolog 1, antagonist of FGF signaling (Drosophila)
SRSF2	serine/arginine-rich splicing factor 2
STC2	stanniocalcin 2
STIL	SCL/TAL1 interrupting locus
STK17B	serine/threonine kinase 17b
SUCO	SUN domain containing ossification factor
SUFU	suppressor of fused homolog (Drosophila)
SURF2	surfeit 2
SVIP	small VCP/p97-interacting protein
SYNPO2	synaptopodin 2
TAF1D	TATA box binding protein (TBP)-associated factor, RNA polymerase I, D, 41kDa
TAF9B	TAF9B RNA polymerase II, TATA box binding protein (TBP)-associated factor, 31kDa
TBC1D15	TBC1 domain family, member 15
TBCK	TBC1 domain containing kinase
TBX20	T-box 20

TGS1	trimethylguanosine synthase 1
THEM4	thioesterase superfamily member 4
TIMM17A	translocase of inner mitochondrial membrane 17 homolog A (yeast)
TIPRL	TIP41, TOR signaling pathway regulator-like (S. cerevisiae)
TMED9	transmembrane emp24 protein transport domain containing 9
TMEM138	transmembrane protein 138
TMEM143	transmembrane protein 143
TMEM14B	transmembrane protein 14B
TMEM161B	transmembrane protein 161B
TMEM182	transmembrane protein 182
TMEM19	transmembrane protein 19
TMEM199	transmembrane protein 199
TMEM230	transmembrane protein 230
TMEM237	transmembrane protein 237
TMEM251	transmembrane protein 251
TMEM55A	transmembrane protein 55A
TMEM67	transmembrane protein 67
TMEM78	transmembrane protein 78
TMX1	thioredoxin-related transmembrane protein 1
TNFSF15	tumor necrosis factor (ligand) superfamily, member 15
TNIK	TRAF2 and NCK interacting kinase
TOMM34	translocase of outer mitochondrial membrane 34
TOP2A	topoisomerase (DNA) II alpha 170kDa
TPM3	tropomyosin 3
TRAPPC8	trafficking protein particle complex 8
TRDMT1	tRNA aspartic acid methyltransferase 1
TRIM6	tripartite motif containing 6
TRMT10B	tRNA methyltransferase 10 homolog B (S. cerevisiae)
TSTA3	tissue specific transplantation antigen P35B
TTC1	tetratricopeptide repeat domain 1
TYW5	tRNA-yW synthesizing protein 5
UBE2F	ubiquitin-conjugating enzyme E2F (putative)
UBE2G2	ubiquitin-conjugating enzyme E2G 2
UBE2S	ubiquitin-conjugating enzyme E2S
UBE2T	ubiquitin-conjugating enzyme E2T (putative)
UBR7	ubiquitin protein ligase E3 component n-recognin 7 (putative)
UGGT2	UDP-glucose glycoprotein glucosyltransferase 2
UNC45B	unc-45 homolog B (C. elegans)
UROS	uroporphyrinogen III synthase
USP15	ubiquitin specific peptidase 15
VEZT	vezatin, adherens junctions transmembrane protein

VPS35	vacuolar protein sorting 35 homolog (S. cerevisiae)
VPS37A	vacuolar protein sorting 37 homolog A (S. cerevisiae)
VPS54	vacuolar protein sorting 54 homolog (S. cerevisiae)
WBP2	WW domain binding protein 2
WDR3	WD repeat domain 3
WDR41	WD repeat domain 41
WDR75	WD repeat domain 75
XRCC2	X-ray repair complementing defective repair in Chinese hamster cells 2
XRN2	5'-3' exoribonuclease 2
YWHAH	tyrosine 3-monooxygenase/tryptophan 5-monooxygenase activation protein, eta polypeptide
ZC2HC1A	zinc finger, C2HC-type containing 1A
ZNF101	zinc finger protein 101
ZNF230	zinc finger protein 230
ZNF300	zinc finger protein 300
ZNF354B	zinc finger protein 354B
ZNF451	zinc finger protein 451
ZNF527	zinc finger protein 527
ZNF557	zinc finger protein 557
ZNF573	zinc finger protein 573
ZNF670	zinc finger protein 670
ZNF774	zinc finger protein 774
ZNF829	zinc finger protein 829
ZRANB2	zinc finger, RAN-binding domain containing 2
ZSWIM7	zinc finger, SWIM-type containing 7
ZWILCH	zwilch kinetochore protein
ZWINT	ZW10 interacting kinetochore protein
ZXDB	zinc finger, X-linked, duplicated B

Table S3. 4 List of qPCR primers used in this study

Oligonucleotide	Sequence
RNA18S	FWD: GCGATGCGGCGGCGTTATTC
	REV: CAATCTGTCAATCCTGTCCGTGTCC
DENV2	FWD: TTGAGTAAACTGTGCAGCCTGTAGCTC
	REV: GGGTCTCCTCTAACCTCTAGTCCT
FASN	FWD: GAAACTGCAGGAGCTGTC
	REV: CACGGAGTTGAGGCGCAT
MVK	FWD: CATGGCAAGGTAGCACTGG
	REV: GATACCAATGTTGGGTAAGCTGA
SREBP2	FWD: CTTTGATATACCAGAATGCAG
	REV: CAGGCTTTGGACTTGAGGCTG
SREBP1c	FWD: ACTTCTGGAGGCATCGCAAGCA
	REV: AGGTTCCAGAGGAGGCTACAAG
LSS	FWD: GCACTGGACGGGTGATTATGG
	REV: TCTCTTCTCTGTATCCGGCTG
SQLE	FWD: GGCATTGCCACTTTCACCTAT
	REV: GGCCTGAGAGAATATCCGAGAAG
HMGCR	FWD: TGATTGACCTTTCCAGAGCAAG
	REV: CTAAAATTGCCATTCCACGAGC
PLA2G4A	FWD: TACCAGCACATTATAGTGGAGCA
	REV: GCTGTCAGGGGTTGTAGAGAT
RNF145	FWD: AGTGAACTGGAGTTTGCCTATG
	REV: ACACACCACCAACTGACCTATT
GPAM	FWD: GATGTAAGCACACAAGTGAGGA
	REV: TCCGACTCATTAGGCTTTCTTTC
ACACA	FWD: ATGTCTGGCTTGCACCTAGTA
	REV: CCCCAAAGCGAGTAACAAATTCT
VSV N	FWD: ATGTCTGTTACAGTCAAGAGAATC
	REV: TCATTTGTCAAATTCTGACTTAGCATA

Table S3. 5 Antibodies used in this study

Primary Antibody	Primary Dilution	Provider	Catalog number
B-tubulin	1:5000	Abcam	610621
FASN	1:1000	Santa-Cruz Biotechnologies	sc-483570
cPLA2 (PLA2G4A)	1:1000	Cell signaling	2832
p-cPLA2	1:500	Cell signaling	2831
LSS	1:1000	ProteinTech	13715-1-AP
SREBP2	1:250	BD Pharmingen	557037
HMGCR	1:1000	ProteinTech	13533-1-AP
SQLE	1:1000	ProteinTech	12544-1-AP
ACACA	1:1000	Cell signaling	3676S
GPAM	1:1000	ThermoScientific	PA584441

6.3 Supplemental information for Chapter 4 "miR-185 inhibits SARS-CoV-2 infection through the modulation of the host's lipid microenvironment"

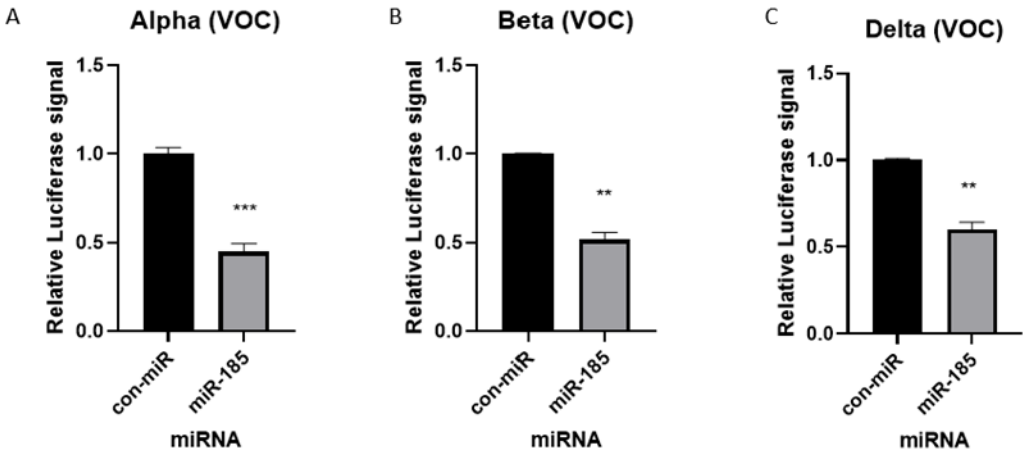

Figure S4. 1 miR-185 inhibits entry of SARS-CoV-2 Alpha, Beta and Delta variants pseudo-typed virus in cell culture. Huh7 cells were transfected with miR-185 mimics or con-miR mimics and 24h post transfection, the cells were infected with 100ul of media containing Sars-CoV-2 S pseudo-typed virus (A) Alpha (B)Beta and (C) delta variants of concern. 48h post infection, cells were lysed in 1X passive lysis buffer and Luciferase activity was measured using a microplate reader. All experiments were read in technical triplicates for at least three biological replicates. Error bars represent the means ±SEM of at least three biological replicates. *P<0.05, **P<0.01, ***P<0.001

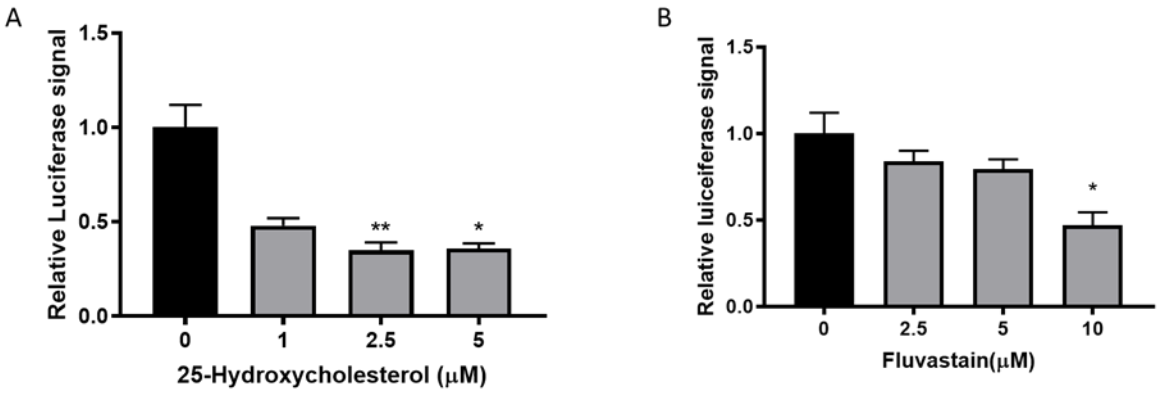

Figure S4. 2 Inhibitors of SREBP2-regulated signaling inhibit SARS-CoV-2 entry. Huh7 cells treated with (A)25-Hydroxycholesterol or (B) Fluvastatin at various concentration, cells were infected with 100ul of media containing Sars-CoV-2 S pseudo-typed virus. 48h post infection, cells were lysed in 1X passive lysis buffer and Luciferase activity was measured using a microplate reader. All experiments were read in technical triplicates for at least three biological replicates. Error bars represent the means ±SEM of at least three biological replicates.*P<0.05, **P<0.01.

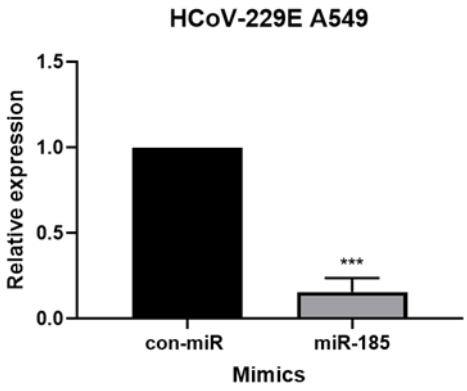

Figure S4. 3 miR-185 inhibits HCoV-229E pathogenesis in A549 cells. Huh7 cells were transfected with miR-185 mimics or con-miR mimics.24 h post-transfection, cells were infected with HCoV-229E at an MOI of 0.05. 48h post-infection cells lysed for RNA analysis of intracellular levels of virus. Error bars represent SEM of three biological replicates, *** $p<0.001$.

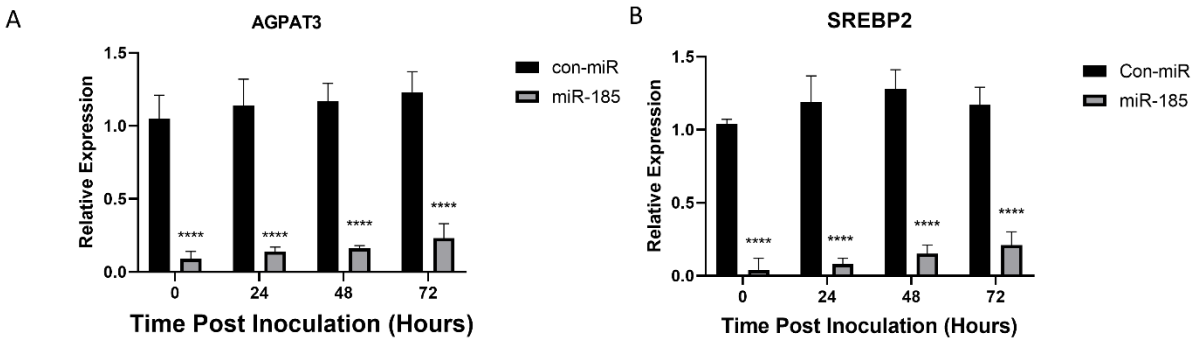

Figure S4. 4 miR-185 decreases the expression of lipogenic genes during SARS-CoV-2 infection. (A and B) Calu-3 cells were transfected with miR-185 mimics or con-miR mimics. Cells were infected with SARS-CoV-2 at various time points at an MOI of 0.01. Cells were lysed for RNA analysis at 0, 24, 48 and 72h post inoculation. RT-qPCR were performed and the levels of SREBP2 and AGPAT3 were evaluated at each time point. Error bars represent SEM of three biological replicates, **** $p<0.0001$.

Table S4. 1 List of qPCR primers used in this study

Oligonucleotide	Sequence
RNA18S	FWD: GCGATGCGGCGGCGTTATTC
	REV: CAATCTGTCAATCCTGTCCGTGTCC
HCoV-229E primers	FWD: TGGCCCCATTAAAAATGTGT
	REV: CCTGAACACCTGAAGCAAT
SREBP2	FWD: CTTTGATATACCAGAATGCAG
	REV: CAGGCTTTGGACTTGAGGCTG
SQLE	FWD: GGCATTGCCACTTTCACCTAT
	REV: GGCCTGAGAGAATATCCGAGAAG
AGPAT3	FWD: CTCCAAGGTCCTCGCTAAGAAG
	REV: CCGCTTGCAGAACACAATCTC
SCARB1	FWD: TCGCAGGCATTGGACAAACT
	REV: CTCCTTATCCTTTGAGCCCTTTT
PPARg	FWD: AGCCTGCGAAAGCCTTTTGG
	REV: GGCTTCACATTCAGCAAACCTGG
ACE2	FWD: CGAAGCCGAAGACCTGTTCTA
	REV: GGGCAAGTGTGGACTGTTCC

Table S4. 2 Antibodies used in this study

Primary Antibody	Primary Dilution	Provider	Catalog number
B-tubulin	1:5000	Abcam	610621
SQLE	1:1000	ProteinTech	12544-1-AP
SREBP2	1:250	BD Pharmingen	557037
Spike	1:2000	GeneTEX	GTX632604